AUSTRALIAN GEOLOGICAL SURVEY ORGANISATION

PETREL SUB-BASIN STUDY

1995-1996

GEOHISTORY MODELLING

by

John M. Kennard

AGSO RECORD 1996/43

DEPARTMENT OF PRIMARY INDUSTRIES AND ENERGY

Minister for Primary Industries and Energy: Hon. J. Anderson, M.P.
Minister for Resources: Senator the Hon. W.R. Parer
Secretary: Paul Barratt

AUSTRALIAN GEOLOGICAL SURVEY ORGANISATION

Executive Director: Neil Williams

ISSN: 1039-0073
ISBN: 0 642 24976 8

PREFACE

AGSO's 1995-96 Petrel Sub-basin Study was undertaken within AGSO's Marine, Petroleum and Sedimentary Resources Division (MPSR) as part of MPSR's North West Shelf Project. The study was aimed at understanding the stratigraphic and structural development of the basin as a framework for more effective and efficient resource exploration. Specifically, the study aimed to:

- define the nature of the major basement elements underlying the Petrel Sub-basin and their influence on the development of the basin through time,
- determine the nature and age of the events that have controlled the initiation, distribution and tectonic evolution of the basin;
- define the nature and age of the basin fill, and the processes that have controlled its deposition and deformation; and, importantly,
- determine the factors controlling the development and distribution of the basin's petroleum systems and occurrences.

This report is the final product of the geohistory modelling component of the study, using the WinBury V2 geohistory modelling package released by Paltech Pty Ltd. The report is intended for use in conjunction with the study's other products, notably the Well Folio, Organic Geochemistry Report and Summary Report. Digital copy of the WinBury models and data files are also available for purchase.

PRODUCTS AVAILABLE FROM THE PETREL SUB-BASIN STUDY

Summary Report *(AGSO Record 1996/40, compiled by J.B. Colwell & J.M. Kennard).*
Summarises major results of the project.

Well Folio *(by J.M. Kennard).*
Provides well composites for 31 key wells in the basin, as well as 6 well-well cross-sections.

Map & Seismic Folio *(by J.B. Colwell, J.E. Blevin & D.J. Wilson).*
Includes 24 time-structure and time-isopach maps as well as select interpreted seismic lines.

Digital Database of Seismic Interpretations.
Covers ~ 8200 line km of AGSO deep- and conventional industry seismic data.

Petrel Stratigraphic Time Chart *(by P.J. Jones et al.).*
Shows latest understanding of the Petrel Sub-basin stratigraphy and event history against biozonations and AGSO's timescale.

Gravity Modelling Report *(AGSO Record 1996/41, by J.B. Willcox)*
Details 2-D gravity modelling undertaken on 3 of the AGSO deep-seismic lines.

Organic Geochemistry Report *(AGSO Record 1996/42, by D. S. Edwards & R. E. Summons).*
Includes carbon isotope and biomarker analyses of oils, oil - source-rock correlations, and a digital source-rock and maturity database.

Geohistory Modelling Report *(AGSO Record 1996/43 , by J.M. Kennard).*
Details geohistory subsidence and thermal maturation modelling of 20 wells and 6 pseudo-wells and hydrocarbon generation and expulsion models for 3 identified source intervals.

CONTENTS

	Page
Abstract	1
Introduction and Methodology	3
Data Input	7
Data Output	9
Subsidence History	10
Phase A: Cambrian-Ordovician-?Silurian	10
Phase B: Frasnian - mid Tournaisian	10
Phase C: late Tournaisian - mid Visean	12
Phase D: late Visean - late Namurian	12
Phase E: latest Namurian- early Asselian	12
Phase F: late Asselian - Anisian	13
Phase G: Ladinian-Sinemurian (Fitzroy Movement and basin inversion)	13
Phase H: Sinemurian-Oxfordian	13
Phase I: late Oxfordian-Maastrichtian	13
Phase J: Tertiary	14
Thermal History	15
Maturity Parameters	15
Palaeo-Heatflow	16
Source Rock Maturation History	19
Mid-Milligans Source Unit	20
Keyling Source Unit	39
Hyland Bay Source Unit	55
Conclusions	61
Acknowledgments	62
References	63
Appendix A: WinBury Geohistory Modelling Flow Diagram	65
Appendix B:	67
Basin Stratigraphy Parameters	67
Observed versus Computed Maturity, Heatflow & Tectonic Subsidence, Geohistory & Hydrocarbon Generation Plots for each well and pseudo-well	68
Appendix C: Kerogen Kinetic Data	113

LIST OF FIGURES page

Figure 1. Location of wells and pseudo-well sites used in this study. 5
Figure 2. Stratigraphy of the Petrel Sub-basin, showing tectonic subsidence cycles and major tectonic events. 6
Figure 3. Tectonic subsidence curves for all wells/pseudo-wells modelled in the Petrel Sub-basin, showing tectonic subsidence Phases A - J. 11
Figure 4. Estimated amount of erosion of Permian Early Triassic sediments during the Fitzroy Movement. 14
Figure 5. Present-day heatflow map for the Petrel Sub-basin. 17
Figure 6. Modelled palaeo-heatflow curves for wells/pseudo-wells. 18
Figure 7. Distribution of the mid-Milligans source rock unit. 21
Figure 8. Bed maturity plot for the mid-Milligans source unit in modelled wells/ pseudo-wells. 22
Figure 9. Present-day bed maturity map for the mid-Milligans source unit. 22
Figure 10. Hydrocarbon generation plots for the mid-Milligans source unit in modelled wells/pseudo-wells. 25
Figure 11. Bed maturity map of the mid-Milligans source unit at the time of deposition of the regional Treachery Shale seal (296 Ma). 36
Figure 12. Comparative hydrocarbon generation plots for the mid-Milligans source rocks in the depocentre north of the Turtle-Barnett High (pseudo-well site HD16-sp400) and the Cambridge Trough south of the Turtle-Barnett High (pseudo-well site CB81-11a). 37
Figure 13. Distribution of the Keyling source rock unit.. 40
Figure 14. Bed maturity plot for the Keyling source unit in modelled wells/pseudo-wells. 41
Figure 15. Present-day bed maturity map for the Keyling source unit. 41
Figure 16. Hydrocarbon generation plots for the Keyling source unit assuming little or no net effective thicknesses of high-quality coaly shales. 43
Figure 17. Hydrocarbon generation plots for the Keyling source unit assuming 10-15 m (i.e., 5 % net TOC), and 40-60 m (i.e., 10 % net TOC) net effective thicknesses of high-quality coaly shales. 49
Figure 18. Distribution of the Hyland Bay source rock unit. 57
Figure 19. Bed maturity plot for the Hyland Bay source unit in modelled wells/ pseudo-wells. 58
Figure 20. Present-day bed maturity map for the Hyland Bay source unit. 58
Figure 21 Hydrocarbon generation plots for the Hyland Bay source unit. 59

LIST OF TABLES

Table 1. Wells analysed in Petrel Sub-basin project. 4
Table 2. Stabilised bottom hole temperatures of wells modelled in this study. 9
Table 3. Wells/pseudo-wells with modelled source rock units. 19

Abstract

Geohistory models of 20 wells and 6 pseudo-well sites in the Petrel Sub-basin are presented to elucidate the complex multi-phase subsidence/uplift history of the basin, and to determine the likely timing of hydrocarbon generation and expulsion from three identified source rock intervals that underpin the basins proven petroleum systems. The models are based on sequence stratigraphic units (second and third order sequences) interpreted to depth of basement, and utilise a new regional understanding of the stratigraphic and structural development of the basin obtained during AGSO's 1995-1996 Petrel Sub-basin Study.

Subsidence models indicate that nine distinct tectonic subsidence phases have controlled the regional basin-fill architecture and stratigraphic history of the Petrel Sub-basin. A phase of Cambrian-Ordovician subsidence (Phase A) was initiated by crustal extension and extrusion of tholeiitic basalts in the Early Cambrian. The major Petrel rift structure was initiated in the late Givetian - Frasnian, and this "syn-rift" extensional phase (Phase B) was terminated by widespread uplift and erosion in the mid Tournaisian. Subsequent tectonic phases (Phases C, D, E and F) appear to have been controlled by re-newed upper and/or lower crustal extension and thermal sag. Compressive tectonism in the Middle Triassic - Early Jurassic (Fitzroy Movement) resulted in widespread uplift and erosion of the flanks of the Petrel Sub-basin, and the formation of inversion anticlines in the central Petrel Deep (Phase G). This compressive basin phase was followed by a phase of minimal net tectonic subsidence throughout most of the Jurassic (Phase H), and two subsidence pulses in the late Oxfordian and Valanginian (jointly Phase I) correlate with the Argo and Gascoyne spreading events along the outer margin of the North West Shelf. A final subsidence phase in the Tertiary (Phase J) is poorly constrained in the Petrel Sub-basin.

Maturation models of three identified source rock units in the Petrel Sub-basin (mid Milligans, Keyling and Hyland Bay source units) provide a much improved understanding of the maturation, expulsion, migration and trapping history of hydrocarbons discovered in the basin, and provides new insights into the basin's future exploration potential.

Composite biodegraded and non-biodegraded oils recovered in the Turtle and Barnett wells were probably charged by hydrocarbons expelled from the mid-Milligans source unit within depocentres to the north and south of the Turtle-Barnett High. Expulsion from the northern source kitchen probably occurred during the mid Carboniferous (Namurian), and this oil was biodegraded as it migrated into shallow, oxidised, fluvial-deltaic reservoirs on the Turtle-Barnett High. Expulsion from the southern source kitchen (Cambridge Trough) probably occurred during the Early Permian following the deposition of the Treachery Shale which forms a regional seal for hydrocarbons sourced from the Milligans Formation. This oil accumulated in the now more deeply buried stacked reservoirs across the Turtle-Barnett High, and was sealed from oxidising groundwaters by the Treachery Shale. Subsequent fault reactivation (probably during the Fitzroy Movement) resulted in partial breach of this seal, and a second phase of oxidation and biodegradation of the shallower oil accumulations.

Untested stratigraphic traps within the Cambridge Trough were probably charged by oil expelled from the mid-Milligans source unit during the Early Permian, and these accumulations are unlikely to be biodegraded since the regional Treachery Shale seal was deposited prior to the expulsion of oil.

Oil shows in the recently drilled Waggon Creek-1 well were probably expelled during the Permian from the mid-Milligans source unit in the central Carlton Sub-basin. These oils could source onlapping turbiditic sand pinchouts against the basal Milligans Supersequence boundary on the flanks of the Carlton Sub-basin, as well as underlying reefal plays in the Ningbing Supersequence.

The Tern Gas Field and the Petrel Gas-Condensate Field were probably charged by gas expelled from the Keyling and/or Hyland Bay source units in the outer and central Petrel Deep during the Late Triassic-Cretaceous (Keyling source) and Tertiary (Hyland Bay source). Shales within the Keyling Supersequence also have the potential to generate minor amounts of oil; in the outer Petrel Deep, this oil was probably expelled during the Late Permian, prior to structuring and trap formation in the Middle Triassic - Early Jurassic (Fitzroy Movement). In the central Petrel Deep, this oil was probably expelled during and shortly after structuring, and may have contributed to the condensate recovered at the Petrel Field. On the shallower southern flank of the Petrel Deep, minor amounts of oil were probably expelled during the Cretaceous and Tertiary.

High-quality, immature to marginally mature, oil-prone, coaly shale source rocks are known to occur in the Kinmore-1 and Flat Top-1 wells, but maturation models suggest that they have expelled little or no hydrocarbons in these wells. If these high-quality source rocks extend to deeper portions of the Petrel Deep, they probably expelled significant quantities of oil and gas during the Early Triassic, prior to the main phase of structuring and trap formation during the Fitzroy Movement. Thus any stratigraphic or combined structural-stratigraphic traps of Permian-Early Triassic age on the flanks of the Petrel Deep may have been charged by oil expelled from the Keyling coaly shale and shale facies in the Petrel Deep during the Early Triassic.

Introduction and Methodology

This record comprises geohistory models for 20 wells and 6 pseudo-wells (sites based on seismic interpretations) in the Petrel Sub-basin (Table 1; Fig. 1). The wells are modelled using the WinBury V2 burial and thermal geohistory modelling package for Windows™ produced by Paltech Pty. Ltd. Wells drilled on and adjacent to inferred and proven salt diapirs (Bougainville-1, Curlew-1, Gull-1, Kinmore-1, Matilda-1, Pelican Island-1 & Sandpiper-1) were not modelled due to stratigraphic disruption and complications involving thermal anomalies. However, stratigraphic and geochemical data from these wells were used to constrain data input for adjacent wells and pseudo-wells.

The wells are modelled on the basis of sequence stratigraphic units (second-order supersequences and third-order sequences) interpreted from well-log and seismic data as summarised on the composite well logs in the AGSO Petrel Sub-basin Well Folio (Kennard, 1996). Full descriptions of the sequences are given in the AGSO Petrel Sub-basin Summary Report (Colwell & Kennard, 1996, Chapter 4), and their stratigraphic relationships and age are summarised in Figure 2. Details of biozone and stratigraphic age relationships are presented on the Petrel Sub-basin Stratigraphic Time Chart (Jones et al., 1996).

All wells are modelled to basement below TD based on seismic stratigraphic interpretations (see Petrel Sub-basin Map & Seismic Folio, Colwell et al., 1996). Additional well data were compiled from well completion reports, composite well logs, and unpublished company and laboratory reports compiled during the AGSO Petrel Sub-basin Project.

The methodology used for WinBury geohistory modelling is summarised in Appendix A. Extensive use has been made of the comprehensive on-line help system provided by WinBury for all data input and manipulation, including on-line geohistory theory and illustrations which assist modelling and interpretation of the data.

In order to ensure consistent subsidence and thermal models within similar structural and tectonic provinces, the 26 wells and pseudo-wells have been grouped into 6 provinces (Fig. 1): 1) Petrel Deep, 2) Lacrosse Terrace, 3) Berkley Platform, Cambridge High and Turtle-Barnett High, 4) Cambridge Trough, Keep Inlet Sub-basin and Kulshill Terrace, 5) Carlton Sub-basin, and 6) northeastern flank of the Petrel Sub-basin.

All geohistory models and data files used for this study are available in digital format; a copy of the WinBury software is required to access this digital data.

PETREL SUB-BASIN WELL ANALYSIS

Well Name	Digital Logs (Wiltshire)	Stratlog Composite	Geohistory Model WinBury
Barnett-1	Y	Y	-
Barnett-2	Y	Y	Y
Berkley-1	Y	Y	Y
Billawock-1	Y	Not for Release	Not for Release
Bonaparte-1	Y	Y	Y
Bonaparte-2	Y	Y	Y
Bougainville-1	Y	Y	(Salt diapir)
Cambridge-1	Y	Y	Y
Curlew-1	Y	Y	(Salt diapir)
Fishburn-1	Y	Not for Release	Not for Release
Flat Top-1	Y	Y	Y
Frigate-1	Y	Y	-
Garimala-1	Y	Y	Y
Gull-1	Y	Y	(Salt diapir)
Keep River-1	Y	Y	Y
Kingfisher- 1	Not Available	Not for Release	Not for Release
Kinmore-1	Y	Y	(Salt diapir)
Kulshill-1	Y	Y	Y
Lacrosse-1	Y	Y	Y
Lesueur-1	Y	Y	Y
Matilda-1	Y	Y	(near Salt diapir)
Ningbing-1	Y	Y	-
Pelican Island-1	Y	Y	(Salt diapir)
Penguin-1	Y	Y	Y
Petrel-1	Y	Y	-
Petrel-1A	Y	Y	Y
Petrel-2	Y	Y	Y
Sandpiper-1	Y	Y	(Salt diapir)
Skull-1	Y	Y	-
Spirit Hill-1	Not Available	Y	-
Sunbird-1	Not Available	Not for Release	Not for Release
Tern-1	Y	Y	Y
Turtle-1	Y	Y	-
Turtle-2	Y	Y	Y
Weaber-2,2A	Y	Y	-
AGSO/1-SP3400	(Outboard of Lacrosse)	-	Y
AGSO/5-SP2800	(midway Kinmore-Bougainville)	-	Y
AGSO/7-SP1100	(Near Gull-1)	-	Y
CB81-11-SP535	(Cambridge Trough)	-	Y
HD16-SP400	(North of Turtle-Barnett High)	-	Y
HD16-SP1050	(North of Turtle-Barnett High)	-	Y

Table 1. Wells analysed in Petrel Sub-basin project. Synthetic well locations shown in italics.

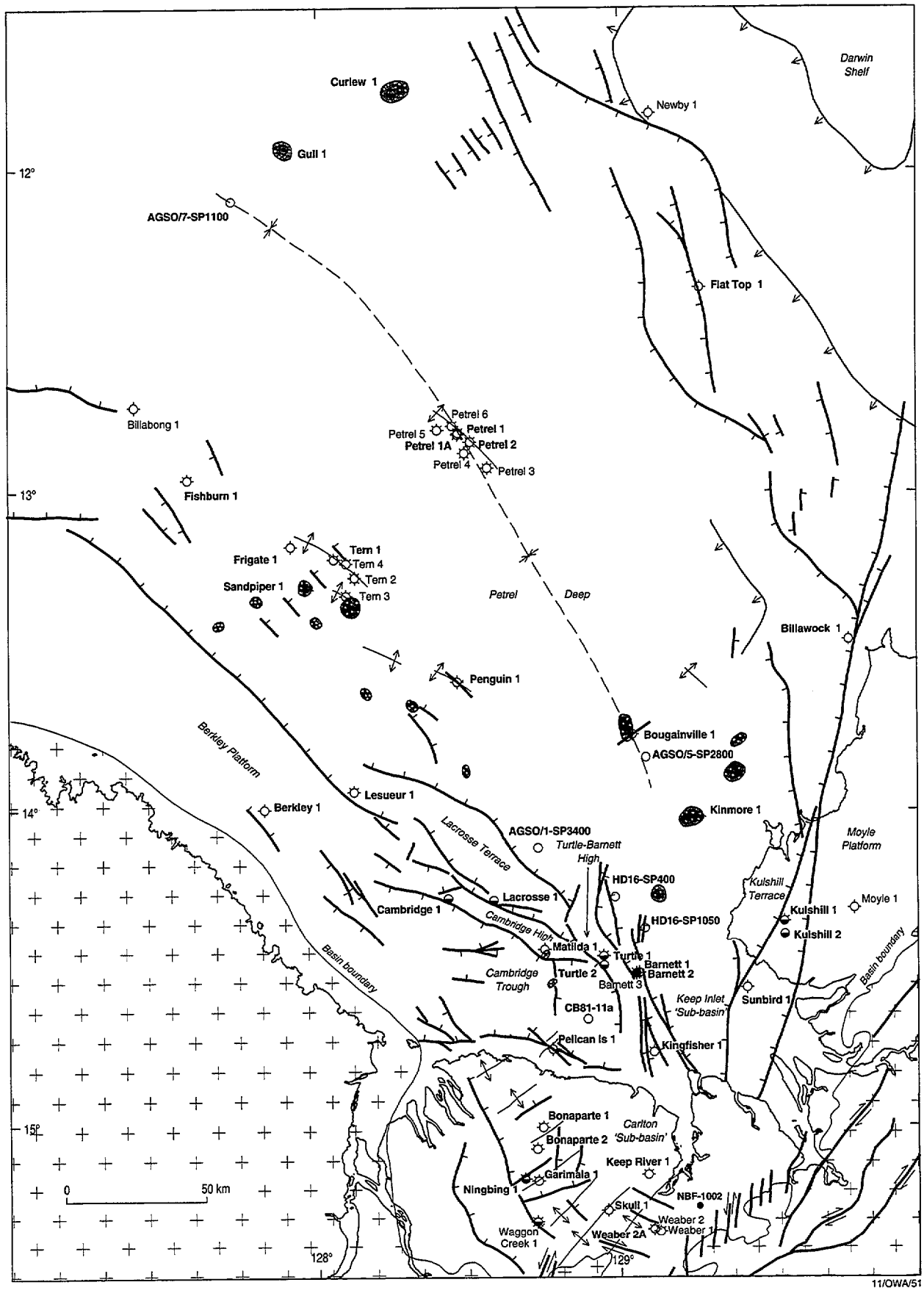

Figure 1. Location of wells and pseudo-well sites used in this study.

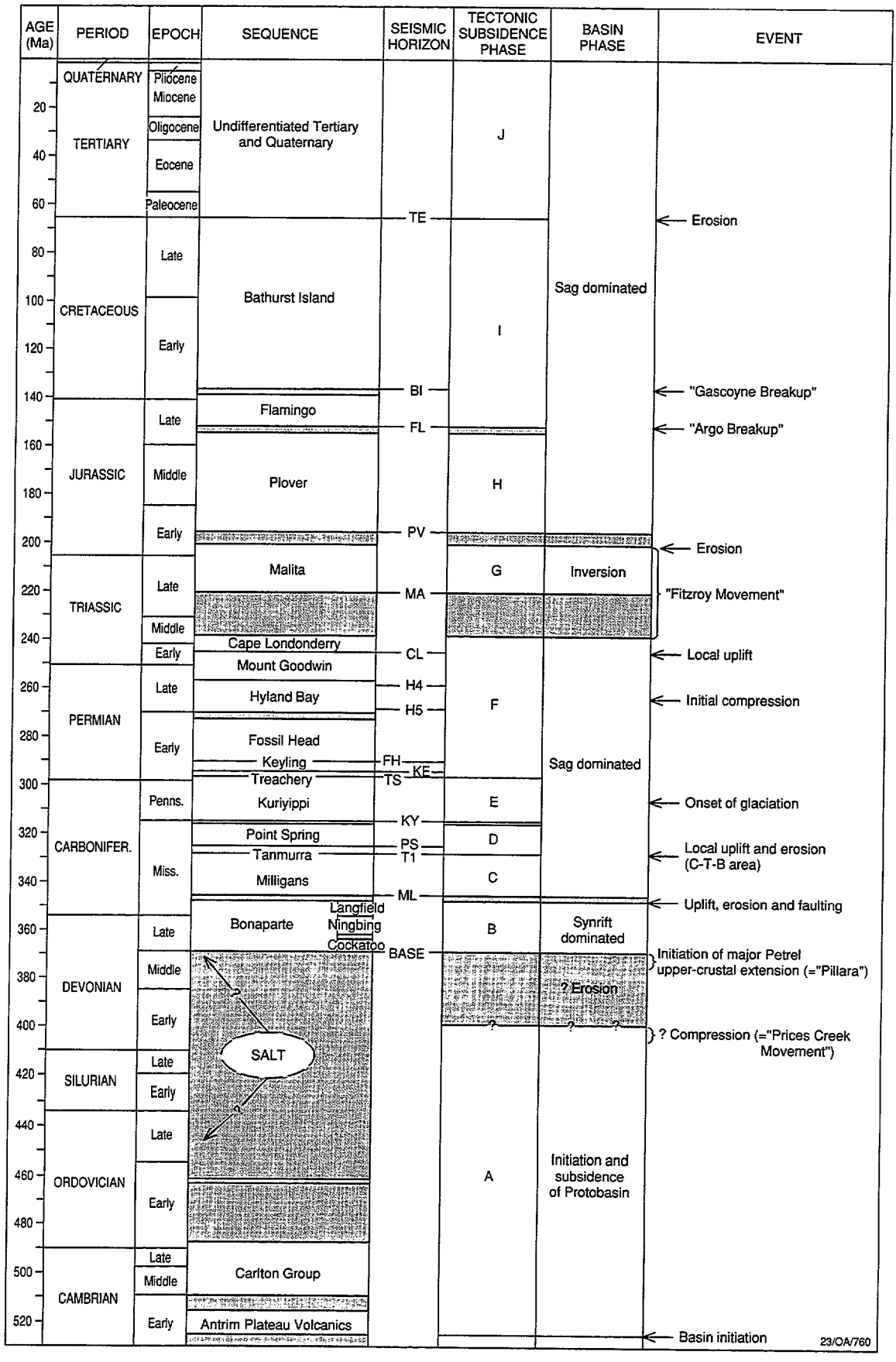

Figure 2. Stratigraphy of the Petrel Sub-basin, showing tectonic subsidence cycles and major tectonic events.

Data Input

Specific aspects of critical data input are discussed below.

Global Lookup Paths/Tables

Chronostratigraphy: Chronostratigraphic ages of sequences are based on the AGSO Petrel Sub-basin Stratigraphic Time Chart (Jones et al, 1996) and are summarised in Appendix B.
Sea Level: The AGSO 1995 long term sea-level curve has been used for the Mesozoic. A Palaeozoic sea-level curve has not been entered since the available Exxon-derived curve (Greenlee & Lehmann, 1993) has not yet been calibrated with the AGSO Timescale at other than Period level. Palaeozoic sea-level is thus assumed to be constant at the present day level.
Maturity Conversion: Thermal Alteration Index (TAI) and Spore Colour Index (SCI) values have been converted to equivalent vitrinite reflectance values using an in-house correlation of maturation indices (C. Foster, AGSO, unpubl., March 1996). Tmax values (from Rock-Eval pyrolysis) have been converted to equivalent vitrinite reflectance values using the WinBury maturity conversion files. Conodont Colour Alteration Index (CAI) values have been converted to equivalent vitrinite reflectance values following Epstein et al. (1977, fig. 11).
Lithology Definitions: The default WinBury Lithologic Parameter File, which defines the compaction rate constants, matrix conductivity and density values, was used.
Kinetic Definitions: Kinetic data for all modelled source rock units were defined by kerogen kinetic analyses (see Appendix C).
Options: All data were converted to the following standard units: Depth-metres, Heatflow-milliwatts, Temperature-centigrade.
Heat Flow Mode - Relative to present day value.
Processing Option - Sweeney (easy Ro).

Well Header Data

Present Surface Temperature: 27°C was used for all wells based on temperature measurements made in the region during water-column gas sampling "sniffer" surveys (Bishop et al., 1992; Bickford et al., 1992) and an Ocean-Bottom Seismometer survey (pers. comm., Chao Shing Lee, AGSO, March 1996).
Bottom Hole Temperature: Corrected bottom hole temperatures (based on Horner plots) have been used where available (e.g., well completion reports), or calculated using the Horner plot facility within WinBury. In those wells where there was insufficient temperature and/or circulation time data to construct Horner plots, the maximum measured log temperature plus up to 10% (depending on time since circulation, and available drill-stem/formation test temperature data) has been used. In the event that reliable bottom-hole, log or drill-stem/formation test temperatures were not available, temperature data were estimated from adjacent wells (within the same structural element and with comparable stratigraphic successions) such that the calculated present-day heatflows of comparable wells are similar. The stabilised bottom hole temperatures entered for each well are shown in Table 2.
Basement Depth: Interpreted from seismic data if below TD (see Map and Seismic Folio, Colwell et al., 1996).

Horizon Data

Stratigraphic Unit, Depth to top of Unit: Based on sequences and sequence boundaries as shown on composite well logs (see Well Folio, Kennard, 1996).
Age: Ages of sequences based on AGSO Petrel Sub-basin Time Chart (Jones et al., 1996).

Hiatuses/Unconformities: Estimations of the thickness, lithology and age of eroded sections and hiatuses were based on understandings gained from regional seismic stratigraphic interpretations and well-well cross-sections. For this purpose, hiatuses and unconformities were initially assessed for wells within a common structural province, and were modified where necessary to achieve the best match between modelled and observed maturity data.

Min/Max Modelled Water Depth: Estimates of palaeo-water depth at top of sequences based on lithofacies, palaeoenvironmental interpretations, and sequence stratigraphic concepts.

Palaeo Sea Bed Temperature: Estimated from lithofacies, palaeoclimate and palaeo-latitude position of Petrel Sub-basin (see Appendix B).

Heatflow: WinBury calculates present-day heatflows from observed/estimated stabilised bottom-hole temperatures, the thermal conductivity of the well lithologies, and the present-day surface temperature. Palaeo-heatflows were modelled by a combination of two approaches; uniformitarian and graphical. In the uniformitarian approach, present-day heatflows for specific tectonic settings (e.g., rifts, post-rift passive margins) were used to guide estimates of heatflows for sequences deposited in similar tectonic settings. In the graphical approach, theoretical heatflow curves in basins formed by differing amounts of crustal extension were used as a guide to model palaeo-heatflow in individual wells and groups of comparable wells. Based on the present-day heatflow, palaeo-tectonic setting and tectonic subsidence curve for each well, an appropriate "bell-shaped" cool-down curve was modelled for each well. This palaeo-heatflow model was validated, and re-modelled as necessary, against observed maturity data (see "Palaeo-Heatflow" section for more details).

Lithology Data: Lithological data was based on well completion reports and composite well logs. It is important to note that the default Lithological Parameter file is based on pure end-member 'matrix lithologies'. Thus a 'sandstone' is a pure quartz arenite with a density of 2.65 gm/cc, conductivity of 16 mcal/cm sec °C, initial porosity of 40 %, and a porosity/depth factor of 0.40. A specific sandstone with a variety of framework grain types, and minor interstitial argillaceous material (inter-framework matrix) should be entered as sandstone-shale mixture (eg., sandstone 80 %, shale 20 %); similarly a calcareous siltstone with silt-sized quartz grains and interstitial calcareous and argillaceous material must be entered as a sandstone-shale-limestone mixture. It was found that the gamma log can generally be used as a guide to determine the proportion of 'matrix lithologies'.

Kerogen Data: Kerogen kinetic data for all modelled source beds are given in Appendix C.

Variable Beds: Halokinetic movements, such as salt diapirs, have not been modelled. Wells drilled on and adjacent to salt diapirs have not been modelled.

Observed Maturity Data

Observed maturity data are used to calibrate the well models by constraining the maturity profile predicted by the model. Six maturity parameters have been used: Vitrinite reflectance, Fluorescence Alteration of Multiple Macerals, Thermal Alteration Index, Spore Colour Index, Tmax (from Rock-Eval pyrolysis) and Conodont Colour Alteration Index. These data were obtained from the compilation presented by Edwards & Summons (1996).

Observed Temperature Data

Maximum recorded log temperatures, drill-stem/formation test temperature data and stabilised bottom hole temperatures (based on Horner plots) have been used. The source of temperature data is identified in an associated flag table.

Observed Porosity and Thermal Conductivity Data

Porosity and thermal conductivity data were not entered for any wells; the WinBury program uses default values for these parameters based on lithological data.

Fluid Inclusion and Fission Track Data

Fluid inclusion and fission track data were not available for any of the wells studied.

Data Output

For each well and pseudo-well the following plots are presented **(see Appendix B):**

- Observed versus Computed Maturity Plot
- Heatflow and Tectonic Subsidence Plot
- Geohistory plot

Bed Maturity Plots, Bed Maturity Maps and Hydrocarbon Generation Plots for each source rock unit are presented as separate text figures.

Well Name	Bottom Hole Temperature °C	Depth m
Barnett-2	102	2811
Berkley-1	56	874
Billawock-1	78	1734
Bonaparte-1	115	3050
Bonaparte-2	98	2136
Cambridge-1	86	2224
Fishburn-1	122.5	2865
Flat Top-1	108	2173
Garimala-1	127	2553
Keep River-1	190	4760
Kingfisher- 1	110	3253
Kulshill-1	155	4394
Lacrosse-1	105	3054
Lesueur-1	116.5	3590
Penguin-1	107	2754
Petrel-2	164	4760
Sunbird-1	117.5	3400
Tern-1	154	4352
Turtle-2	97	2760

Table 2. Stabilised bottom hole temperatures of wells modelled in this study.

Subsidence History

Tectonic subsidence models indicate that the Petrel Sub-basin has undergone a complex, multi-phase, tectonic history (Fig. 3). Nine distinct subsidence phases are evident in most wells/pseudo-wells (Phases B to J), although Phase E is evident only in the outer portion of the basin (e.g., Petrel-1A, 2, Fishburn-1, Tern-1 and Penguin-1). Several of these phases are characterised by an initial rapid subsidence (or local uplift) stage, followed by a more prolonged stage of waning subsidence, a pattern consistent with extension and subsequent thermal sag (McKenzie, 1978). Some of these extension-sag cycles were interrupted by subsequent events, such that the initial rapid mechanical subsidence stage of a new extensional-sag cycle has been superimposed on, and thereby masks, the slow thermal subsidence stage of the preceding phase.

Total tectonic subsidence ranges from 7-9 km for wells in the outer and central Petrel Deep (Petrel-1A, 2, pseudo-well site ASGO Line 7-sp1100), to about 5 km in the inner Petrel Deep (Fishburn-1, Tern-1, Penguin-1), about 2-3 km in the Carlton Sub-basin, Cambridge Trough, Keep Inlet Sub-basin, Kulshill and Lacrosse Terraces, and less than 2 km on the Turtle-Barnett and Cambridge Highs and Eastern Ramp margin. Given that the maximum thermal subsidence of the present ocean basins is about 6 km, a single rift event and subsequent thermal sag cannot explain the observed amount of tectonic subsidence in the Petrel Sub-basin. A full discussion of other possible subsidence mechanisms is presented by Baxter (1996).

Phase A: Cambrian-?Silurian

An initial, "pre-rift" Cambrian-?Silurian tectonic phase is thought to represent initial subsidence of the basin following extension and extrusion of tholeiitic basalts of the Antrim Plateau Volcanics in the Early Cambrian. However, these sediments have not been intersected in exploration wells, and the subsidence pattern during this phase has not been modelled in this study. This phase was terminated by gentle folding, regional uplift and erosion prior to initiation of the Late Devonian Petrel Rift.

Phase B: Frasnian - mid Tournaisian

This phase is characterised by rapid subsidence following the initiation of the Petrel Rift at the end of the Givetian. More detailed characterisation of this phase is only possible in wells in the onshore Carlton Sub-basin, and to a lesser extent Kulshill-1, where tectonic subsidence curves indicate very rapid initial subsidence during deposition of the Cockatoo Supersequence, and decreasing subsidence rates during deposition of the Ningbing and Langfield Supersequences (Fig. 3). Seismic data show clear evidence of large growth faults and rotated fault blocks during this phase (see AGSO Lines 100/1, 2 & 3, Seismic and Map Folio, enclosures 1-3). Similarly, the thickening of coarse clastic facies of the Cockatoo Supersequence against the eastern fault margin of the Carlton Sub-basin (Mory & Beere, 1988, fig. 52) indicates active fault movement at the beginning of this phase. Up to 2.5 km of tectonic subsidence occurred during this phase which appears to have affected all areas of the Petrel Sub-basin.

This "syn-rift" extensional phase was terminated by widespread uplift and erosion in the mid Tournaisian, especially across the Cambridge and Turtle-Barnett Highs. Although the amount

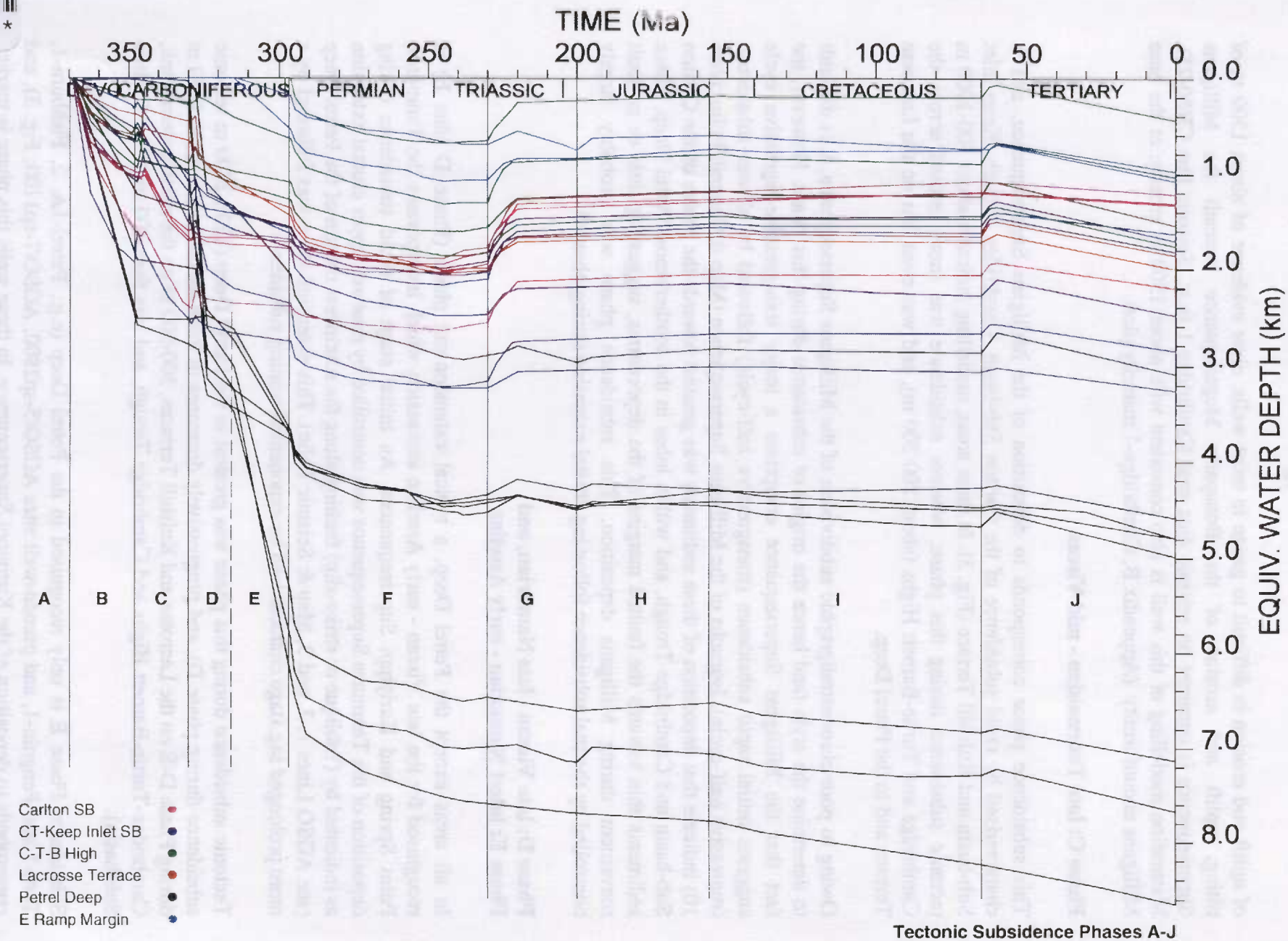

Figure 3. Tectonic subsidence curves for all wells/pseudo-wells modelled in the Petrel Sub-basin, showing tectonic subsidence Phases A-J. SB = Sub-basin; CT = Cambridge Trough; C-T-B High = Cambridge & Turtle-Barnett Highs. Kulshill-1 included in Keep Inlet SB.

of uplift and erosion is difficult to gauge in most wells, clear evidence of about 1500 m of tilting, uplift and erosion of the Bonaparte Megasequence beneath the Milligans Supersequence is apparent on seismic data near Cambridge-1 (e.g., Seismic line CB80-25). Maturation modelling of this well is also consistent with about 1500 m erosion at the base Milligans unconformity (Appendix B, Cambridge-1 maturity plot).

Phase C: late Tournaisian - mid Visean

This subsidence phase corresponds to deposition of the Milligans Supersequence, and is characterised by rapid subsidence of the Carlton Sub-basin, Cambridge Trough, Keep Inlet Sub-basin and Kulshill Terrace (Fig. 3). In these areas, modelling indicates about 500-1000 m tectonic subsidence during this phase, whereas subsidence was more limited across the Cambridge and Turtle-Barnett Highs (about 200-300 m), and was even less on the Lacrosse Terrace and in the Petrel Deep.

Owing to poor chronostratigraphic subdivision of the Milligans Supersequence, it is difficult to determine the style (and hence the origin) of subsidence during this phase. However, the fact that the Milligans Supersequence comprises a major transgressive-regressive cycle suggests initial rapid subsidence (transgressive half-cycle) followed by slower subsidence (regressive half-cycle). Isopachs of the Milligans Supersequence (Map & Seismic Folio, plate 10) indicate that deposition of these sediments was greatest towards the centre of the Carlton Sub-basin and Cambridge Trough, and within lobes in the southernmost Petrel Deep. These sediments thin towards the faulted margins of the depocentres, suggesting little or no fault movement during Milligans deposition. This subsidence phase was probably largely controlled by thermal subsidence following crustal extension during phase B.

Phase D: late Visean - late Namurian, and
Phase E: latest Namurian - early Asselian

In all areas except the Petrel Deep, a typical extension-sag phase (Phase D plus E) is recognised for the late Visean - early Asselian succession which incorporates the Tanmurra, Point Spring and Kuriyippi Supersequences. An initial stage of rapid subsidence during deposition of the Tanmurra Supersequence was controlled by renewed upper crustal extension as indicated by (?oblique or strike-slip) faulting along the southwest margin of the Petrel Deep (see AGSO Lines 1, 2, and 3, Map & Seismic Folio). This extension stage was followed by a more prolonged sag stage characterised by exponential waning subsidence.

Tectonic subsidence during this phase was greatest in the Petrel Deep (1200-2400 m tectonic subsidence during phase D), and progressively decreases in more inboard areas (800-1000 m during Phase D-E on the Lacrosse and Kulshill Terraces, 300-500 m on the northeastern flank, Cambridge-Turtle-Barnett Highs and Cambridge Trough, and less than 200 m in the Carlton Sub-basin).

Subsidence Phase E is only recognised in the Petrel Deep (e.g., Petrel-1A, 2, Fishburn-1, Tern-1 and Penguin-1, and pseudo-well sites AGSO/5-sp2800, AGSO/7-sp1100; Fig. 3), and corresponds to deposition of the Kuriyippi Supersequence. In these wells this phase is marked by a rapid increase in tectonic subsidence, especially in more outboard positions (e.g., Petrel-1A, 2, and pseudo-well site AGSO/7-sp1100). This phase may be controlled by Late Carboniferous (latest Namurian) NW-SE extension in the Malita Graben which may signal the initiation of the Westralian Superbasin (Etheridge & O'Brien, 1994). Flexural isostatic

modelling indicates that NW-SE extension centred on an inferred major NE-SW fault in the vicinity of Gull-1 may have controlled the rapid increase in subsidence in the Petrel Deep during this phase (Baxter, 1996; see Colwell & Kennard, 1996, chapter 5), but any such fault is poorly imaged on existing deep seismic data. Mory & Beere (1988) also recognised local active faulting in the onshore portion of the basin at this time, based on the recognition of fan-delta facies within outcrops of the Keep Inlet Formation adjacent to uplifted fault blocks.

Phase F: late Asselian - Anisian

This phase incorporates the Treachery, Keyling, Fossil Head - Hyland Bay and Mt Goodwin - Cape Londonderry Supersequences. It is characterised by rapid early subsidence during deposition of the Treachery Sequence, followed by a relatively prolonged stage (about 50 Ma.) of waning subsidence (Fig. 3). Tectonic subsidence during this phase ranges from 800-1200 m in the Petrel Deep, decreasing to about 400-800 m in more inboard areas. In the Carlton Sub-basin, virtually all of the sediments deposited during this phase were subsequently stripped during the Fitzroy Movement, but modelling of maturation profiles for wells in this area suggest about 200 m tectonic subsidence during this phase.

Tectonic subsidence decreases to zero near the end of this phase, and many wells show minor uplift (less than 100 m) at the end of this phase. This apparent uplift probably indicates the first pulses of the Fitzroy Movement, but since much of the younger sediments of this phase were subsequently stripped during the Fitzroy Movement, the thickness of these eroded sediments may have been underestimated (the modelled thicknesses of eroded sediments are based on the minimal amount required to match observed maturity profiles).

The rapid and then waning subsidence pattern of this phase is consistent with renewed extension and subsequent thermal sag, but there is no clear seismic evidence of significant upper crustal fault movement during this phase. Extension during this phase may thus have been partitioned within the lower crust beneath the Petrel Sub-basin.

This phase of tectonic subsidence was terminated by uplift and erosion associated with the Fitzroy Movement, the peak of which occurred during the late Middle Triassic (Ladinian).

Phase G: Ladinian-Sinemurian (Fitzroy Movement and basin inversion)

This phase incorporates uplift and erosion during the Fitzroy Movement, and deposition of the "syn-tectonic" Malita Supersequence (Fig. 3). This compressive movement affected all areas of the Petrel Sub-basin, and a substantial thickness of Permian and Early Triassic sediment was eroded from the southern and southwestern flanks of the sub-basin at this time (Fig. 4; 400-800 m on the Berkley Platform, Cambridge and Turtle-Barnett Highs, Cambridge Trough and Keep Inlet Sub-basin, and about 1000 m on the western flank of the Carlton Sub-basin). Large-scale inversion anticlines developed within the Petrel Deep at this time, and form traps for the Petrel and Tern Gas Fields.

Phase H: Sinemurian-Oxfordian

This phase of minimal net tectonic subsidence incorporates the Plover Supersequence, and appears to be uniformly expressed throughout all provinces of the Petrel Sub-basin (Fig. 3).

Phase I: late Oxfordian-Maastrichtian

This phase incorporates the Flamingo and Bathurst Island Supersequences, and is characterised by a moderate net increase in tectonic subsidence during the late Oxfordian to late Berriasian, followed by net minimal subsidence throughout the remainder of the Cretaceous (generally less than 100 m total net tectonic subsidence; Fig. 3). Detailed analysis of the subsidence history during this phase was not attempted during this study. Nevertheless, sequence stratigraphic concepts suggest two distinct pulses of rapid subsidence: the first in the late Oxfordian-Kimmeridgian corresponding to widespread transgression at the base of the Frigate Shale, and the second in the Valanginian corresponding to widespread transgression at the base of the very condensed Darwin Shale section. These pulses are correlated with the Argo and Gascoyne break-up events. This phase was terminated by regional uplift and channel incision at the base of the Tertiary Supersequence (e.g., ASGO Line 5, Map & Seismic Folio).

Phase J: Tertiary

The pattern of subsidence during this phase is not known due to inadequate chronostratigraphic subdivision of Tertiary strata in the basin. About 100-200 m tectonic subsidence occurred in all areas during this phase (Fig. 3).

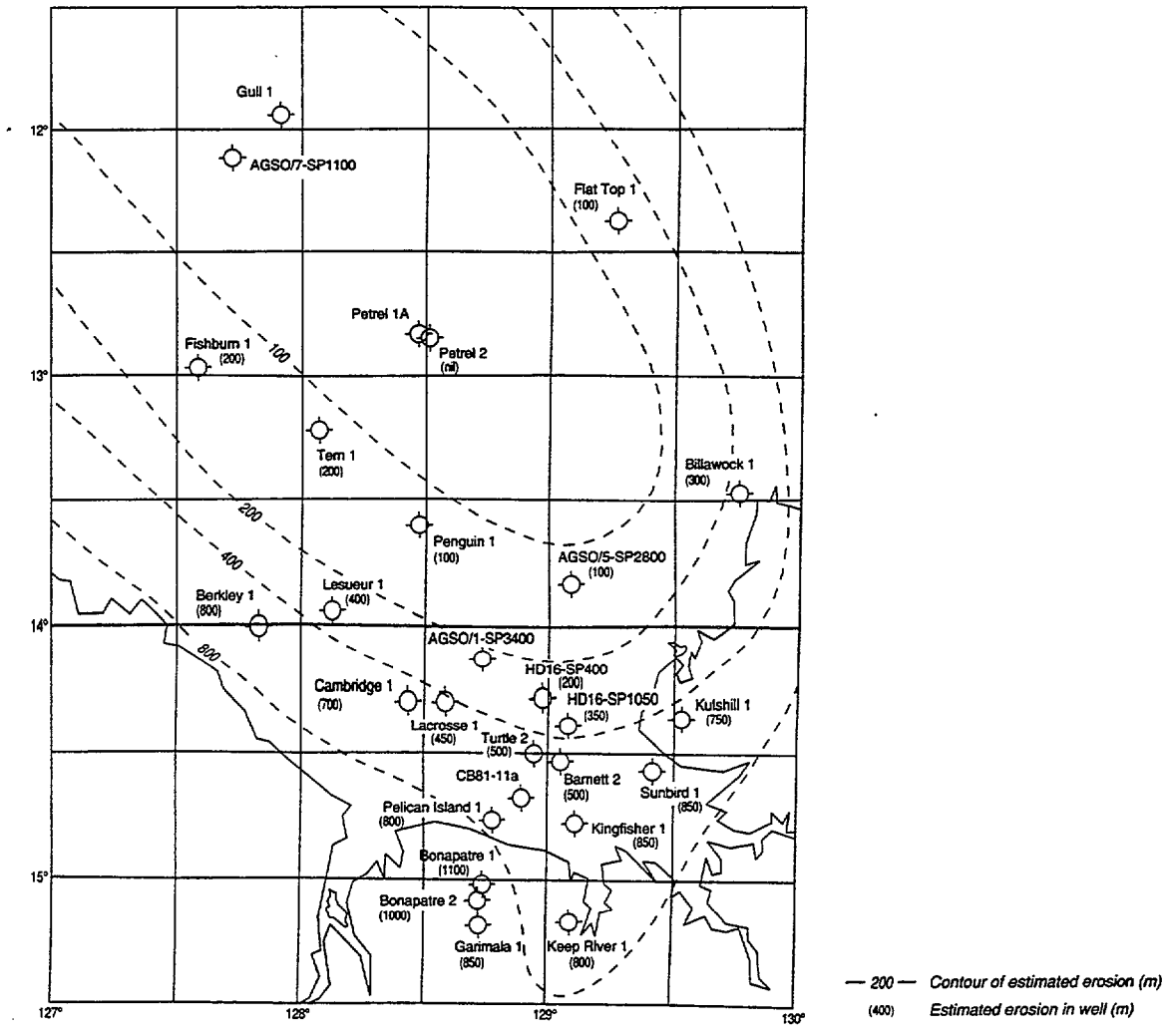

Figure 4. Estimated amount of erosion of Permian - Early Triassic sediments during the Fitzroy Movement. Estimates based on minimal amount of eroded section required to model observed maturity profiles in each well.

Thermal History

Two critical factors in modelling the thermal history of the wells are:

- the assessment and selection of reliable maturity parameters, and
- the establishment of palaeo-heatflow curves.

Maturity Parameters

Six maturity parameters were used in this study: Vitrinite reflectance (Rv), Fluorescence Alteration of Multiple Macerals (FAMM), Thermal Alteration Index (TAI), Spore Colour Index (SCI), Tmax and Conodont Colour Alteration Index (CAI). These data were obtained from the database compiled by Edwards & Summons (1996).

Plots of observed maturity parameters versus depth for each well (Appendix B) commonly indicate that some parameters are internally inconsistent (that is, they do not show an expected progressive increase in maturity down the well) and highly variable, or that the maturity value of one parameter contradicts that indicated by other parameters. Rv, FAMM, CAI and, to a lesser degree, TAI were generally found to be the most consistent and reliable maturity parameters in the studied wells.

Vitrinite Reflectance: Rv values were generally the most widely available and reliable maturity parameter in the studied wells. Spurious data attributed to measurement of macerals other than vitrinite was excluded (see Edwards & Summons, 1996), but several wells show disparate values which could be attributed to either oxidation (in the laboratory or in nature), oil staining of the organic matter, and contamination by cavings. In some wells, disparate Rv values are clearly attributed to different analytical laboratories (e.g., Keep River-1, Petrel-2). The most consistent Rv data comes from the most recently drilled wells (e.g., confidential data for Kingfisher-1 and Sunbird-1).

Fluorescence Alteration of Multiple Macerals: FAMM data was only available for Bonaparte-2 (analyses by R. Wilkins, CSIRO). This technique was applied to test problems associated with Rv measurements of mixed macerals in the older Carboniferous succession. The data is internally consistent, shows minimal scatter below an equivalent Rv value of 1.2 %, and is consistent with other maturity indicators (Rv, TAI and CAI). On this basis, the FAMM data in this well is considered a very reliable maturity parameter.

Thermal Alteration Index and Spore Colour Index: TAI and SCI values (based on discolouration of organic material) are routinely equated with Rv values, but are somewhat subjective, and are often expressed on a different scale by different workers. In this study, TAI determinations by C. Foster (AGSO) and R. Purcell (Consultant) have been converted to equivalent Rv values using an in-house Correlation Chart of Maturation Indices (C. Foster, AGSO, unpubl., March 1996). These data are internally consistent in all wells, but generally equate to broad ranges of Rv values; thus this parameter is not a sensitive measure of maturation level.

TAI determinations for Penguin-1 and Petrel-2 (PAU Laboratory, France, in Well Completion Report) and SCI data for Flat Top-1, Lacrosse-1, Petrel-2 and Tern-1 (Well Completion Reports) have also been converted to Rv values using this in-house correlation chart of maturation indices. Using this conversion, the SCI data for Lacrosse-1, Petrel-2 and Tern-1

appear to be consistent with measured Rv data, but the converted SCI data in Flat Top-1 are consistently lower than measured Rv data. TAI data for Penguin-1 and Petrel-2 (PAU, France) are evidently based on a different scale to that used by Foster (unpubl., AGSO, March 1996) and cannot be converted to equivalent Rv values using this chart.

Tmax: Tmax, the temperature at which maximum generation of pyrolysate (S_2) occurs, is widely used as an indicator of maturity, and is commonly plotted against the Hydrogen Index (HI) in a standard Van Krevelan diagram (this diagram purports to identify the generic type and origin of the organic matter). This parameter might be expected to systematically increase with depth down a well, however this is seldom the case for the majority of wells studied here. All pyrolysis data were initially screened according to S_2 values and PI index (see Edwards & Summons, 1996), and dubious Tmax values due to possible migrated hydrocarbons have been separately flagged on the well maturity plots (shown as Tmax(?), Appendix B). Regardless of this quality control, Tmax values show considerable variation in most wells, and are thus generally of limited value as a maturity indicator. However, in many wells the upper envelope of the observed Tmax distribution appears to provide a reasonable indication of maturity level (see Maturity Plots for Barnett-2, Berkley-1, Cambridge-1, Kulshill-1 & Tern-1, Appendix B).

Conodont Colour Alteration: Limited CAI data (R. Nicoll, AGSO, unpubl.) is available for four onshore wells (Bonaparte-1, 2, Keep River-1, Kulshill-1). CAI values were converted to equivalent Rv values based on the data presented in Epstein et al. (1977, fig. 11). Although this parameter is semi-qualitative (based on a visual comparison of conodont colour with a standard colour index), it appears to be a reliable measure of maturity in these wells.

Palaeo-Heatflow

The establishment of a palaeo-heatflow curve for each well was an iterative process based initially on present-day heatflows, and successive attempts to match observed and predicted maturity data. It quickly became obvious that elevated palaeo-heatflows were required to achieve a match with observed maturity data, especially for the older Devonian-Carboniferous section.

A present-day heatflow map for the Petrel Sub-basin is presented as Figure 5. The sub-basin has a maximum heatflow of 70-74 mW m^{-2} in the southern Carlton Sub-basin (Garimala-1 and Keep River-1), decreasing to 60-70 mW m^{-2} in the northern Carlton Sub-basin and the SW and NE flank of the offshore portion of the sub-basin, and 50-60 mW m^{-2} in the Petrel Deep.

Modelled palaeo-heatflow curves for all wells/pseudo-wells are presented in Figure 6. A major Late Devonian heating episode has been modelled during the initial development of the Petrel Rift (tectonic subsidence Phase B), together with superimposed heating pulses for subsequent major subsidence events identified on the tectonic subsidence plots (Phases D and F). The peak values of the heating episodes were compared to present-day heatflows in comparable tectonic settings (e.g., rifts, post-rift sag basins), and the shape of the heating and subsequent cool-down curves were modelled from theoretical heatflow curves corresponding to different amounts of crustal extension (see Deighton, 1992; WinBury on-line help plots). Wells within each structural province were assumed to have a similar heatflow history (Fig. 6), and modelled heatflow curves were validated against observed maturity data in each well,

and modified as necessary to achieve a best match between observed and modelled maturity trends.

Initial very high heatflows of 110-140 mW m^{-2} were modelled during the initiation of the Petrel Rift, and subsequent minor heat pulses (additional 5-10 mW m^{-2}) were superimposed on the cool-down curve of that event during subsidence Phases D and F. Although these palaeo-heatflows exceed values typical of modern rift settings (70-110 mW m^{-2}, average 80 mW m^{-2}; Allen & Allen, 1990), and active strike-slip basins (80-120 mW m^{-2} average 100 mW m^{-2}; *ibid.*), these high values were required to match observed maturity levels in the Devonian-Carboniferous section. These elevated palaeo-heatflows may indicate former thermal plumes beneath the Petrel Sub-basin, and much of the extreme total tectonic subsidence experienced by the sub-basin (up to 7-9 km) may have been controlled by subsequent thermal decay of these plumes.

Based on the approach outlined above, a reasonable match was achieved between observed and modelled maturity parameters for all wells (see Appendix B).

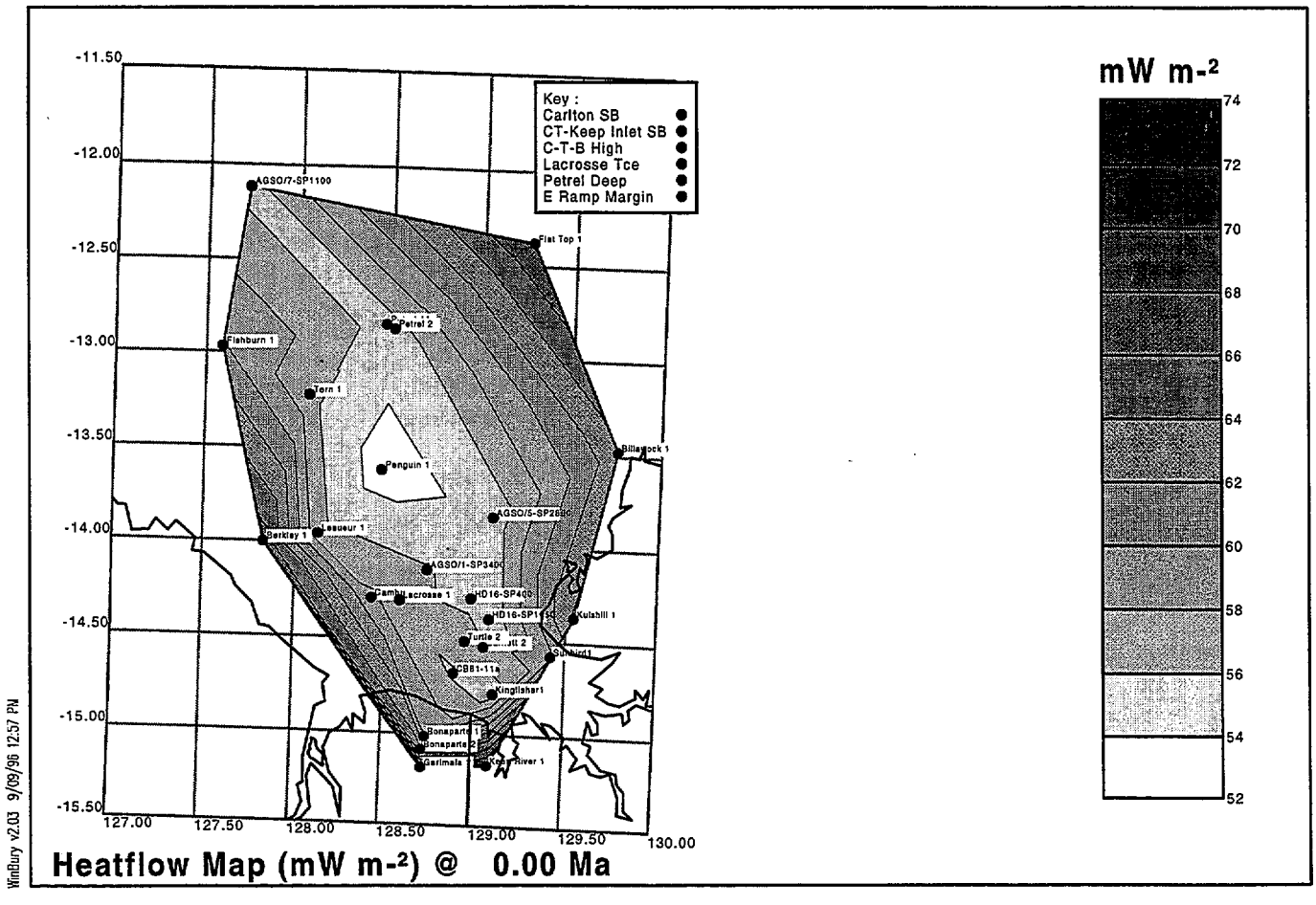

Figure 5. Present-day heatflow map for the Petrel Sub-basin.

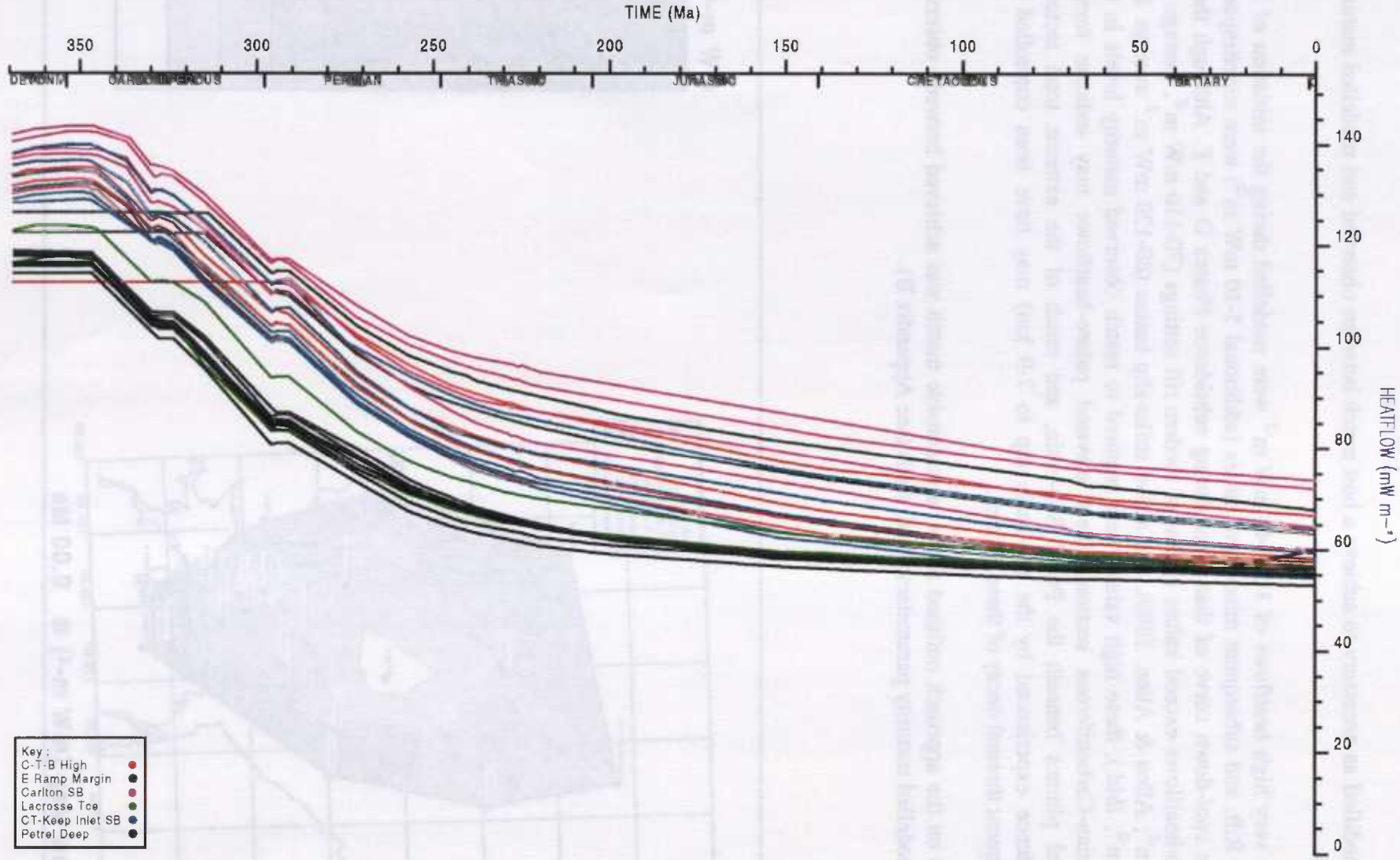

Figure 6. Modelled palaeo-heatflow curves for wells/pseudo-wells.

Source Rock Maturation History

Integration of structural, sequence stratigraphic, biostratigraphic and geochemical data indicates four probable source rock units that underpin three active Petroleum Systems in the Petrel Sub-basin (Colwell & Kennard, 1996; Edwards & Summons, 1996):

- Marine shales and carbonates in the Ningbing reef complex and Bonaparte Formation (Ningbing-Bonaparte Petroleum System)
- Marine shales in the mid Milligans Formation (Milligans Petroleum System)
- Coaly shales throughout the Keyling Formation (Keyling-Hyland Bay Petroleum System)
- Marine shales within the Hyland Bay Formation (Keyling-Hyland Bay Petroleum System)

The nature and quality of these source units are discussed in detail in Edwards & Summons (1996), and the petroleum systems are described in detail in Colwell & Kennard (1996).

MODELLED SOURCE ROCK UNITS			
Well/Pseudo-well	**Mid Milligans**	**Keyling**	**Hyland Bay**
Barnett-2	(Y)	-	-
Berkley-1	-	-	-
Billawock-1	-	Y	-
Bonaparte-1	Y	-	-
Bonaparte-2	Y	-	-
Cambridge-1	-	Y	-
Fishburn-1	-	Y	Y
Flat Top-1	-	Y	Y
Garimala-1	Y	-	
Keep River-1	Y	-	-
Kingfisher- 1	Y	-	-
Kulshill-1	(Y)	-	-
Lacrosse-1	(Y)	-	-
Lesueur-1	-	Y	Y
Penguin-1	-	Y	Y
Petrel-1A	-	-	-
Petrel-2	-	Y	Y
Sunbird-1	Y	-	-
Tern-1	-	Y	Y
Turtle-2	(Y)	-	-
AGSO/1-SP3400	Y	Y	-
AGSO/5-SP2800	-	Y	Y
AGSO/7-SP1100	-	Y	Y
CB81-11-SP535	Y	-	-
HD16-SP400	Y	Y	-
HD16-SP1050	Y	-	-

(Y) No effective source rocks

Table 3. Wells/pseudo-wells with modelled source rock units.

Although several oil and gas shows have been recorded in the Ningbing Limestone and overlying Langfield Group (e.g., Garimala-1, Ningbing-1, Keep River-1 and onshore mineral holes), effective source rocks within the Ningbing-Bonaparte Petroleum System have only been intersected in Spirit Hill-1 where they have limited dry gas potential (Edwards & Summons, 1996). Maturation modelling of potential source units within this system have not been undertaken since the quality and distribution of potential source units are poorly known, and this system is thought to have only limited hydrocarbon potential.

The mid-Milligans source unit has been modelled in 14 wells/pseudo-wells, the Keyling source unit in 12 wells/pseudo-wells, and the Hyland Bay source unit in 8 wells/pseudo-wells (Table 3). Effective source rocks were identified on the basis of the following parameters (see further discussion in Edwards & Summons, 1996): 1) TOC > 1 %; 2) Hydrogen Index; HI > 300 (oil-prone), 150 < HI < 300 (condensate-prone), HI < 150 gas-prone; and 3) Gamma-log value greater than about 100-125 API.

Mid-Milligans Source Unit

This source unit comprises marine shales of the Milligans Formation. Sequence stratigraphic analysis indicates that the most organic-rich intervals penetrated by petroleum exploration wells (as indicated by TOC and HI values) generally occur in the upper portion of the second-order transgressive systems tract of the Milligans Supersequence (Sequences Milligans A5 and A6; see Well Folio). This organic-rich interval is characterised by high gamma, low sonic log values, and is about 200-250 m thick. Well and seismic data suggest that this source unit extends throughout the Carlton Sub-basin, Cambridge Trough, Keep Inlet Sub-basin and the Milligans depocentre north of the Turtle-Barnett High (Fig. 7). In the Cambridge Trough, this source unit represents a condensed transgressive section beneath prominent progradational highstand clinoforms that are sourced from the south-southwest.

Rock-Eval pyrolysis data, maceral analyses and palynological evaluation of kerogen (Edwards & Summons, 1996) indicate that shales within the Milligans Supersequence generally comprise mixed marine and land-derived organic matter and are largely gas-prone. However, samples of immature, oil-prone, marine ?algal-rich shales have been intersected in mineral hole NBF1002, and carbon isotopic and biomarker data suggest that oils recovered at Waggon Creek-1, Turtle-1 and 2 and Barnett-1 and 2 were sourced from similar source rocks (Edwards & Summons, 1996). Maturation modelling of the mid-Milligans source interval is thus based on kerogen kinetic analysis of the marine ?algal-rich shale in mineral hole NBF1002 (Sample No. 7925, genetic potential 300 mg/gm TOC). This type of kerogen generates oil and gas over a narrow range of activation energies, generally within the range Rv = 0.7 % to 0.9 % for the modelled wells.

An average TOC of 2 % and effective thickness of 200-250 m was modelled for the mid-Milligans source interval in 14 wells/pseudo-wells (Table 3). Although Barnett-2, Turtle-2, Kulshill-1 and Lacrosse-1 lack effective source rocks within the Milligans Supersequence, they have been included in order to map maturity trends. A modelled age of 336 Ma has been used for the top of this source unit.

The mid-Milligans source unit first entered the oil and gas maturity zone during the Early Carboniferous (Visean), and attained maximum maturity during the Late Permian to Early

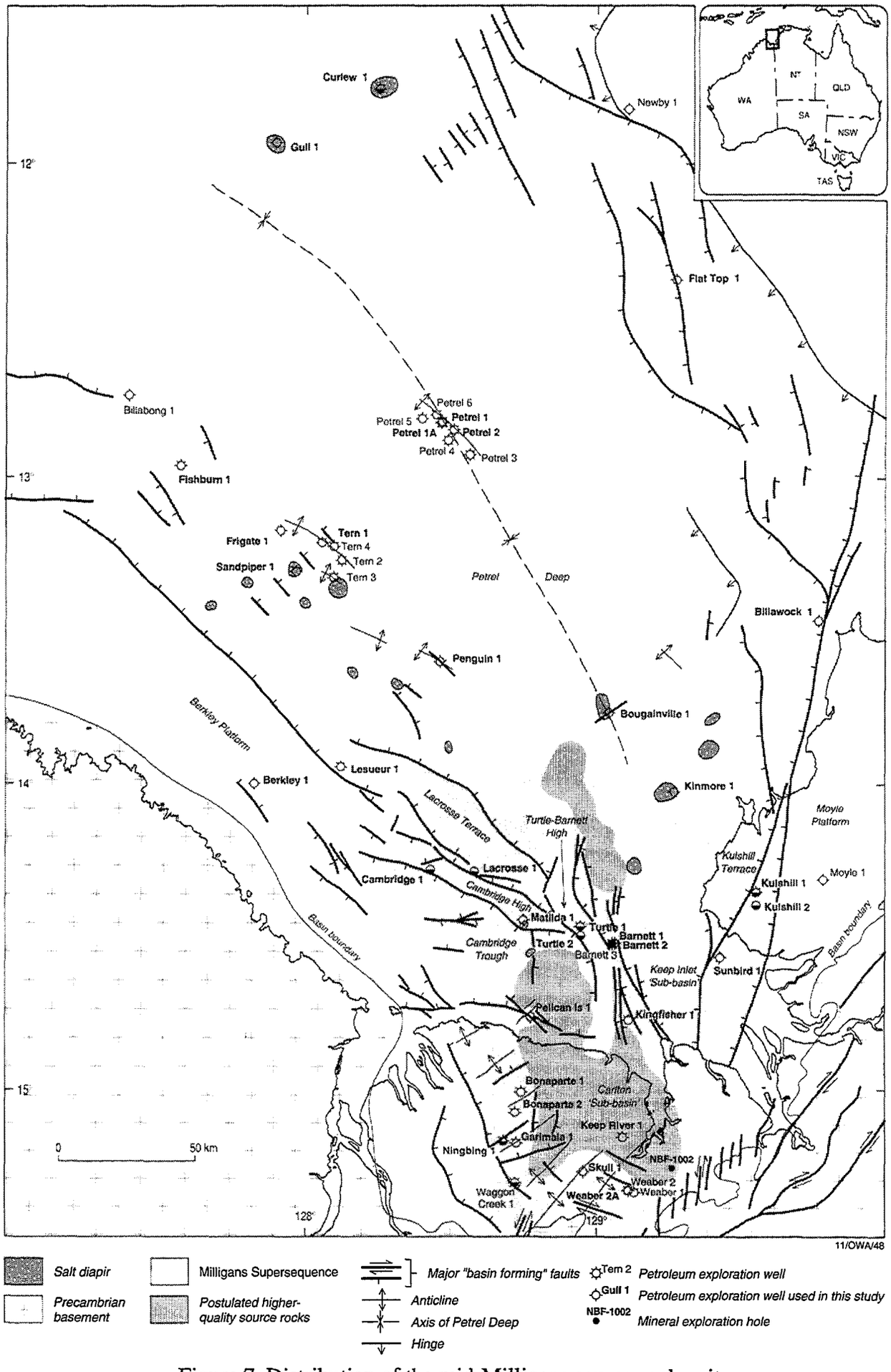

Figure 7. Distribution of the mid-Milligans source rock unit.

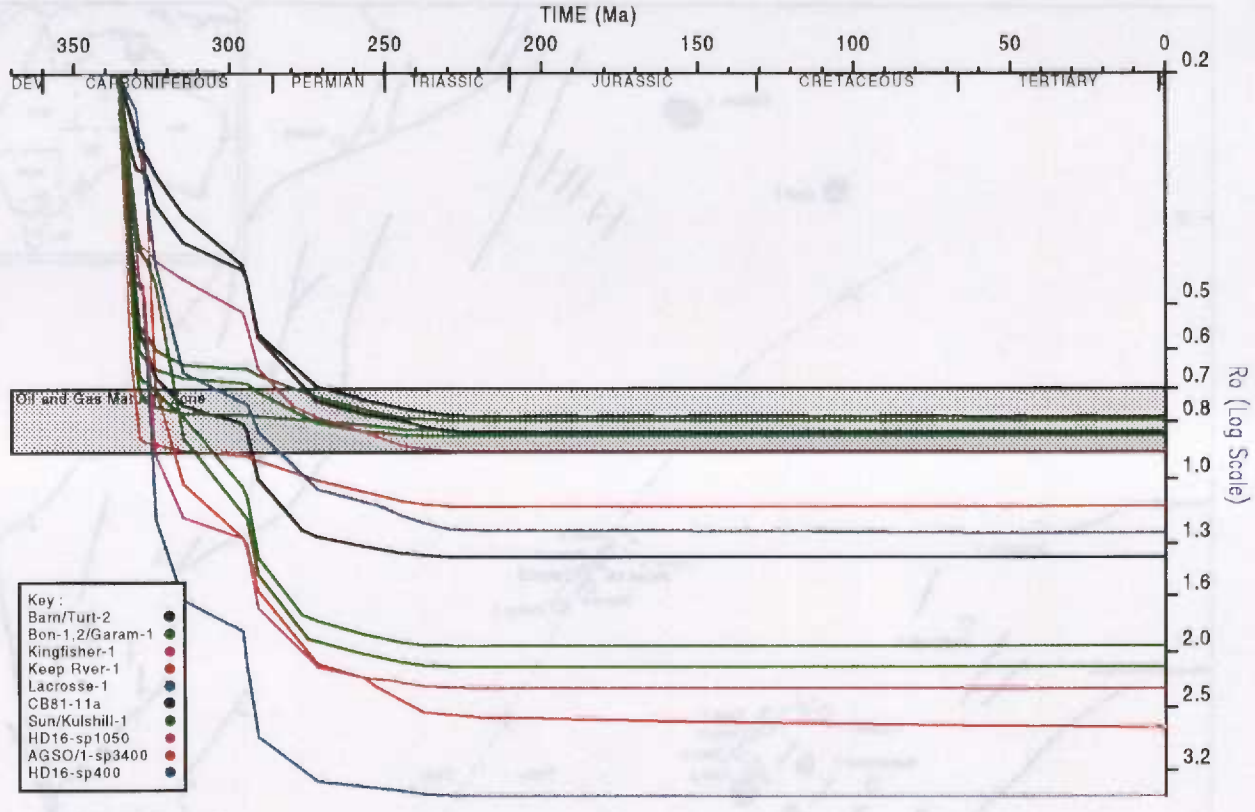

Figure 8. Bed maturity plot for the mid-Milligans source unit in modelled wells/pseudo-wells.

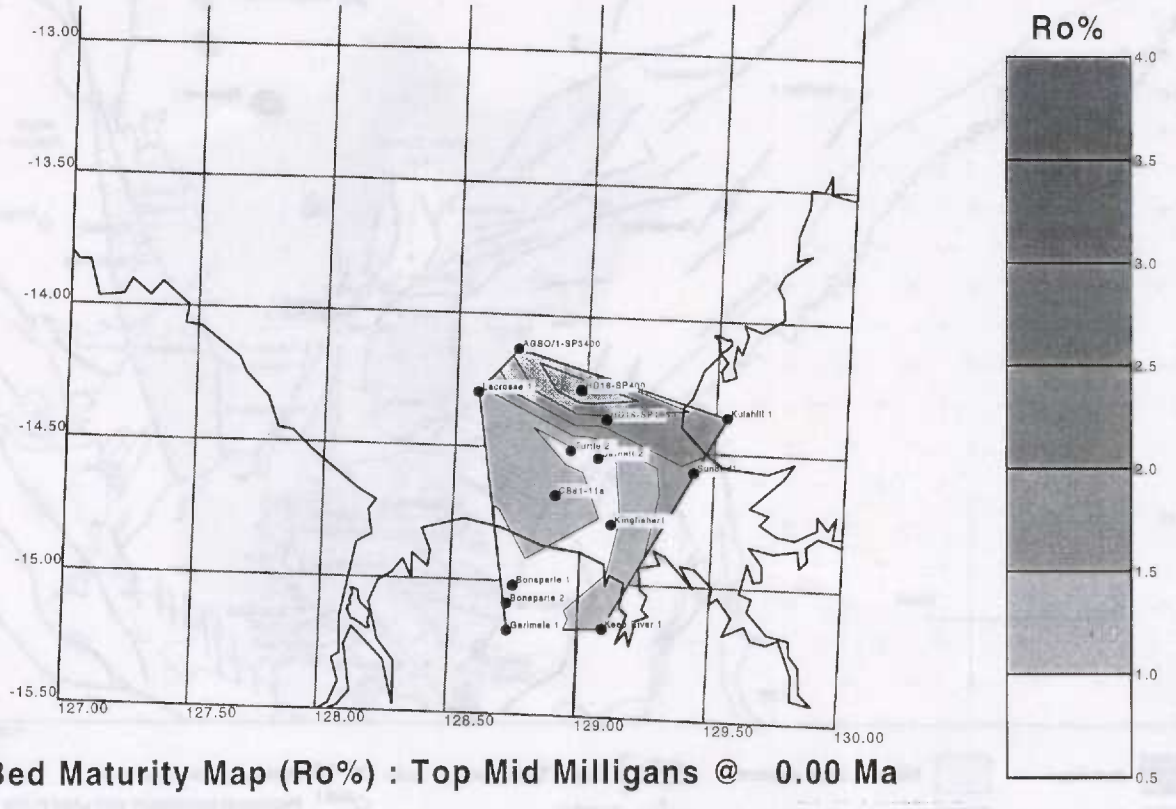

Figure 9. Present-day bed maturity map for the mid-Milligans source unit.

Triassic (subsidence Phase F), prior to uplift and erosion during the Fitzroy Movement (Fig. 8). It is presently in the oil and gas maturity zone in Bonaparte-1 and 2, Garimala-1, Kingfisher-1, Barnett-2 and Turtle-2, and is overmature in all other modelled wells/pseudo-wells (Figs. 8 & 9).

Hydrocarbon generation plots (Fig. 10A-L) suggest that oil and gas was first expelled from the mid-Milligans source unit during the Early Carboniferous (Namurian) from depocentres north of the Turtle-Barnett High (pseudo-wells AGSO/1-sp3400, HD16-sp400, HD16-sp1050), and that expulsion from the Keep Inlet Sub-basin, Cambridge Trough and deeper parts of the Carlton Sub-basin (e.g., Sunbird-1, Kingfisher-1, CB81-11a, Keep River-1) occurred during the Early Permian.

The regional seal for hydrocarbons generated from the mid-Milligans source unit is provided by the Early Permian Treachery Shale, although this seal was locally breached by fault re-activation over the Turtle-Barnett High. The relative timing of hydrocarbon expulsion and emplacement of this regional seal has important consequences for the prospectivity of the Milligans Petroleum System. Figures 11 and 12 indicate that in the depocentres north of the Turtle-Barnett High, the mid Milligans source unit expelled oil and gas during the mid Carboniferous prior to deposition of the Treachery seal, whereas equivalent source rocks in the Cambridge Trough and Keep Inlet Sub-basins expelled oil and gas during the Early Permian, immediately after deposition of this regional seal. This contrasting expulsion history is believed to explain the observed occurrence of composite biodegraded and non-biodegraded oils in Turtle-1 and 2 and Barnett-1 and 2. Jefferies (1988) concluded that these oils formed during two phases of migration, the first being severely biodegraded prior to migration of the second. The present maturation and expulsion models suggest the following scenario:

1. Oil expelled during the Early Carboniferous (Namurian) from source kitchens north of the Turtle-Barnett high was biodegraded as it migrated into shallow Early-Late Carboniferous fluvial/deltaic reservoirs on the Turtle-Barnett High under oxidising conditions.
2. In contrast, oil expelled during the Early Permian from source kitchens south of the Turtle-Barnett High (Cambridge Trough and Keep Inlet Sub-basin) accumulated in now more deeply buried Early-Late Carboniferous reservoirs on the Turtle-Barnett High which were sealed from oxidising groundwaters by the overlying Treachery Shale.
3. Subsequent fault re-activation across the Turtle-Barnett High (probably during the Middle-Late Triassic Fitzroy Movement) resulted in partial breach of the Treachery seal, and a second phase of oxidation and biodegradation of the shallower oil accumulations.

In contrast, any hydrocarbon accumulations within more deeply-buried stratigraphic traps to the north or south of the Turtle-Barnett High would not have suffered biodegradation since they were protected from oxidising meteoric groundwaters by intraformational seals. Thus upper slope carbonate mounds identified within the Tanmurra Supersequence north of the Turtle-Barnett High and stratigraphic pinchouts and basin-floor fans identified in the lower Milligans Supersequence in the Cambridge Trough (see Colwell & Kennard, 1996, chapter 7) are considered prospective oil-charged targets.

Oil shows in the recently drilled Waggon Creek-1 well (see Edwards & Summons, 1996, and Colwell & Kennard, 1996, chapter 7) were probably expelled during the Permian from the mid-Milligans source unit in the central Carlton Sub-basin. These oils could source onlapping turbiditic sand pinchouts against the basal Milligans Supersequence boundary on the flanks of the Carlton Sub-basin, as well as underlying reefal plays in the Ningbing Supersequence.

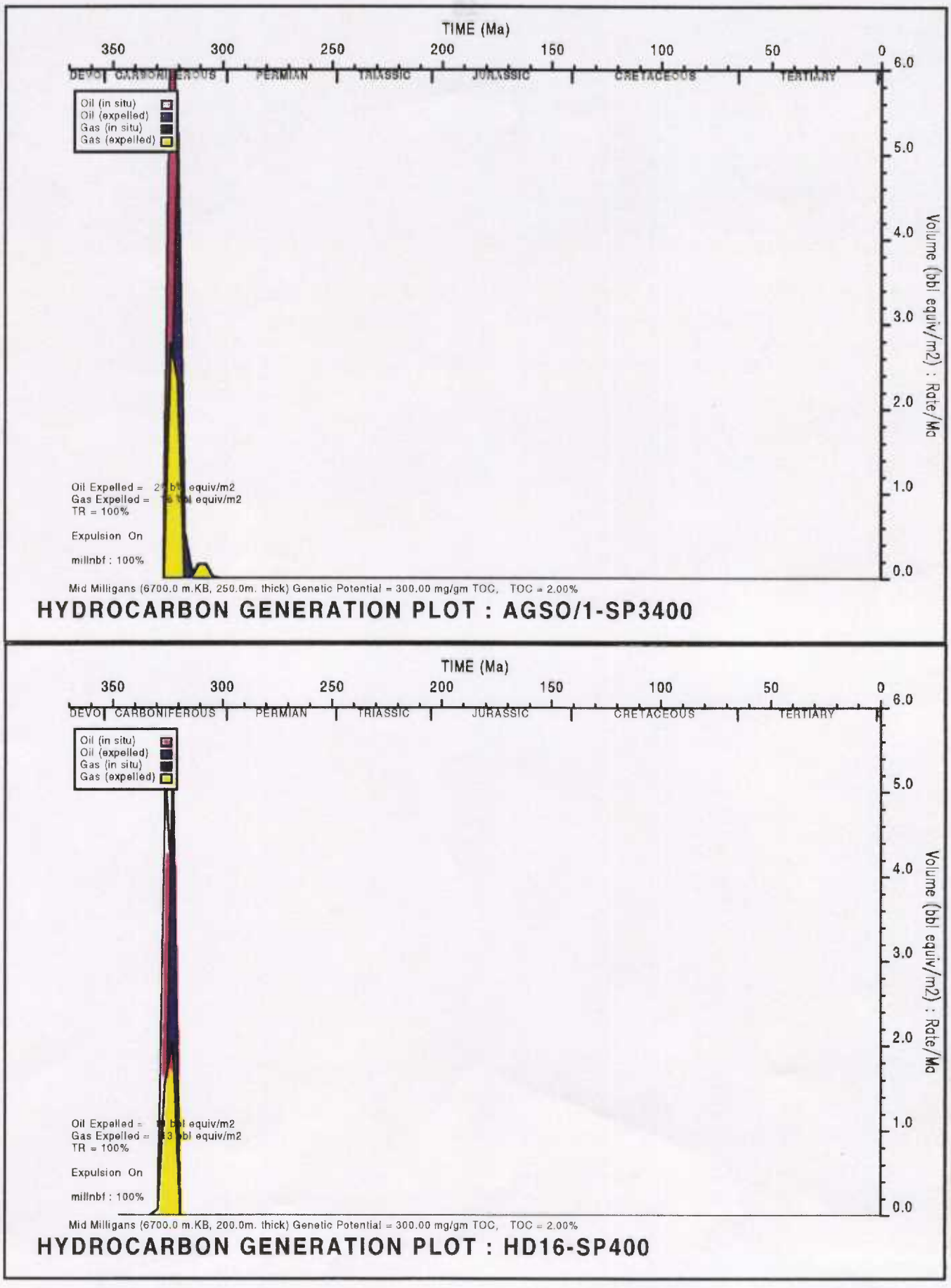

Figure 10 A, B. Hydrocarbon generation plots for the mid-Milligans source unit in: A) Pseudo-well AGSO/1-sp3400, and B) Pseudo-well HD16-sp400.

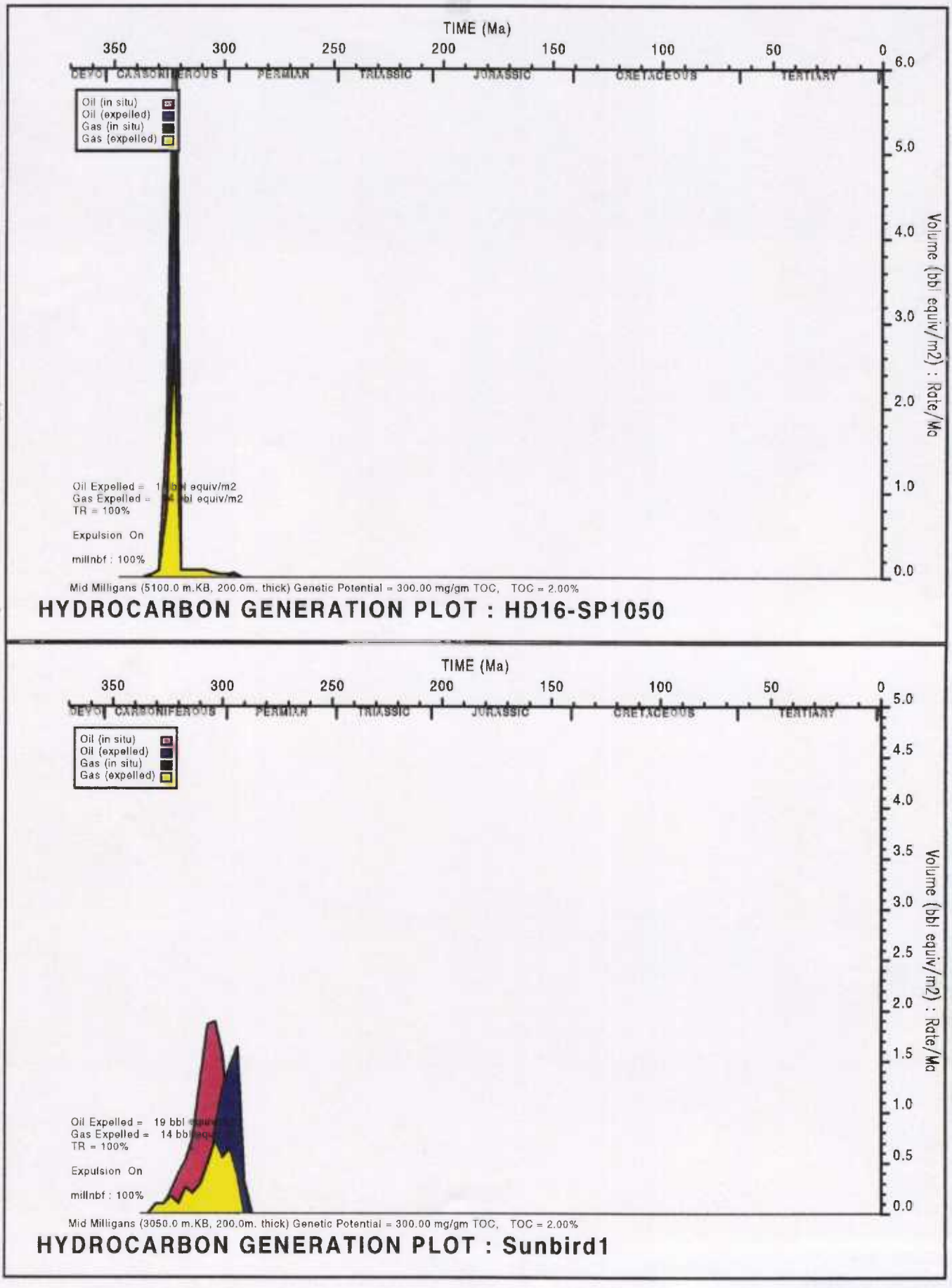

Figure 10 C, D. Hydrocarbon generation plots for the mid-Milligans source unit in: C) Pseudo-well HD16-sp1050, and D) Sunbird-1.

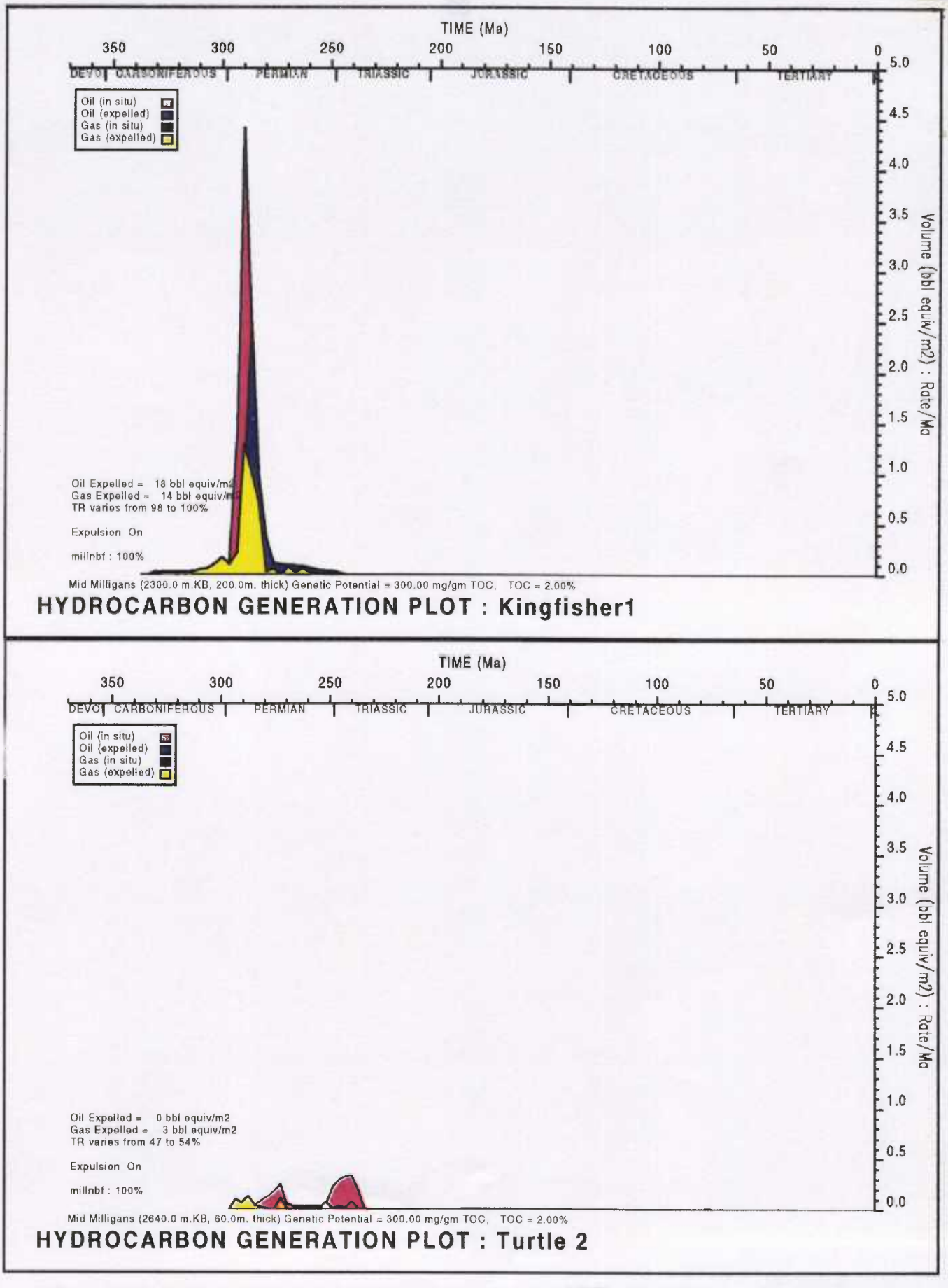

Figure 10 E, F. Hydrocarbon generation plots for the mid-Milligans source unit in: E) Kingfisher-1, and F) Turtle-2.

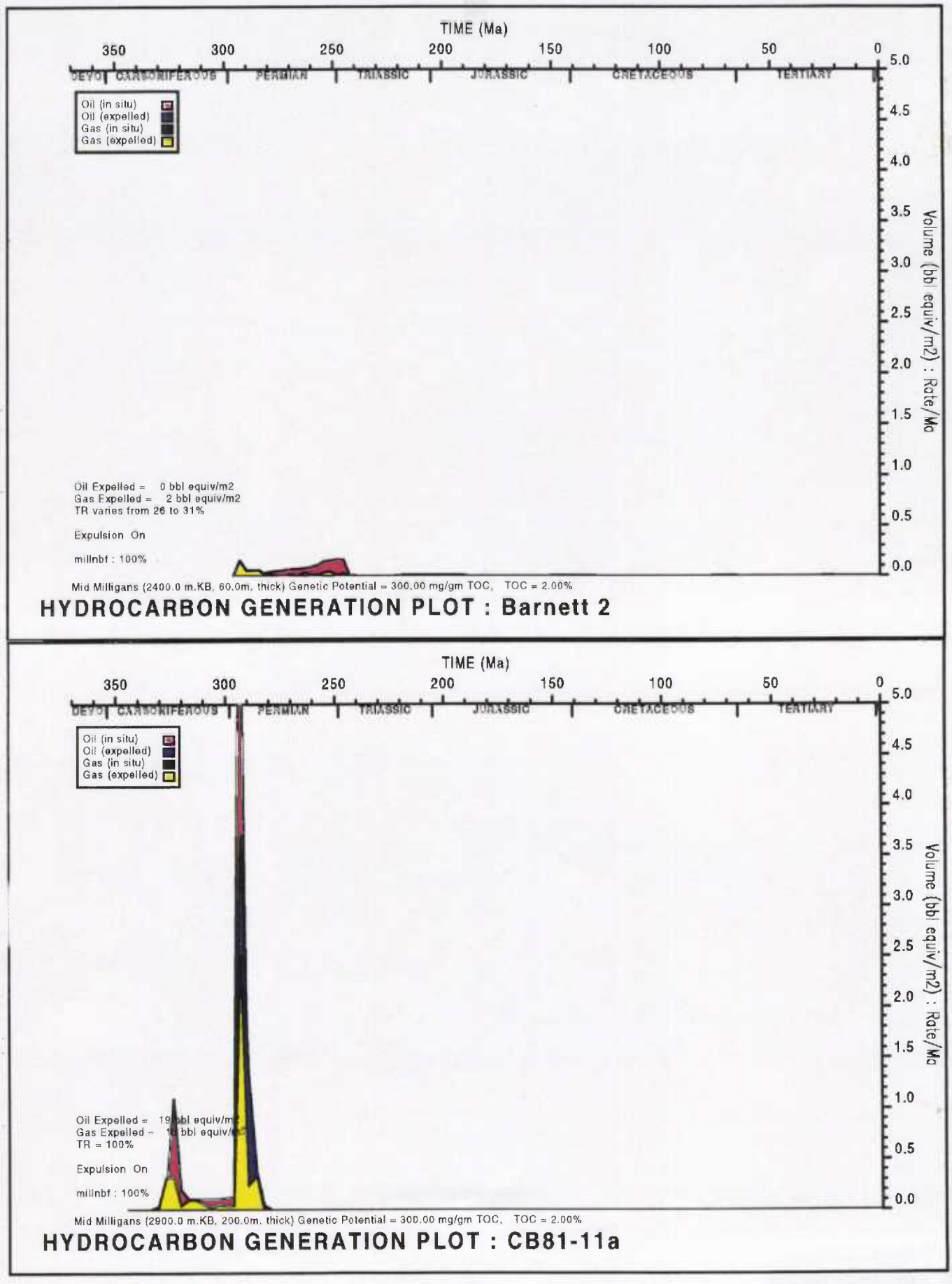

Figure 10 G, H. Hydrocarbon generation plots for the mid-Milligans source unit in: G) Barnett-2, and H) Pseudo-well CB-81-11a.

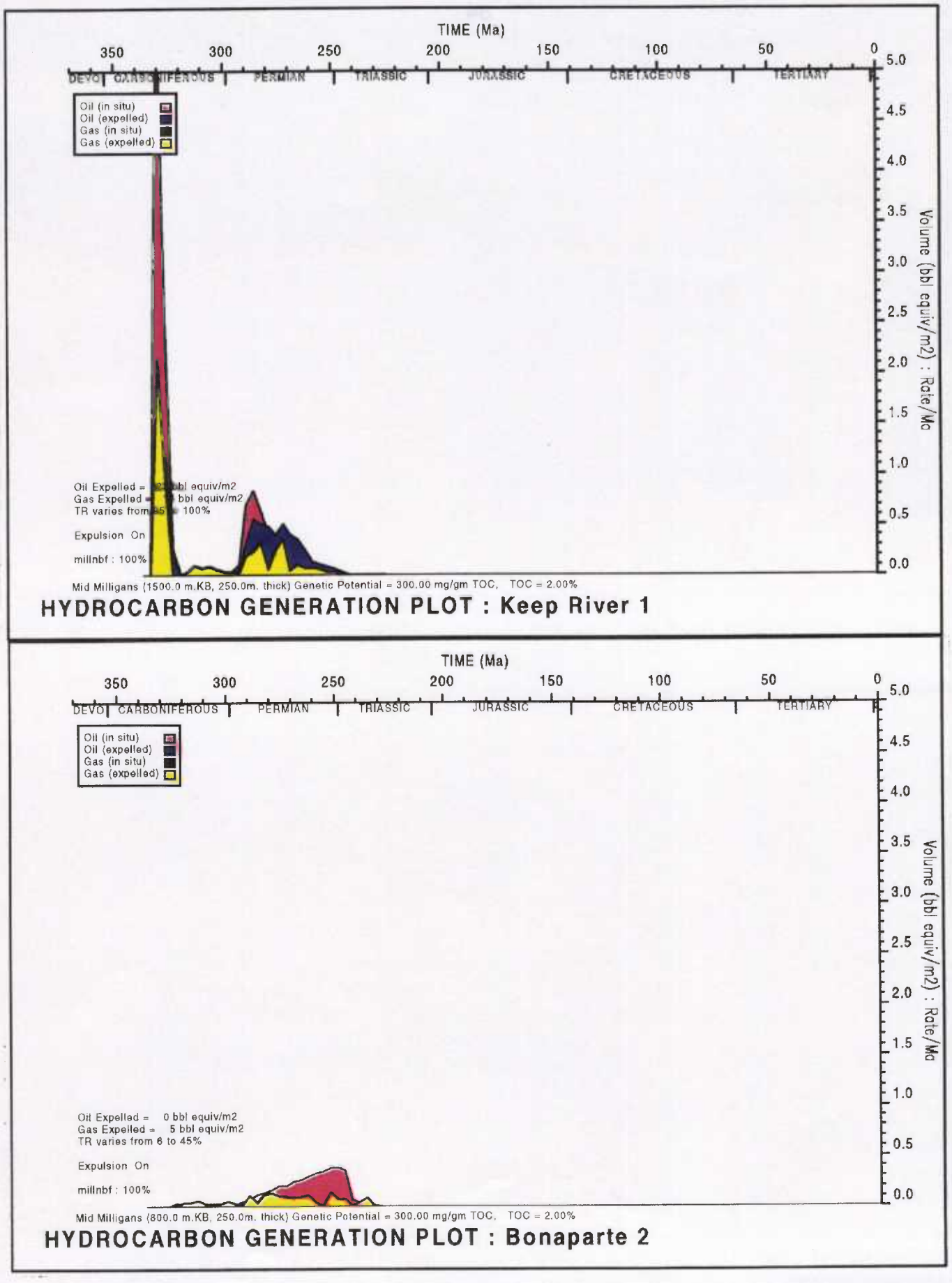

Figure 10 I, J. Hydrocarbon generation plots for the mid-Milligans source unit in:
I) Keep River-1, and K) Bonaparte-2.

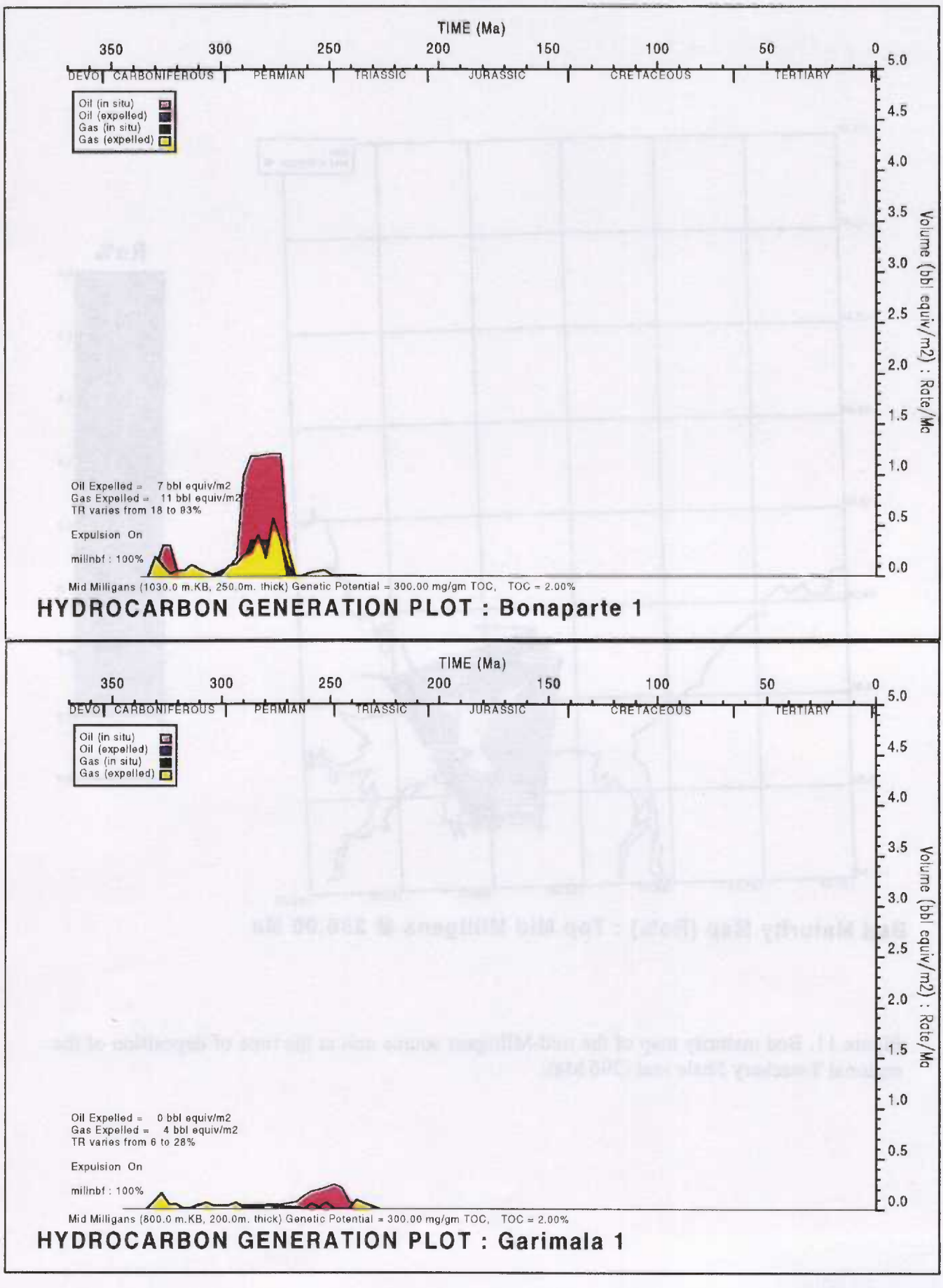

Figure 10 K, L. Hydrocarbon generation plots for the mid-Milligans source unit in: K) Bonaparte-1, and L) Garimala-1.

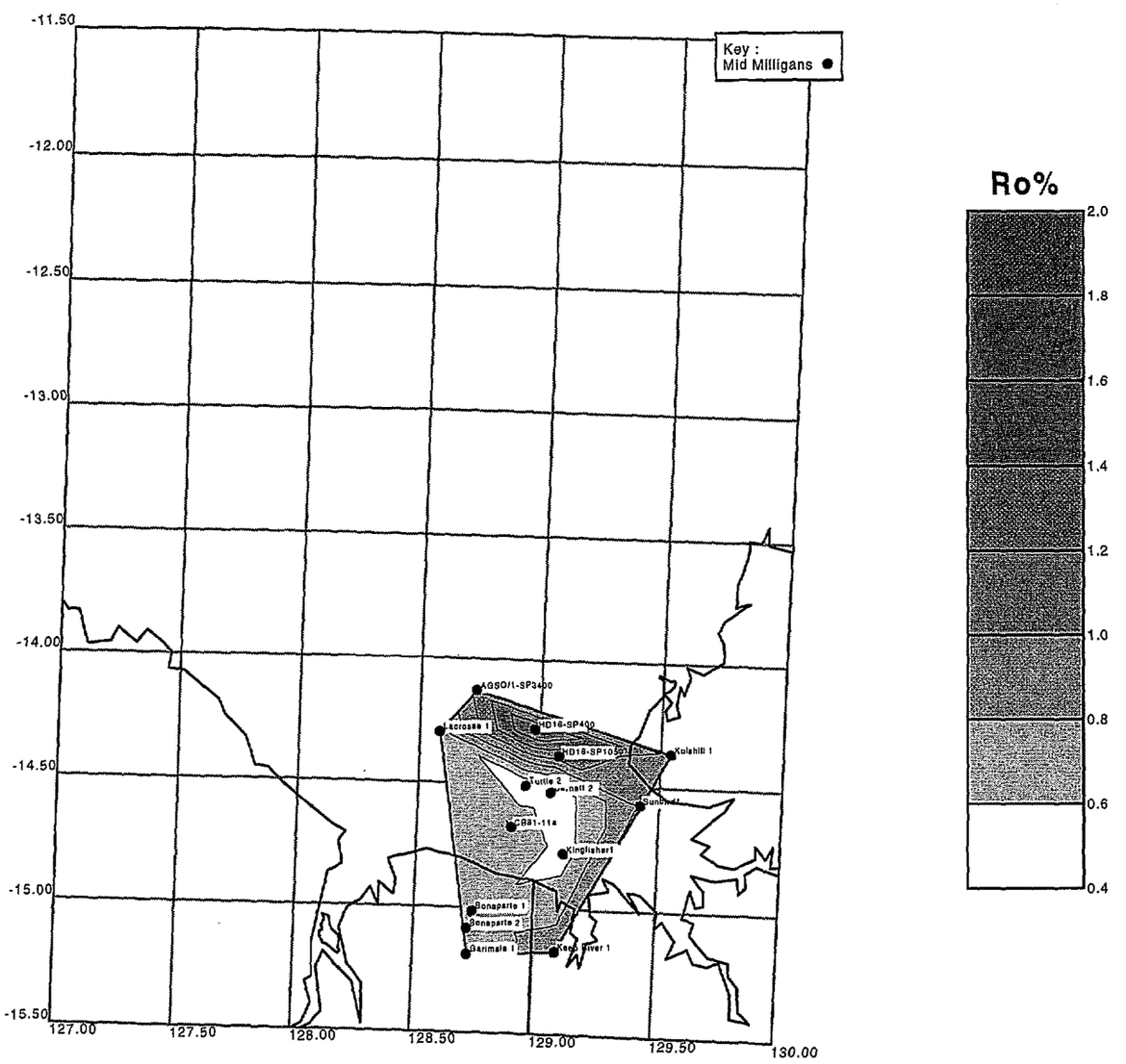

Bed Maturity Map (Ro%) : Top Mid Milligans @ 296.00 Ma

Figure 11. Bed maturity map of the mid-Milligans source unit at the time of deposition of the regional Treachery Shale seal (296 Ma).

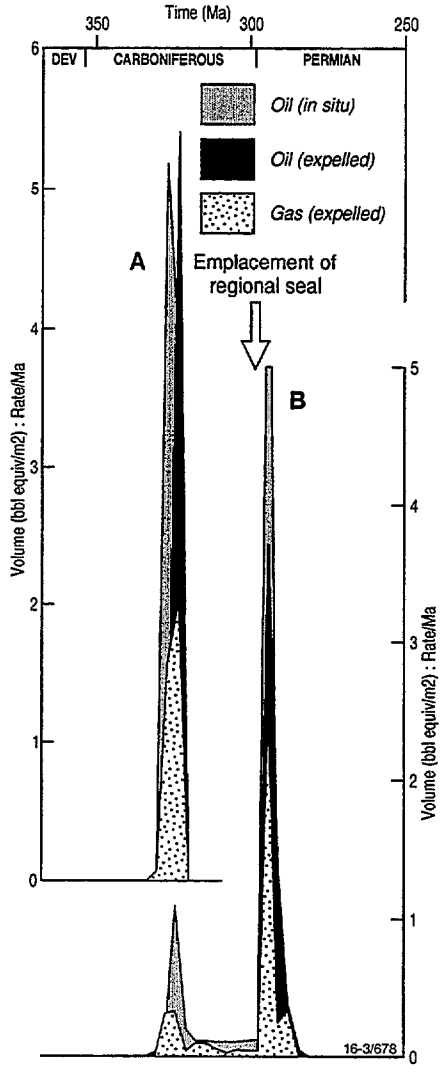

Figure 12. Comparative hydrocarbon generation plots for the mid-Milligans source rocks in:
A) The depocentre north of the Turtle-Barnett High (pseudo-well site HD16-sp400).
B) The Cambridge Trough south of the Turtle-Barnett High (pseudo-well site CB81-11a).

Keyling Source Unit

Edwards & Summons (1996) identified two source facies within the Keyling Supersequence; marginal marine shales and non-marine coaly shales. The shales have fair source potential, ranging from dry gas-prone Type III/IV kerogen to oil and condensate-prone Type II/III kerogen (mean TOC = 2.8 %, mean HI = 95, mean $S_1 + S_2$ = 3.6 kg hydrocarbons per tonne). The coaly shales are characterised by Type II/III kerogen and have good oil and gas generative potential (mean TOC = 35.2 %, mean HI = 230, mean $S_1 + S_2$ = 78 kg hydrocarbons per tonne). Whereas the shales occur throughout the Keyling Supersequence, the higher source-quality coaly shales occur within fluvial and delta plain facies which tend to be concentrated within the second-order lowstand and highstand systems tracts in the lower and upper portions of the supersequence, respectively. However, these coaly sediments only occur as thin interbeds and laminae, and volumetrically probably represent only a few percent of the total succession. Previous source rock sampling strategies do not permit an evaluation of the net effective thickness of these high source-quality coaly shales.

The Keyling Supersequence is widespread throughout the offshore portion of the Petrel Sub-basin, and organic-rich shales appear to occur throughout its areal distribution (Fig. 13). Coaly shales have been intersected in several wells in inboard, marginal areas (e.g., Barnett-1, Flat Top-1, Kinmore-1, Kulshill-1, Matilda-1 and Turtle-1), but high-quality coaly source rocks have only been identified in Flat Top-1 and Kinmore-1 (Rock-Eval data; Edwards & Summons, 1996). A fairway of possible high-quality source rocks is thus proposed on the eastern flank of the Petrel Deep (Fig. 12), but the basinal continuation of this fairway is unknown (the Keyling Supersequence occurs below TD at Penguin-1 and Petrel-1, 1A and 2).

Maturation models for the Keyling source unit are presented for 12 wells/pseudo-wells (Table 3). Modelled TOC values reflect average TOC of shales analysed in each well (ranging from 1.5 % TOC in Billawock-1 and Cambridge-1, to 4 % TOC in Flat Top-1) and a net effective source thickness of 200-300 m. Maturation modelling of the Keyling source unit is based on kinetic analyses of an organic-rich shale and a coaly shale in Kinmore-1 (AGSO # 8989 and 8484, respectively; Appendix C). Both samples have a genetic potential of approximately 300 mg/gm TOC, and a similar distribution of activation energies. In the modelled wells, this kerogen type generates oil within the approximate range Rv = 0.65 to 1.0 %, wet gas at Rv = 1 to 1.6 %, and dry gas at Rv > 1.6 %.

Due to uncertainties in the net effective thickness of the higher source-quality coaly shales, this source facies has only been modelled in Flat Top-1, pseudo-well site AGSO/5-sp2800 (near Kinmore-1 which was not modelled due to problems associated with salt intrusion), Penguin-1, and Petrel-2. In these wells/pseudo-wells, three scenarios were modelled for mixed shale and coaly shale source rocks; 1) with nil coaly shales, 2) with 10-15 m net effective thicknesses of coaly shales (representing 5 % of total modelled shale thickness), and 3) with 40-60 m net effective thicknesses of coaly shales (representing 20 % of total modelled shale thickness). These three models are equivalent to average net TOC values of about 3-4 %, 5 % and 10 %, respectively, over the total thickness of the Keyling source interval in these wells/pseudo-wells.

The Keyling source unit is presently at maximum attained maturity level in all modelled wells/pseudo-wells (Fig. 14). Maximum attained maturity levels steadily increased throughout the Permian and Early Triassic (subsidence Phase F), increased slightly or remained essentially constant from the Middle Triassic to Jurassic (subsidence Phases G and H), and

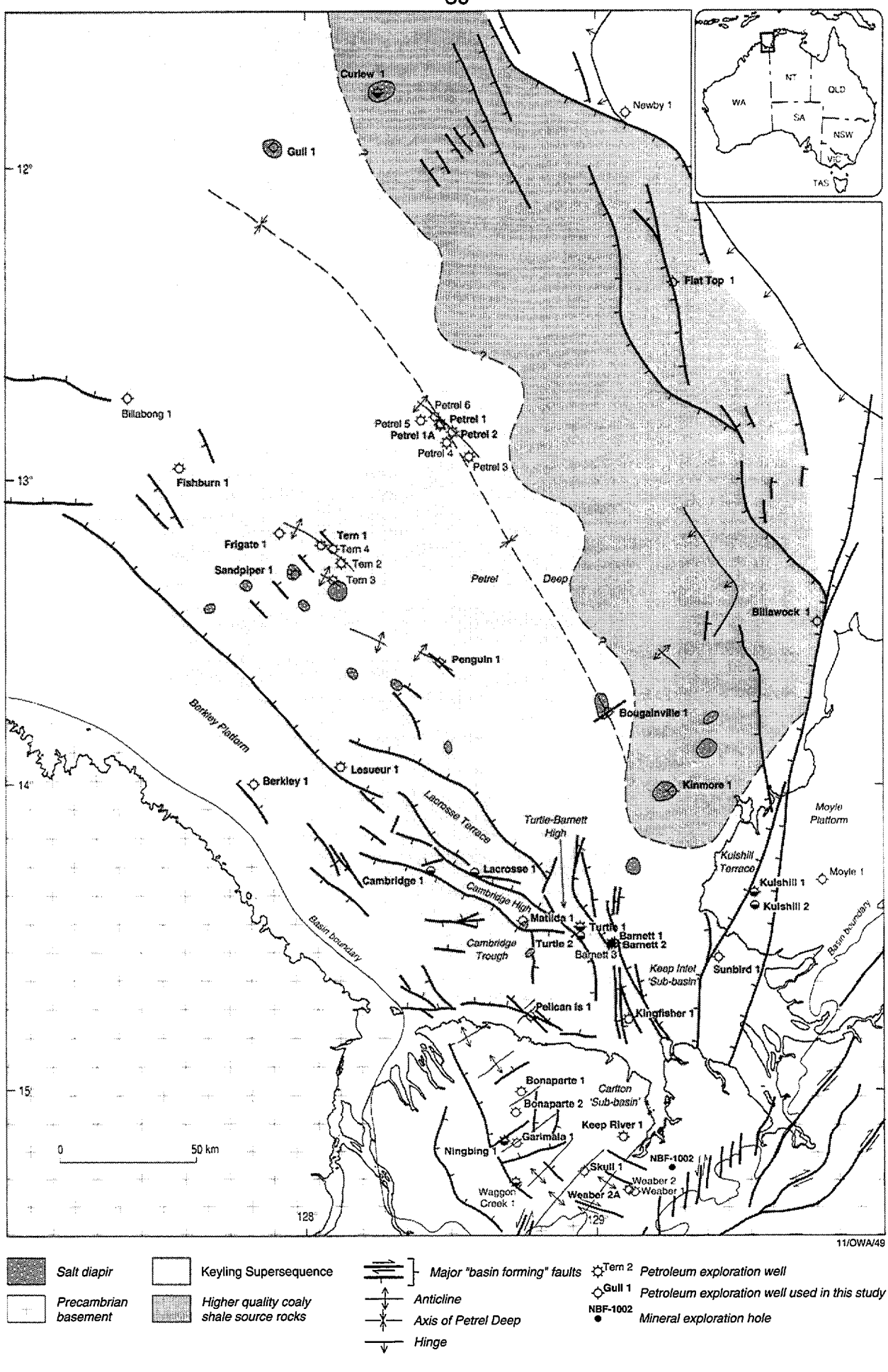

Figure 13. Distribution of the Keyling source rock unit.

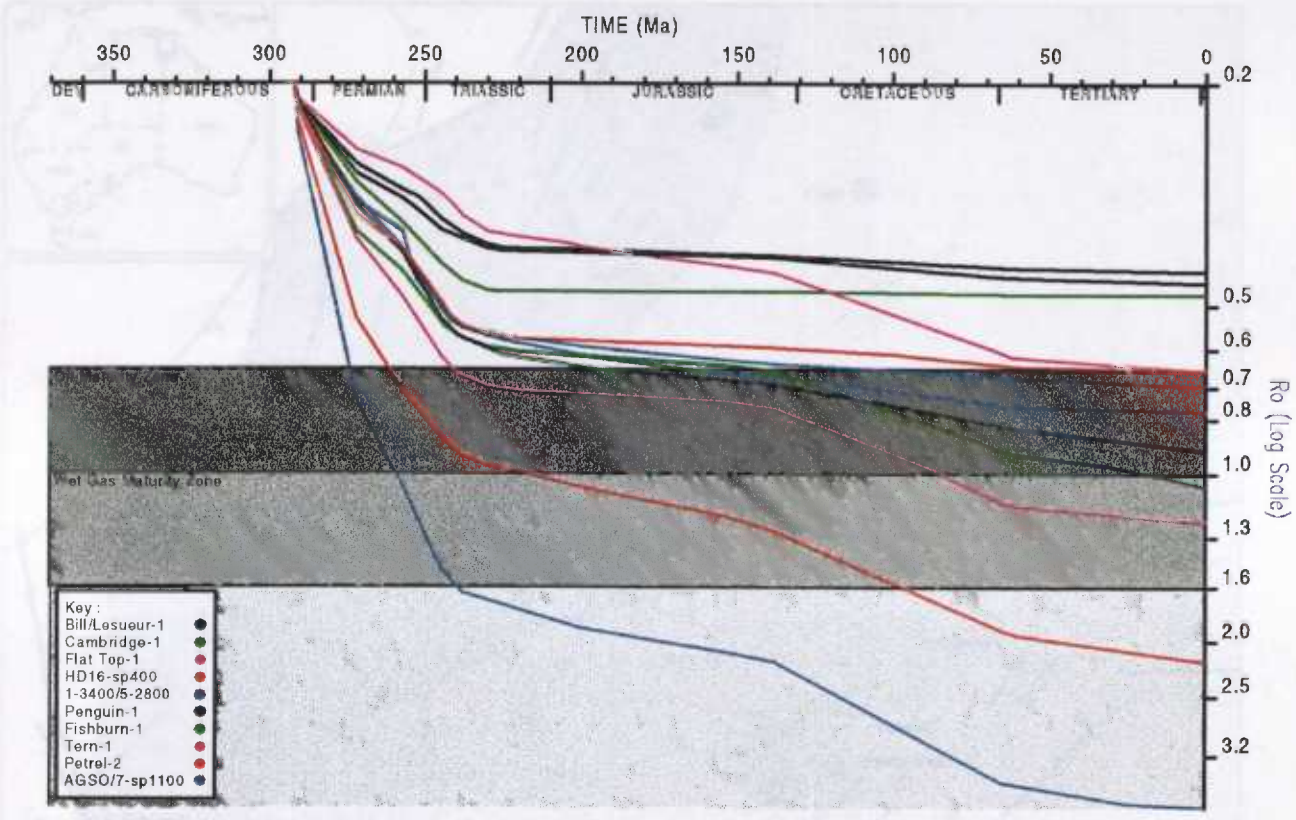

Bed Maturity vs TIME : TOP Keyling

Figure 14. Bed maturity plot for the Keyling source unit in modelled wells/pseudo-wells.

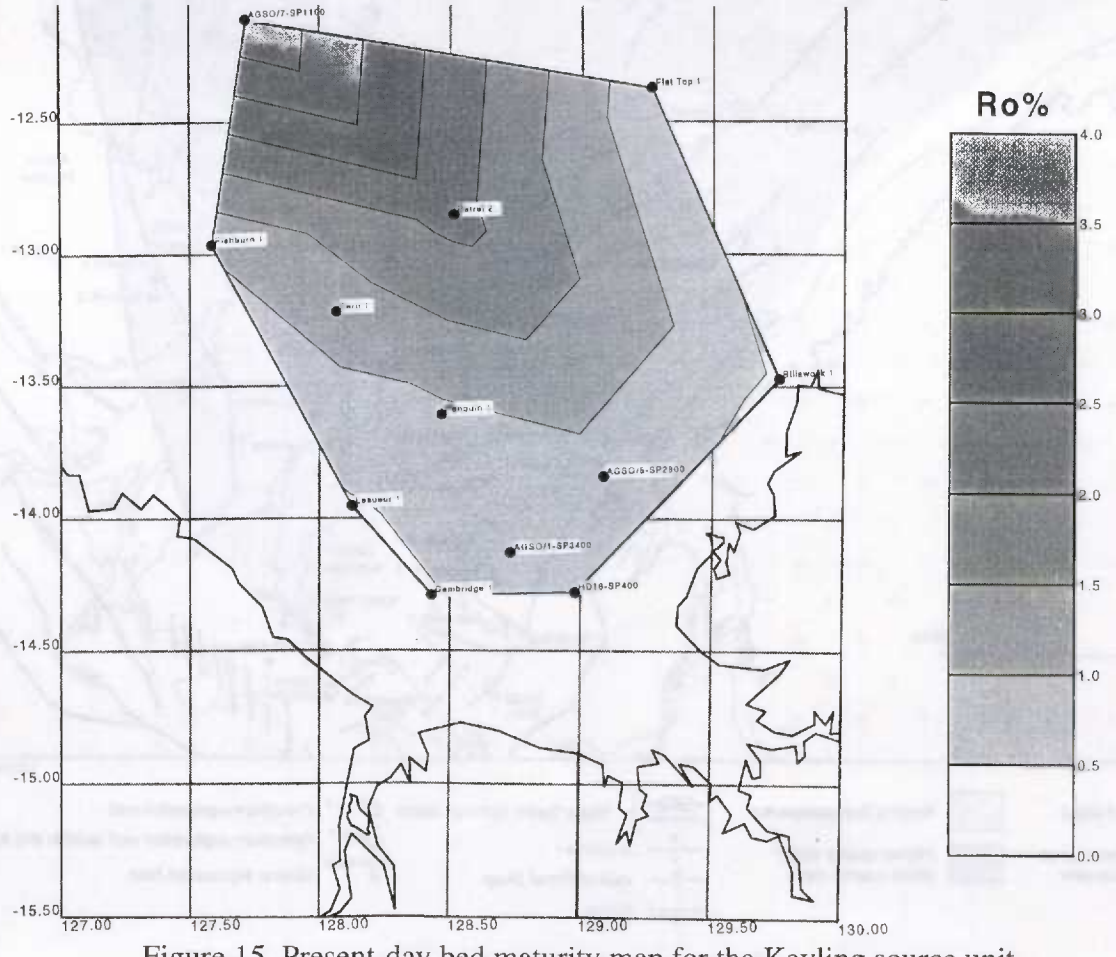

Figure 15. Present-day bed maturity map for the Keyling source unit.

then increased throughout the Cretaceous (subsidence Phase I) to about present-day maturity levels. Figures 14 and 15 indicate the following present-day maturity levels for the Keyling source interval:

- Immature in Billawock-1, Lesueur-1, Cambridge-1, Flat Top-1 and pseudo-well HD16-sp400.
- Oil maturity zone in pseudo-wells AGSO/1-sp3400, AGSO/5-sp2800 (near Kinmore-1) and Penguin-1.
- Wet gas maturity zone in Fishburn-1 and Tern-1.
- Dry gas maturity zone in Petrel-2 and pseudo-well AGSO/7-sp1100.

Wells in the outer and central Petrel Deep (e.g., pseudo-well AGSO/7-sp1100, Petrel-2 and Tern-1) entered the oil maturity zone during the Permian or Early Triassic (that is, prior to the Fitzroy Movement structuring events), whereas wells on the flanks of the Petrel Deep (e.g., Fishburn-1, Penguin-1 and pseudo-well sites AGSO/5-sp2800 and AGSO/1-sp3400) entered the oil maturity zone during the Jurassic-Cretaceous (Fig. 14). However, hydrocarbon generation plots for these well/pseudo-wells (Fig. 16) indicate that the time of peak expulsion of hydrocarbons generally occurred substantially later than the time indicated by bed maturity. For example, although the Keyling source interval at Tern-1 first entered the oil maturity zone during the Early Triassic, peak expulsion of oil probably did not occur until the Cretaceous (Fig. 16C), well after the Middle Triassic - Early Jurassic Fitzroy Movement structuring. Similarly, this source unit first entered the oil window at Fishburn-1 during the Jurassic, but peak oil expulsion probably occurred in the Tertiary (Fig. 16 D). In pseudo-well site AGSO/1-sp3400, nil hydrocarbons have been expelled from the Keyling source unit.

Hydrocarbon generation plots for Petrel-2 indicate critical relationships between modelled net effective thickness of the Keyling coaly shales, timing of peak hydrocarbon expulsion, and time of structuring. If the high-quality coaly shales have a low net effective thickness (net TOC = 3 %), modelled peak expulsion of liquid hydrocarbons occurred during the Late Triassic synchronous with Fitzroy Movement structuring (Fig. 16B). However, if the high-quality coaly shales have a net effective thickness of 15-60 m (net TOC = 5-10%), then the peak expulsion of liquid hydrocarbons probably occurred during the Early Triassic prior to the main Fitzroy Movement structuring (Fig. 17A, B). Liquid hydrocarbons generated at this time may have thus migrated to traps on the flanks of the Petrel Deep prior to the formation of the Petrel and Tern Anticlines in the Middle-Late Triassic. However, seismic data suggests that these structures may have started to grow in the Late Permian (see Colwell & Kennard, 1996, chapter 3), and thus they may have been partially charged by hydrocarbons expelled from the Keyling coaly shales in the Early Triassic. Regardless of the proportion of high-quality coaly shales, significant amounts of gas were probably expelled both prior to and after structuring.

At Penguin-1, a low net effective thicknesses of high-quality coaly shales (net TOC = 3 %) results in minor expulsion of gas (but no oil) throughout the Cretaceous and Tertiary (Fig. 16E), whereas a net effective thicknesses of 10-40 m coaly shales (net TOC = 5-10%,) results in minor expulsion of oil during the Tertiary in addition to Cretaceous-Tertiary gas expulsion history (Fig. 17C, D). At pseudo-well site AGSO/5-sp2800 (near Kinmore-1), gas and oil expulsion is negligible for all modelled proportions of high-quality coaly shales (Figs. 16F, 17E, F).

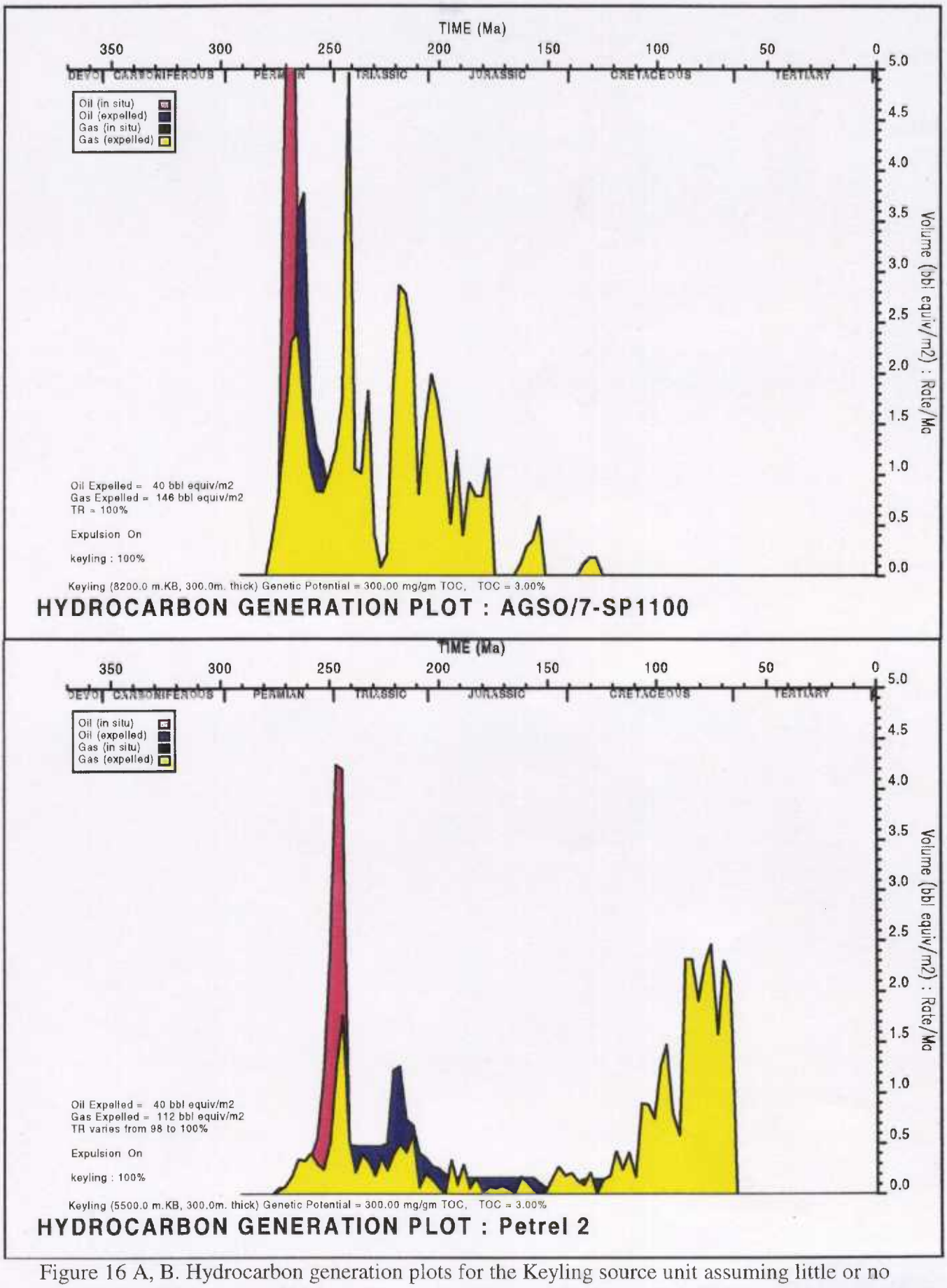

Figure 16 A, B. Hydrocarbon generation plots for the Keyling source unit assuming little or no net effective thicknesses of high-quality coaly shales: A) Pseudo-well AGSO/7-sp1100, B) Petrel-2.

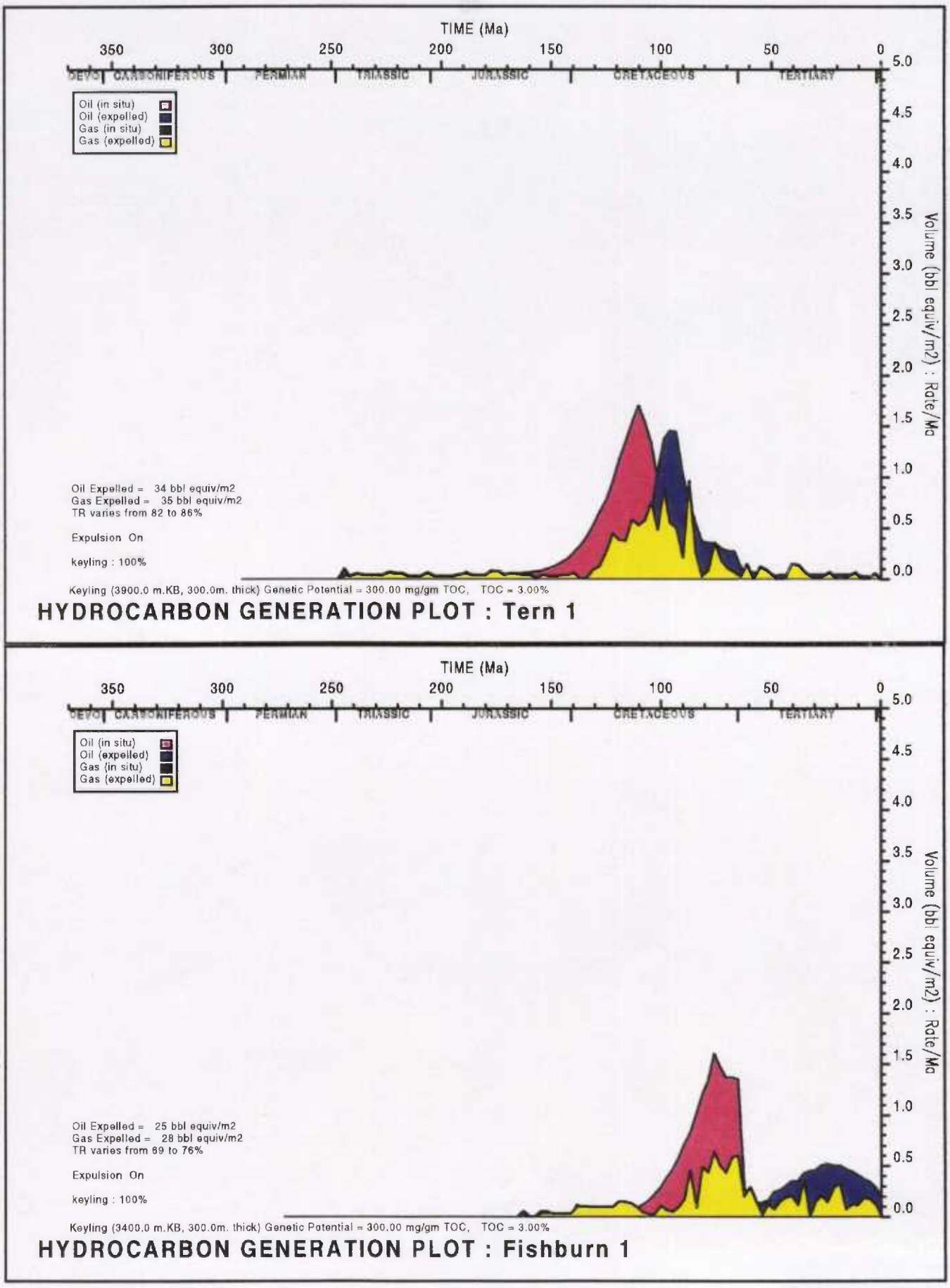

Figure 16 C, D. Hydrocarbon generation plots for the Keyling source unit assuming little or no net effective thicknesses of high-quality coaly shales: C) Tern-1, D) Fishburn-1.

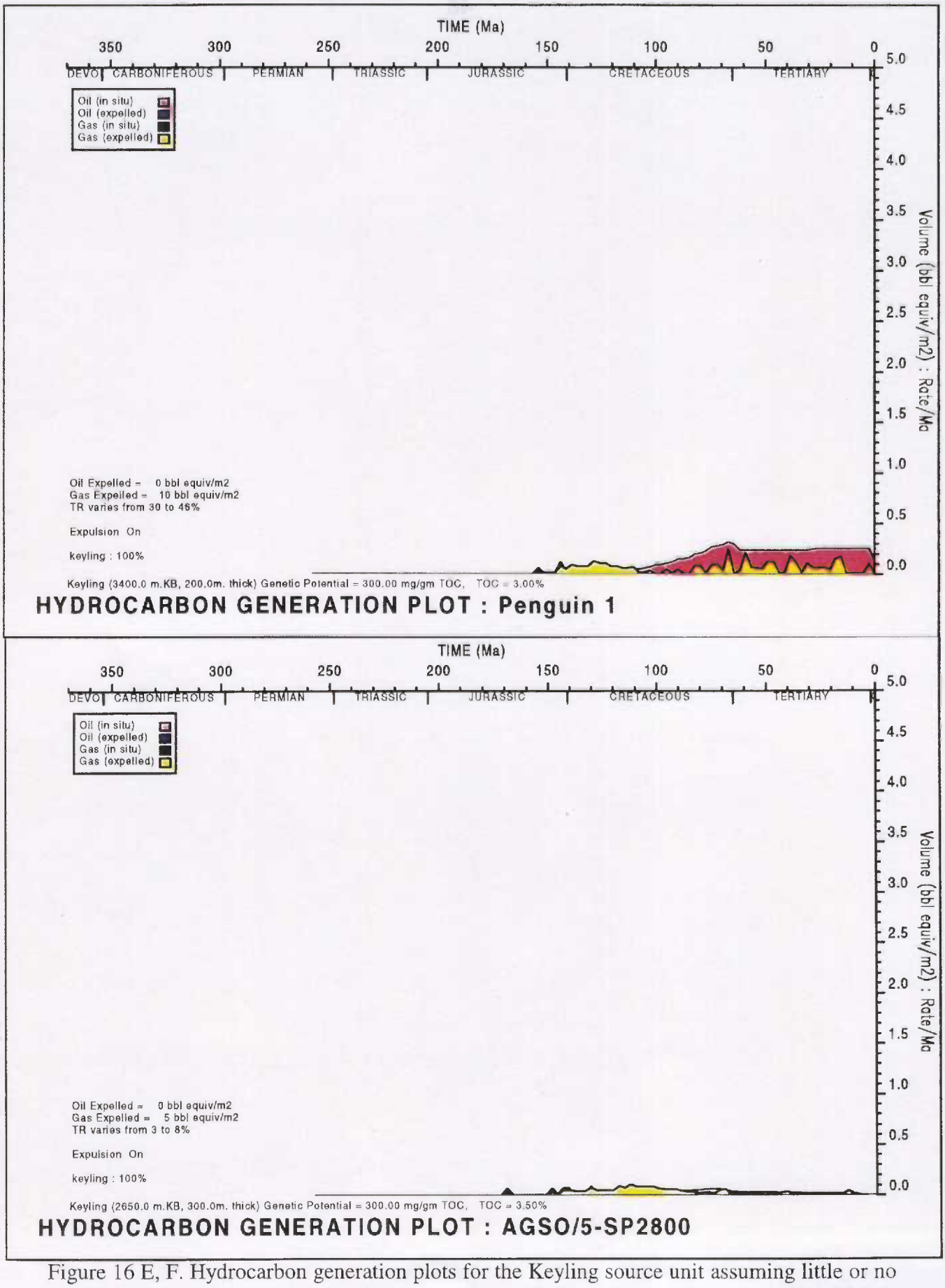

Figure 16 E, F. Hydrocarbon generation plots for the Keyling source unit assuming little or no net effective thicknesses of high-quality coaly shales: E) Penguin-1, F) Pseudo-well AGSO/5-sp2800.

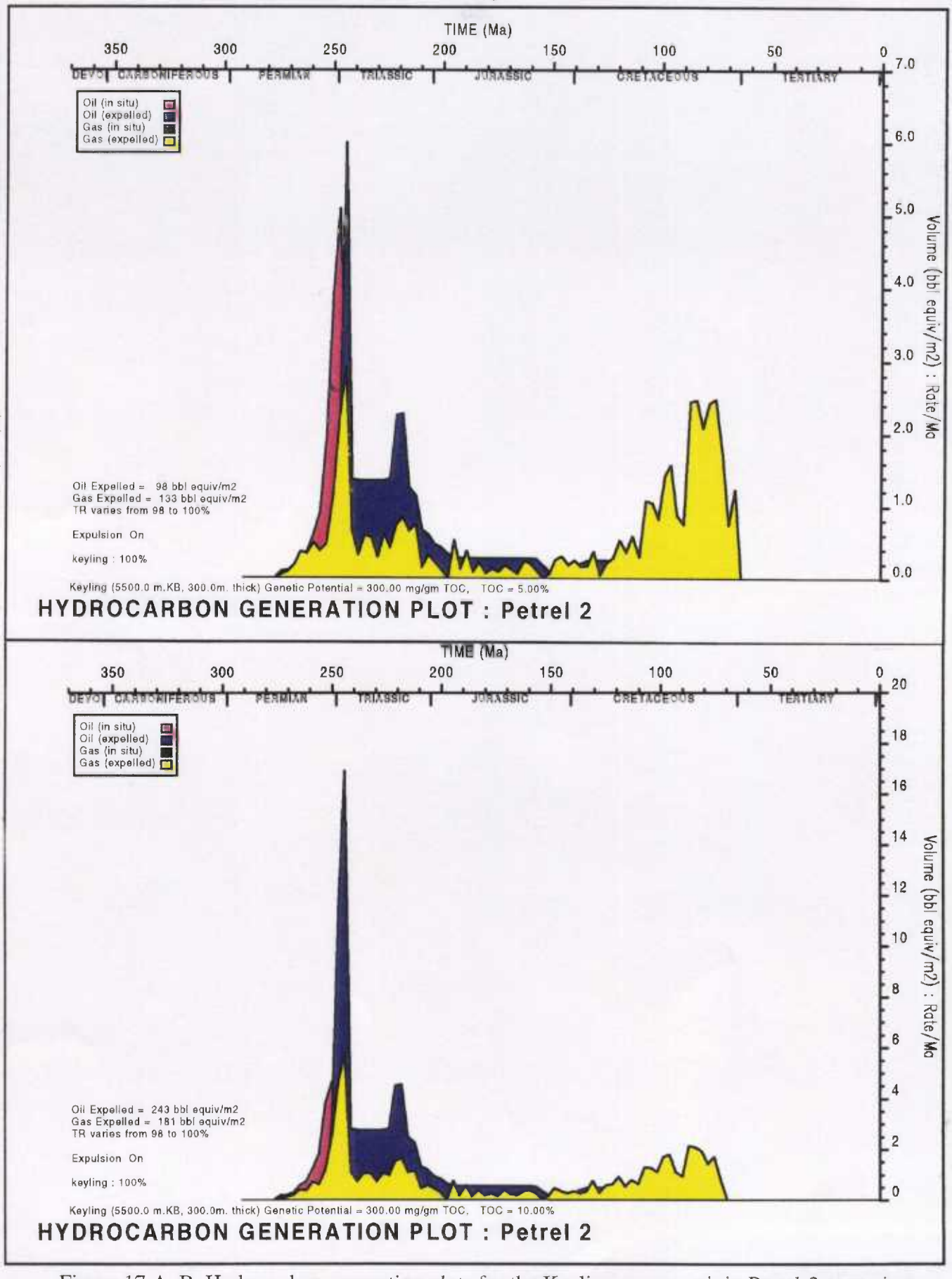

Figure 17 A, B. Hydrocarbon generation plots for the Keyling source unit in Petrel-2 assuming A) 10-15 m (i.e., 5 % net TOC), and B) 40-60 m (i.e., 10 % net TOC) net effective thicknesses of high-quality coaly shales.

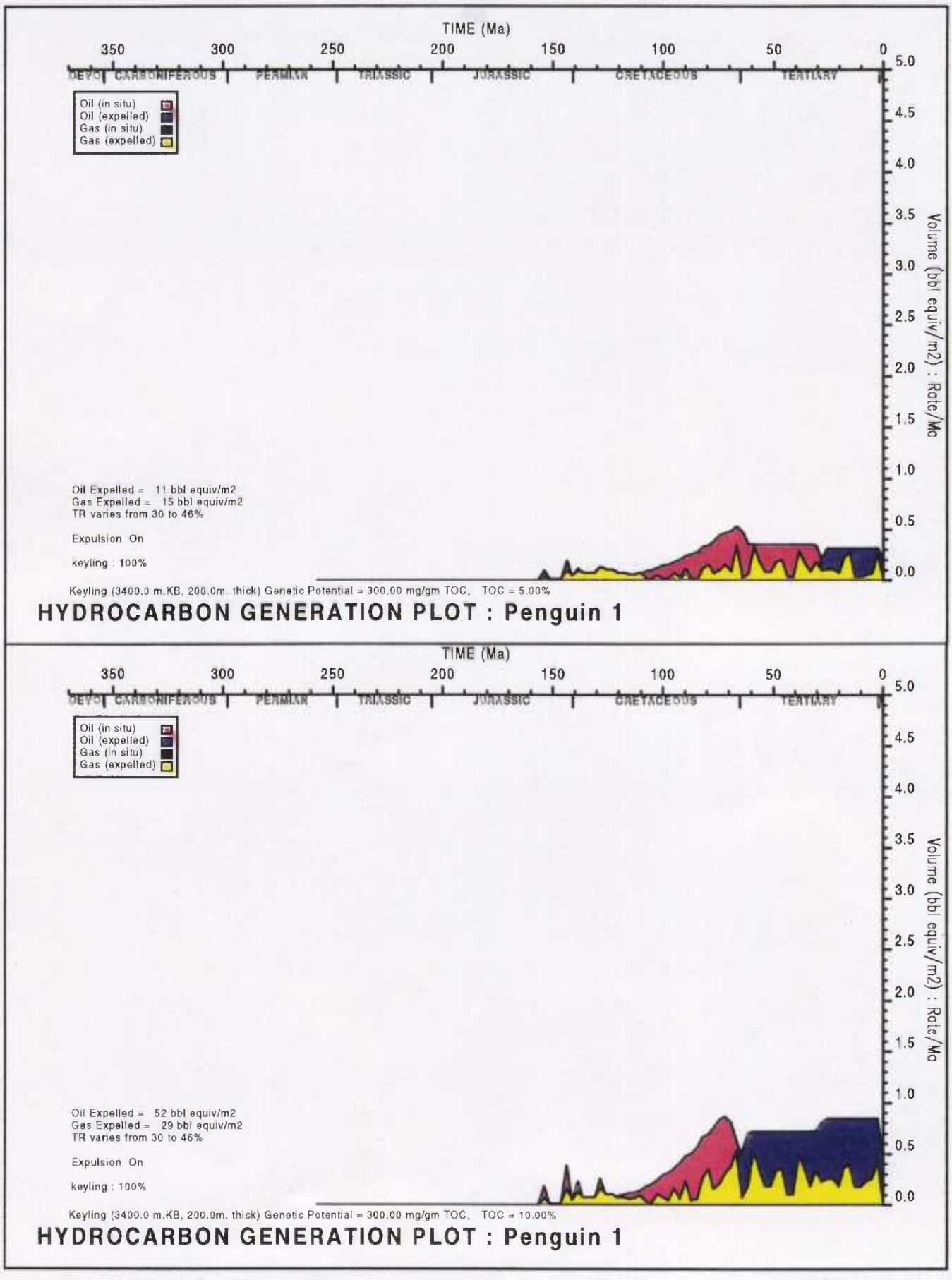

Figure 17 C, D. Hydrocarbon generation plots for the Keyling source unit in Penguin-1 assuming C) 10-15 m (i.e., 5 % net TOC), and D) 40-60 m (i.e., 10 % net TOC) net effective thicknesses of high-quality coaly shales.

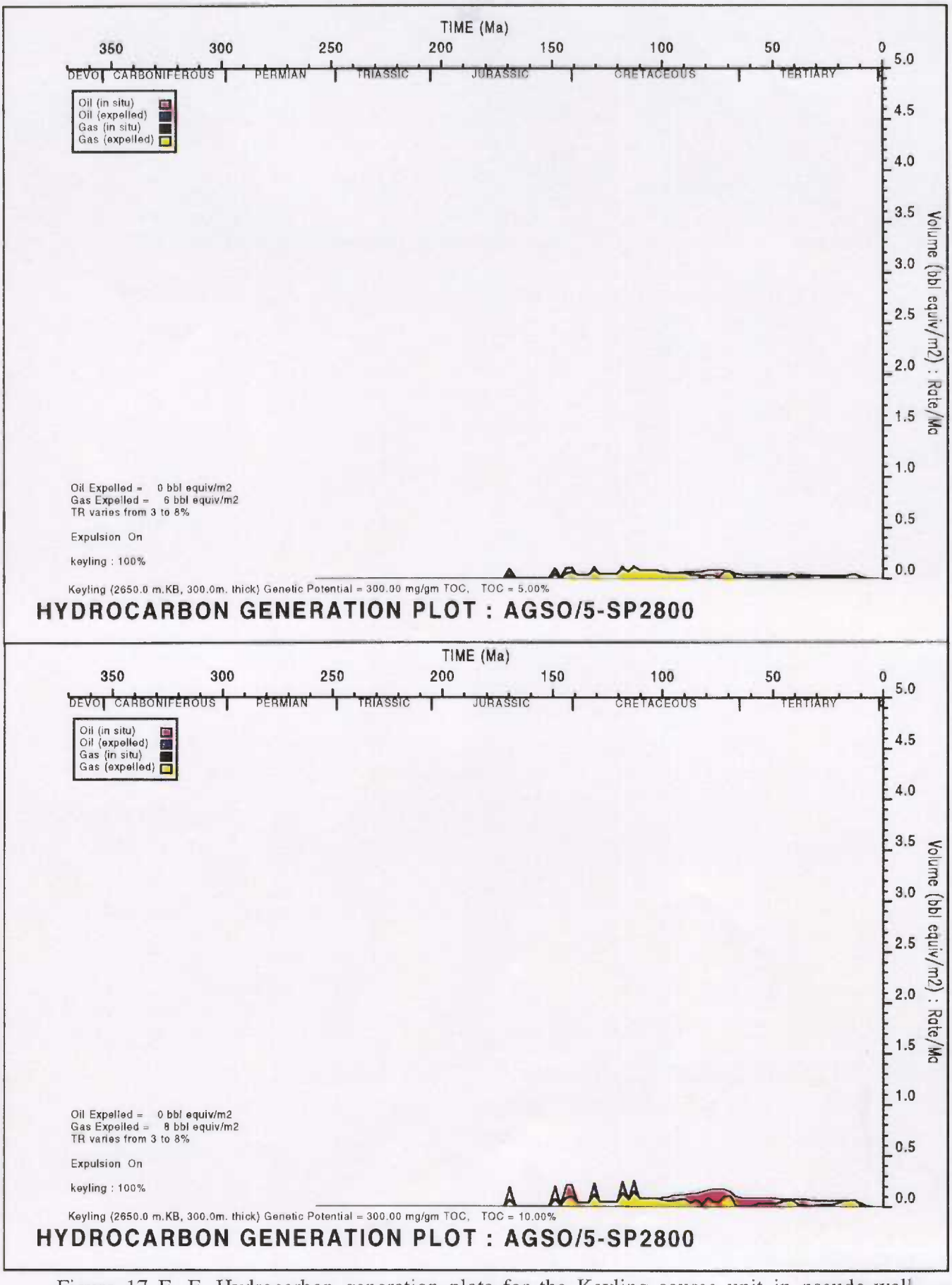

Figure 17 E, F. Hydrocarbon generation plots for the Keyling source unit in pseudo-well AGSO/5-sp2800 assuming E) 10-15 m (i.e., 5 % net TOC), and F) 40-60 m (i.e., 10 % net TOC) net effective thicknesses of high-quality coaly shales.

Hyland Bay Source Unit

Marine shales and siltstones of the Hyland Bay Formation generally have poor source potential (mean TOC = 2%; mean HI = **55**; mean S1 + S2 = 1.3 kg hydrocarbons/tonne; Edwards & Summons, 1996). These sediments contain Type III/IV kerogen which is at best gas-prone.

Sequence stratigraphic analysis of well sections (see Well Folio) indicates that the most organic-rich intervals occur within transgressive pro-delta and early highstand delta-slope facies in the lower portion of the Hyland Bay Member. These source rocks are widespread throughout the Petrel Deep (Fig. 18). Higher source quality sediments may occur in the outer portions of Petrel Deep and could have contributed, at least in part, to the gas and condensate accumulations at the Petrel and Tern Fields. Edwards & Summons (1996) concluded that the condensate at Petrel-4 has a diagnostically heavy carbon isotopic signature consistent with it being generated from mature Permian clay-rich sediments containing mixed land-plant and marine algal material.

Maturation models of the Hyland Bay source interval are presented for 8 wells/pseudo-wells (Table 3). Modelled TOC values reflect average TOC of shales/siltstones analysed in each well (ranging from 1 to 2.5 %), and a net effective source thickness of 250-300 m in outboard wells, decreasing to 50-150 m in inboard wells. Maturation modelling of the Hyland Bay source interval is based on the kinetic analysis of similar kerogen material in the Keyling source unit, but with a lower genetic potential (HI = 150). In the modelled wells, this kerogen type generates oil within the approximate range Rv = 0.65 - 1.0 %, wet gas at Rv = 1 - 1.6 %, and dry gas at Rv > 1.6 %.

The Hyland Bay source unit is presently at maximum attained maturity level in all modelled wells/pseudo-wells (Fig. 19). Figures 19 and 20 indicate the following present-day maturity levels for the Hyland Bay source interval:

- Immature in Lesueur-1, Flat Top-1 and pseudo-well AGSO/5-sp2800.
- Oil maturity zone in Penguin-1, Fishburn-1 and Tern-1.
- Wet gas maturity zone in Petrel-2
- Dry gas maturity zone pseudo-well AGSO/7-sp1100.

Potential Hyland Bay source rocks in the outer Petrel Deep (AGSO/7-sp1100) first entered the oil maturity zone during the Middle Jurassic, well after Fitzroy Movement structuring. In the central Petrel Deep, Petrel-2 first entered the oil maturity zone at the start of the Cretaceous, and the remaining wells in shallow portions of the Petrel Deep first entered this zone during the Late Cretaceous-Tertiary.

Hydrocarbon generation plots (Fig. 21) indicate that potential Hyland Bay source rocks in the outer Petrel Deep probably expelled significant quantities of gas during the Tertiary, and to a lesser extent, the Cretaceous. In the central Petrel Deep, however, these source rocks probably expelled only minor amounts of gas during the Late Cretaceous, and a significant proportion of the original kerogen has yet to been transformed into hydrocarbons (TR = 35-62 %: Fig. 21B). In the shallower portions of the Petrel Deep (e.g., Penguin-1, Fishburn-1 and Tern-1), maturation modelling suggests that little or no hydrocarbons have been generated or expelled from the Hyland Bay source unit.

This modelling suggests that the Hyland Bay source unit may have contributed to the gas accumulations in the Petrel and Tern Fields, but that expulsion of gas from this source was probably limited to areas of that source in the outer portion of the Petrel Deep (Fig. 18).

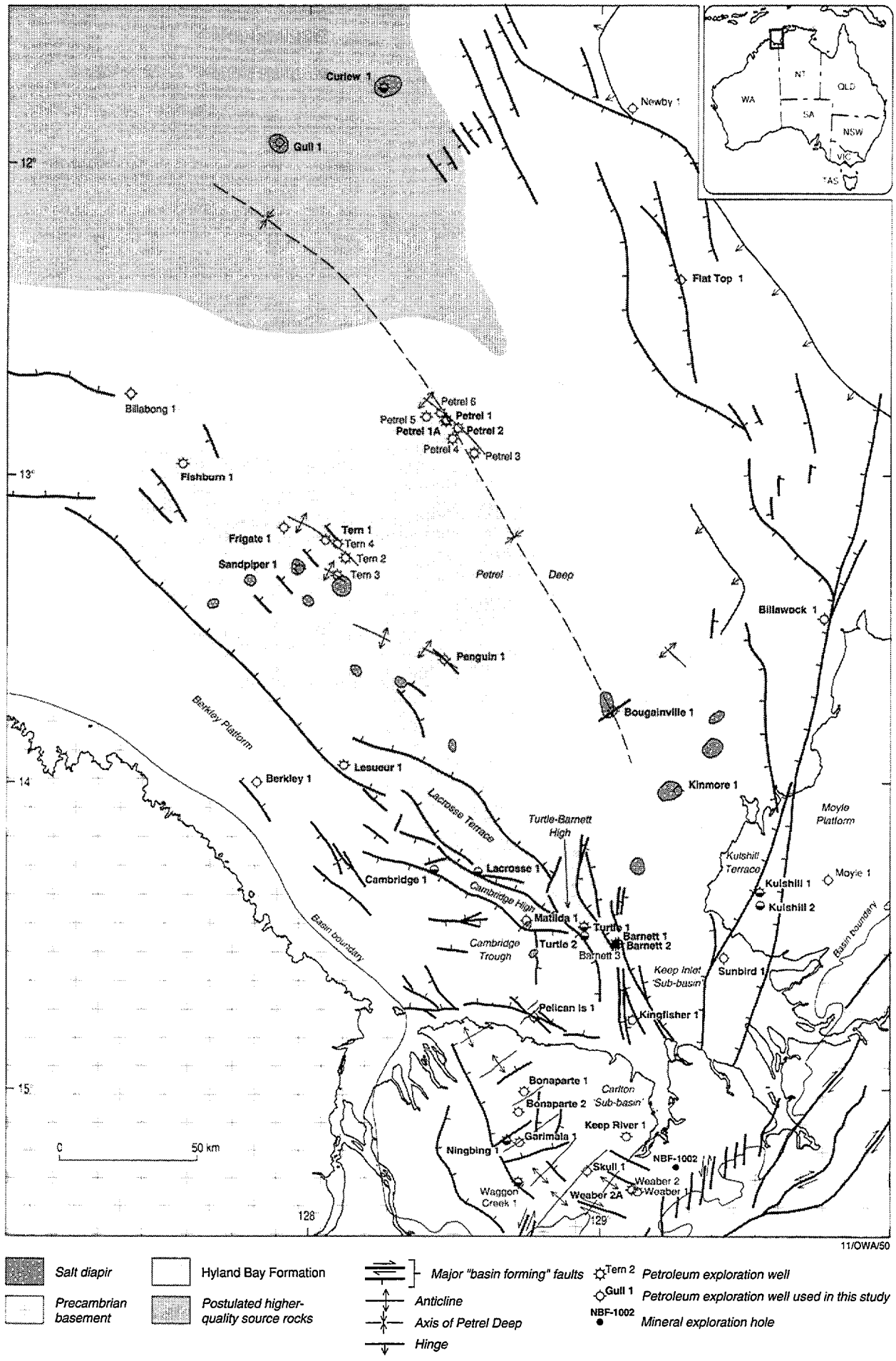

Figure 18. Distribution of the Hyland Bay source rock unit.

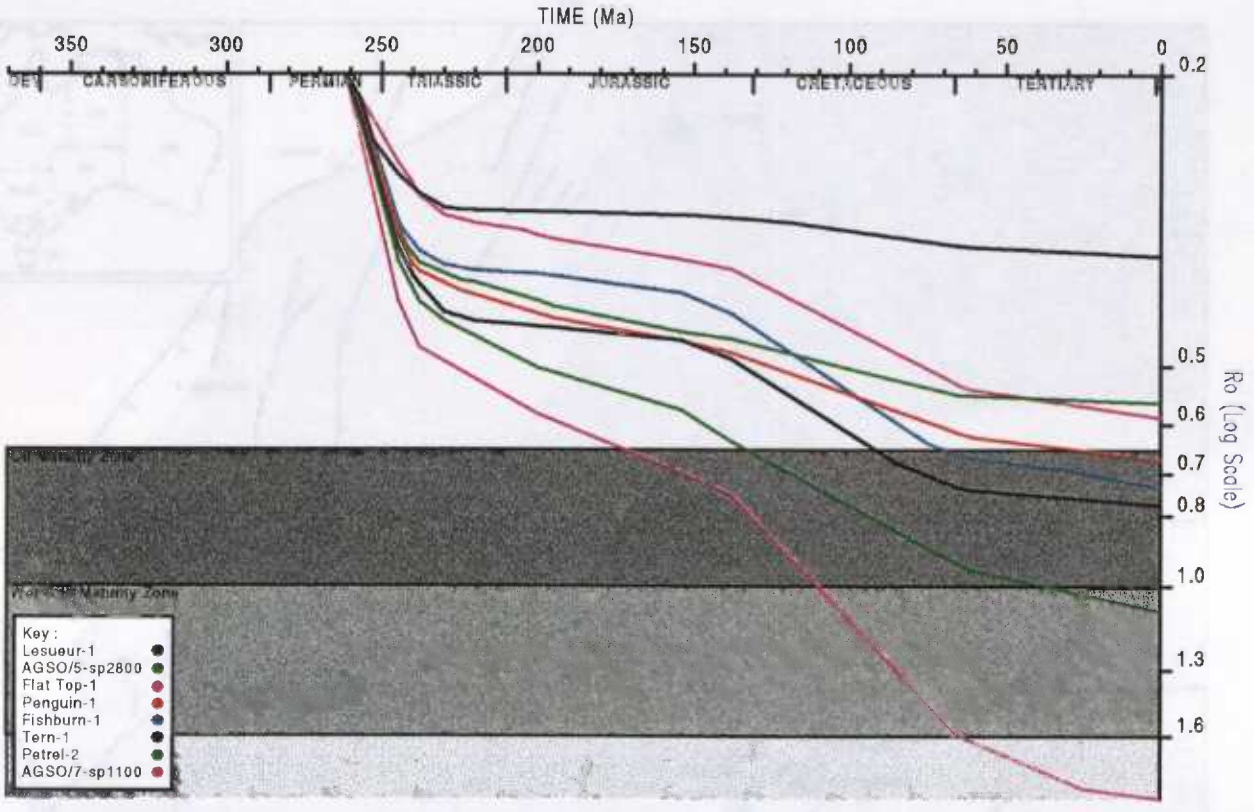

Bed Maturity vs TIME : TOP Hyland Bay

Figure 19. Bed maturity plot for the Hyland Bay source unit in modelled wells/pseudo-wells.

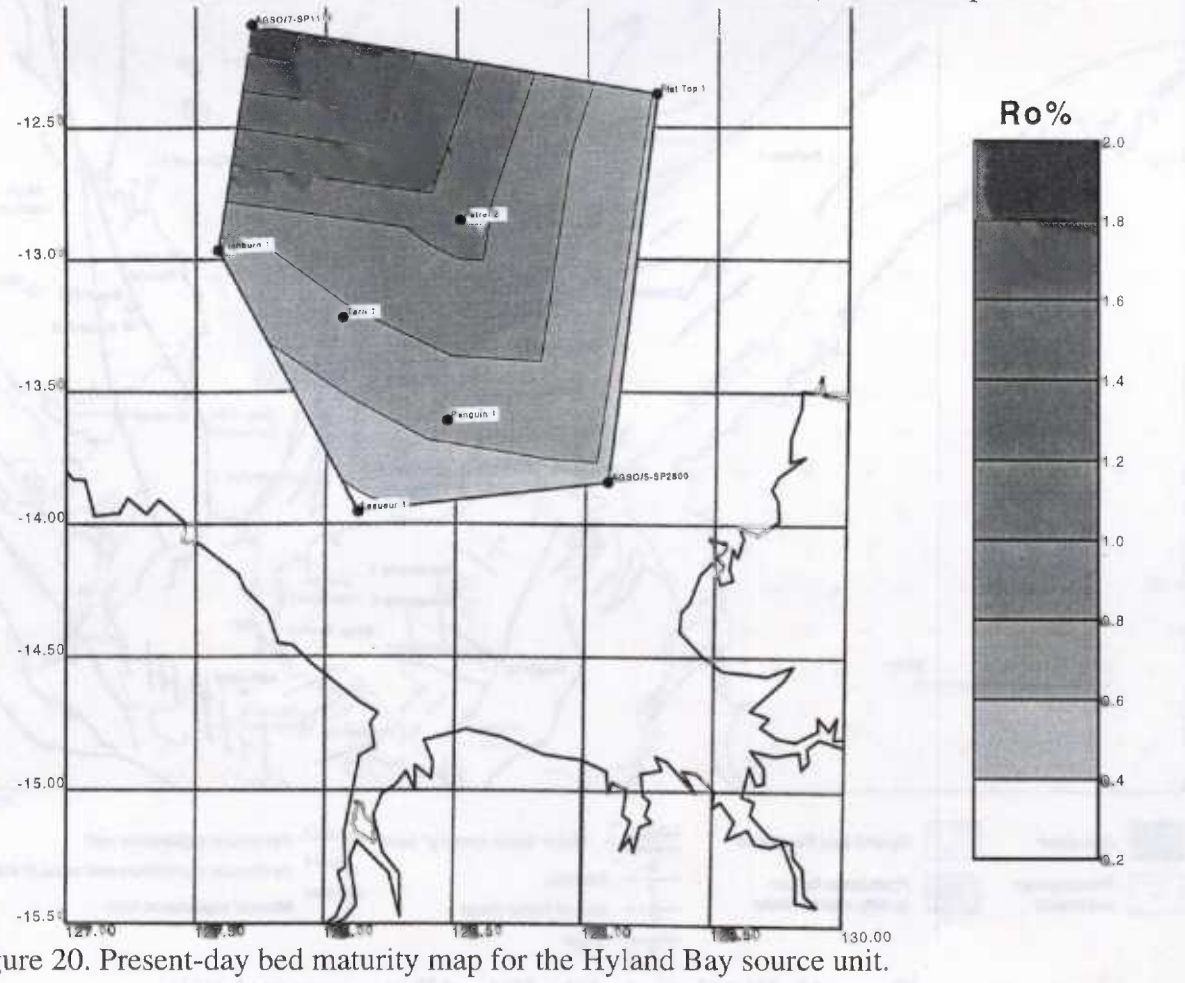

Figure 20. Present-day bed maturity map for the Hyland Bay source unit.

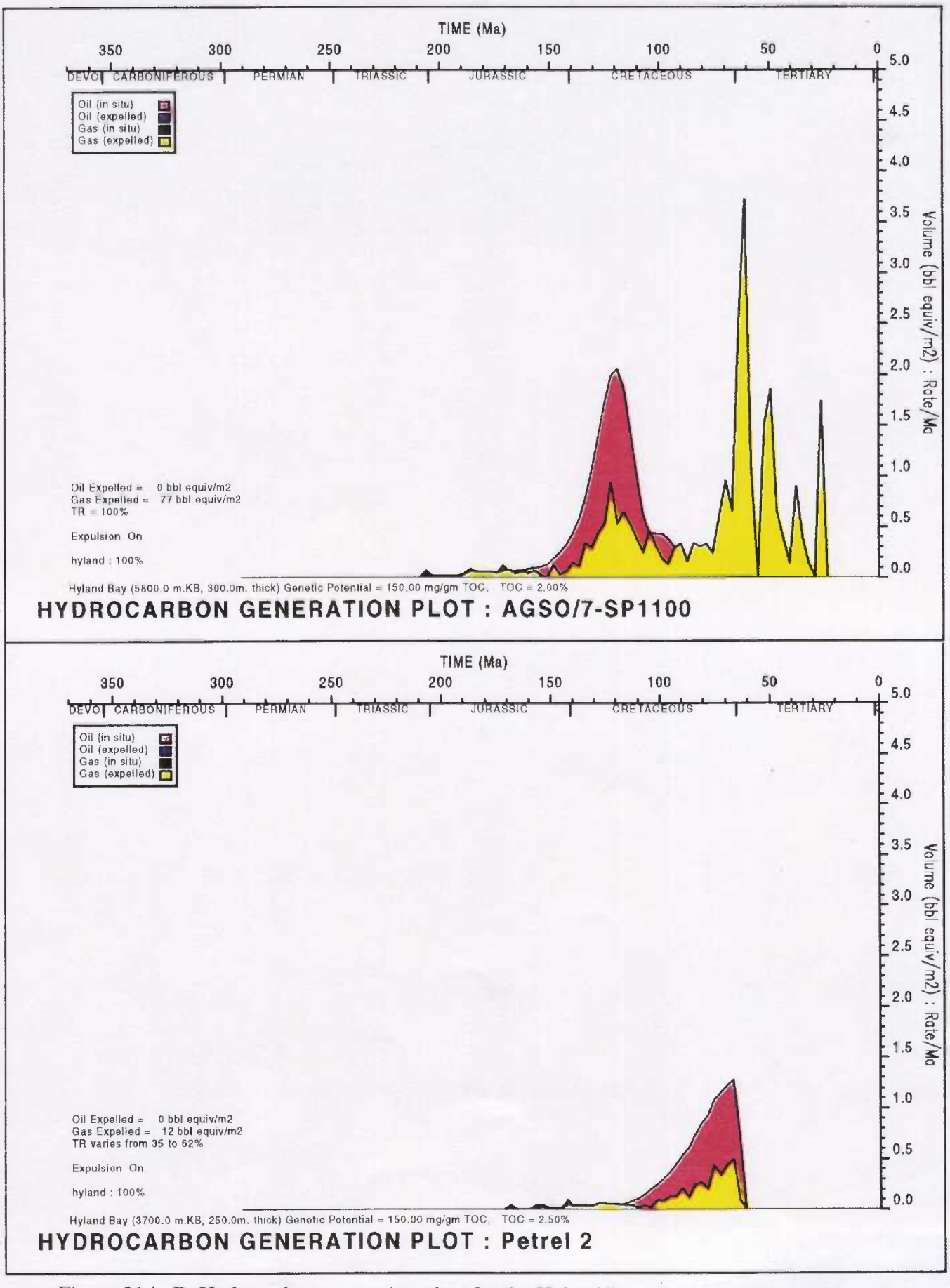

Figure 21A, B. Hydrocarbon generation plots for the Hyland Bay source unit in:
A) Pseudo-well AGSO/7-sp1100, B) Petrel-2.

Conclusions

Subsidence modelling has identified nine distinct tectonic subsidence phases that controlled the regional basin-fill architecture and stratigraphic history of the Petrel Sub-basin. A phase of Cambrian-Ordovician subsidence (Phase A) was initiated by crustal extension and extrusion of tholeiitic basalts in the Early Cambrian. The major Petrel rift structure developed in the late Givetian-Frasnian, and this "syn-rift" extensional phase (Phase B) was terminated by widespread uplift and erosion in the mid Tournaisian. Subsequent tectonic phases (Phases C, D, E and F) appear to have been controlled by re-newed upper and/or lower crustal extension and subsequent thermal sag. Many of these extensional-sag cycles were interrupted by subsequent events, such that the initial rapid mechanical subsidence stage of a new tectonic cycle was superimposed on the slow thermal sag stage of the preceding phase(s).

Compressive tectonism during the Middle Triassic - Early Jurassic (Fitzroy Movement) resulted in widespread uplift and erosion of the flanks of the Petrel Sub-basin, and the formation of inversion anticlines in the central Petrel Deep (Phase G). This compressive basin phase was followed by a phase of minimal net tectonic subsidence throughout most of the Jurassic (Phase H). Two subsequent pulses of relative rapid to slow subsidence in the late Oxfordian and Valanginian (jointly Phase I) correlate with the Argo and Gascoyne spreading events along the outer margin of the North West Shelf. A final subsidence phase in the Tertiary (Phase J) is poorly constrained in the Petrel Sub-basin.

Maturation modelling of three identified source rock units in the Petrel Sub-basin (mid Milligans, Keyling and Hyland Bay source units) has led to a much improved understanding of the maturation, expulsion, migration and trapping history of hydrocarbons discovered in the basin, and provides new insights into the basin's future exploration potential.

Composite biodegraded and non-biodegraded oils recovered in the Turtle and Barnett wells were probably charged by hydrocarbons expelled from the mid-Milligans source unit within depocentres to the north and south of the Turtle-Barnett High. Expulsion from the northern source kitchen probably occurred during the mid Carboniferous (Namurian), and this oil was biodegraded as it migrated into shallow, oxidised, fluvial-deltaic reservoirs on the Turtle-Barnett High. Expulsion from the southern source kitchen (Cambridge Trough) probably occurred during the Early Permian following the deposition of the Treachery Shale which forms a regional seal for hydrocarbons sourced from the Milligans Formation. This oil accumulated in the now more deeply buried stacked reservoirs across the Turtle-Barnett High, and was sealed from oxidising groundwaters by the Treachery Shale. Subsequent fault reactivation, probably during the Fitzroy Movement, resulted in partial breach of this seal, and a second phase of oxidation and biodegradation of the shallower oil accumulations.

Stratigraphic traps within the Cambridge Trough (stratigraphic pinchouts and basin floor fans in the lower Milligans Supersequence) were probably charged by oil expelled from the mid-Milligans source unit during the Early Permian, and these accumulations are unlikely to be biodegraded since the regional Treachery Shale seal was deposited prior to the expulsion of oil. Any stratigraphic or combined stratigraphic-structural traps to the north of the Turtle-Barnett High (e.g., upper slope carbonate mounds within the Tanmurra Sequences) would have been sealed by intraformational shales.

Oil shows in the recently drilled Waggon Creek-1 well were probably expelled during the Permian from the mid Milligans source unit in the central Carlton Sub-basin. These oils could source onlapping turbiditic sand pinchouts against the basal Milligans Supersequence boundary on the flanks of the Carlton Sub-basin, as well as underlying reefal plays in the Ningbing Supersequence.

The Tern Gas Field and the Petrel Gas-Condensate Field were probably charged by gas expelled from the Keyling and/or Hyland Bay source units in the outer and central Petrel Deep during the Late Triassic-Cretaceous (Keyling source) and Tertiary (Hyland Bay source). Shales within the Keyling Supersequence also have the potential to generate minor amounts of oil; in the outer Petrel Deep, this oil was probably expelled during the Late Permian, prior to structuring and trap formation in the Middle Triassic - Early Jurassic (Fitzroy Movement). In the central Petrel Deep (e.g., Petrel-2), this oil was probably expelled during and shortly after structuring, and may have contributed to the condensate recovered at the Petrel Field. On the shallower southern flank of the Petrel Deep (e.g., Tern-1, Fishburn-1), minor amounts of oil were probably expelled during the Cretaceous and Tertiary.

High-quality, immature to marginally mature, oil-prone, coaly shale source rocks are known to occur in the Kinmore-1 and Flat Top-1 wells, but maturation models suggest that they have expelled little or no hydrocarbons in these wells. If these high-quality source rocks extend to deeper portions of the Petrel Deep (e.g., below TD at Petrel-2), they probably expelled significant quantities of oil and gas during the Early Triassic, prior to the main phase of structuring and trap formation during the Fitzroy Movement. Thus, any stratigraphic or combined structural-stratigraphic traps of Permian-Early Triassic age on the flanks of the Petrel Deep may have been charged by oil expelled from the Keyling coaly shale and shale facies in the Petrel Deep during the Early Triassic.

Acknowledgments

I wish to thank Ian Deighton, Paltech Pty. Ltd., for valuable assistance on all aspects of the WinBury program, and on geohistory analysis in general. AGSO colleagues Jim Colwell and Jane Blevin are thanked for input of seismic interpretation data and discussions on structural aspects of the Petrel Sub-basin, and Dianne Edwards and Chris Boreham for assistance with source rock and kerogen kinetic data. Ken Baxter (CSIRO, AGCRC) is thanked for discussions on tectonic subsidence patterns and subsidence mechanisms. Heike Struckmeyer, Jim Colwell, Dianne Edwards and Tom Loutit are thanked for their constructive comments and review of this report.

References

ALLEN, P.A., & ALLEN, J.R., 1990. Basin Analysis, Principals and Applications. Blackwell Scientific Publications, Oxford, 451 pp.

BAXTER, K., 1996. Flexural isostatic modelling of the Petrel Sub-basin, Australian North West Shelf. CSIRO Internal Report.

BICKFORD, G.P., BISHOP, J.H., O'BRIEN, G.W. & HEGGIE, D.T., 1992. Light hydrocarbon geochemistry of the Bonaparte Gulf Basin, including the Sahul Syncline, Malita Graben and northern Petrel Sub-basin: Rig Seismic Survey 99. Bureau of Mineral Resources, Australia, Record 1992/50.

BISHOP, J.H., O'BRIEN, G.W., BICKFORD, G.P. & HEGGIE, D.T., 1992. Light hydrocarbon geochemistry of the Bonaparte Gulf Basin, including the Sahul Syncline, Malita Graben and southern Petrel Sub-basin: Rig Seismic Survey 100. Bureau of Mineral Resources, Australia, Record 1992/47.

COLWELL, J.B., BLEVIN, J. B., & WILSON, D.J., 1996. Petrel Sub-basin Study 1995-1996, Map and Seismic Folio. Australian Geological Survey Organisation.

COLWELL, J.B., & KENNARD, J.M, (compilers) 1996. Petrel Sub-basin Study 1995-1996, Summary Report. Australian Geological Survey Organisation, Record 1996/40.

DEIGHTON, I., 1992. Burial and thermal geohistory analysis: A short course. Sedimentologists Specialist Group, Geological Society of Australia, August 1992, 84 pp.

EDWARDS, D.S., & SUMMONS, R.E., 1996. Petrel Sub-basin Study 1995-1996, Organic Geochemistry of oils and source rocks. Australian Geological Survey Organisation, Record 1996/42.

EPSTEIN, A.G., EPSTEIN, J.B., & HARRIS, L.D., 1977. Conodont colour alteration - an index to organic maturity. United States Geological Survey Professional Paper 995, 27 pp.

ERTHERIDGE, M.A., & O'BRIEN, G.W., 1994. Structural and tectonic evolution of the Western Australian basins system. The PESA Journal, 22, 45-63.

GREENLEE, S.M., & LEHMANN, P.J., 1993. Stratigraphic framework of productive carbonate buildups. In: Loucks, R.G., & Sarg, J.F. (Eds), Carbonate Sequence Stratigraphy, Recent Developments and Applications. American Association of Petroleum Geologists Memoir 57, 43-62.

JONES, P.J., NICOLL, R.S., SHERGOLD, J.H., FOSTER, C.B., KENNARD, J.M., & COLWELL, J.B., 1996. Petrel Sub-basin Stratigraphic Time Chart. Australian Geological Survey Organisation, Chart 1/96.

KENNARD, J.M., 1996. Petrel Sub-basin Study 1995-1996, Well Folio. Australian Geological Survey Organisation.

McKENZIE, D., 1978. Some remarks on the development of sedimentary basins. Earth & Planetary Sciences Letters, 40, 25-32.

MORY, A.J., 1991. Geology of the offshore Bonaparte Basin, northwestern Australia. Geological Survey of Western Australia, Report 29, 47 pp.

MORY, A.J., & BEERE, G.M., 1988. Geology of the onshore Bonaparte and Ord Basins in Western Australia. Geological Survey of Western Australia, Bulletin 134, 184 pp.

Appendix A: WinBury Geohistory Modelling Flow Diagram

1. Subsidence / Uplift Modelling
   ⇓ ⇑
2. Thermal Modelling
3. Source Rock Maturation Modelling

1. Subsidence / Uplift Modelling

A. Single Well Mode

Stratigraphy:

- Sequences (Mega-, Super-)
- Thickness in wells
- Sub TD seismic interpretation
- Age based on biostratigraphic/sequence chart
- Palaeo-water depth (min/max): sedimentology & palaeogeography
- Lithology: default porosity/compaction & thermal conductivity

Unconformities / eroded section

- Thickness, age of deposition/erosion, lithology

Sea level curve

- Exxon Mesozoic converted to AGSO Timescale
- ?Palaeozoic

Subsidence/Uplift history

- Stripped-basement Tectonic Subsidence
- Sediment loading, Compaction, Water depth removed
- 'Fine-tune' profile to subsidence/uplift models
  Concave extension , convex foreland loading
  Adjust water-depth, age; modify unconformities

B. Multiple Well (Basin) Mode

- Compare wells from same/adjacent tectonic elements
- Ensure consistent subsidence model for each tectonic element

2. Thermal Modelling

A. Single Well Mode

Surface & Bottom Hole Temperature:

- OBS & sniffer sea bed temperatures 28 °C all depths
- Observed well temperature: Log runs, DST
- Estimate stable BHT:
  Horner plots: temp & time since circulation
  Max observed Temperature plus < 10 %

Present-day Heatflow: Surface Temp, BHT, Conductivity

Palaeo-sea bed temperature for each sequence

- Palaeo-water depth, palaeo-latitude, palaeo-climate

Observed maturity data

- Rv, FAMM, TAI, SCI, Tmax, CAI, AFTA
- Convert each parameter to equivalent Rv level

Palaeo-Heat Flow:

- Tectonic events/processes (Extension & Thermal Sag)
- Iterative to match Modelled & Observed maturity
- Modify subsidence/unconformity models as necessary:
  - Thickness, Age, Lithology of eroded section

B. Multiple Well (Basin) Mode

- Present-day Heat Flow Model
- Palaeo-Heat Flow Model for each tectonic element

Re-evaluate & re-iterate everything to achieve best model !!

3. Source Rock Maturation Modelling

Define Source Unit in Each Well and Pseudo-Well Source Kitchen

- Depth to top of source unit
- Thickness of source unit
- Average TOC of source unit
- Type of kerogen(s)

Define Distribution of Source Unit

- Create well file for wells/pseudo-wells with source unit

Define Age of Source Unit

- Create source unit File and define age of top of source unit

Hydrocarbon Generation Plots: Select View Type

• Summary:	Time (well total)	bbl equiv./m2
	Time (all layers)	bbl equiv./m2
	Depth & Calibration	bbl equiv./m2
• Layer	Volume	bbl equiv./m2
	Rate	bbl equiv./m2
• Sub-layer	Cumulative Volume	bbl equiv./m3
	Cumulative HC	HC generated mg/g TOC
	Rate Volume	bbl equiv./m3: Rate/Ma
	Rate HC	HC generated mg/g TOC: Rate/Ma

Bed Maturity Plots

- Generate for well/pseudo-well source unit file

Bed Maturity Maps

- Generate for present day maturity (Ma = 0)
- Generate for times of critical importance (time of structuring, seal emplacement etc.)

Appendix B:

Basin Stratigraphy Parameters

Observed versus Computed Maturity, Heatflow and Tectonic Subsidence, Geohistory & Hydrocarbon Generation Plots for each well and pseudo-well (alphabetical order)

BASIN STRATIGRAPHY PARAMETERS

Sequence	Age Top (Ma.)	Age Base (Ma.)	Min Water (m)	Max Depth (m)	Seabed Temp. (°C)	Palaeo Lat. (° S/N)
Tertiary	000.0	060.0	-20	30	27.0	14
Hiatus/Erosion 5	060.0	065.0	20	200	25.0	35
Bathurst Island	065.0	136.0	20	200	25.0	40
Flamingo	138.0	152.0	10	50	21.0	50
Plover	154.0	195.0	-20	20	20.0	45
Hiatus/Erosion 4	195.0	200.0	-20	10	16.0	40
Malita	200.0	220.0	-20	10	16.0	35
Fitzroy Erosion	220.0	230.0	-20	20	14.0	30
Hiatus 3	230..0	238.0	-20	20	12.5	30
Cape Londonderry	238.0	245.0	-20	20	11.0	35
H4 + Mt Goodwin	245.0	257.0	10	50	9.0	35
Hyland Bay	257.0	270.0	10	50	7.0	40-45
Fossil Head	272.0	291.0	30	100	5.0	50
Keyling	291.0	294.5	-20	30	5.0	50
Treachery	294.5	296.0	-10	30	5.0	45
Kuriyippi	296.0	314.0	-20	30	5.0	40
Point Spring	315.0	324.0	10	60	12.0	40
Tanmurra 2	324.0	327.0	20	100	18.0	15
Tanmurra 1	327.0	328.0	20	100	19.5	15
Erosion 2	328.0	330.0	20	100	20.0	15
Milligans A5-8	330.0	337.0	30	100	21.0	15
Milligans A1-4	337.0	345.0	30	100	23.0	10
Milligans praecipua	345.0	347.0	10	30	24.0	10
Langfield	347.0	354.0	10	60	24.5	5
Ningbing	354.0	361.0	10	60	25.0	5
Erosion/Hiatus 1	361.0	363.0	10	60	25.0	5
Cockatoo	363.0	369.0	-10	60	25.0	5
?Devonian Salt	369.0	375.0	-10	20	25.0	5

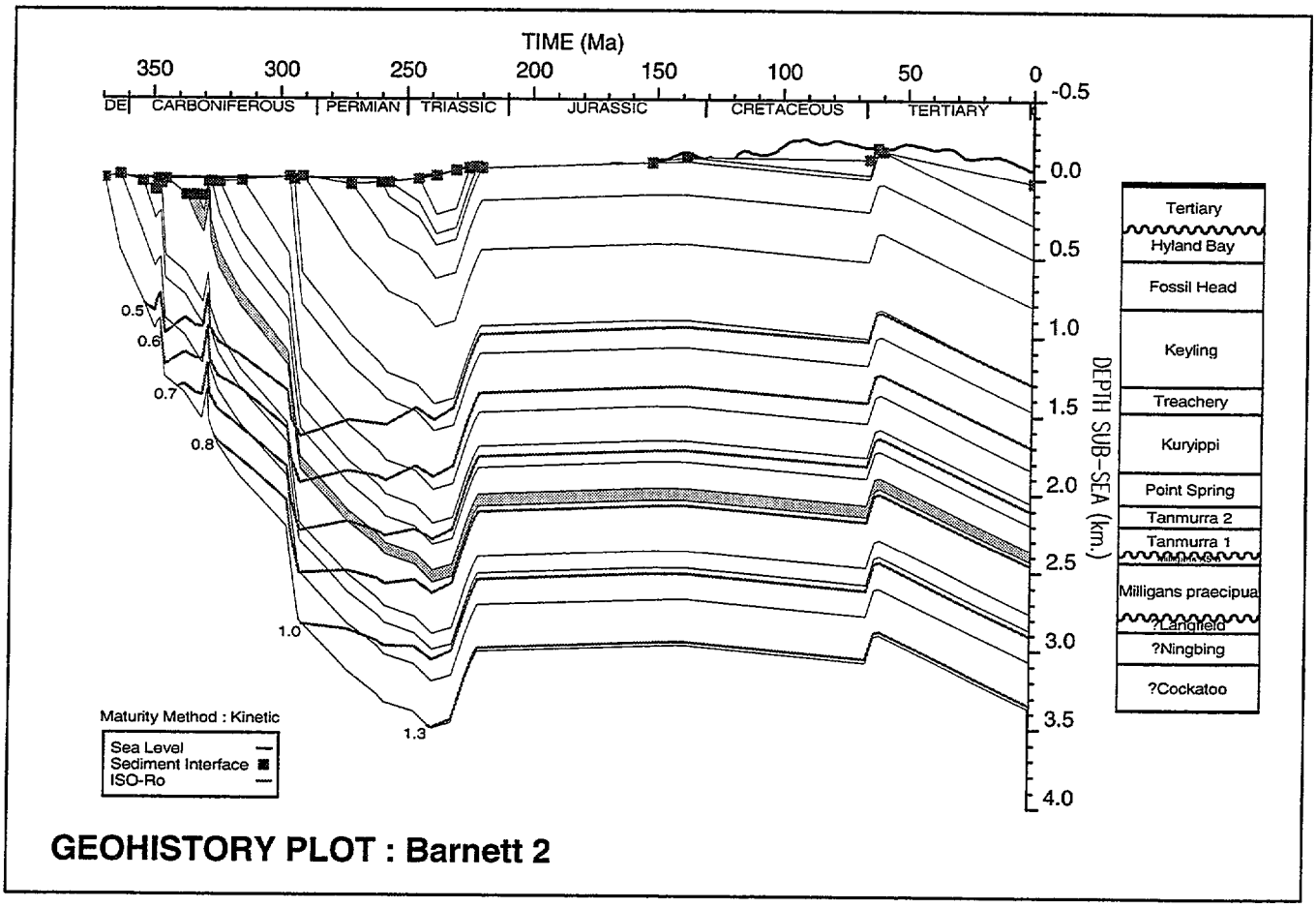

GEOHISTORY PLOT : Barnett 2

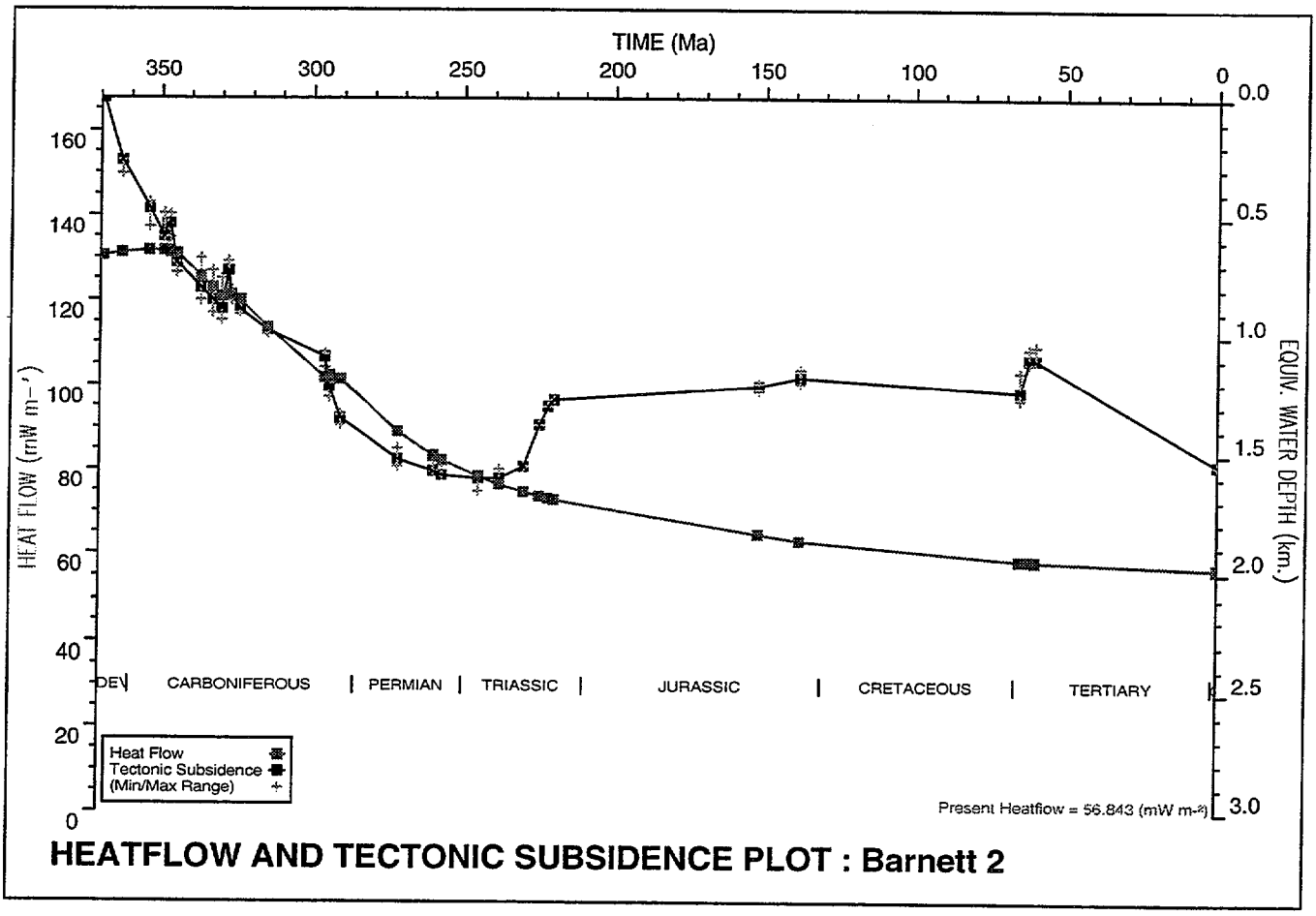

HEATFLOW AND TECTONIC SUBSIDENCE PLOT : Barnett 2

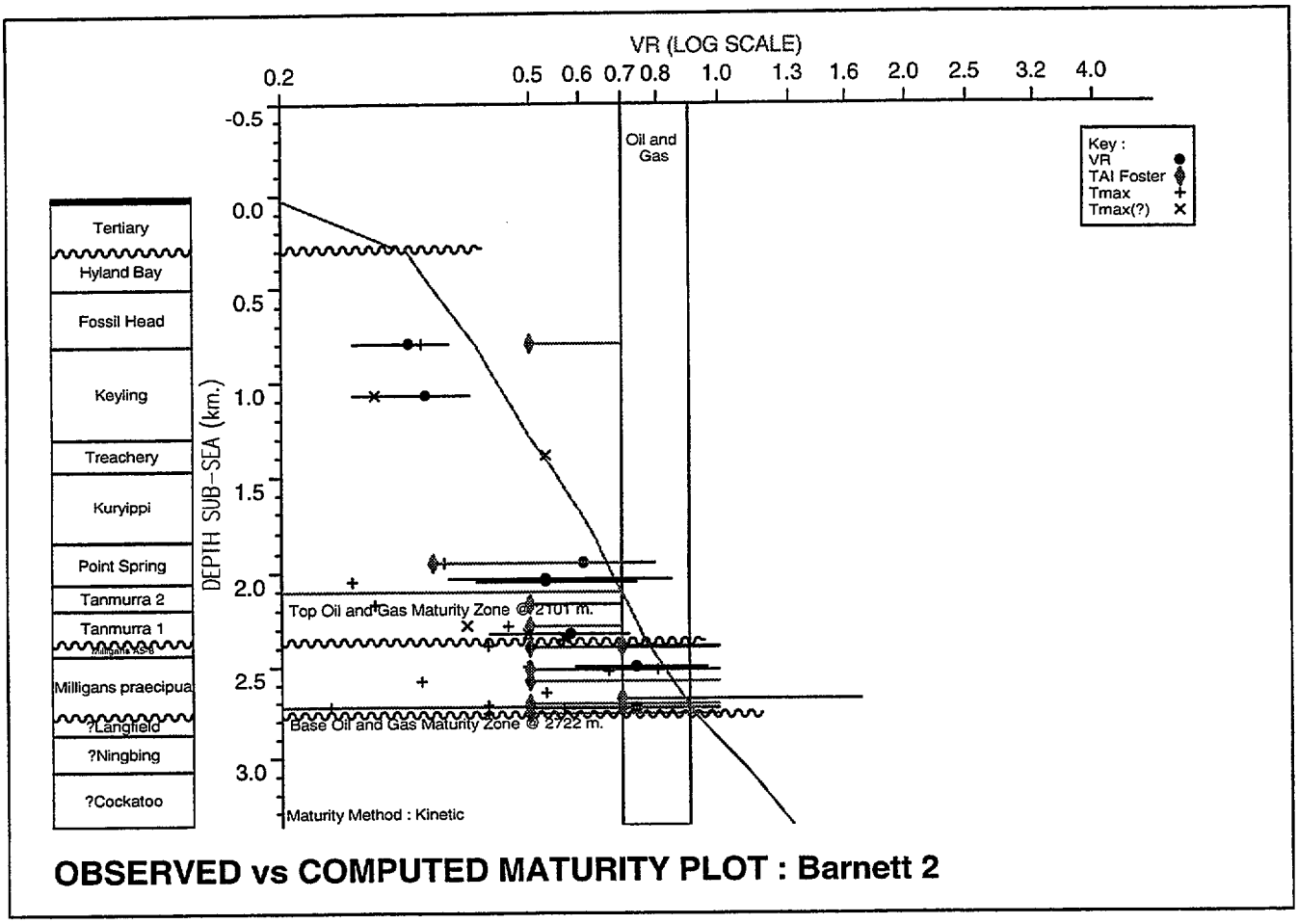

OBSERVED vs COMPUTED MATURITY PLOT : Barnett 2

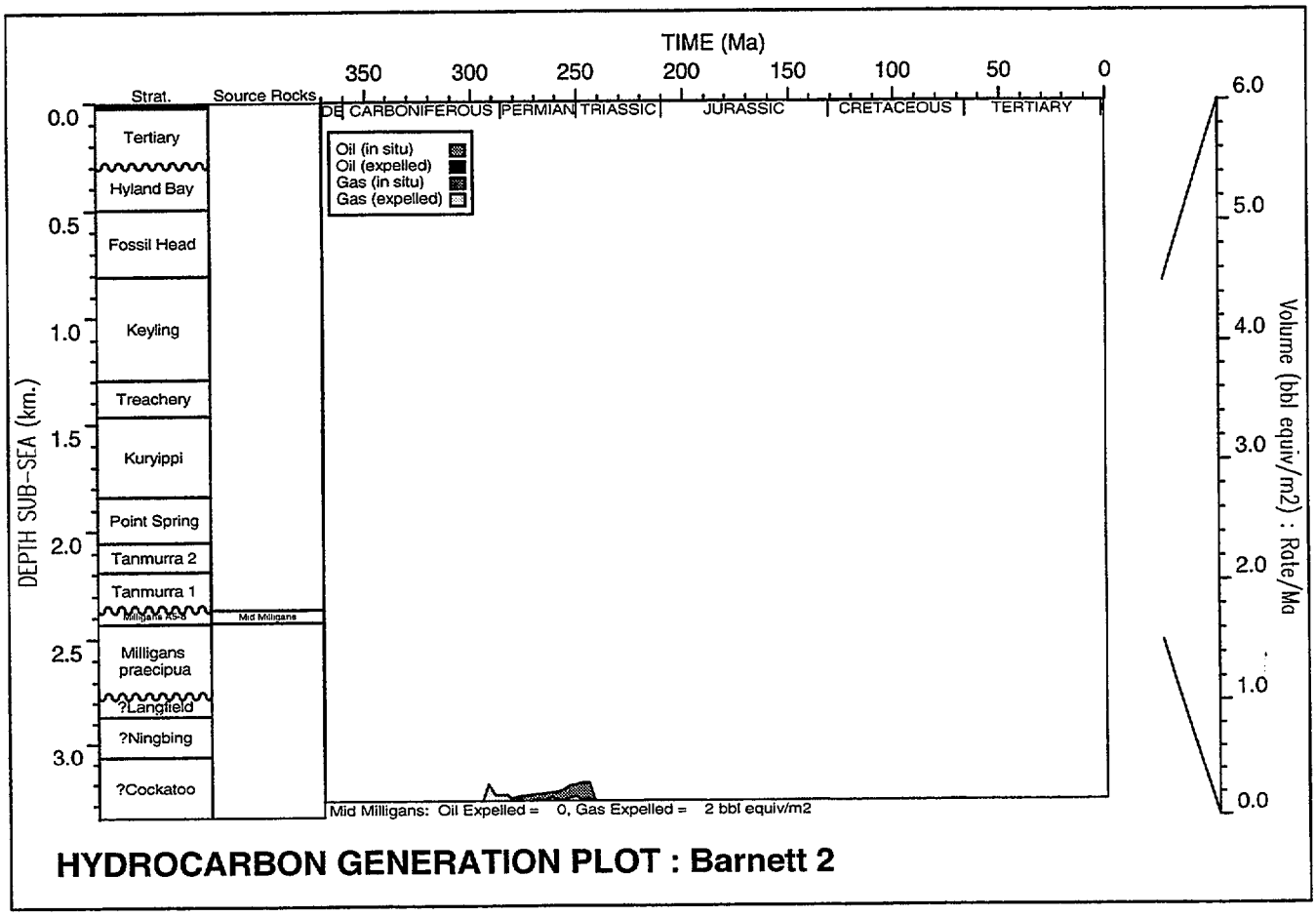

HYDROCARBON GENERATION PLOT : Barnett 2

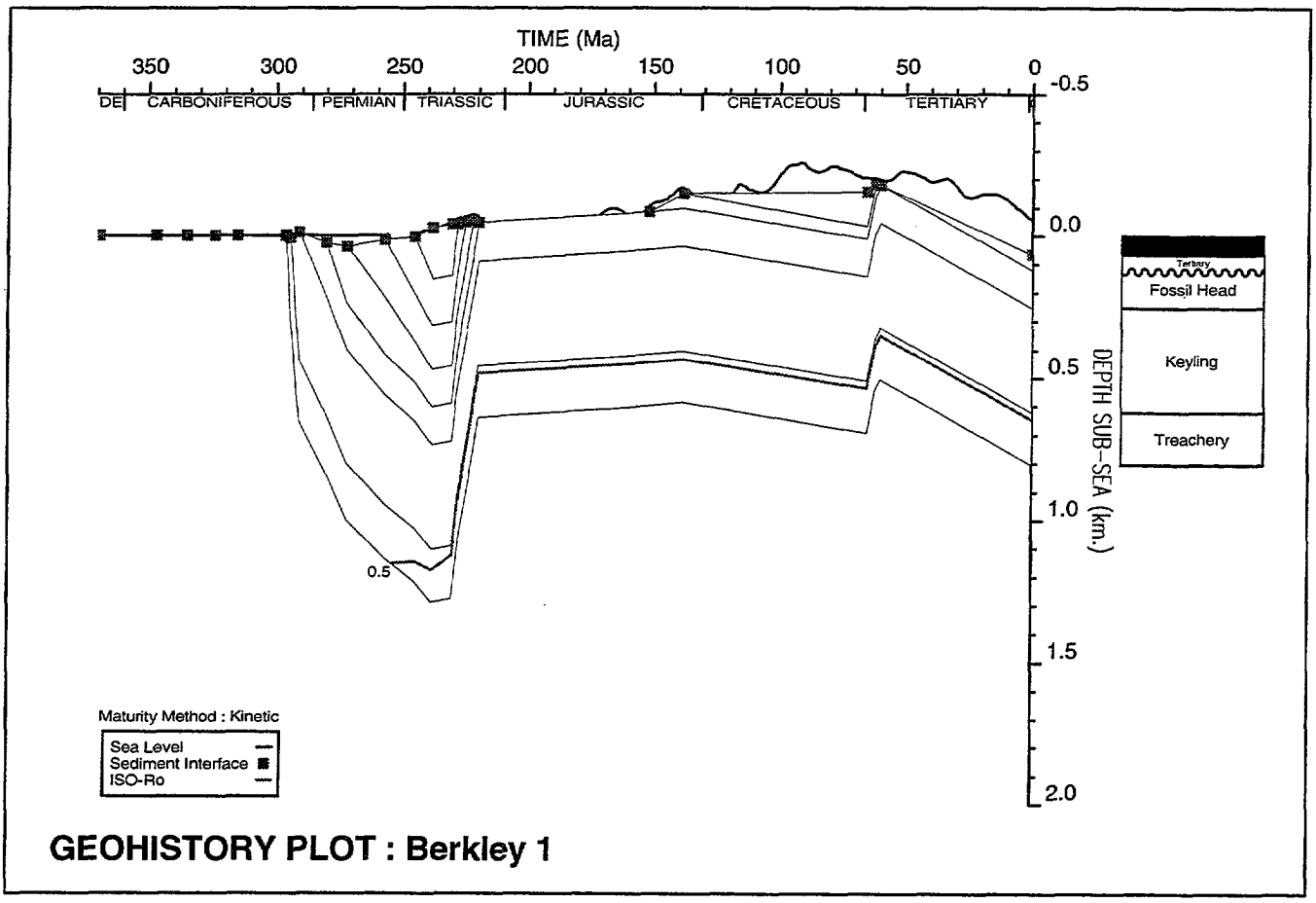

GEOHISTORY PLOT : Berkley 1

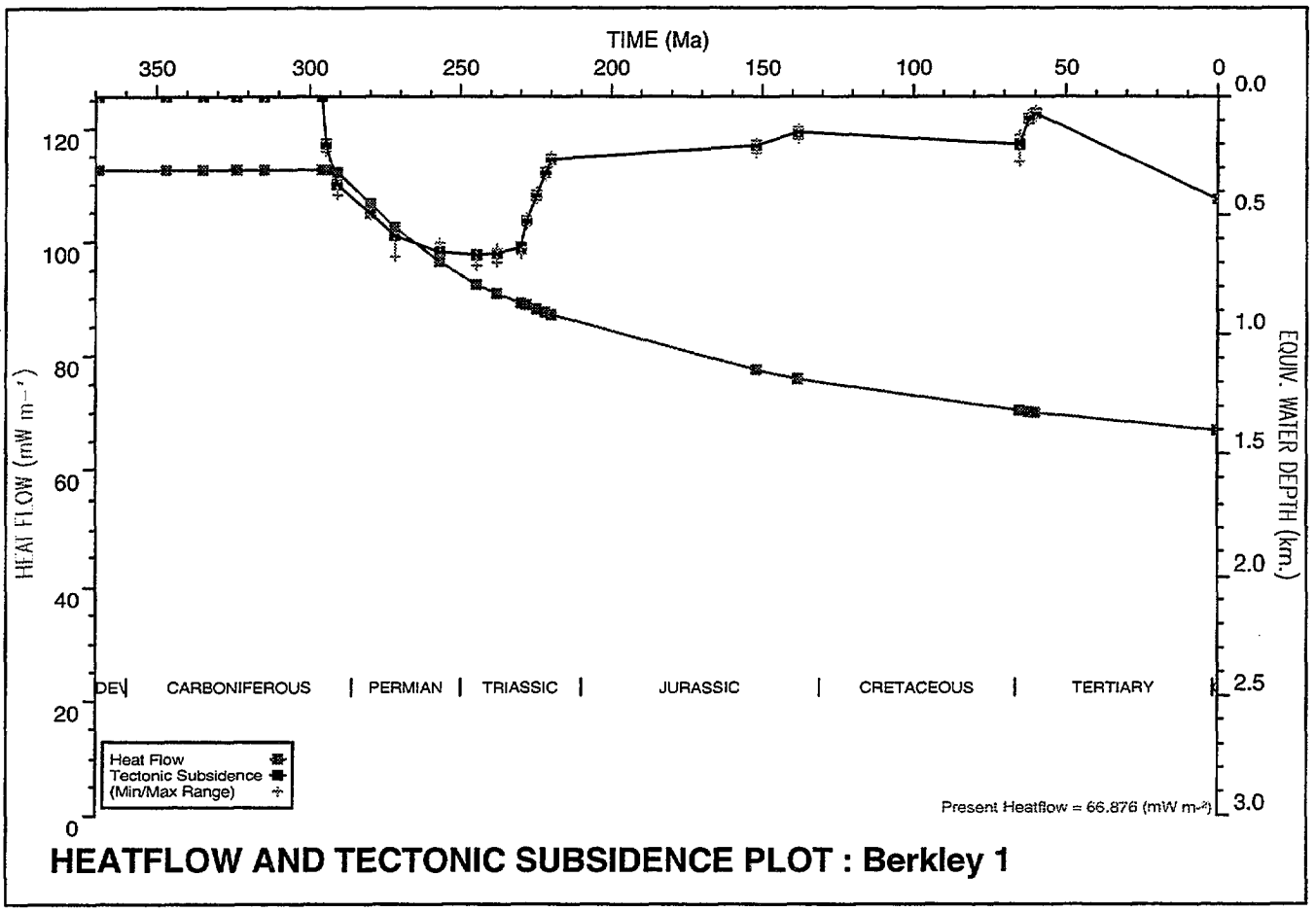

HEATFLOW AND TECTONIC SUBSIDENCE PLOT : Berkley 1

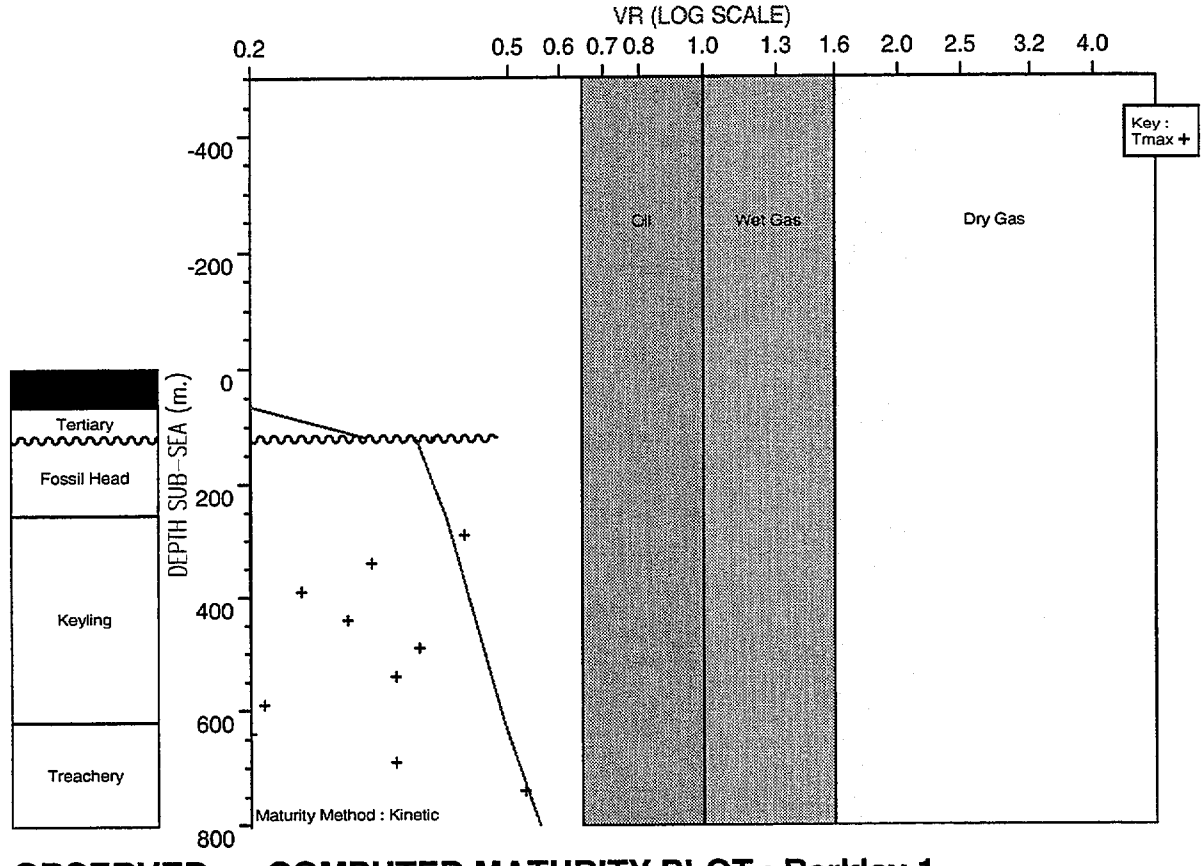

OBSERVED vs COMPUTED MATURITY PLOT : Berkley 1

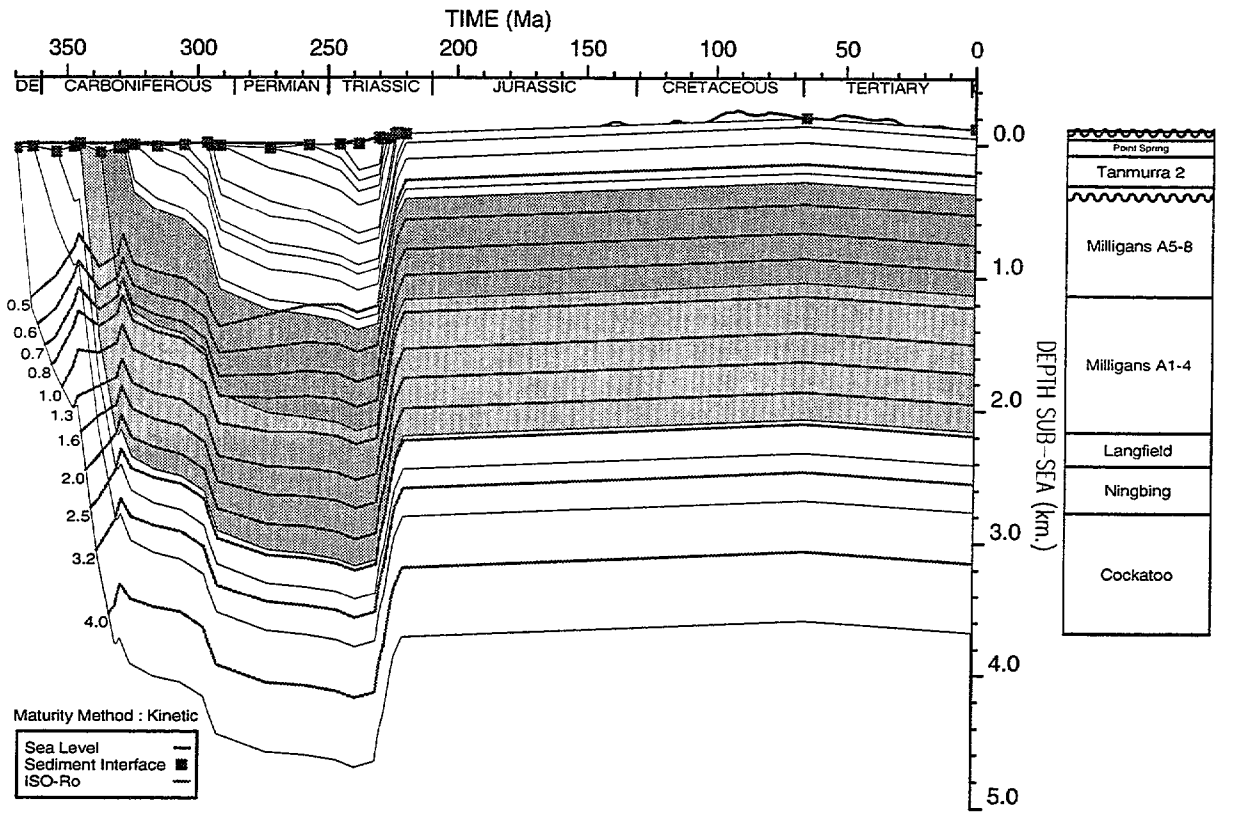

GEOHISTORY PLOT : Bonaparte 1

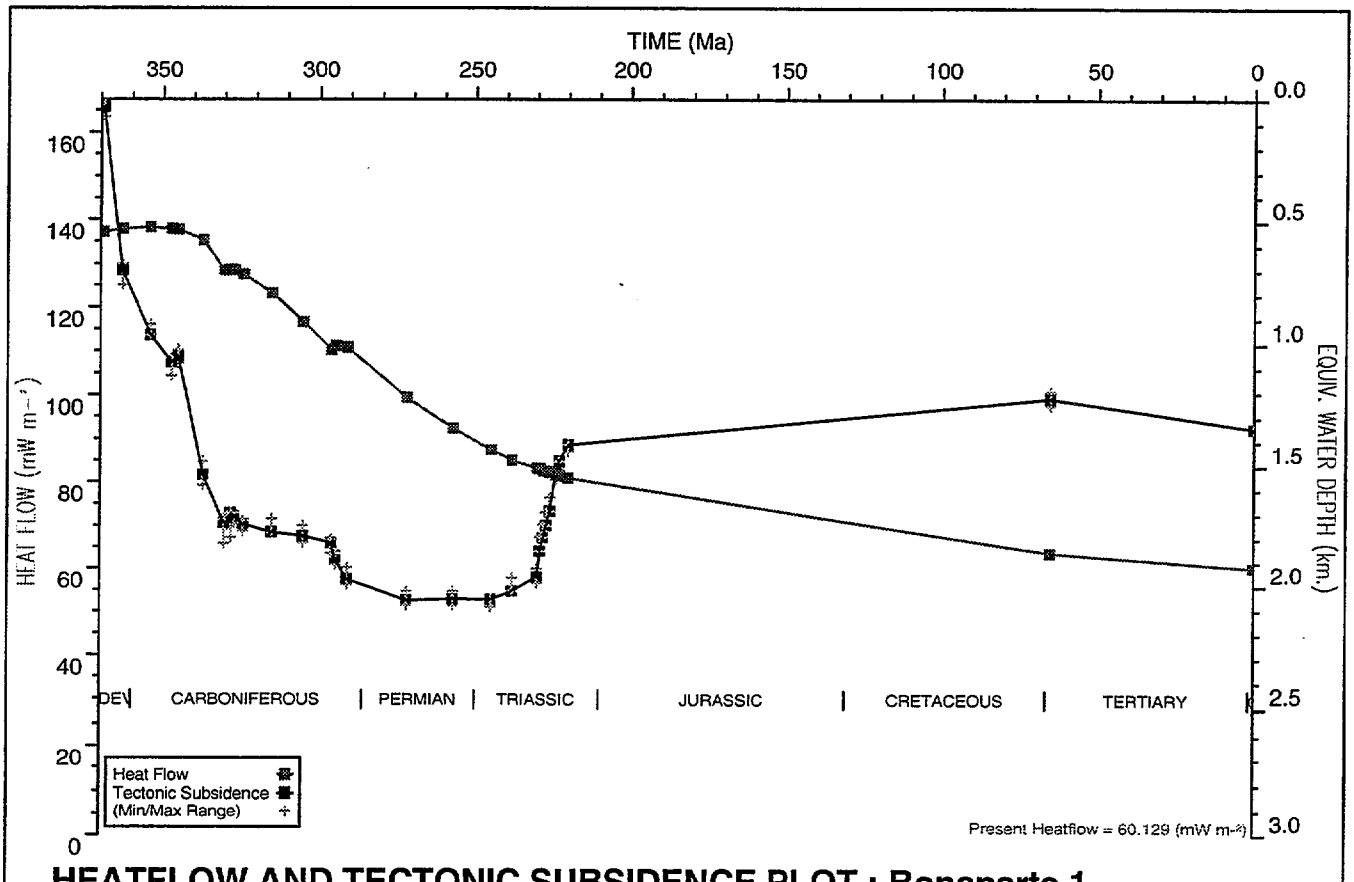

HEATFLOW AND TECTONIC SUBSIDENCE PLOT : Bonaparte 1

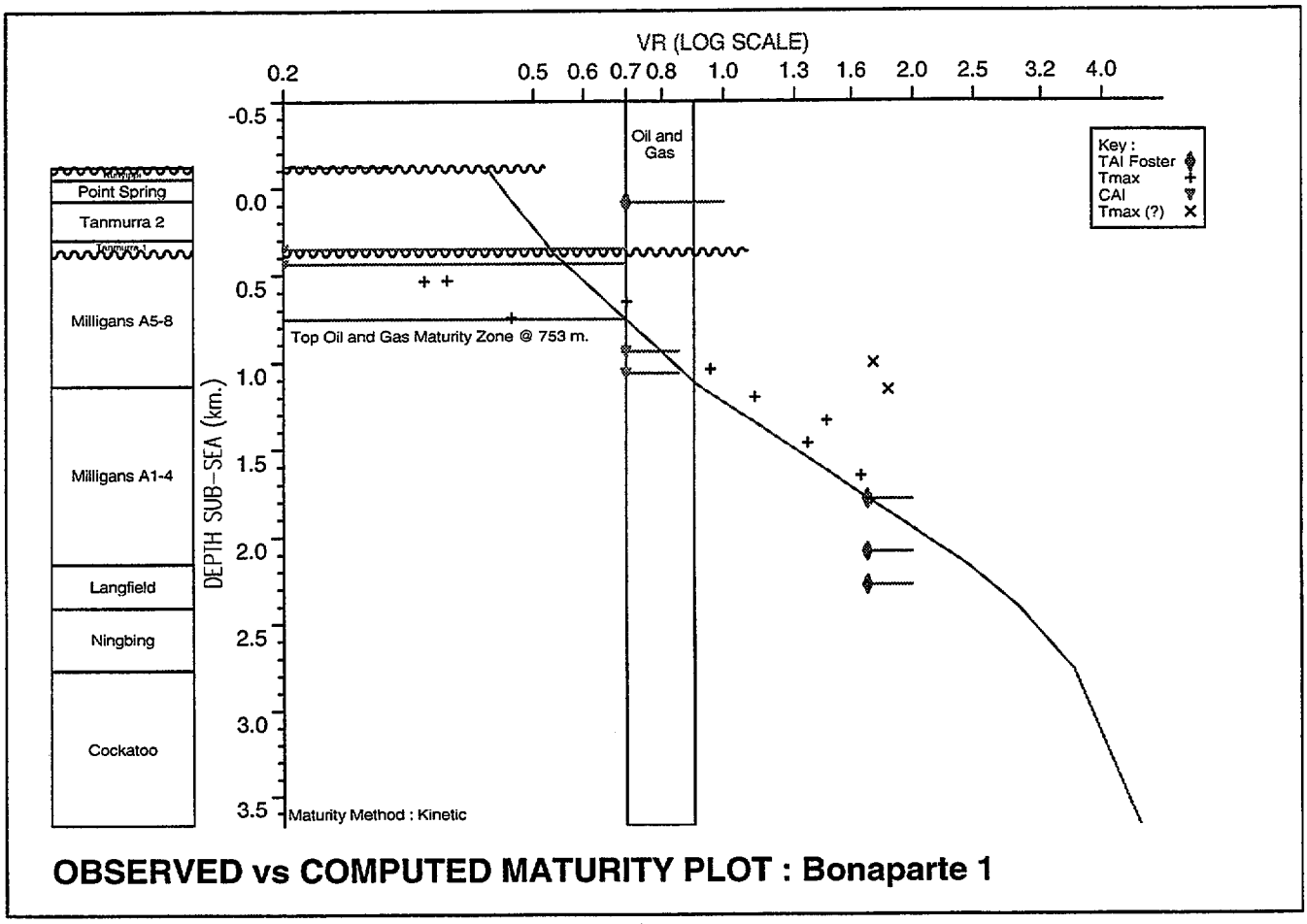

OBSERVED vs COMPUTED MATURITY PLOT : Bonaparte 1

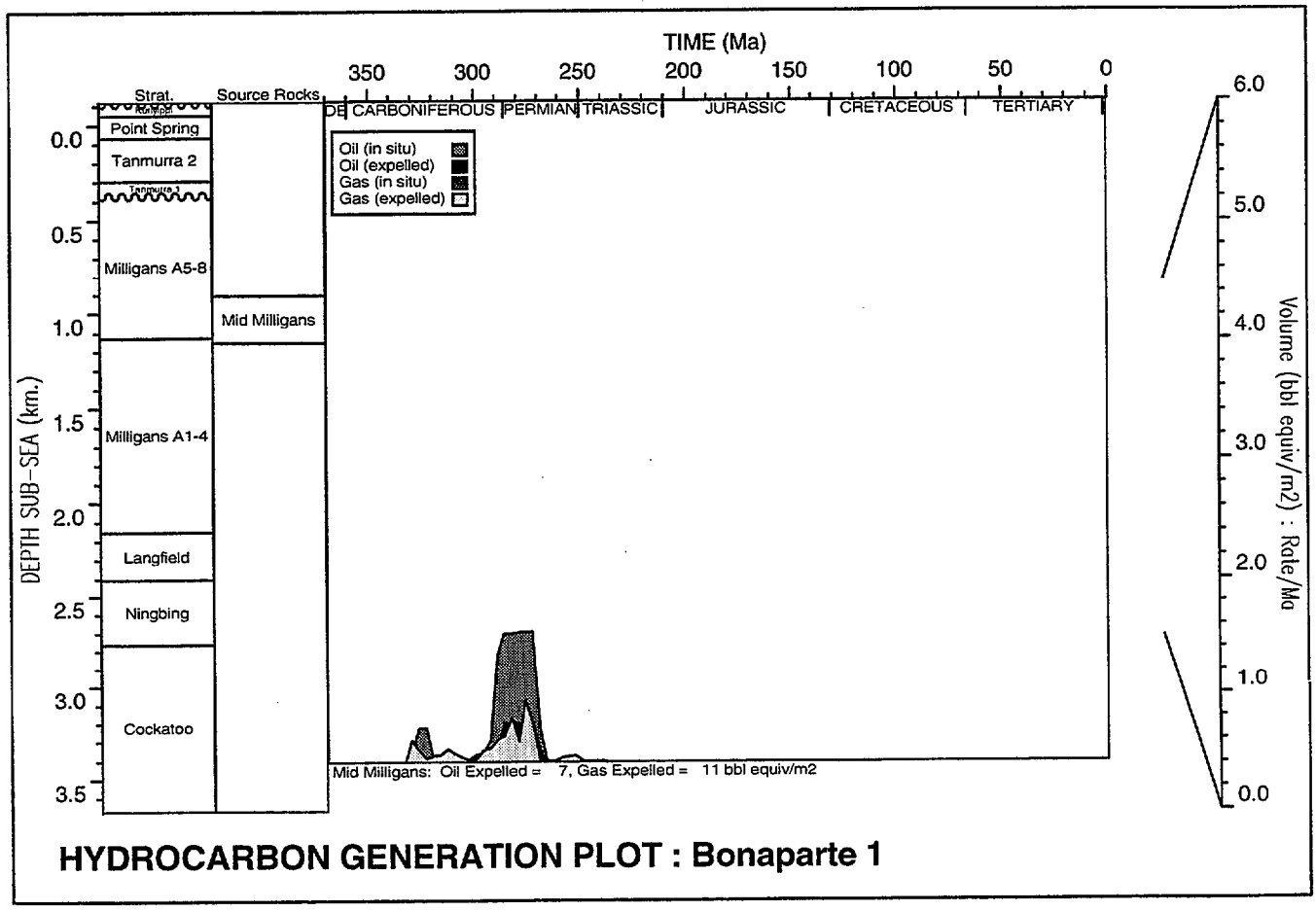

HYDROCARBON GENERATION PLOT : Bonaparte 1

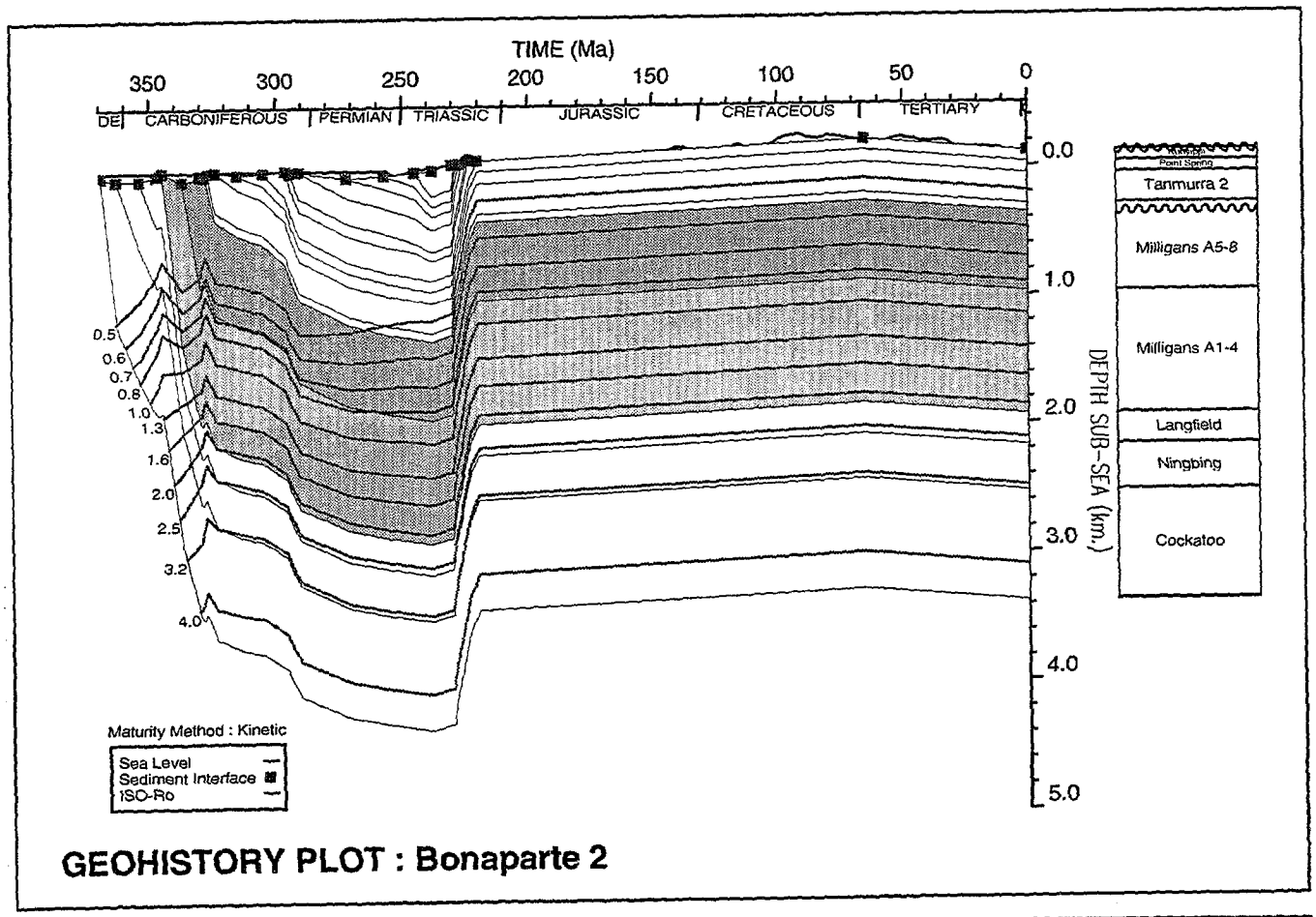

GEOHISTORY PLOT : Bonaparte 2

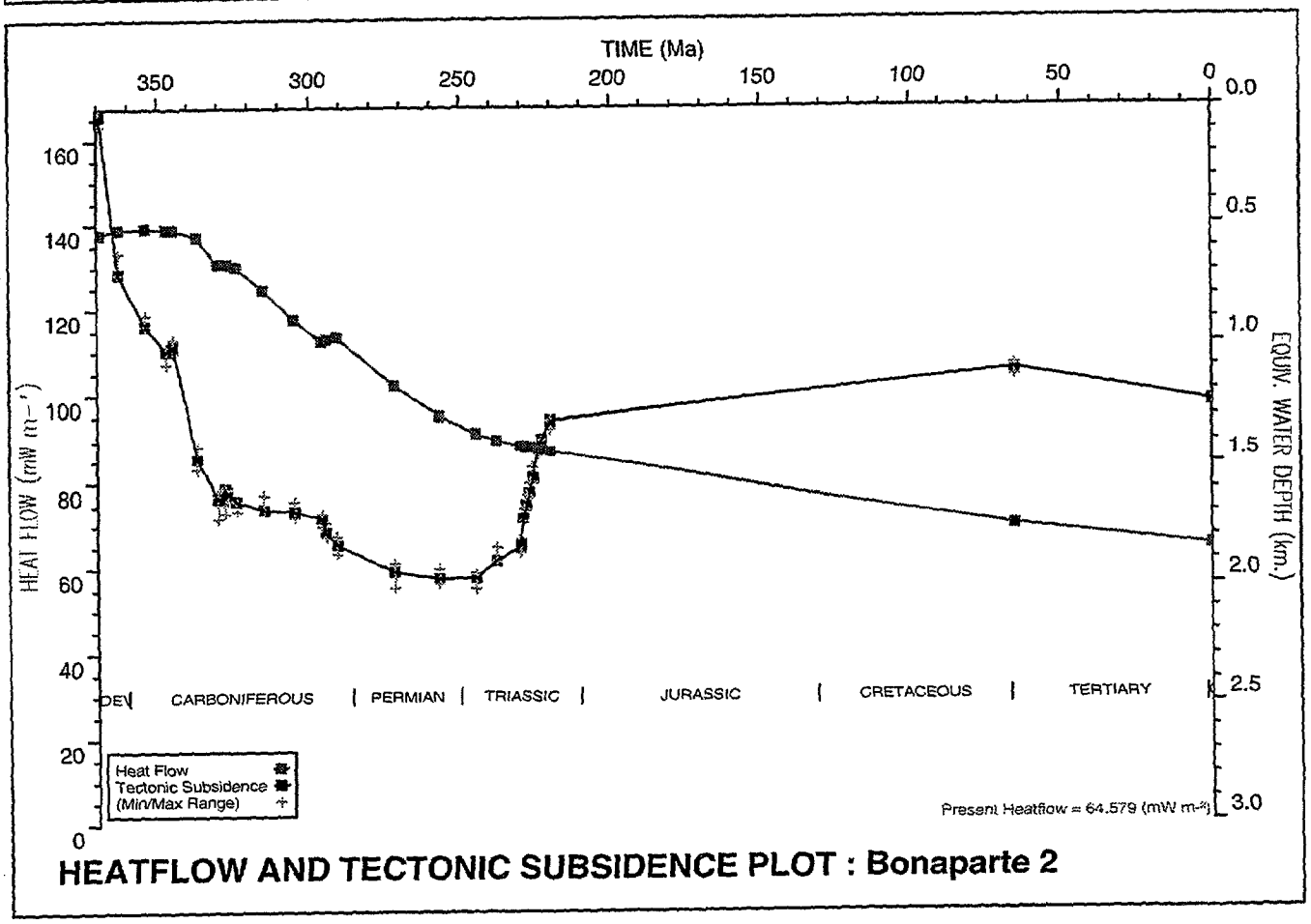

HEATFLOW AND TECTONIC SUBSIDENCE PLOT : Bonaparte 2

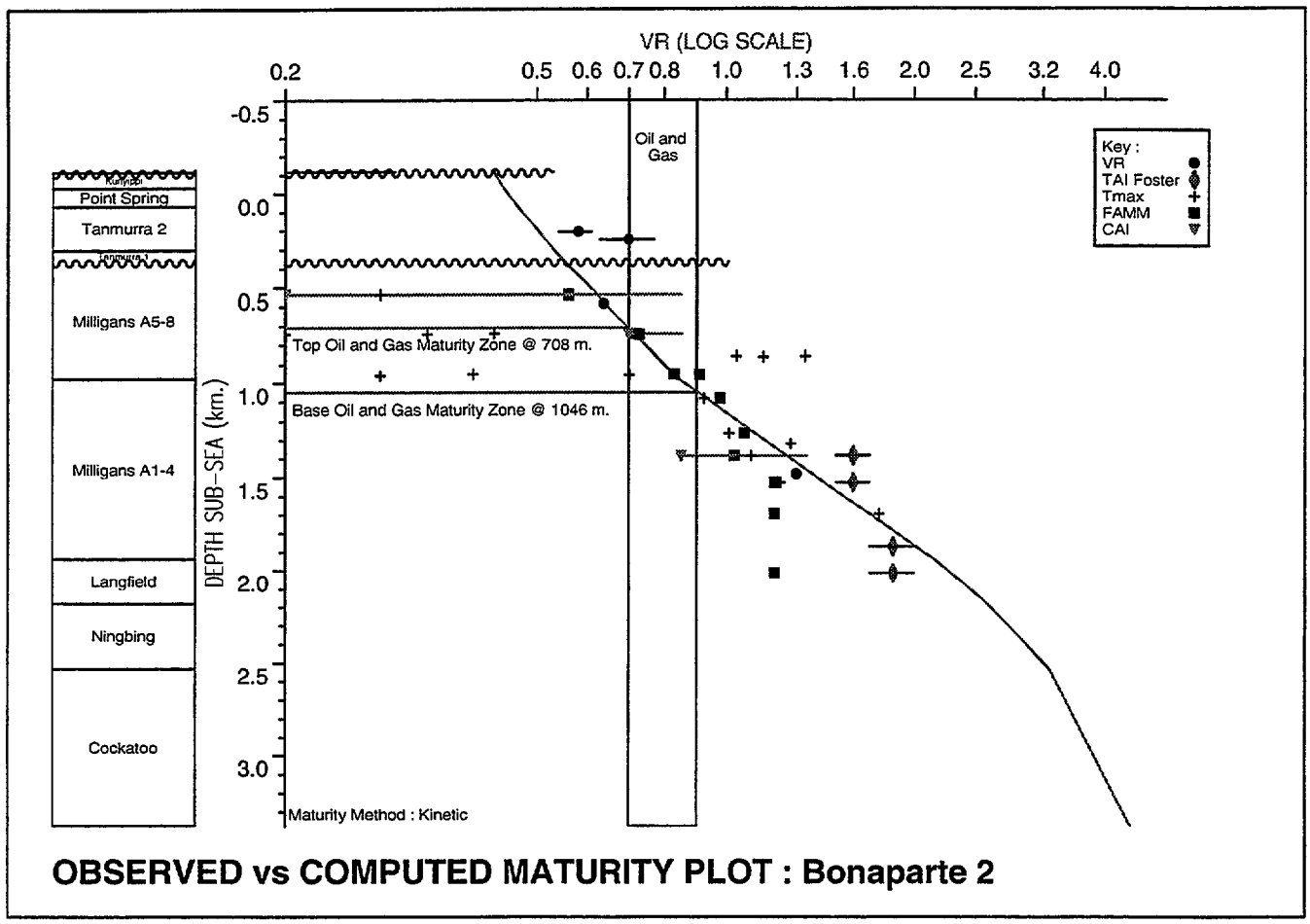

OBSERVED vs COMPUTED MATURITY PLOT : Bonaparte 2

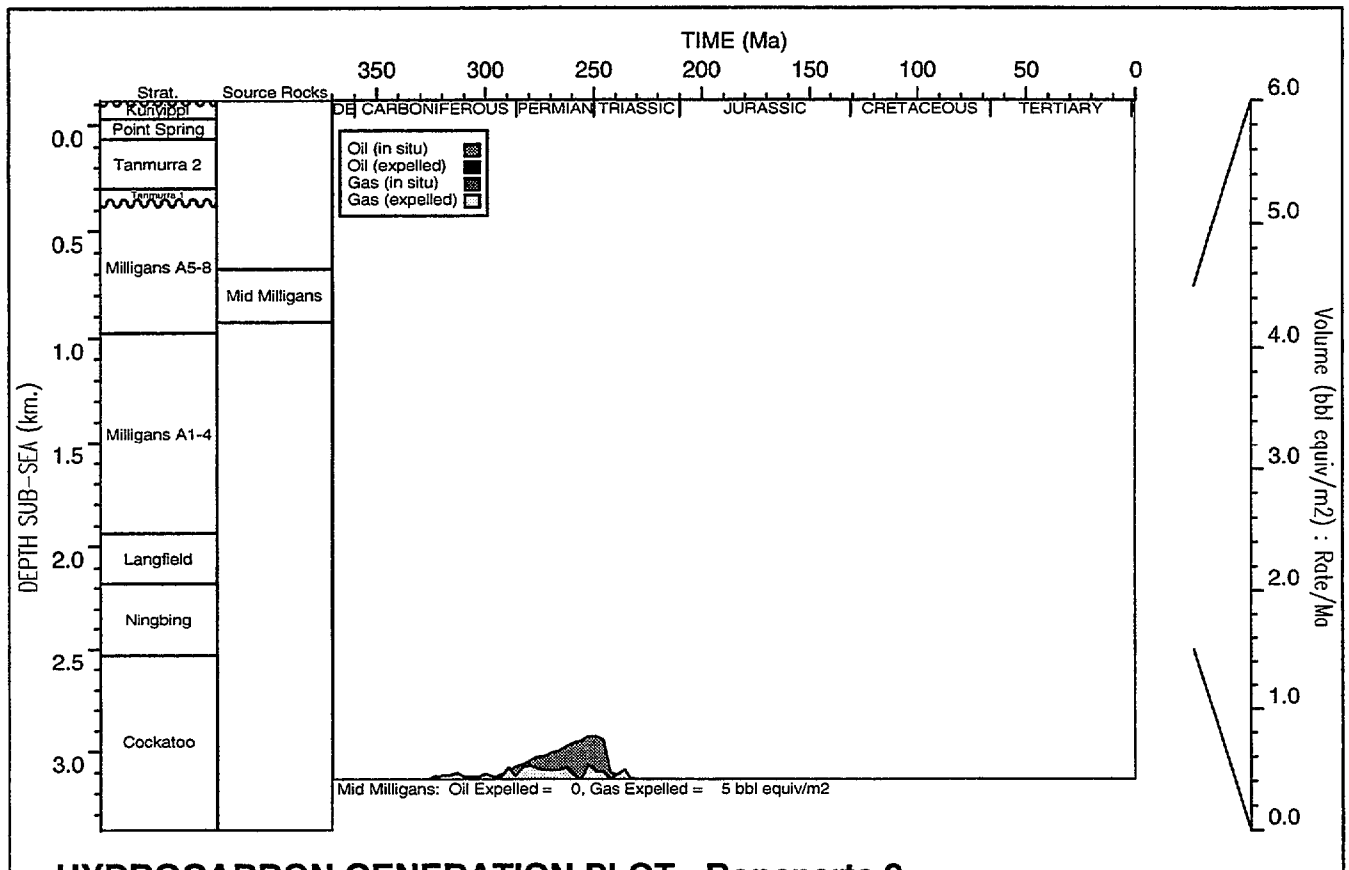

HYDROCARBON GENERATION PLOT : Bonaparte 2

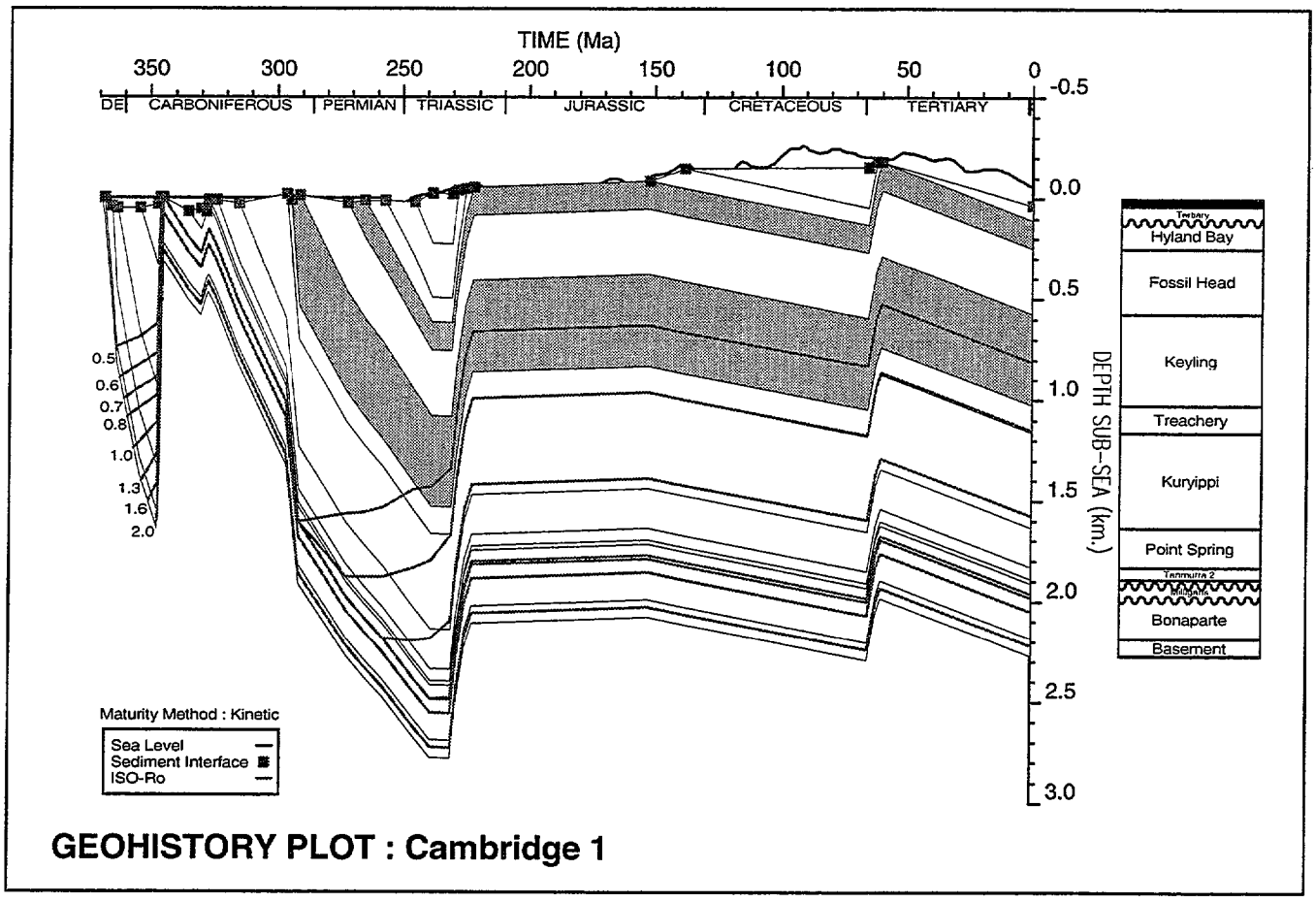

GEOHISTORY PLOT : Cambridge 1

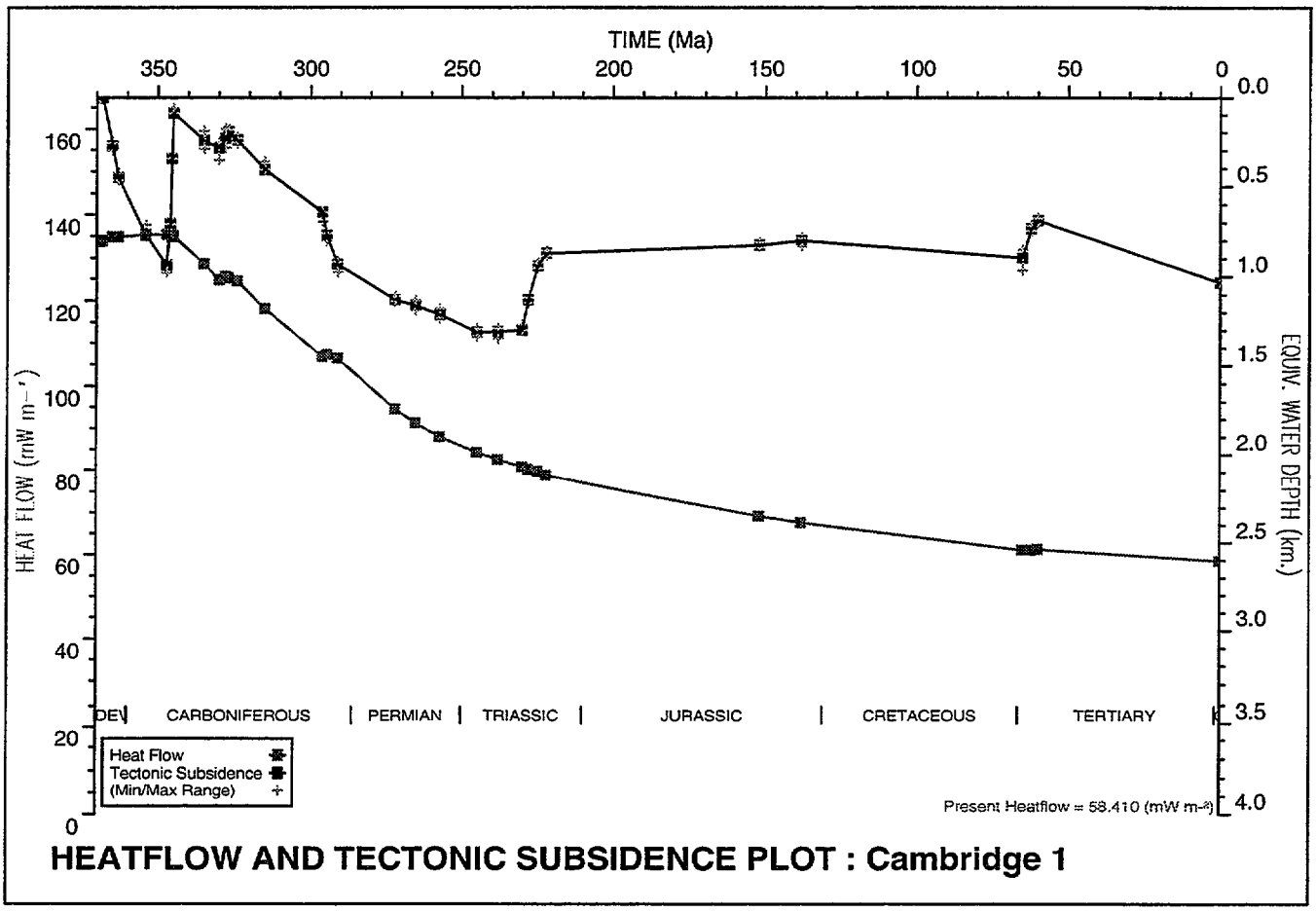

HEATFLOW AND TECTONIC SUBSIDENCE PLOT : Cambridge 1

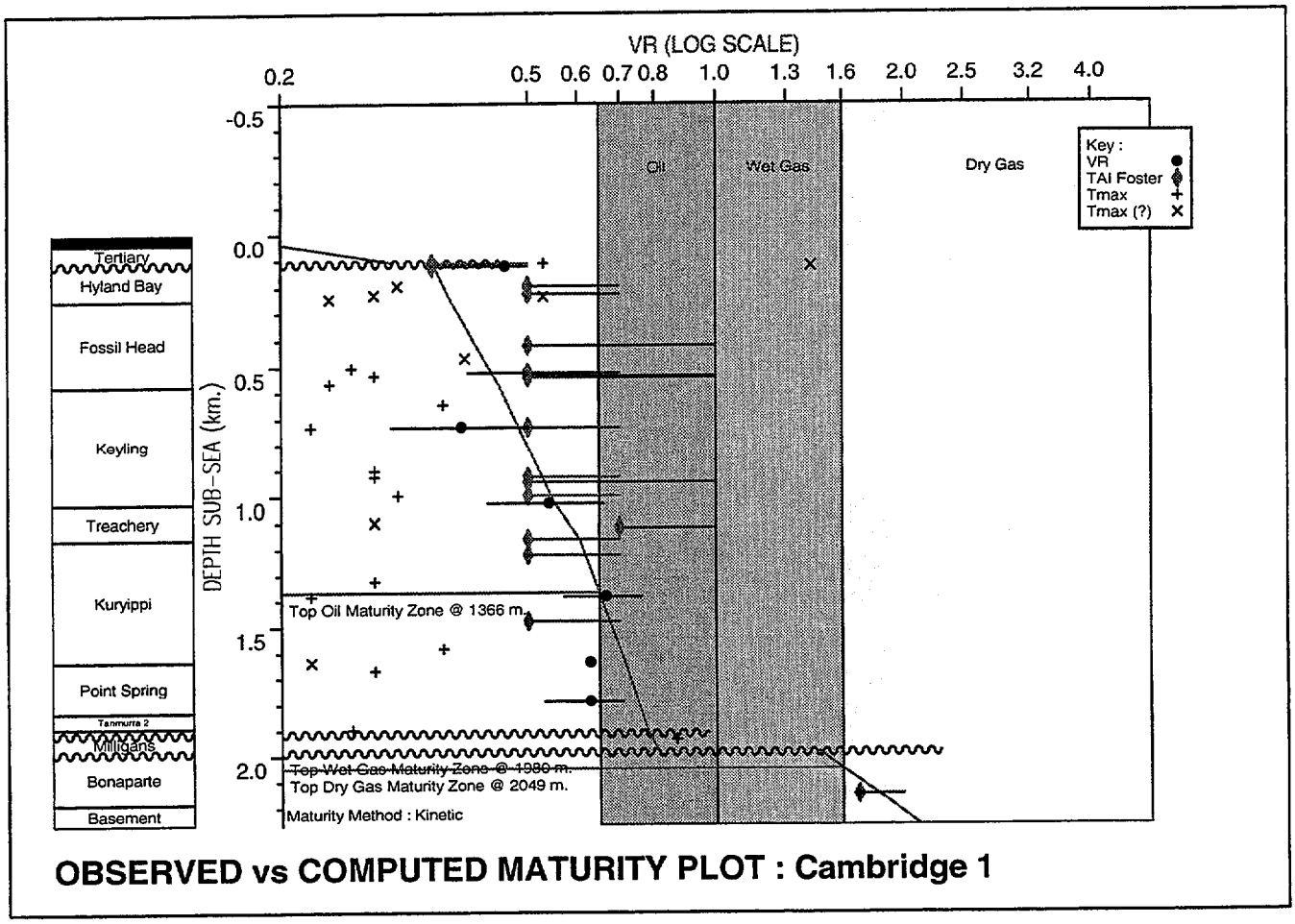

OBSERVED vs COMPUTED MATURITY PLOT : Cambridge 1

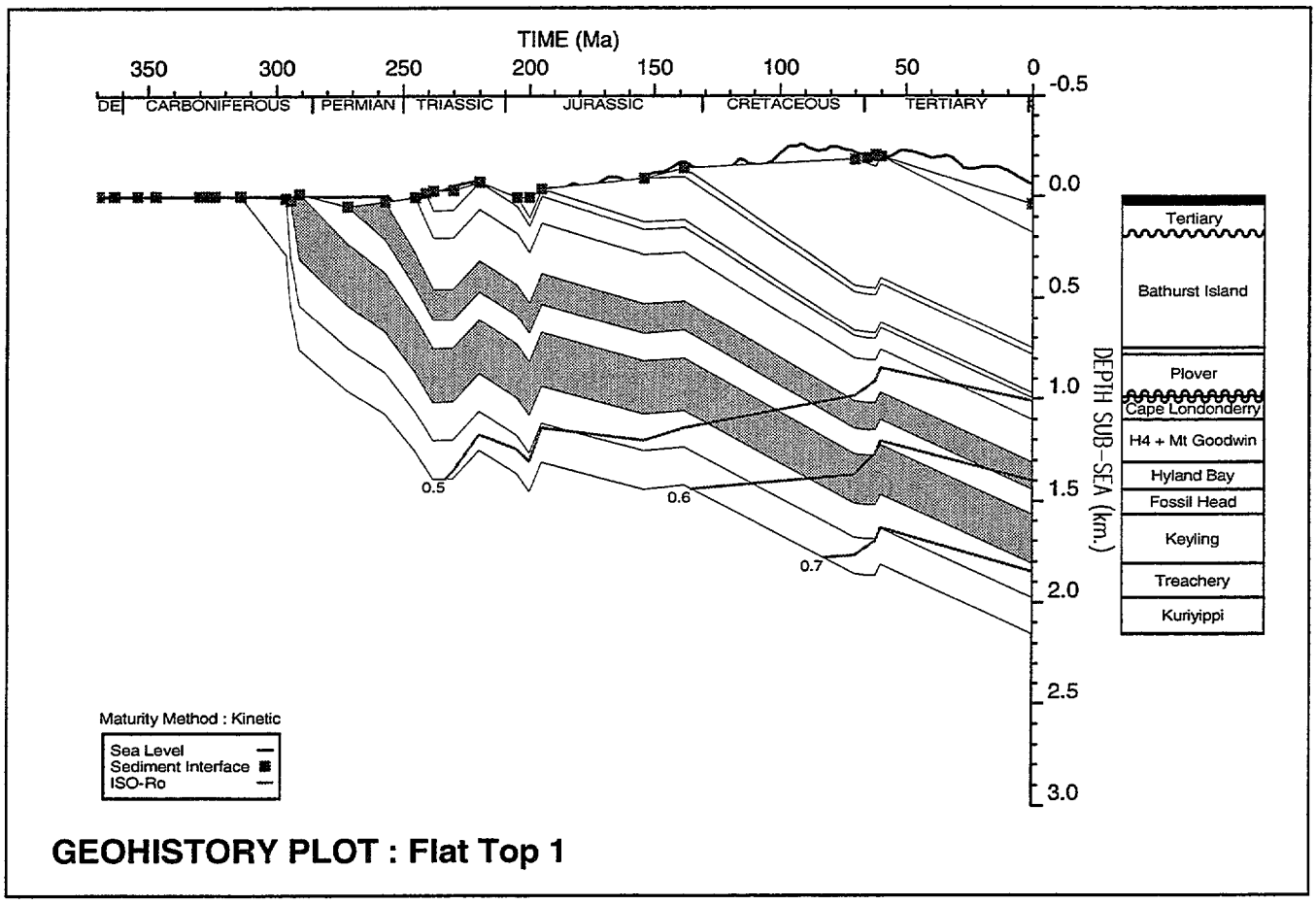

GEOHISTORY PLOT : Flat Top 1

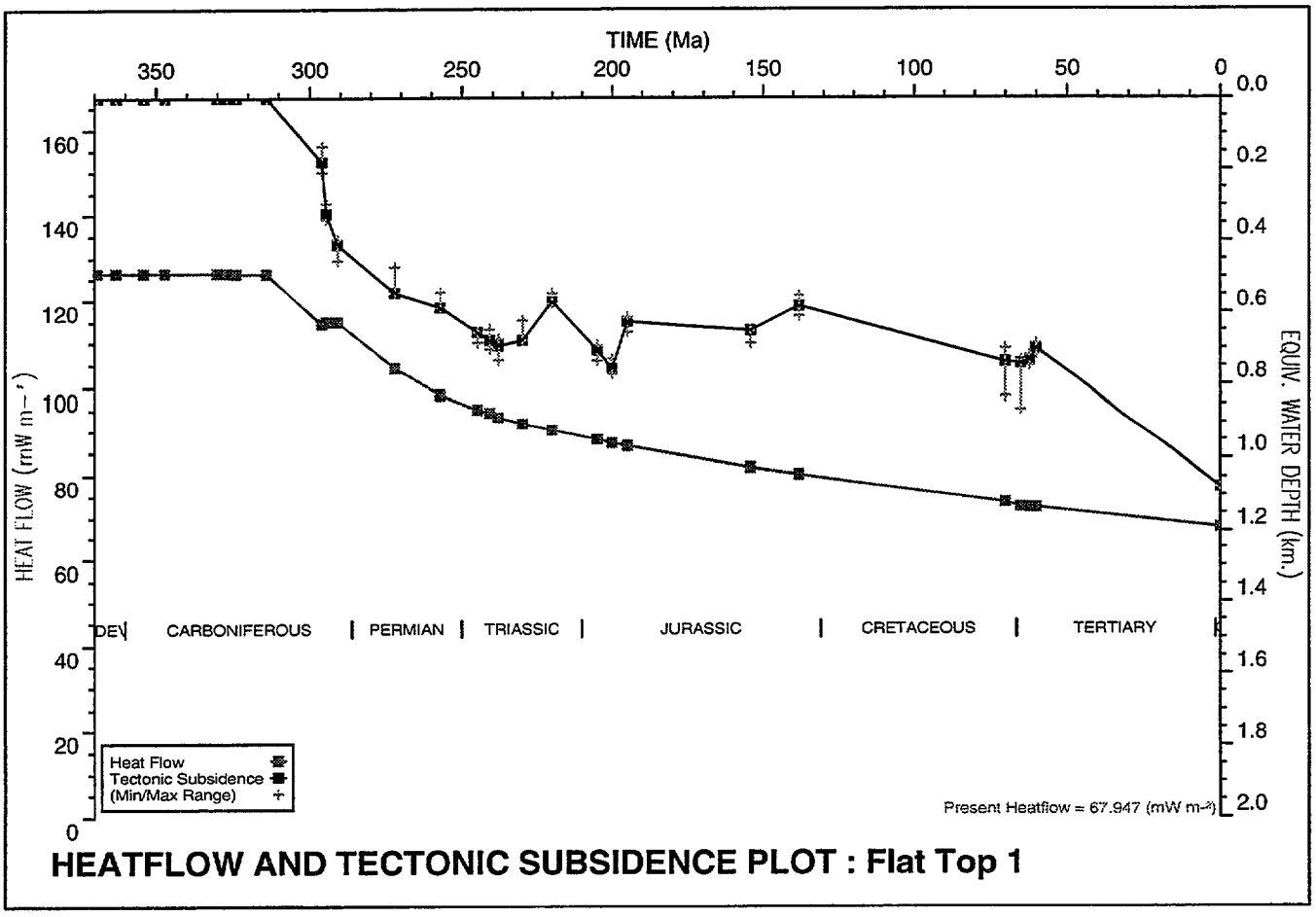

HEATFLOW AND TECTONIC SUBSIDENCE PLOT : Flat Top 1

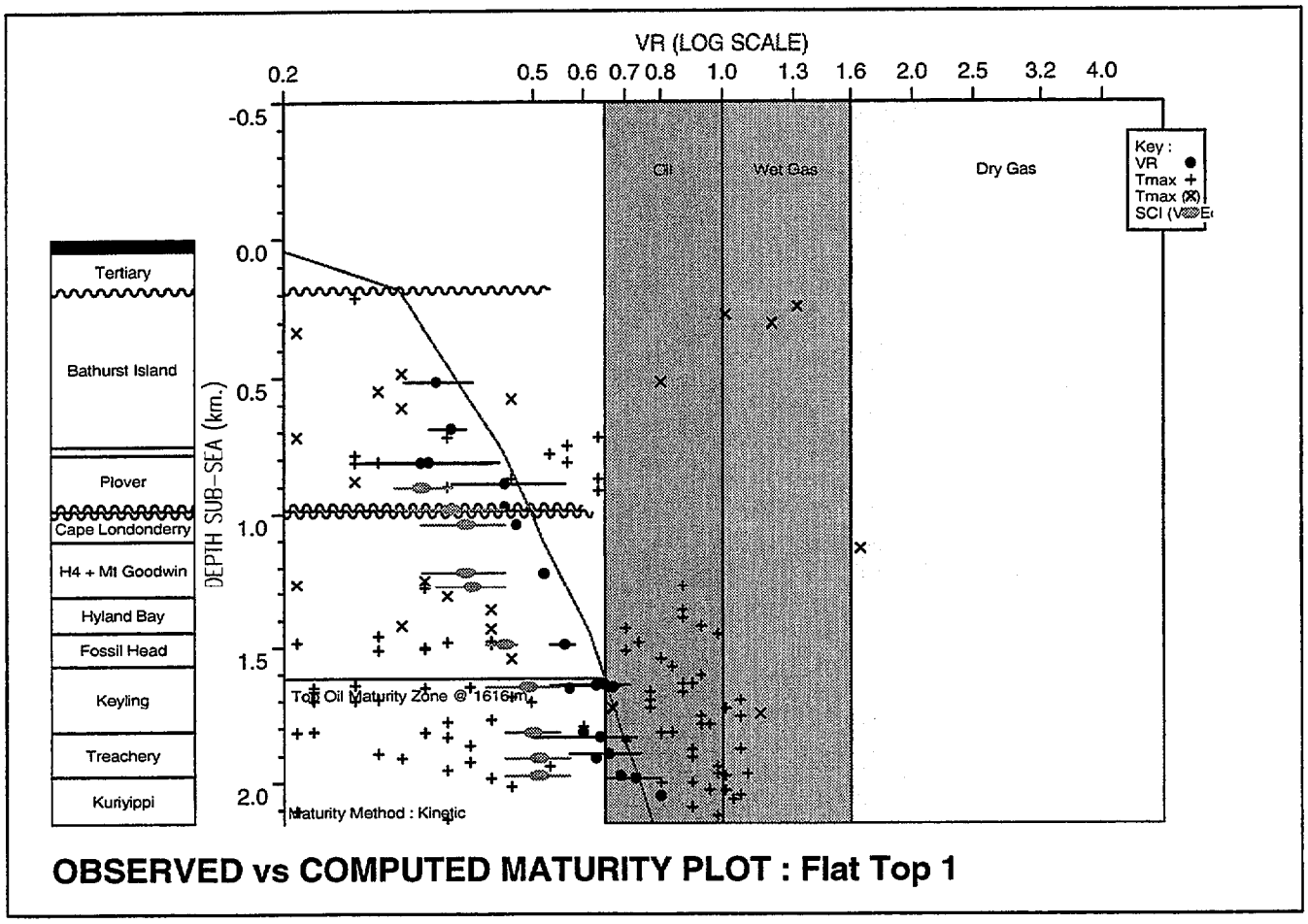

OBSERVED vs COMPUTED MATURITY PLOT : Flat Top 1

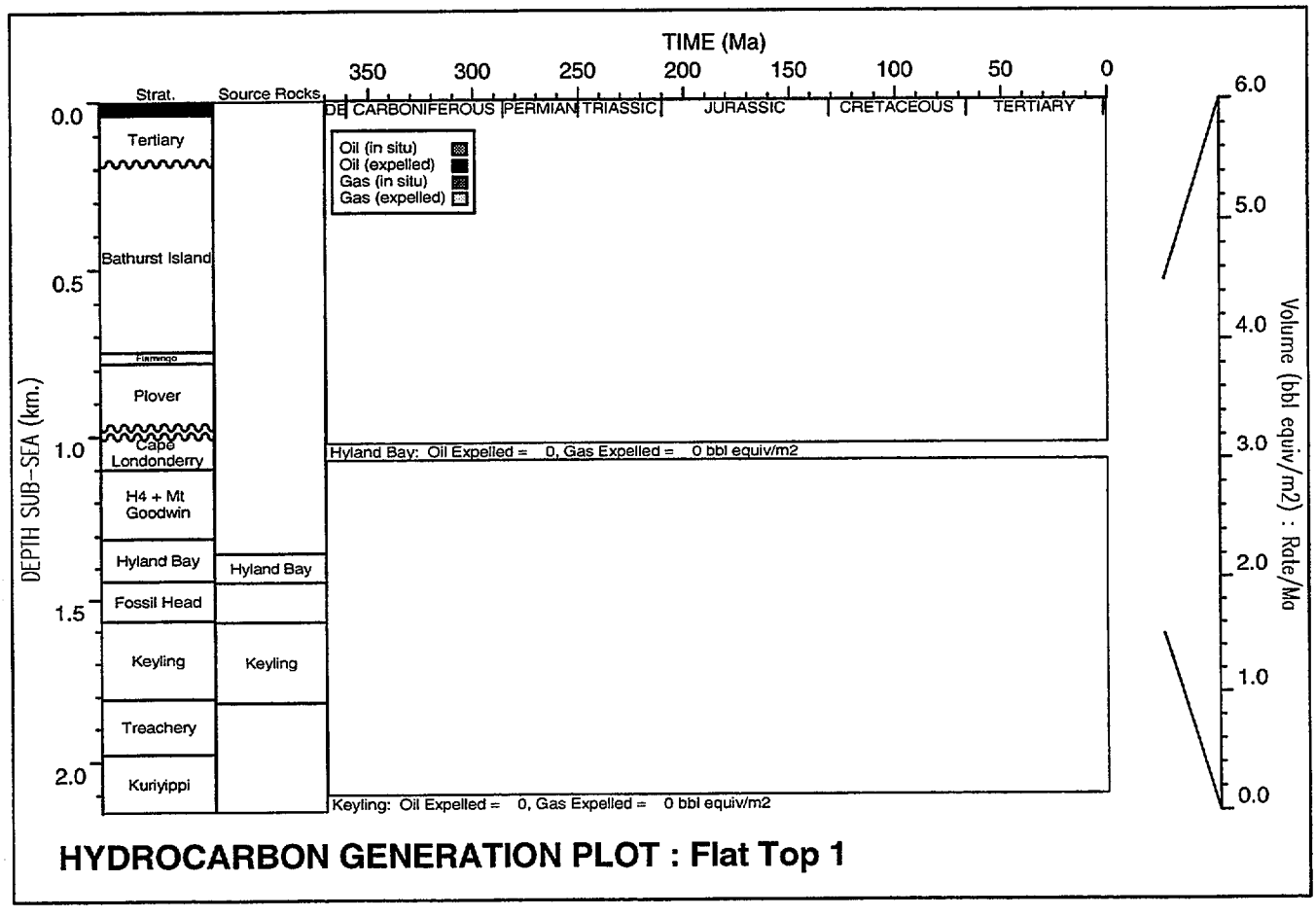

HYDROCARBON GENERATION PLOT : Flat Top 1

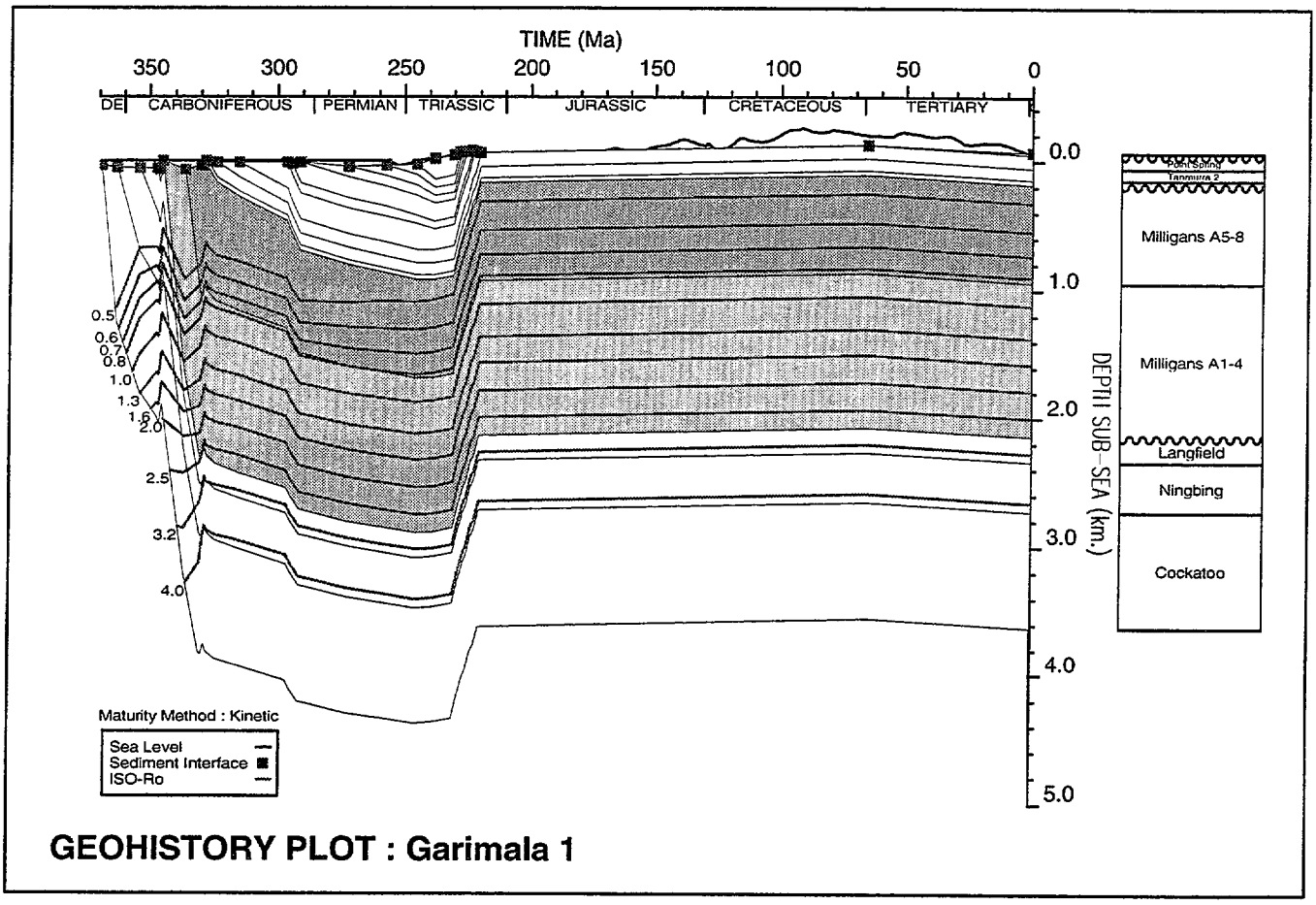

GEOHISTORY PLOT : Garimala 1

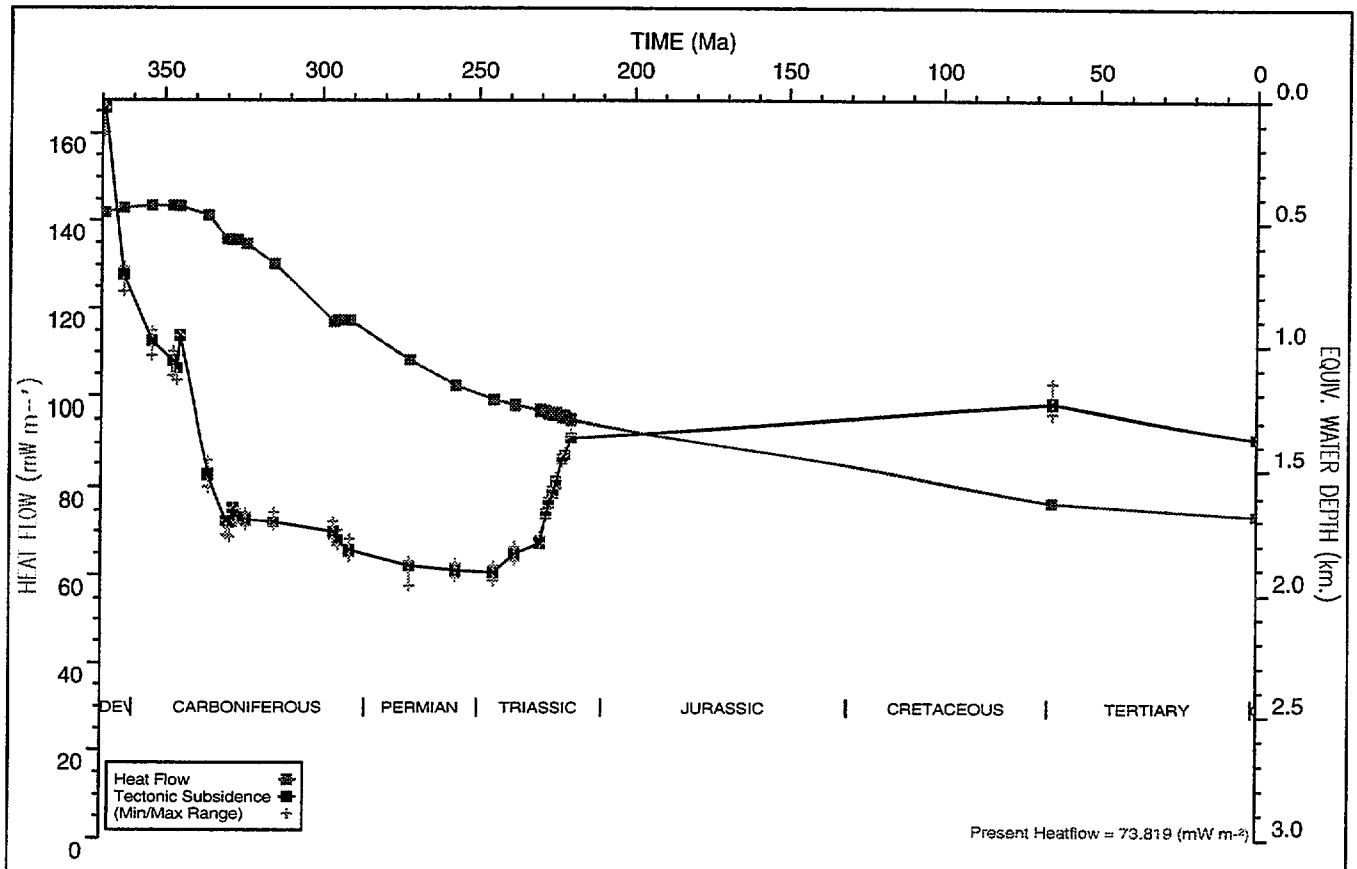

HEATFLOW AND TECTONIC SUBSIDENCE PLOT : Garimala 1

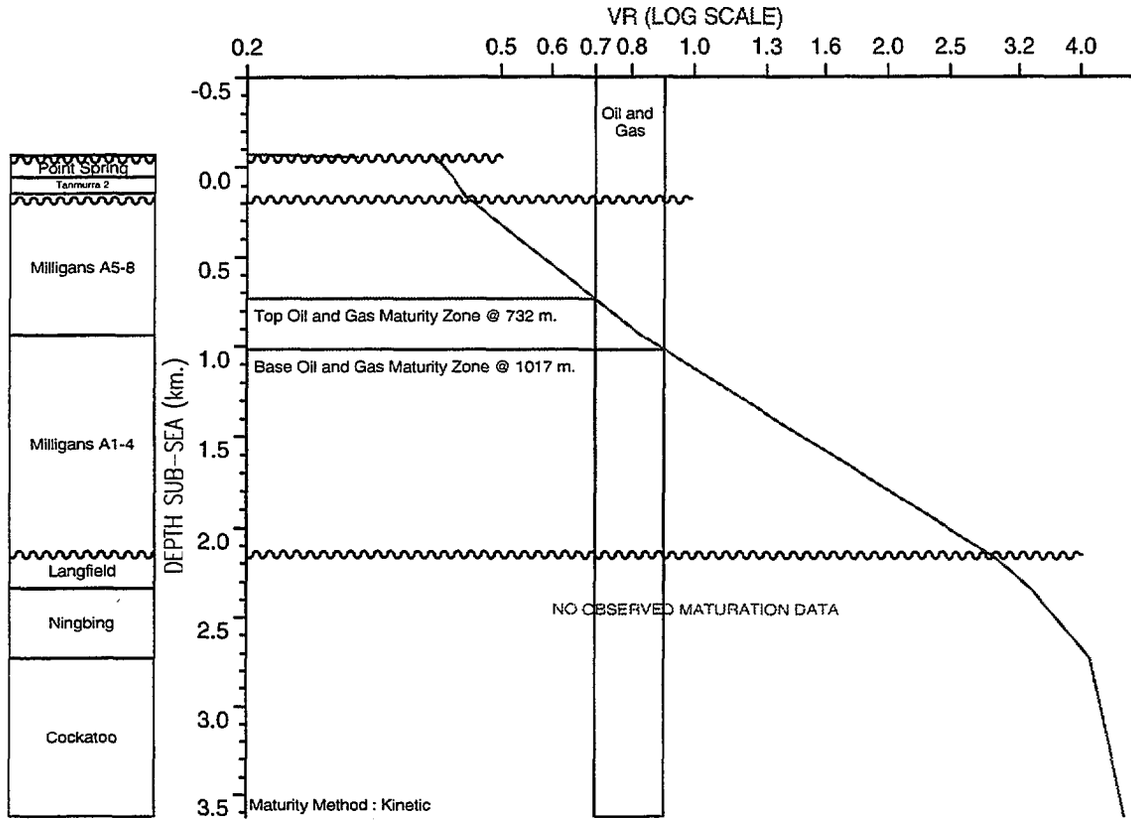

OBSERVED vs COMPUTED MATURITY PLOT : Garimala 1

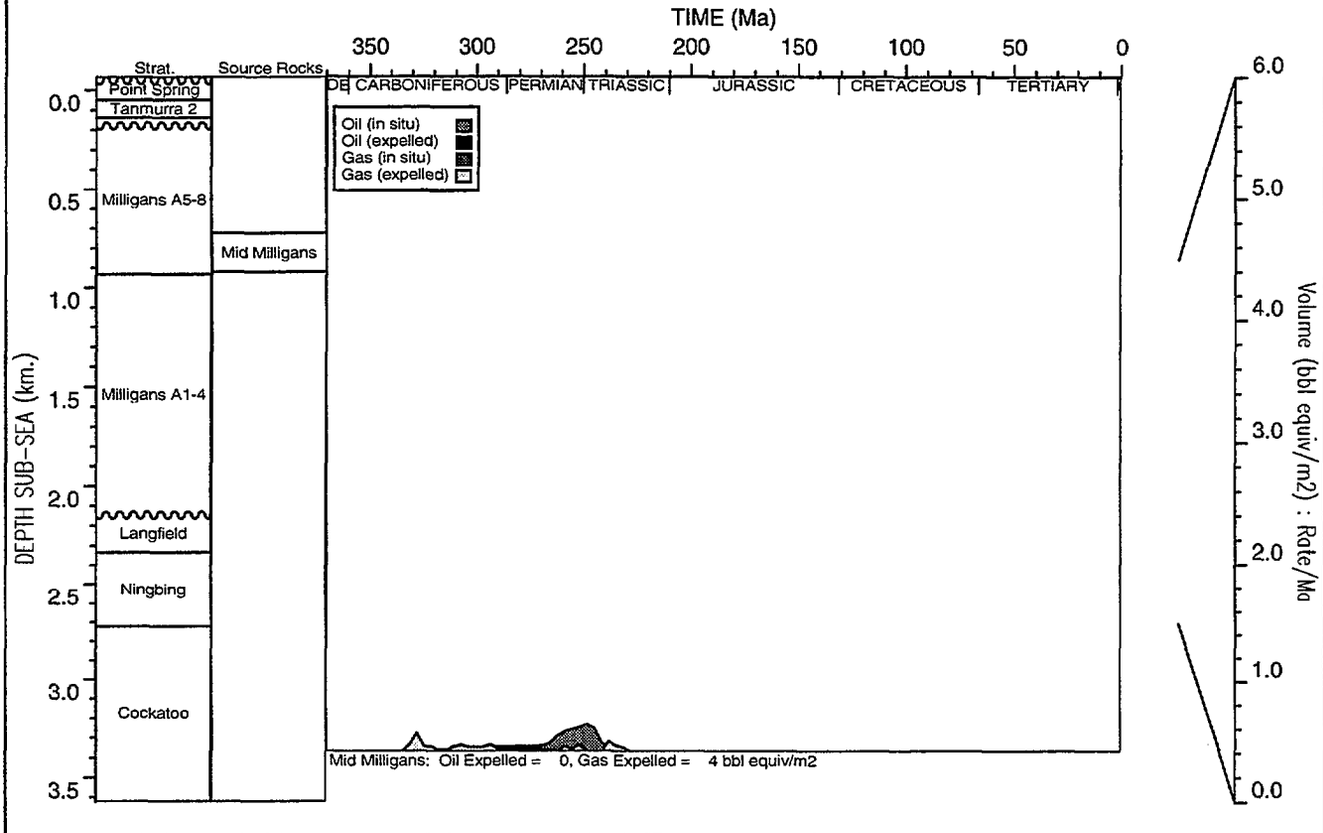

HYDROCARBON GENERATION PLOT : Garimala 1

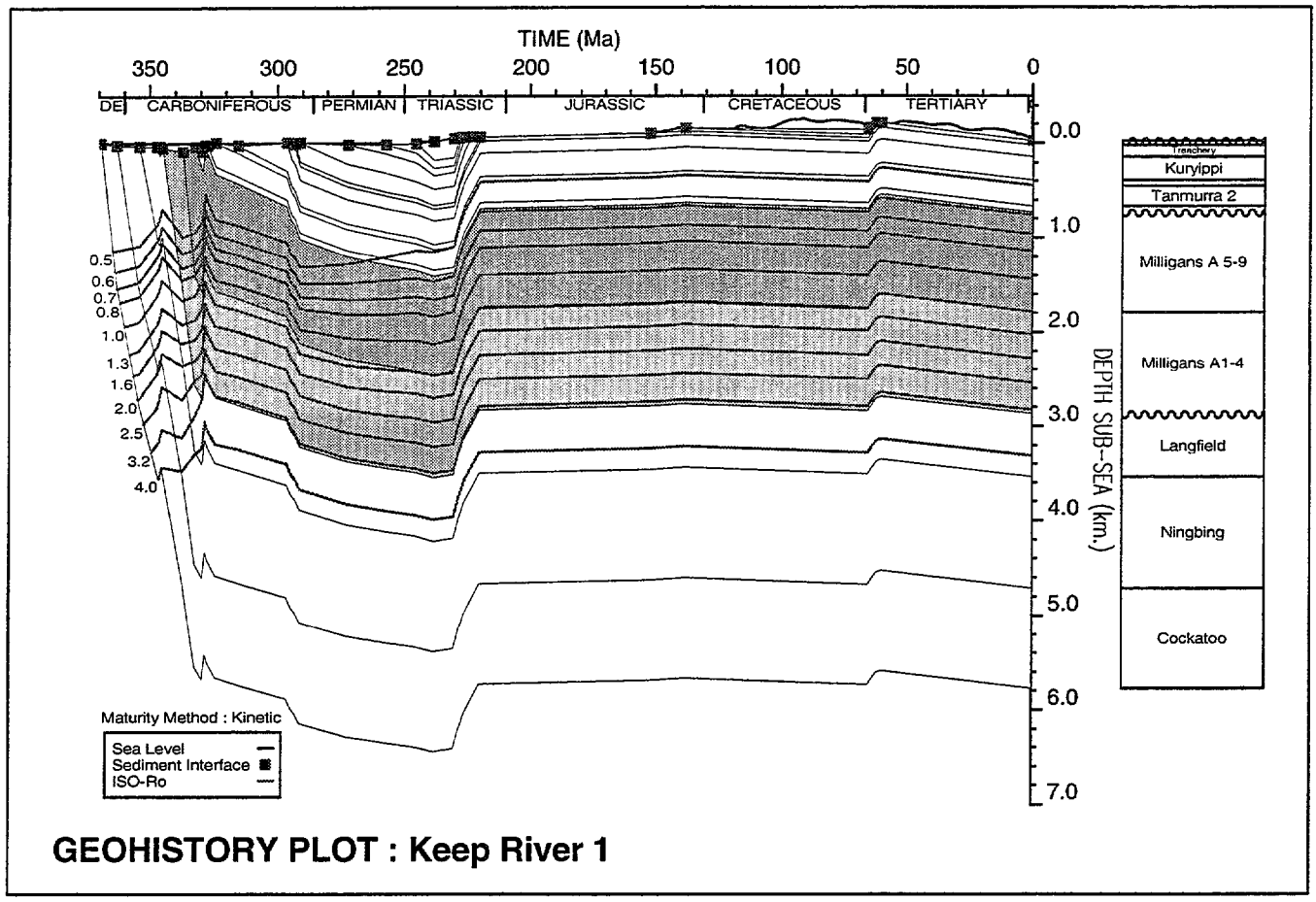

GEOHISTORY PLOT : Keep River 1

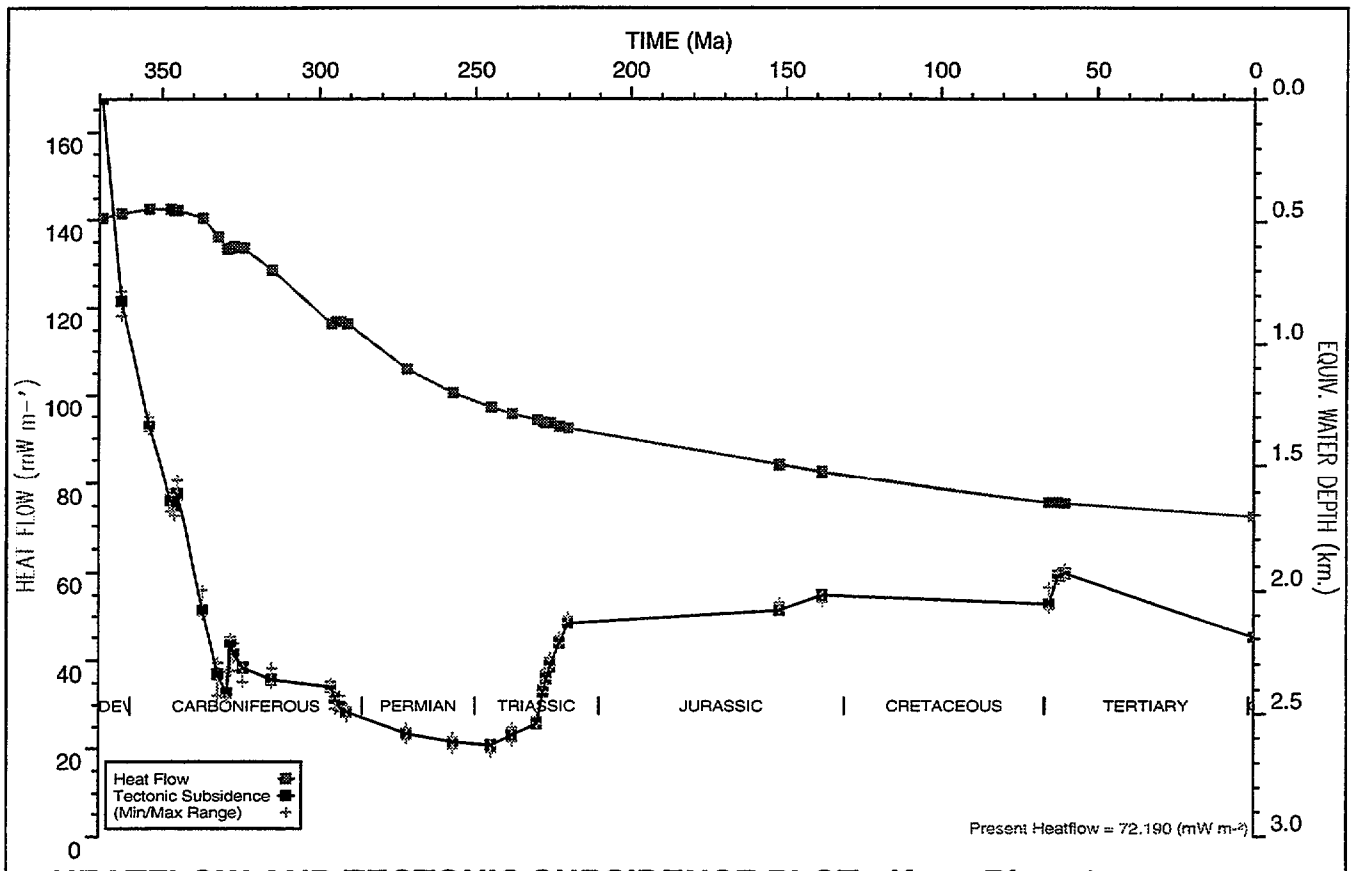

HEATFLOW AND TECTONIC SUBSIDENCE PLOT : Keep River 1

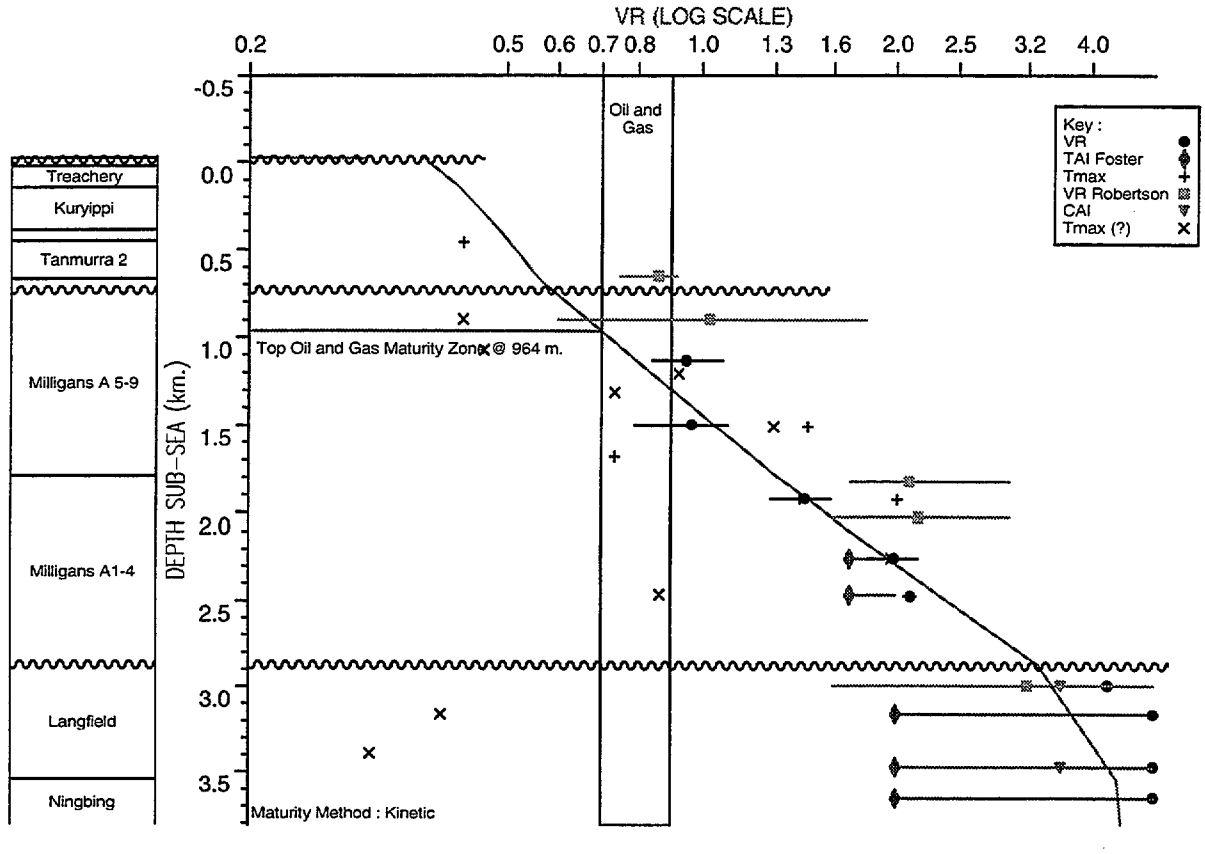

OBSERVED vs COMPUTED MATURITY PLOT : Keep River 1

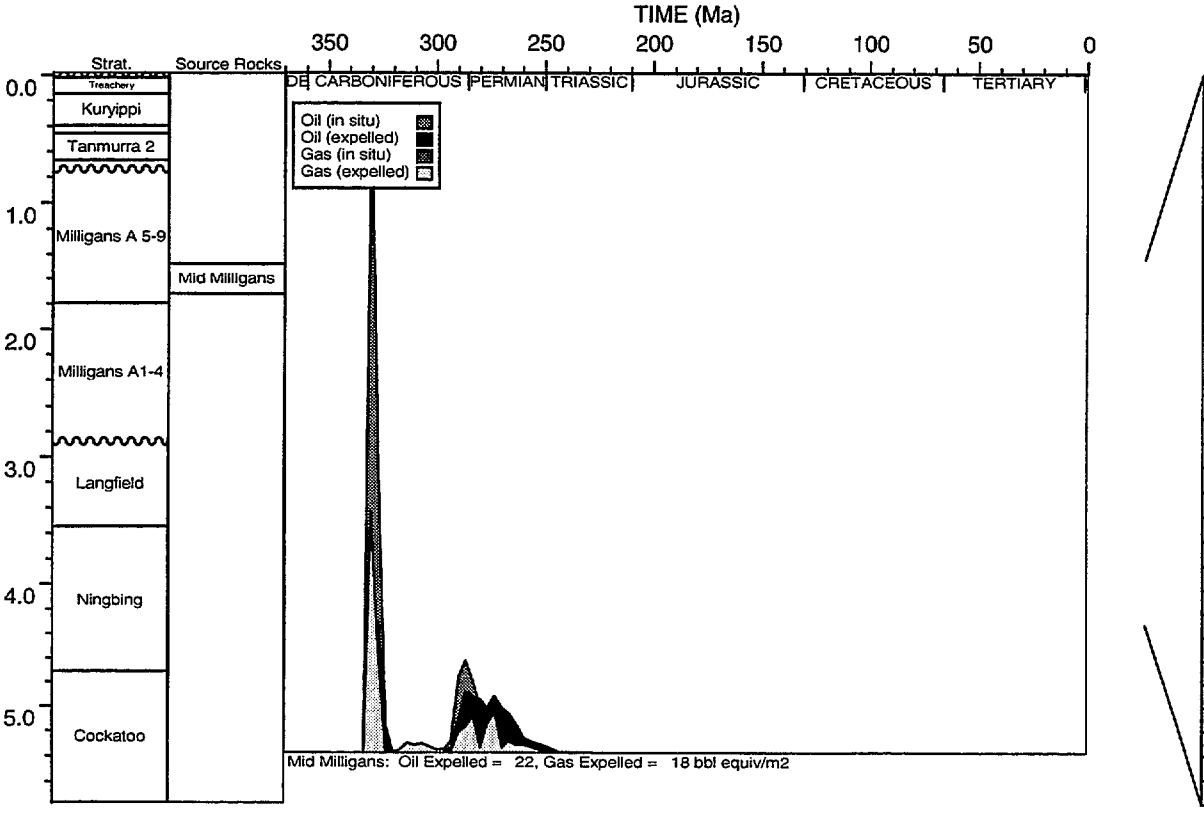

HYDROCARBON GENERATION PLOT : Keep River 1

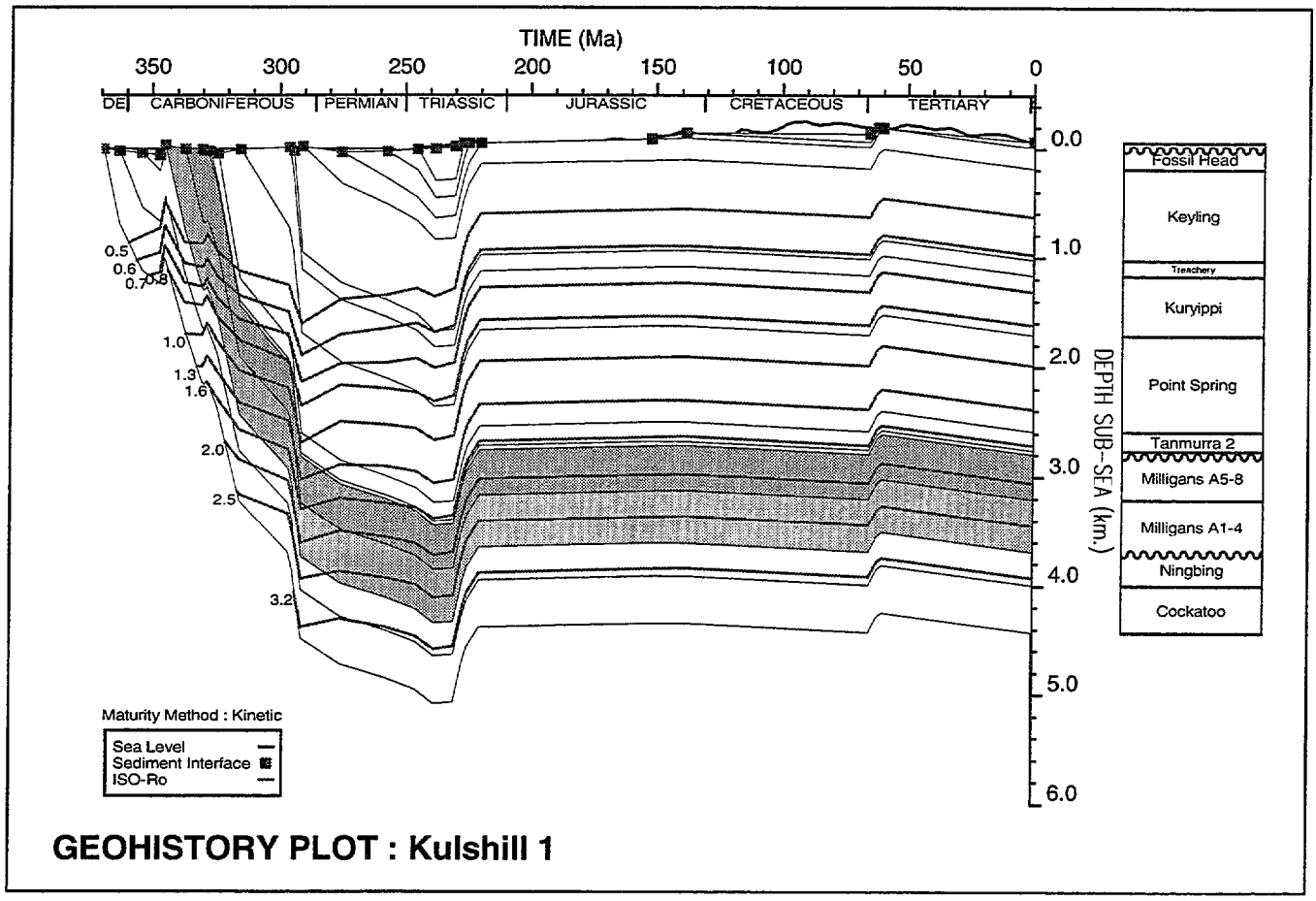

GEOHISTORY PLOT : Kulshill 1

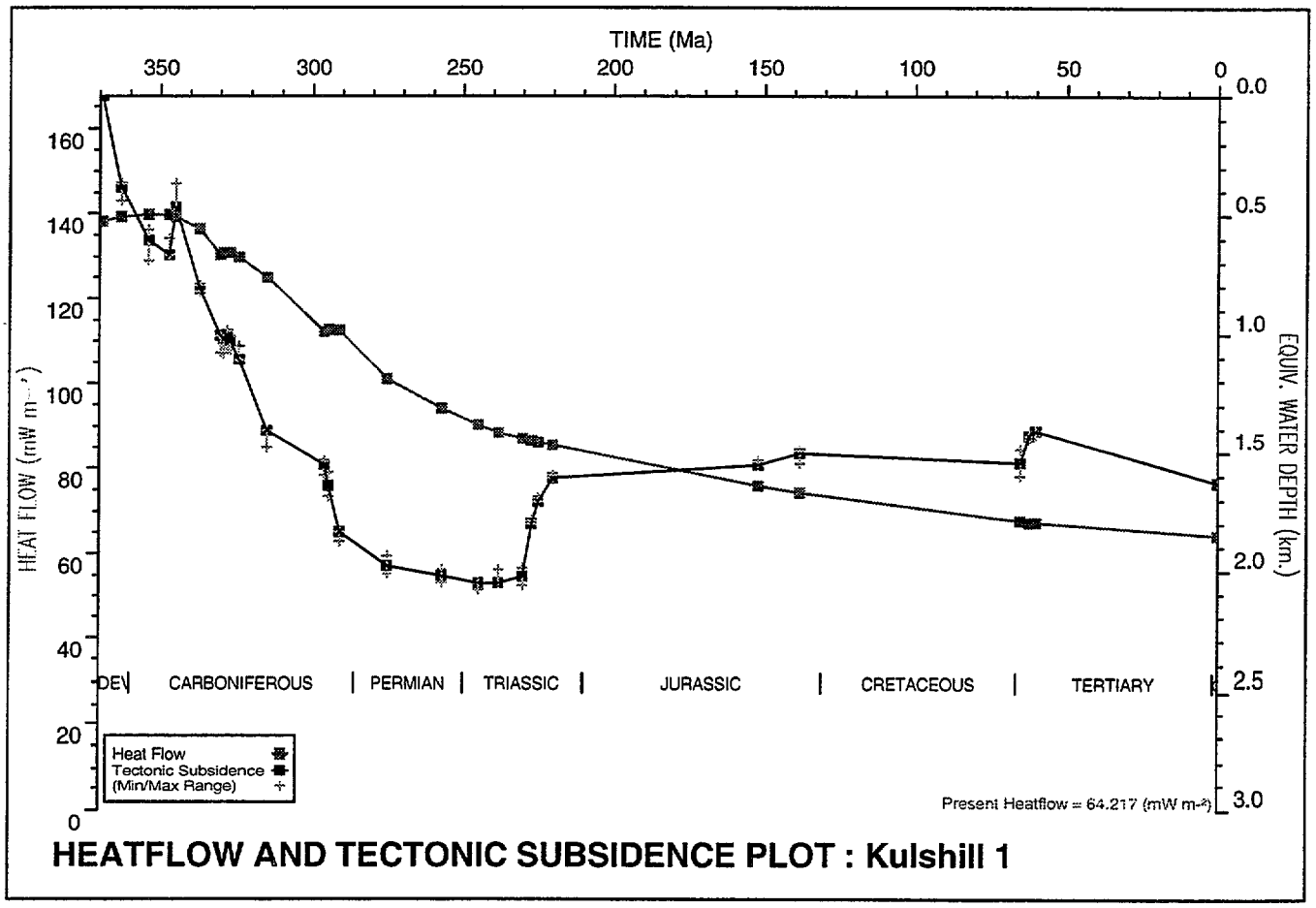

HEATFLOW AND TECTONIC SUBSIDENCE PLOT : Kulshill 1

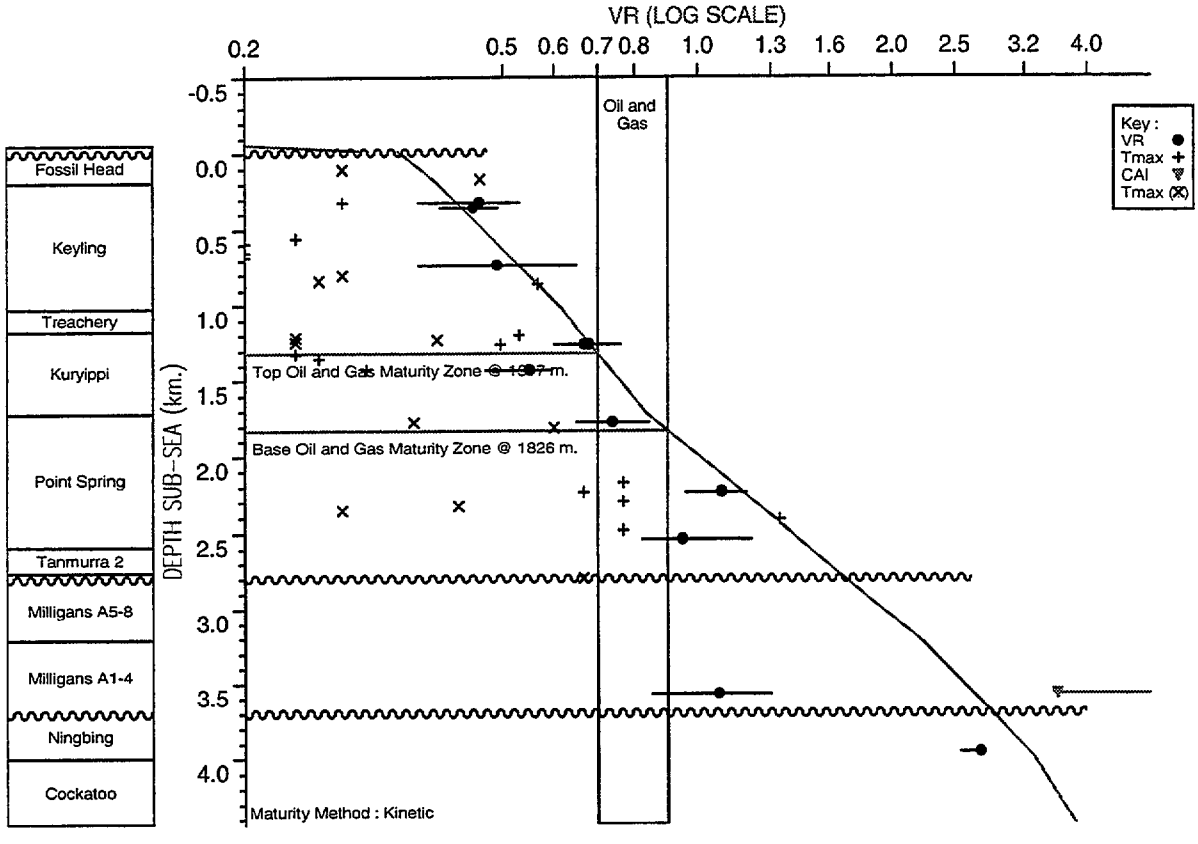

OBSERVED vs COMPUTED MATURITY PLOT : Kulshill 1

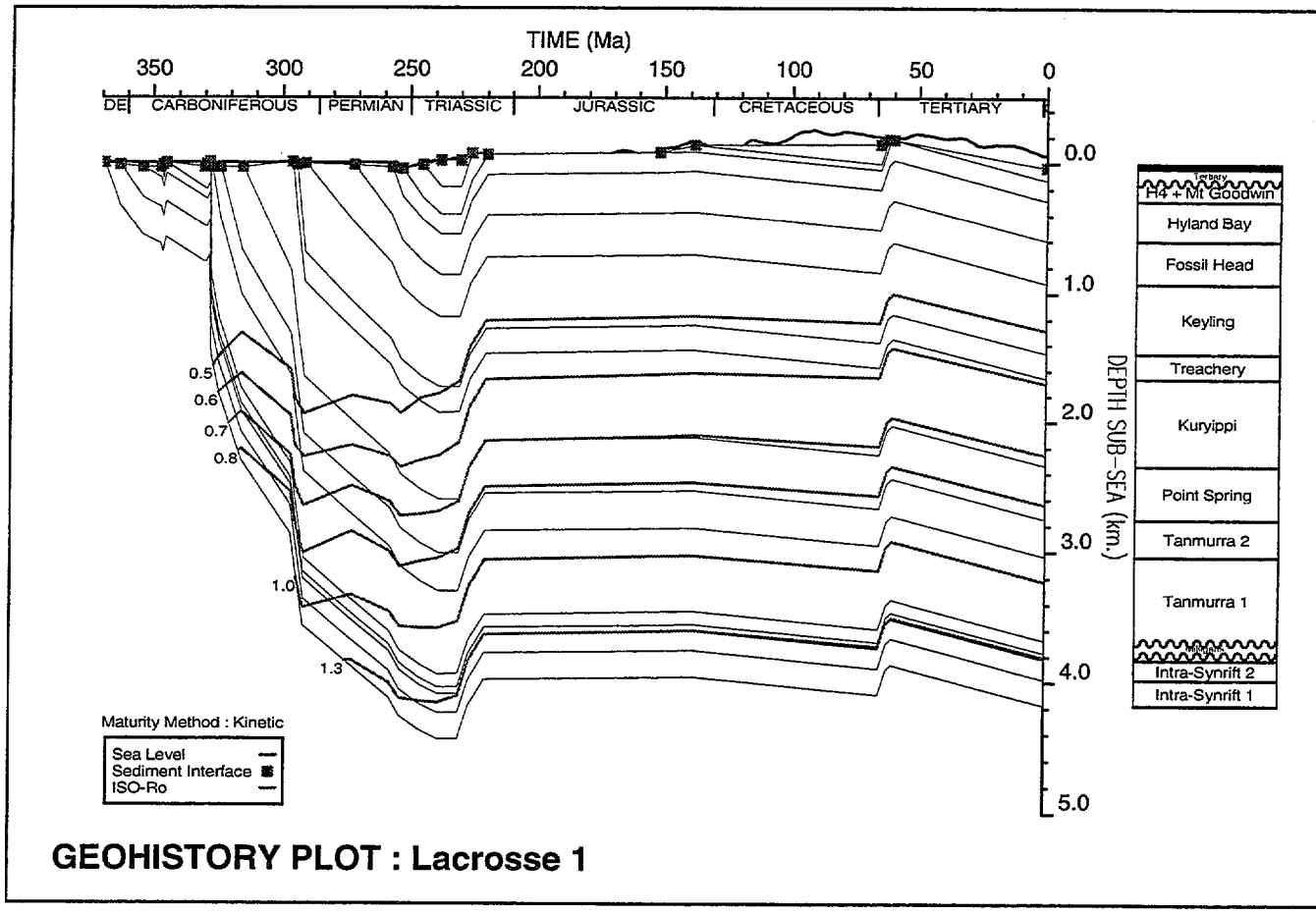

GEOHISTORY PLOT : Lacrosse 1

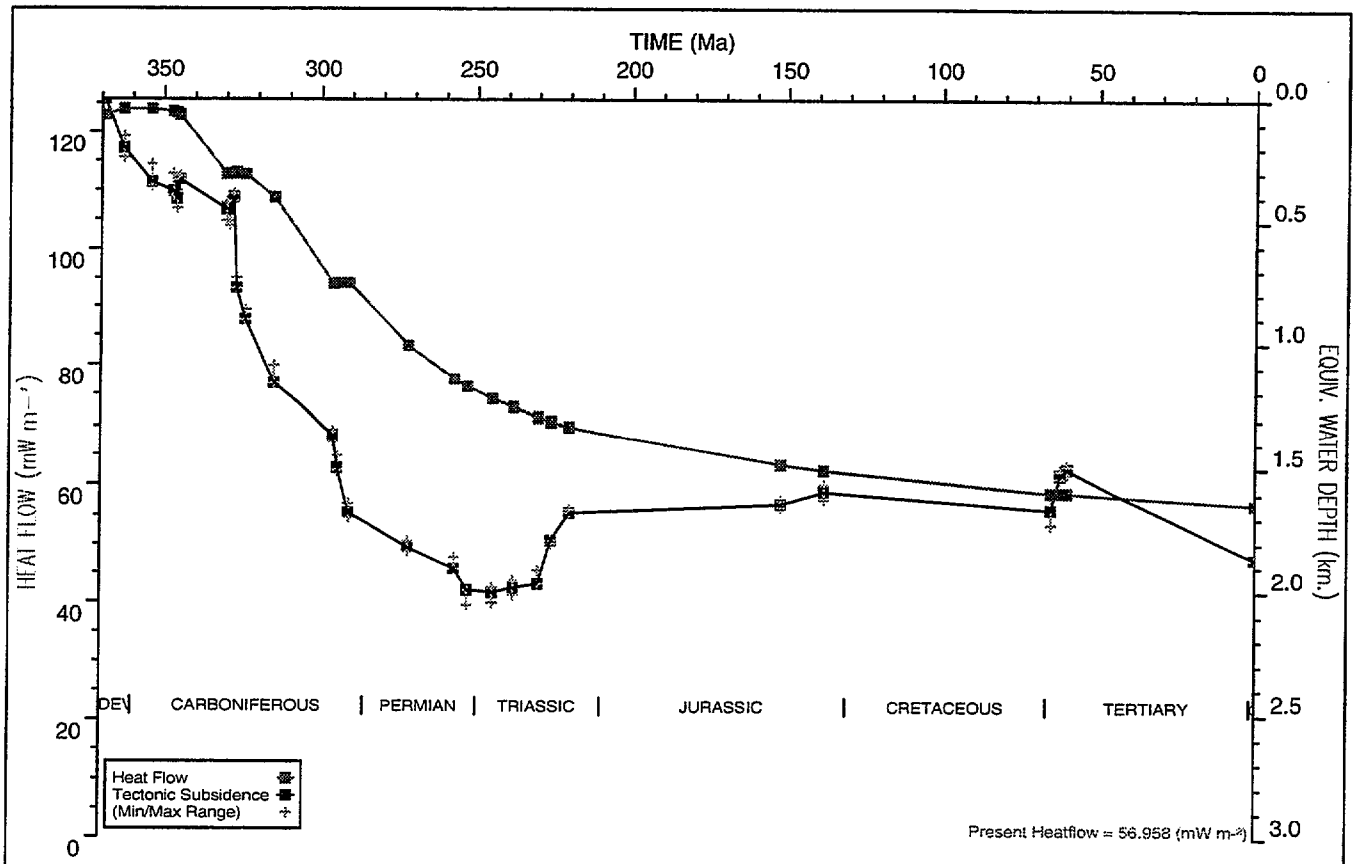

HEATFLOW AND TECTONIC SUBSIDENCE PLOT : Lacrosse 1

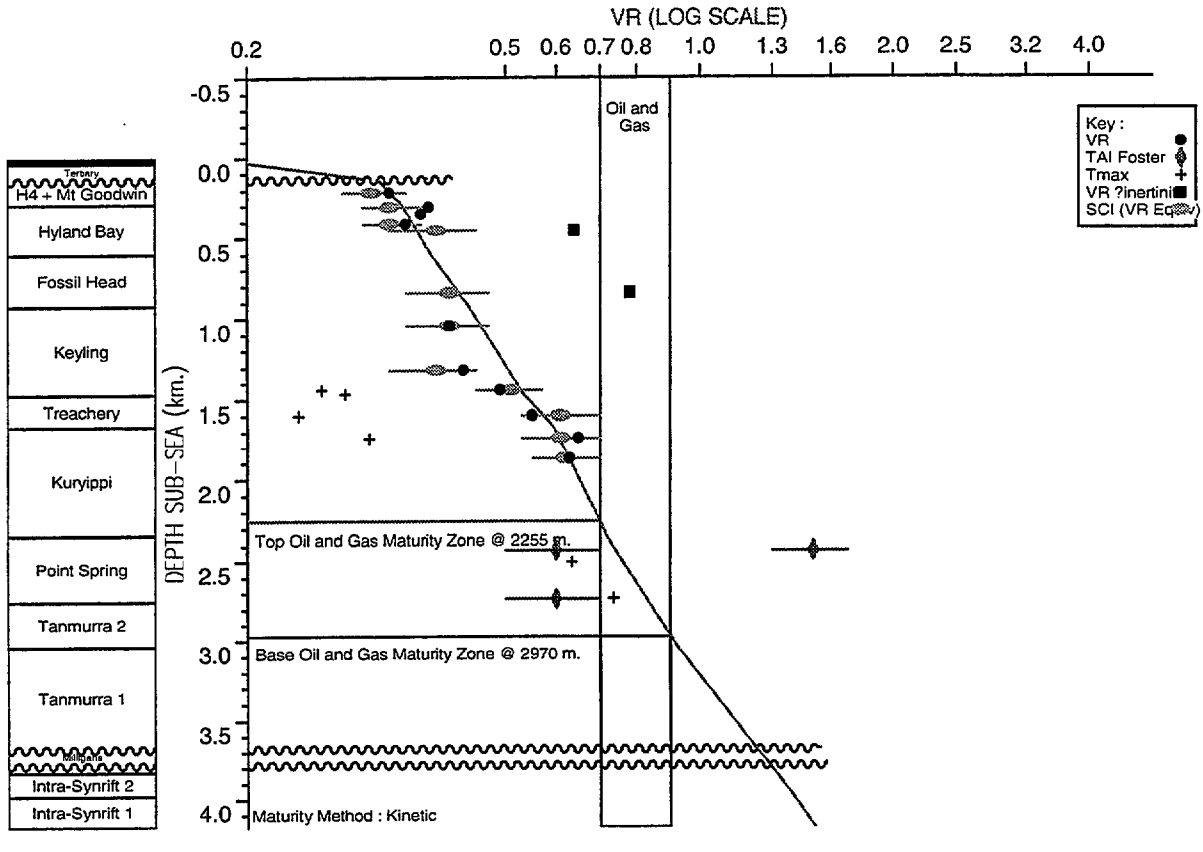

OBSERVED vs COMPUTED MATURITY PLOT : Lacrosse 1

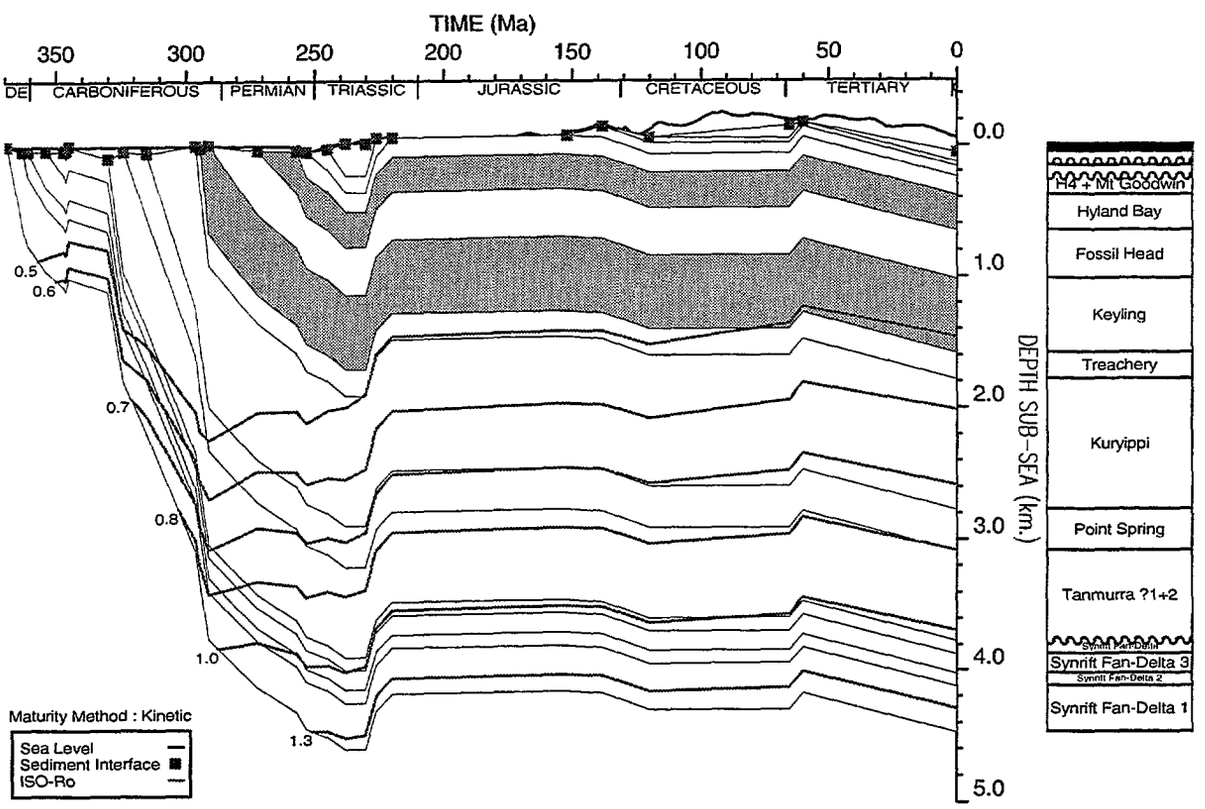

GEOHISTORY PLOT : Lesueur 1

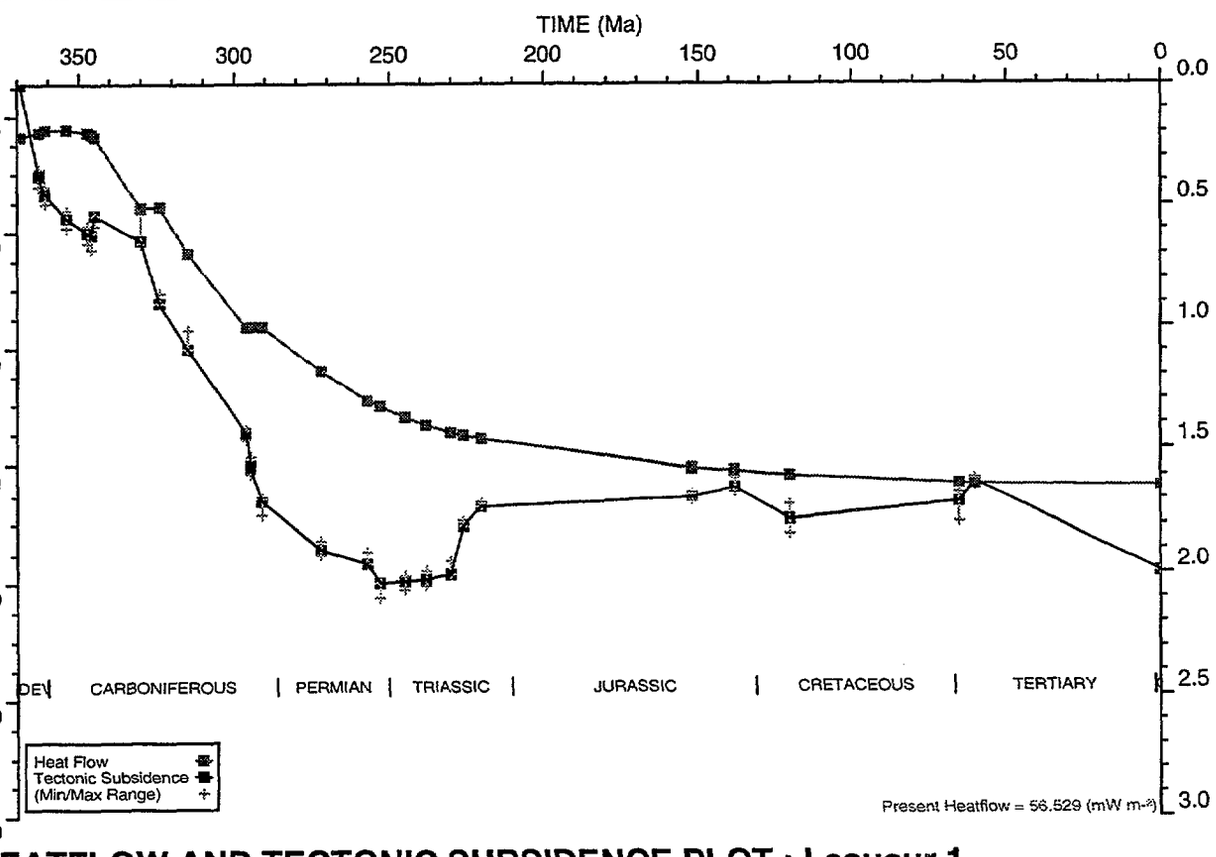

HEATFLOW AND TECTONIC SUBSIDENCE PLOT : Lesueur 1

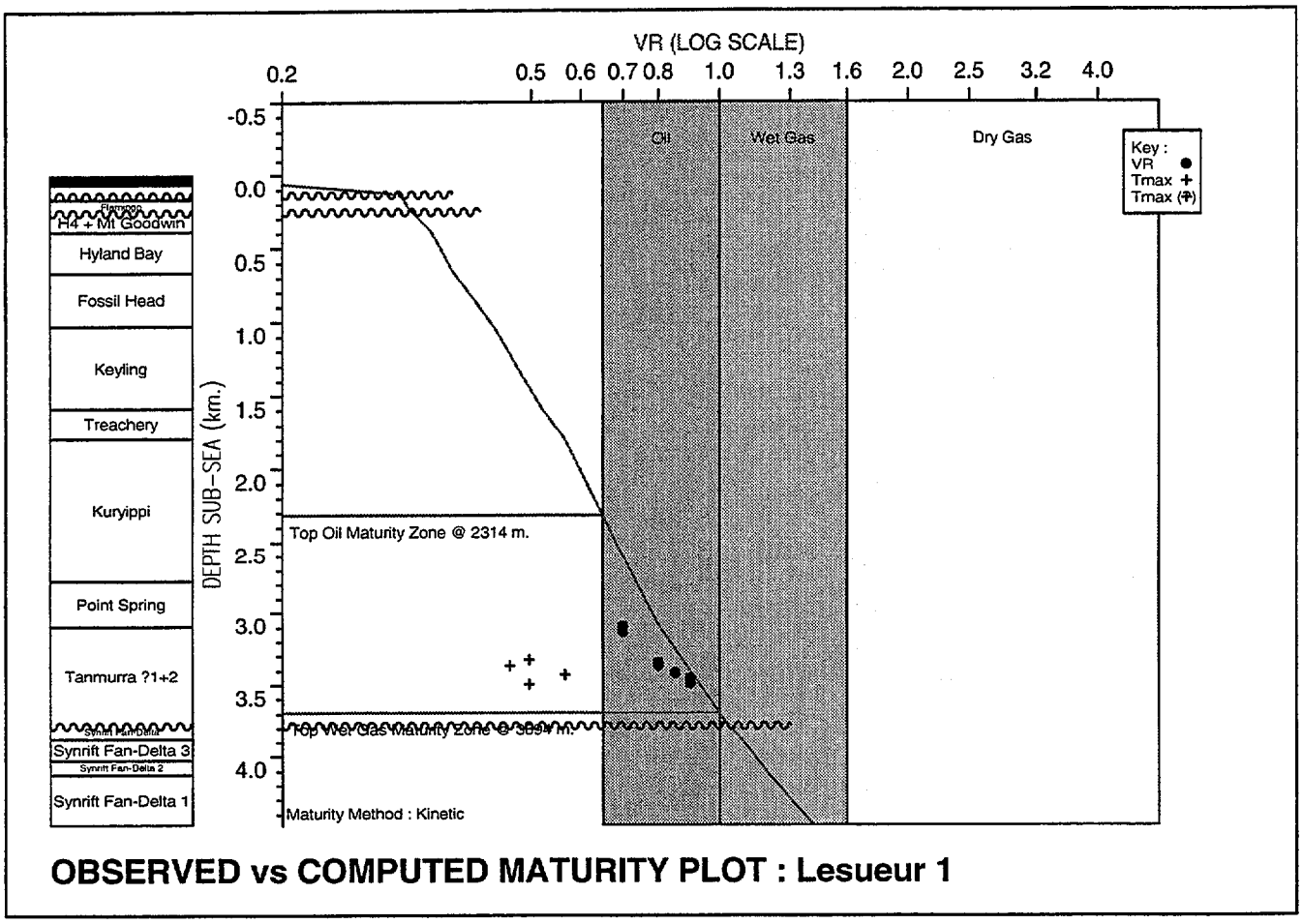

OBSERVED vs COMPUTED MATURITY PLOT : Lesueur 1

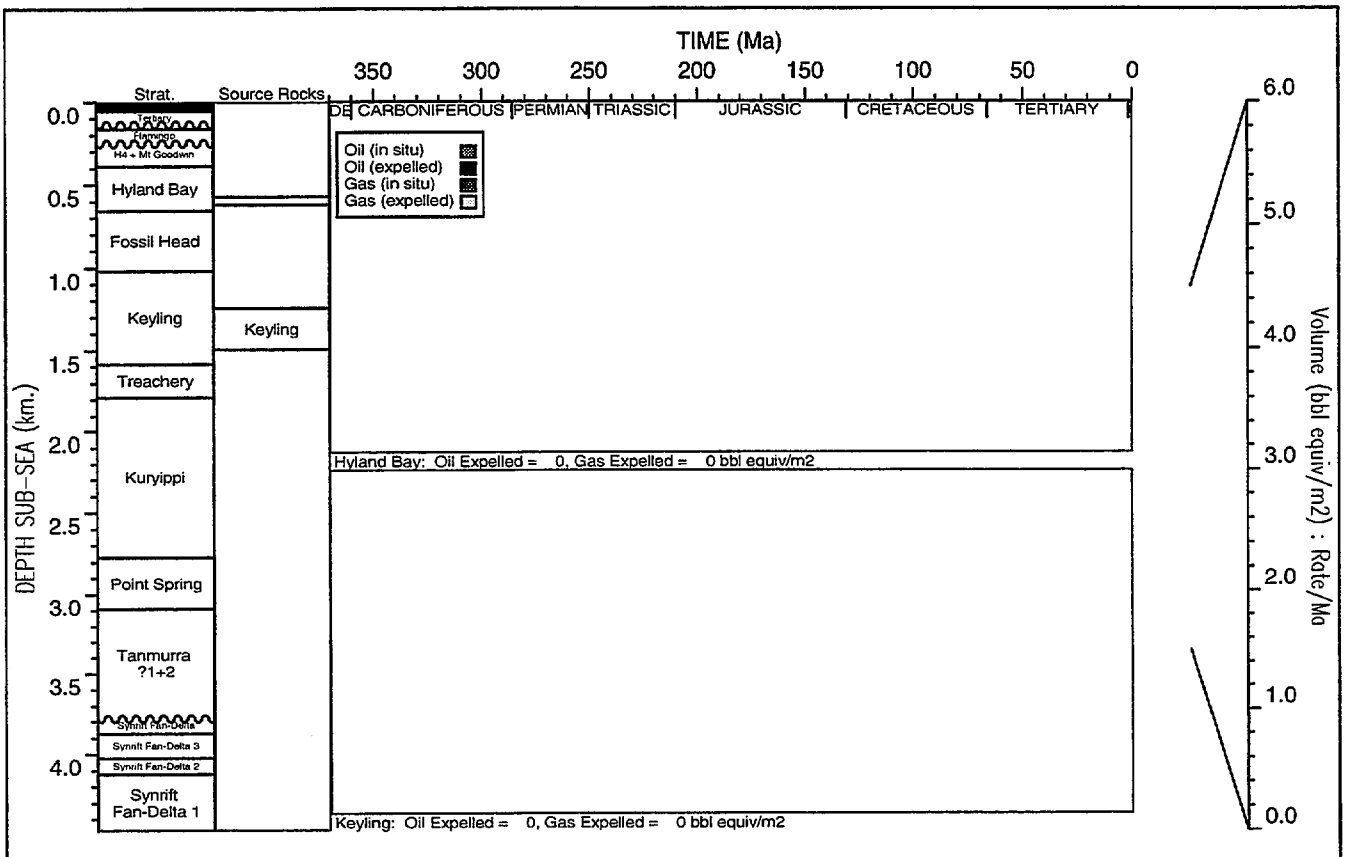

HYDROCARBON GENERATION PLOT : Lesueur 1

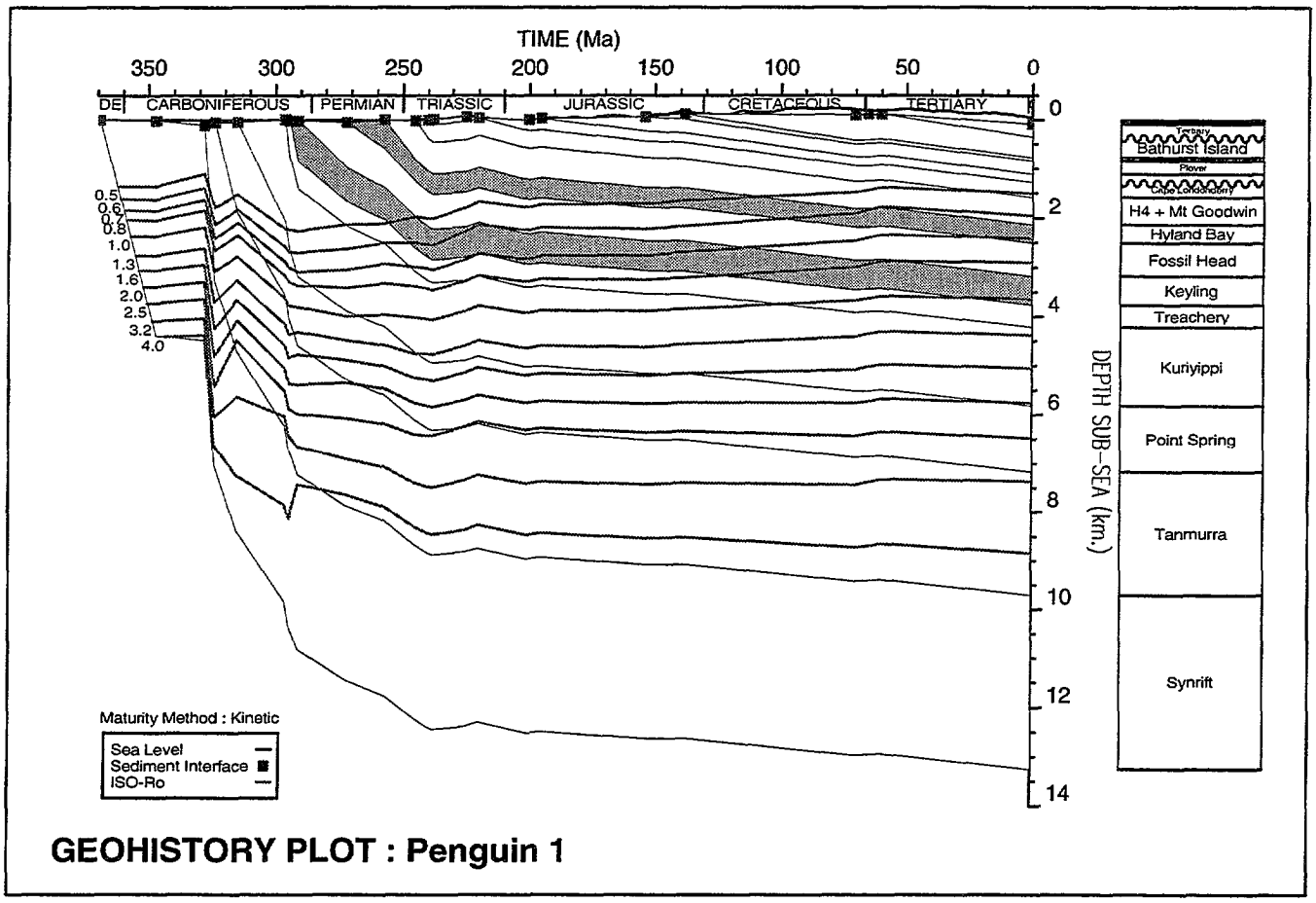

GEOHISTORY PLOT : Penguin 1

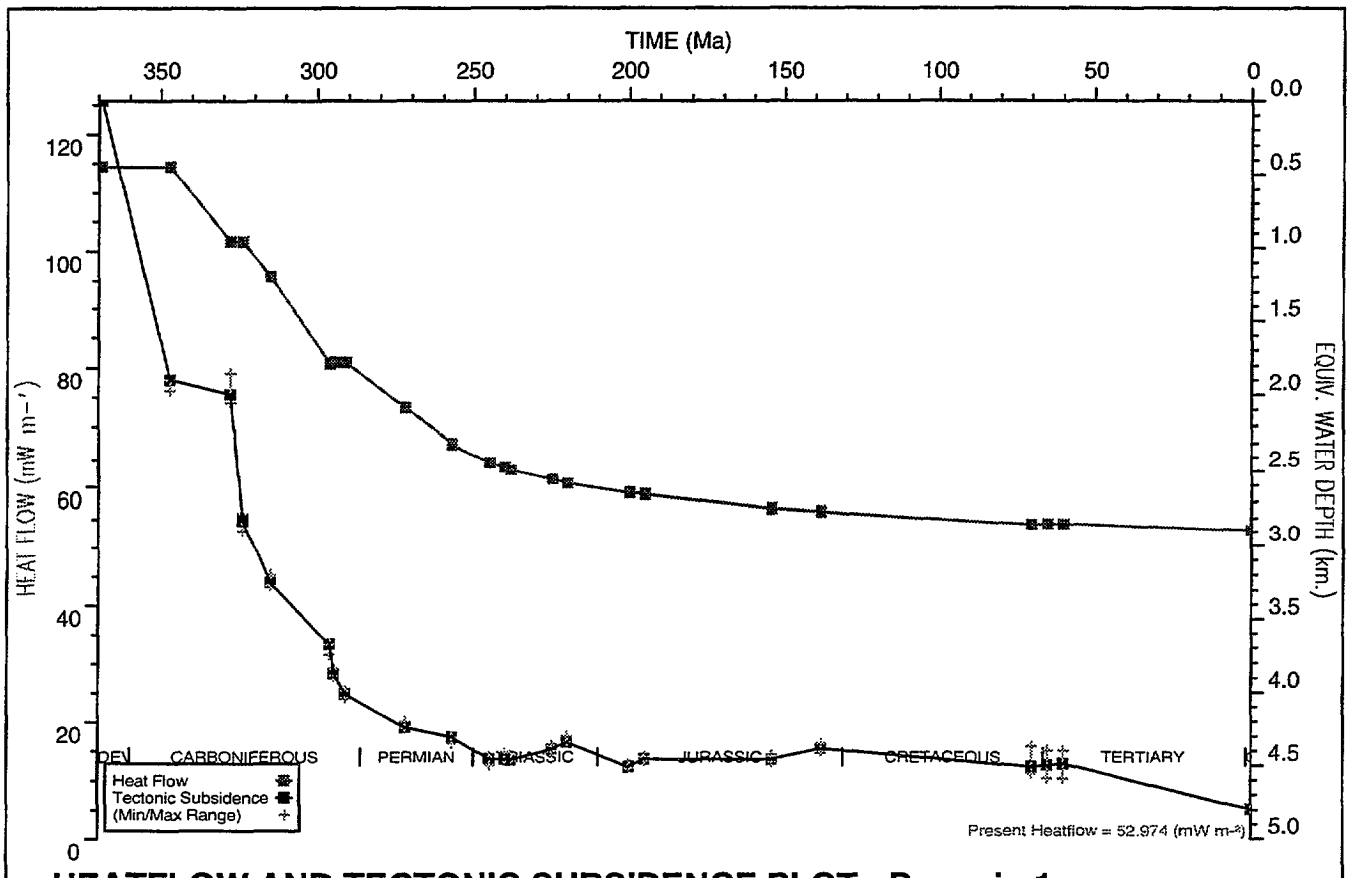

HEATFLOW AND TECTONIC SUBSIDENCE PLOT : Penguin 1

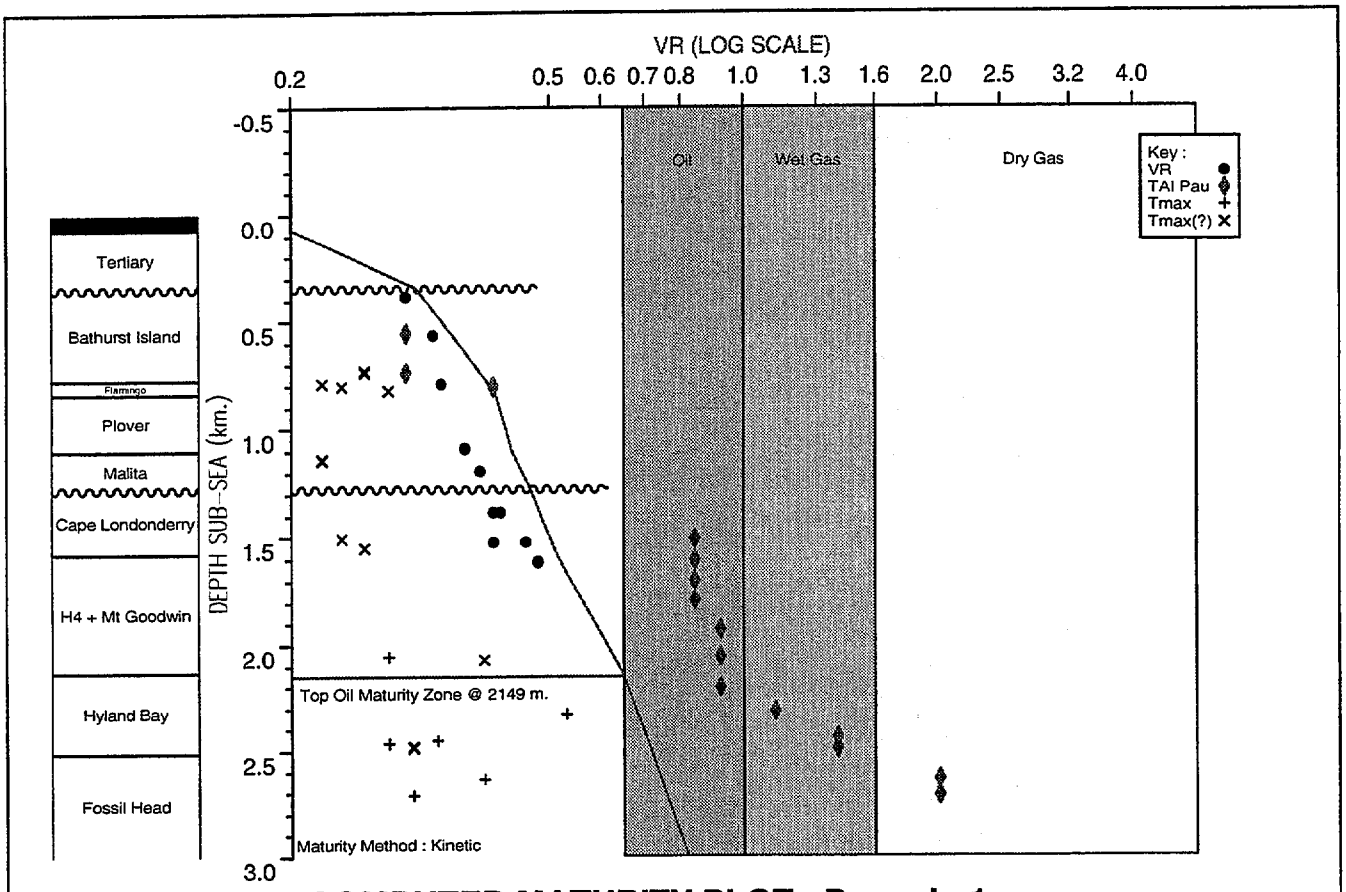

OBSERVED vs COMPUTED MATURITY PLOT : Penguin 1

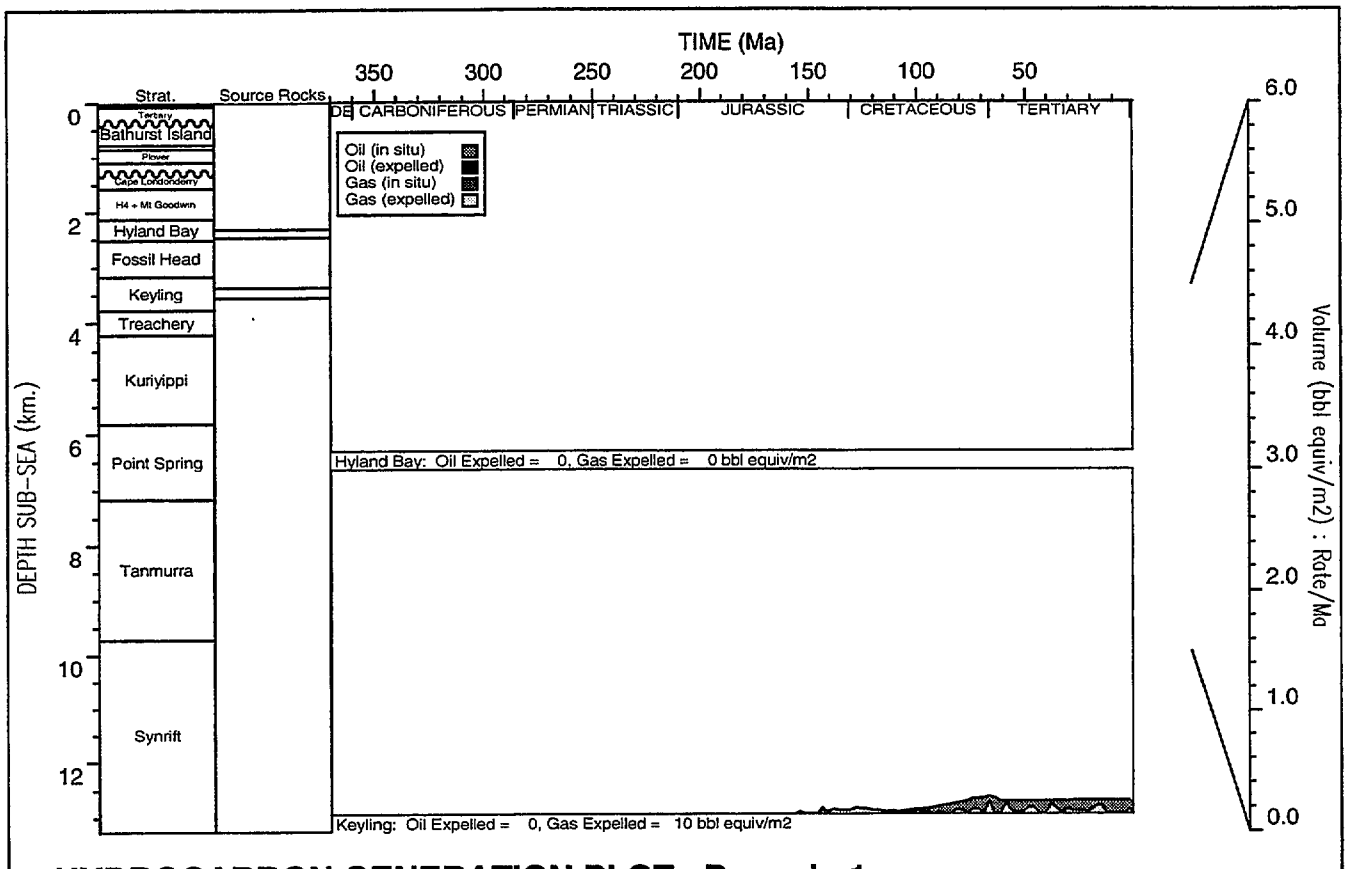

HYDROCARBON GENERATION PLOT : Penguin 1

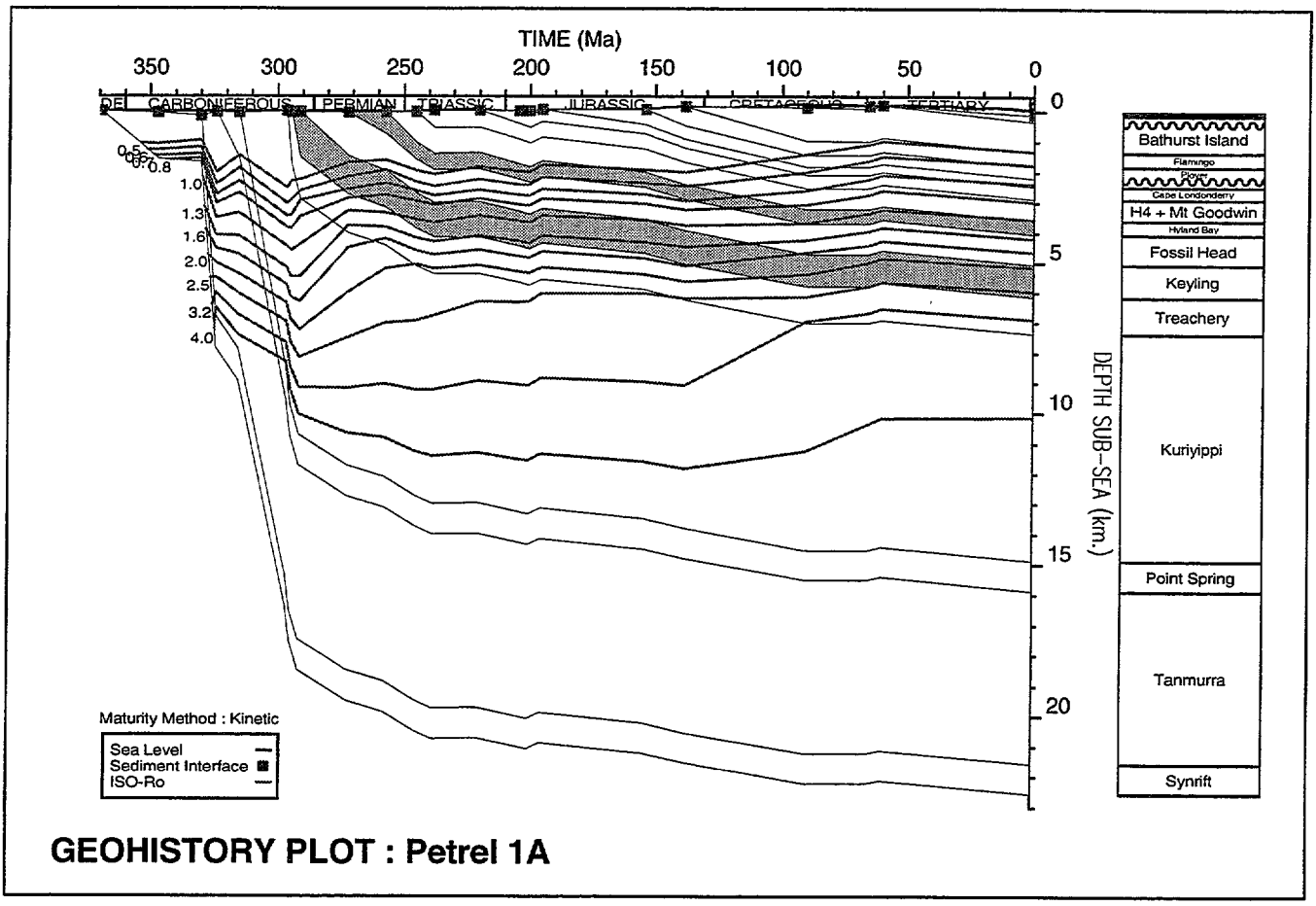

GEOHISTORY PLOT : Petrel 1A

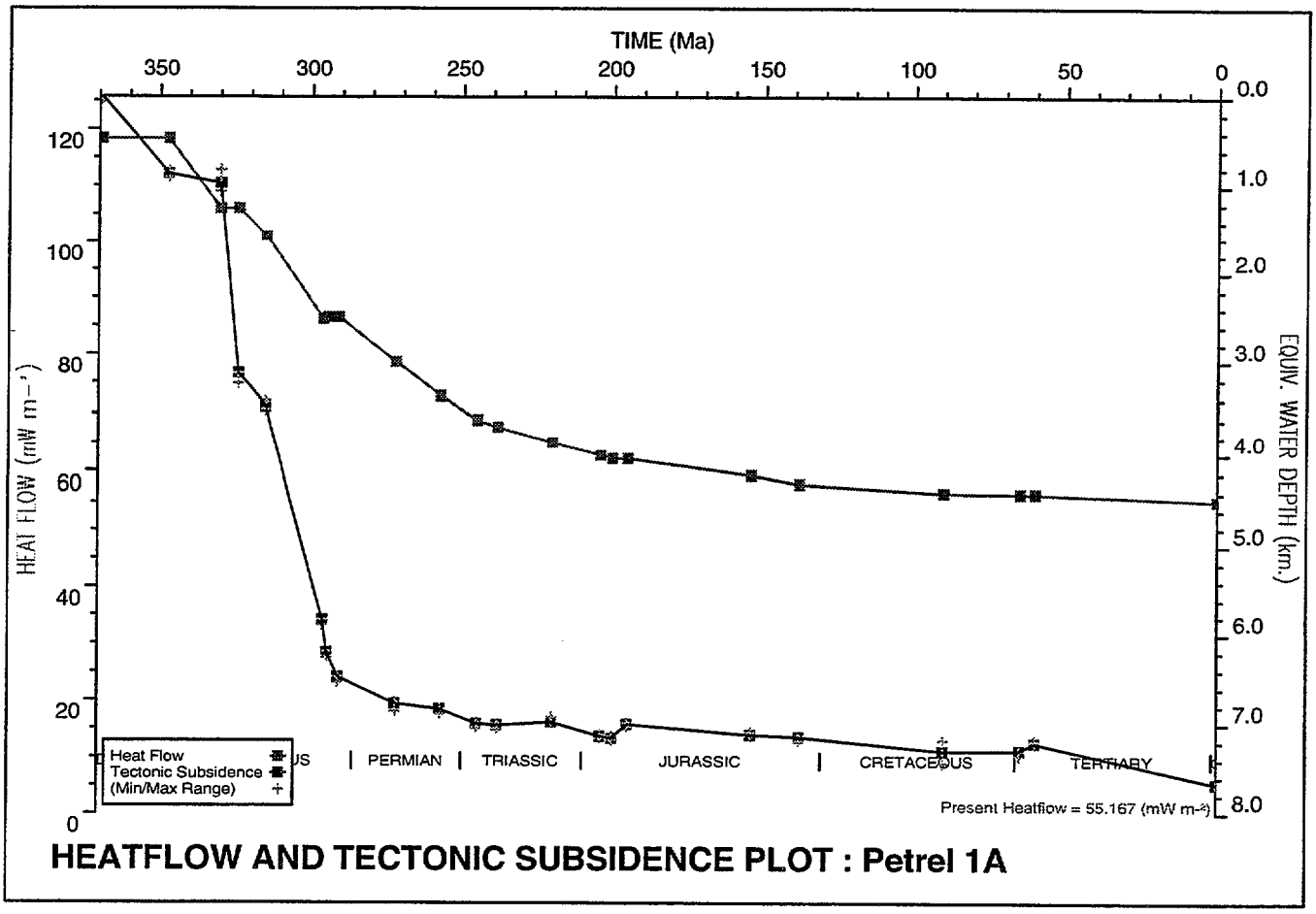

HEATFLOW AND TECTONIC SUBSIDENCE PLOT : Petrel 1A

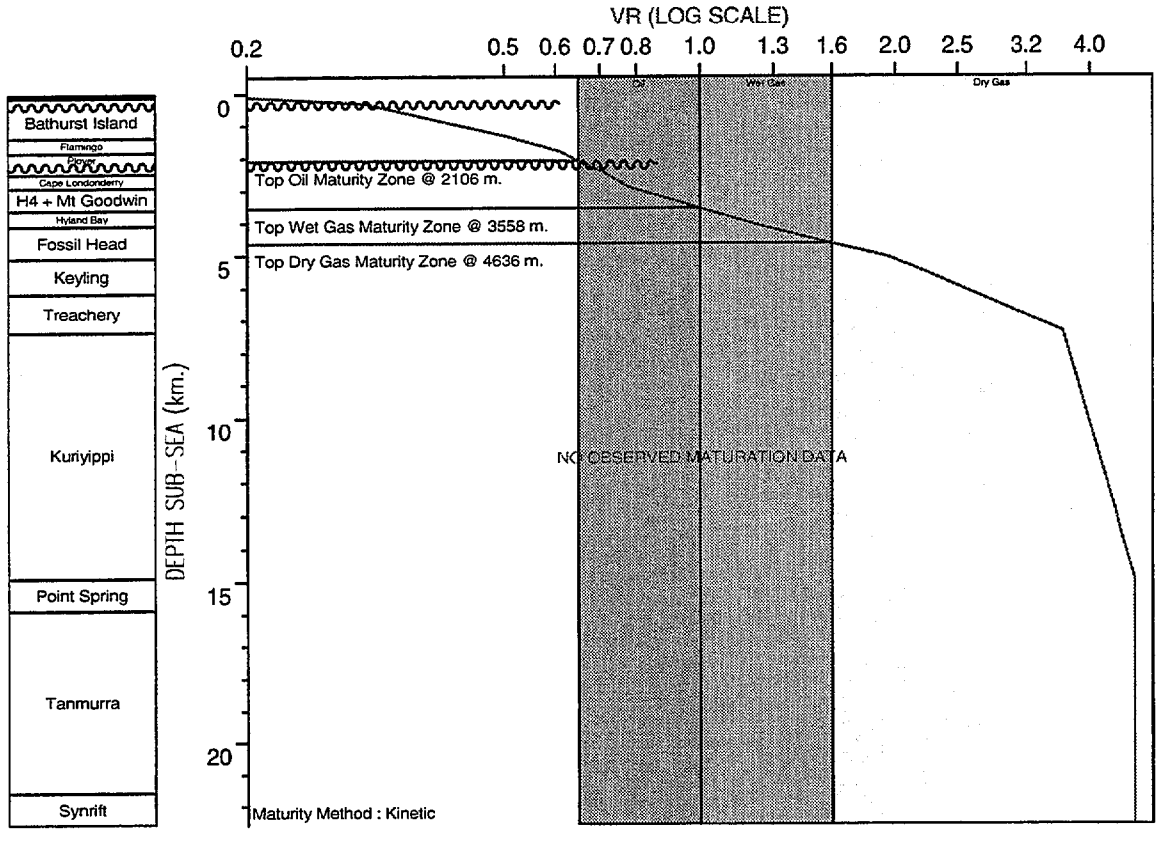

OBSERVED vs COMPUTED MATURITY PLOT : Petrel 1A

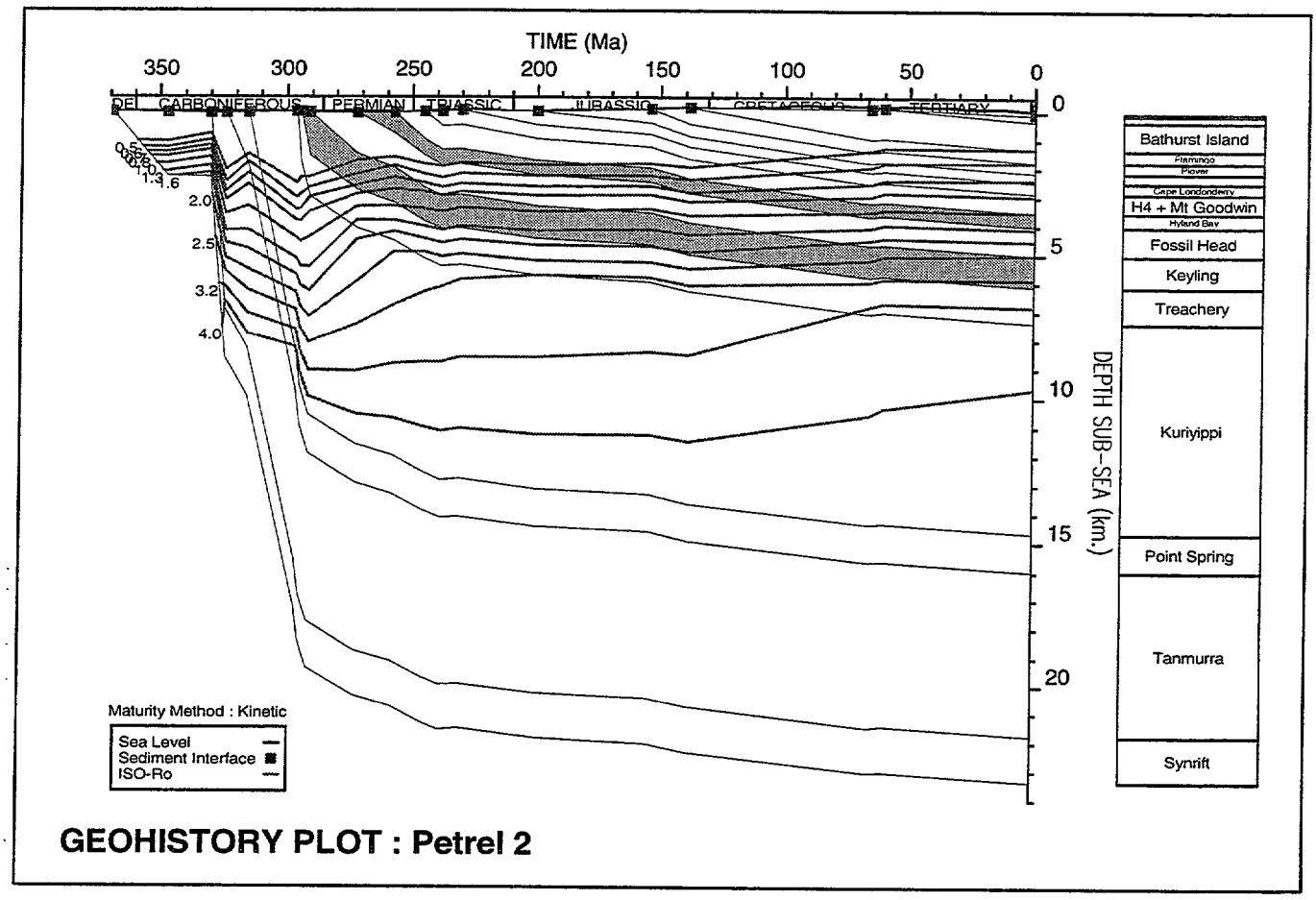

GEOHISTORY PLOT : Petrel 2

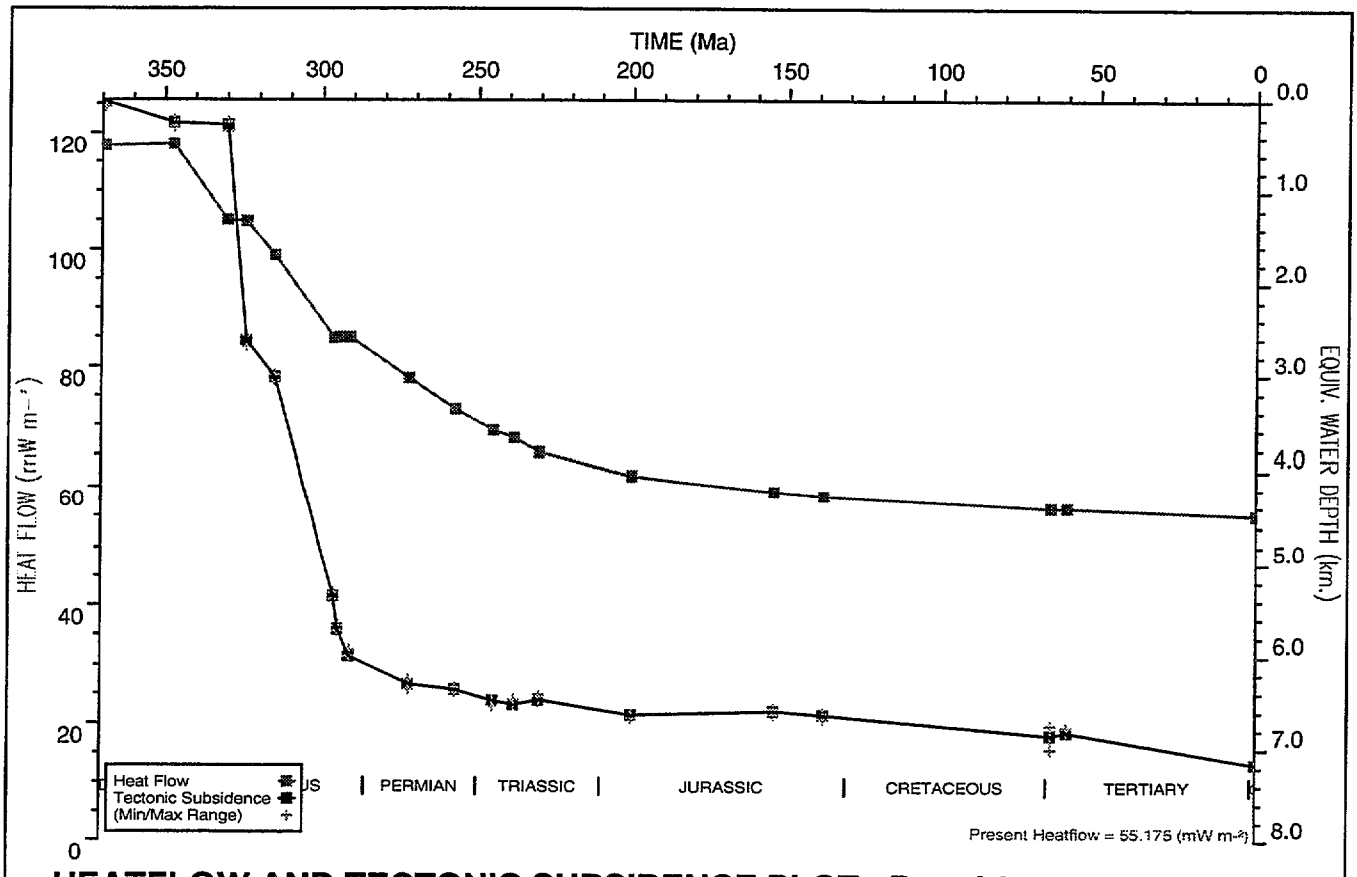

HEATFLOW AND TECTONIC SUBSIDENCE PLOT : Petrel 2

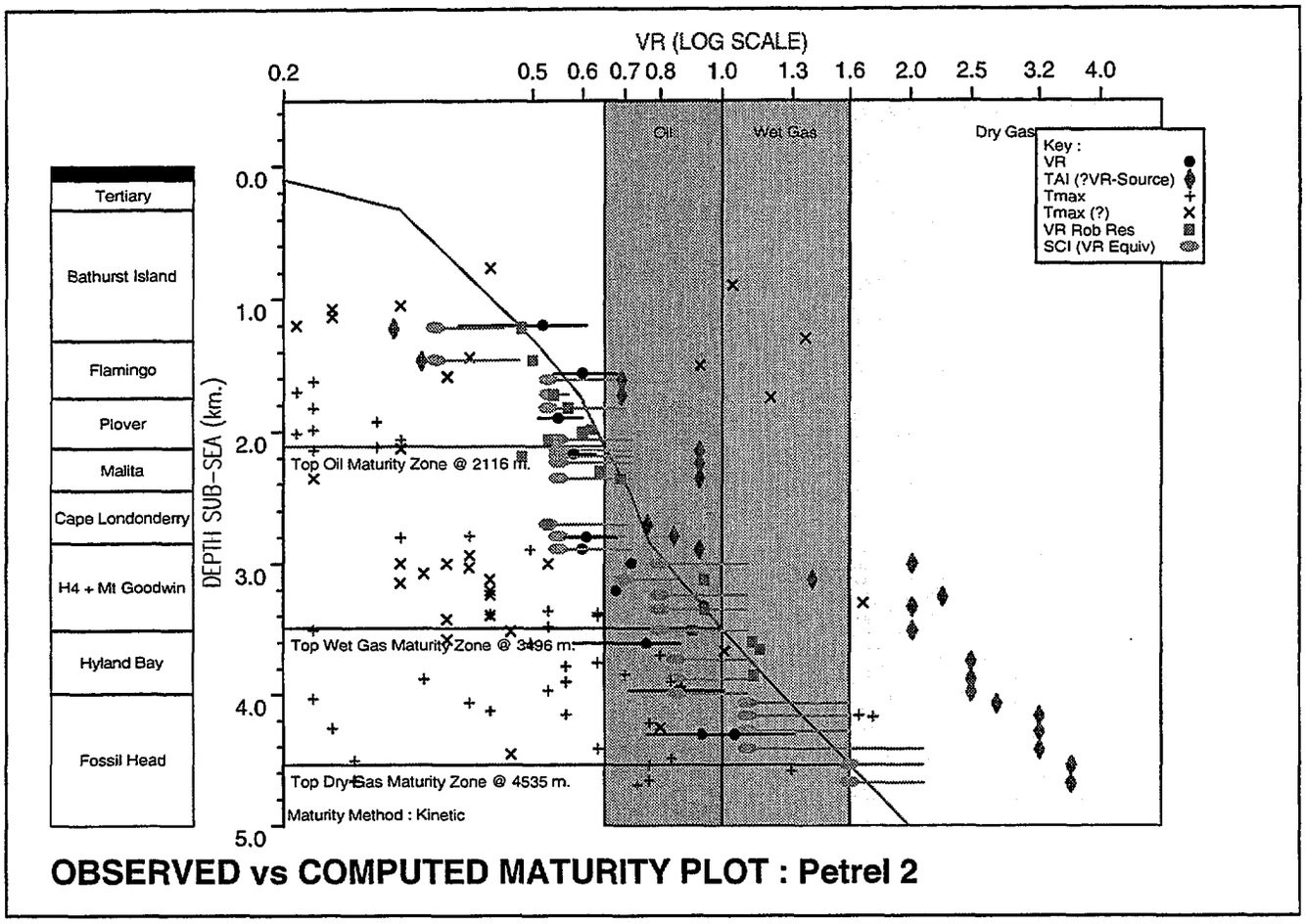

OBSERVED vs COMPUTED MATURITY PLOT : Petrel 2

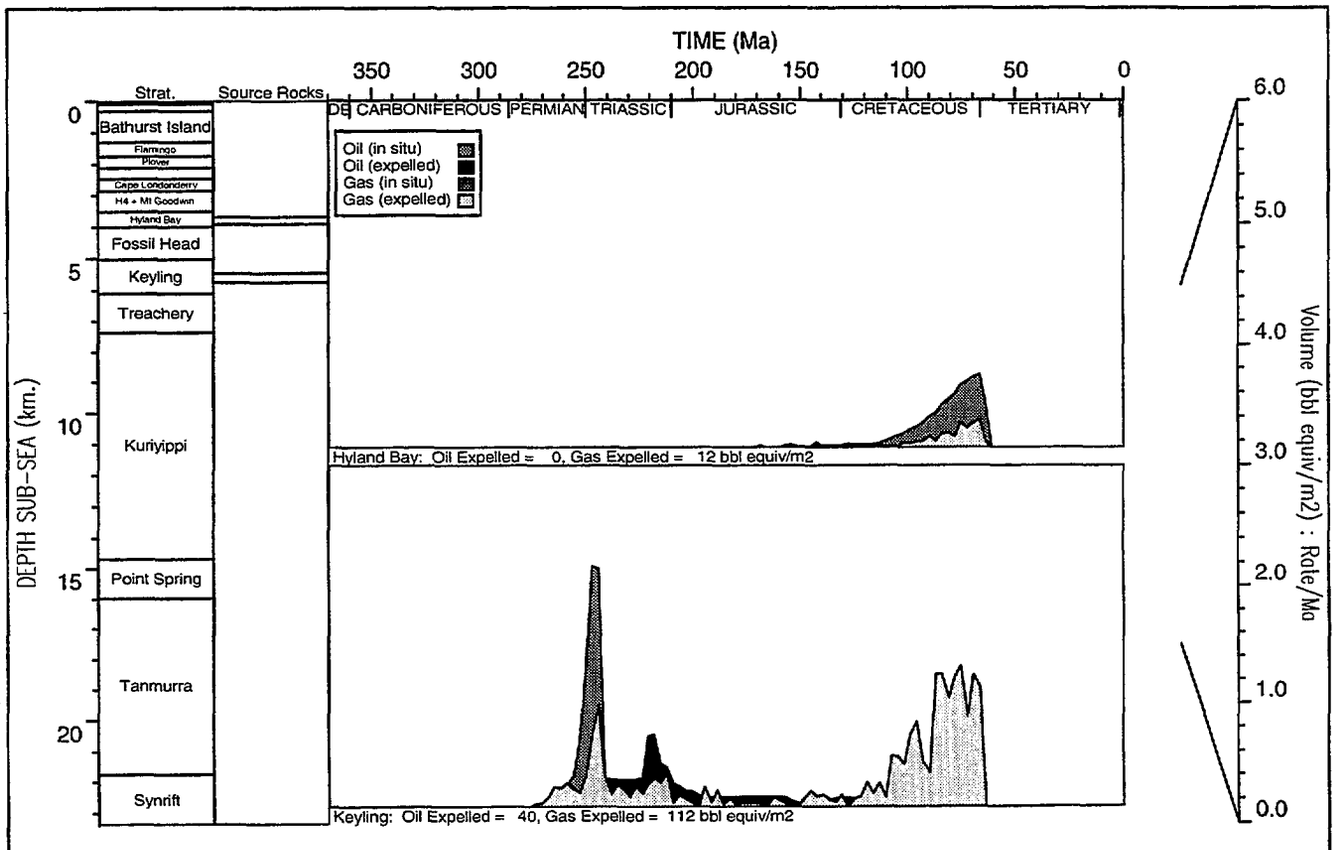

HYDROCARBON GENERATION PLOT : Petrel 2

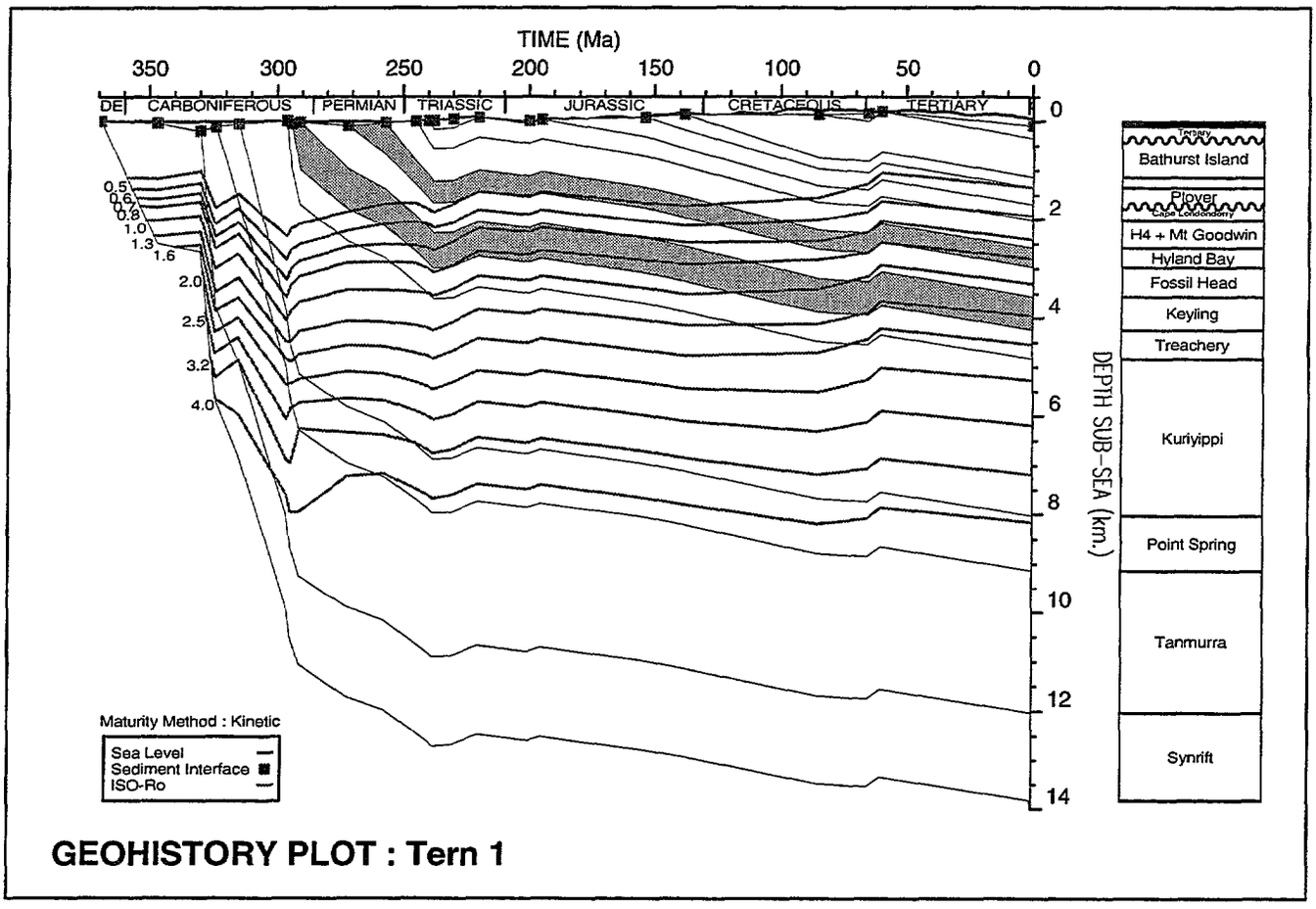

GEOHISTORY PLOT : Tern 1

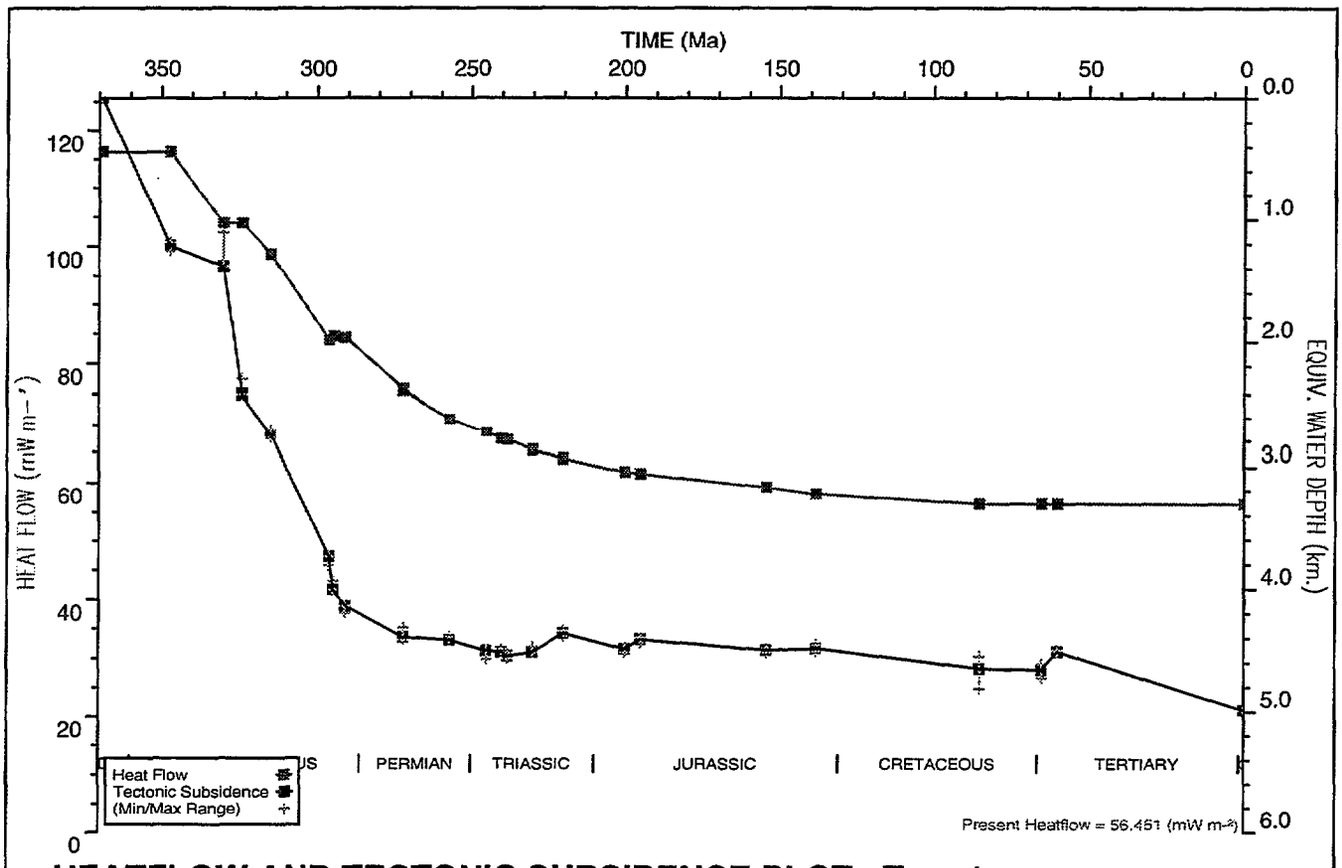

HEATFLOW AND TECTONIC SUBSIDENCE PLOT : Tern 1

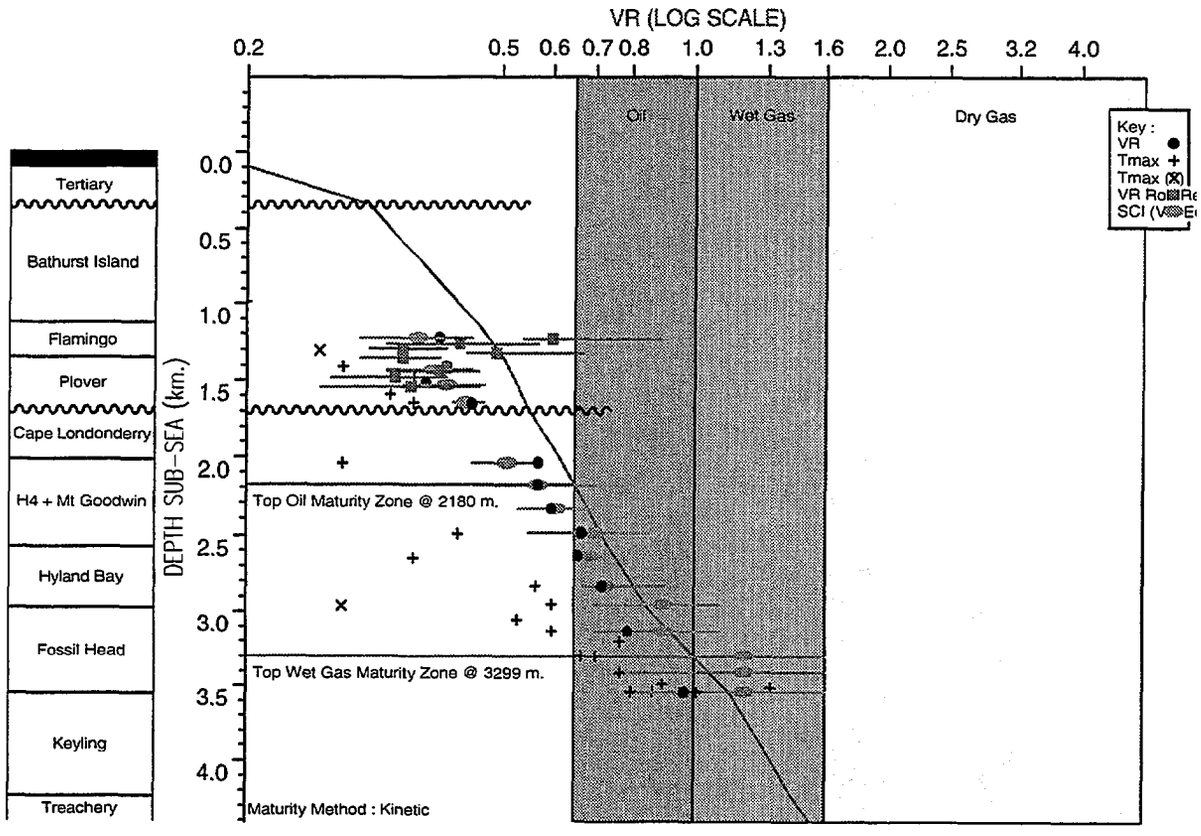

OBSERVED vs COMPUTED MATURITY PLOT : Tern 1

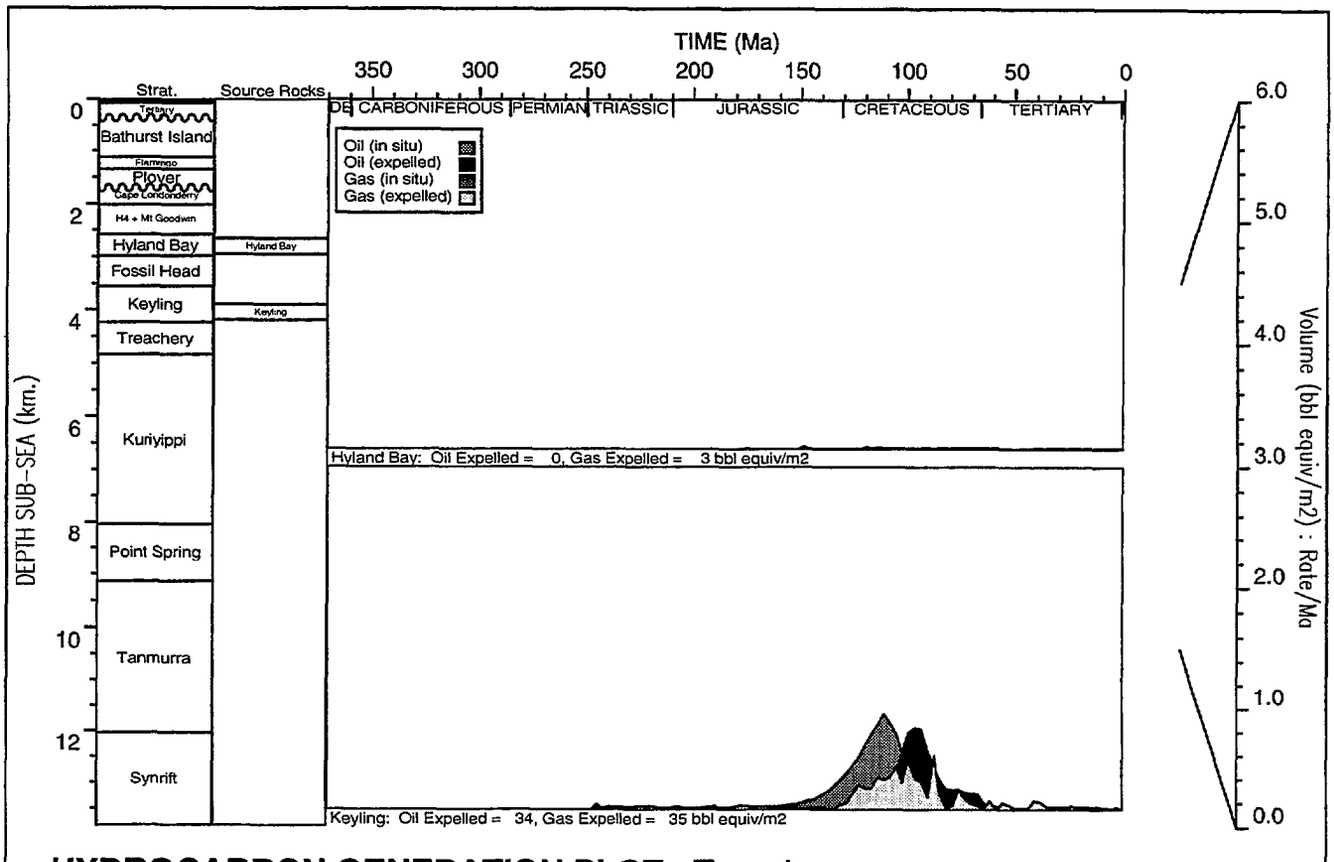

HYDROCARBON GENERATION PLOT : Tern 1

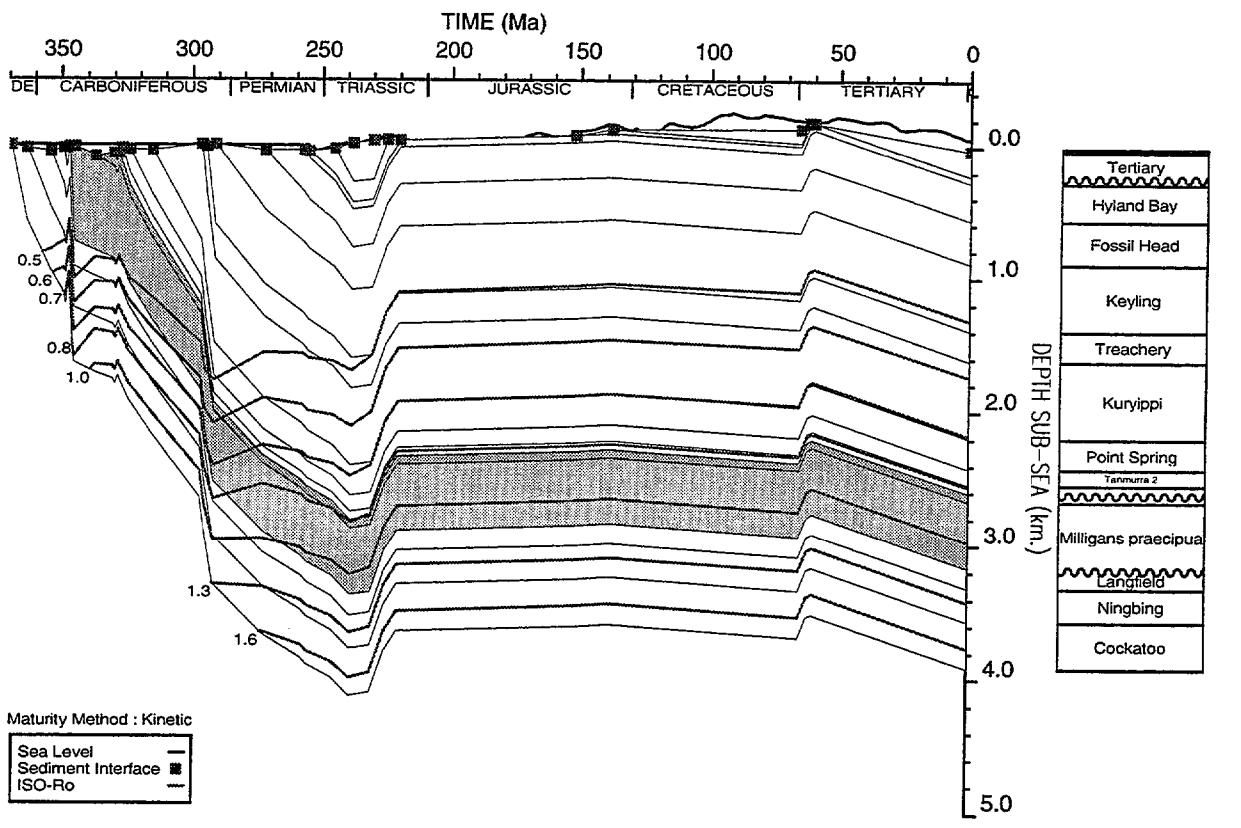

GEOHISTORY PLOT : Turtle 2

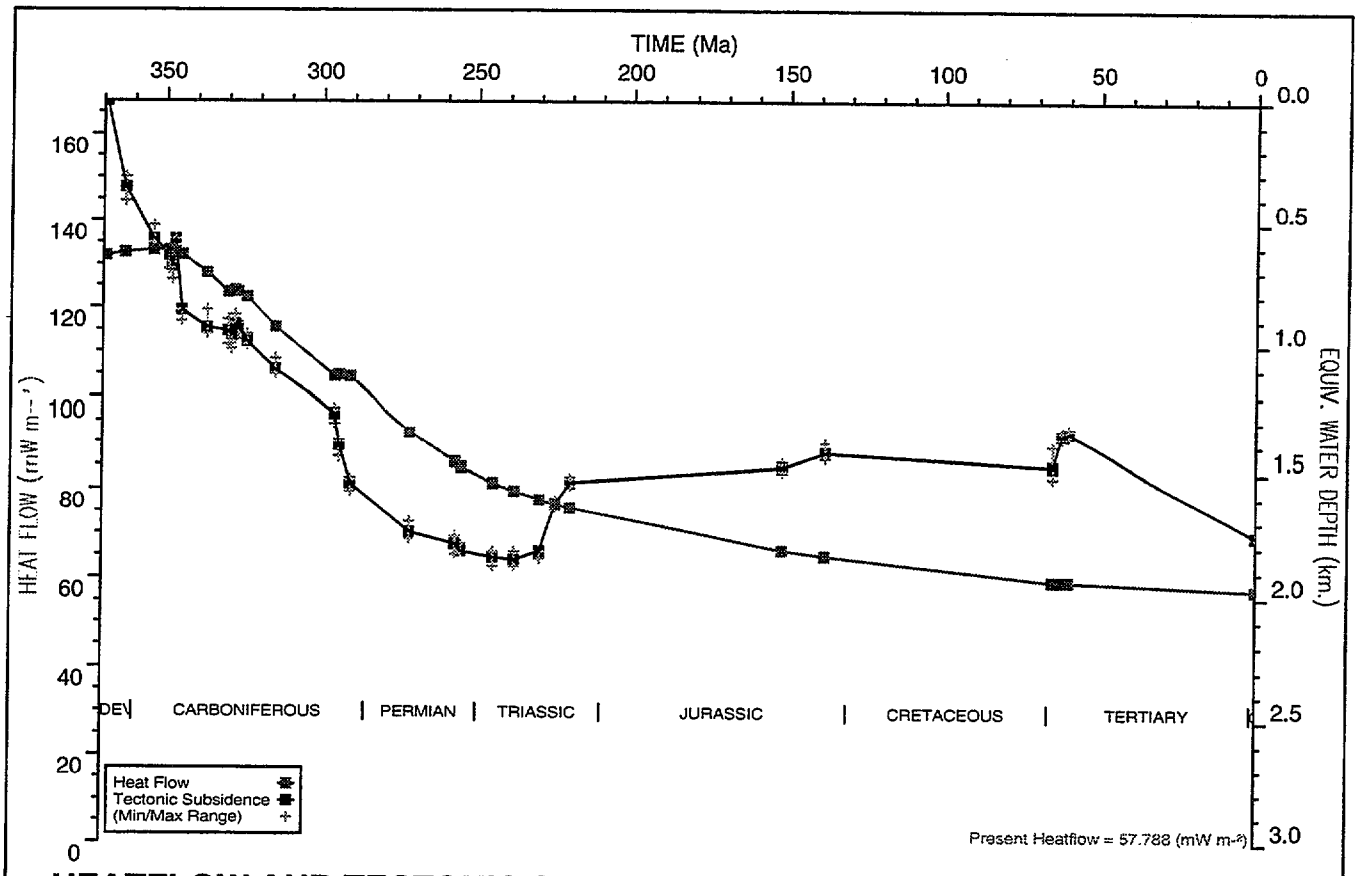

HEATFLOW AND TECTONIC SUBSIDENCE PLOT : Turtle 2

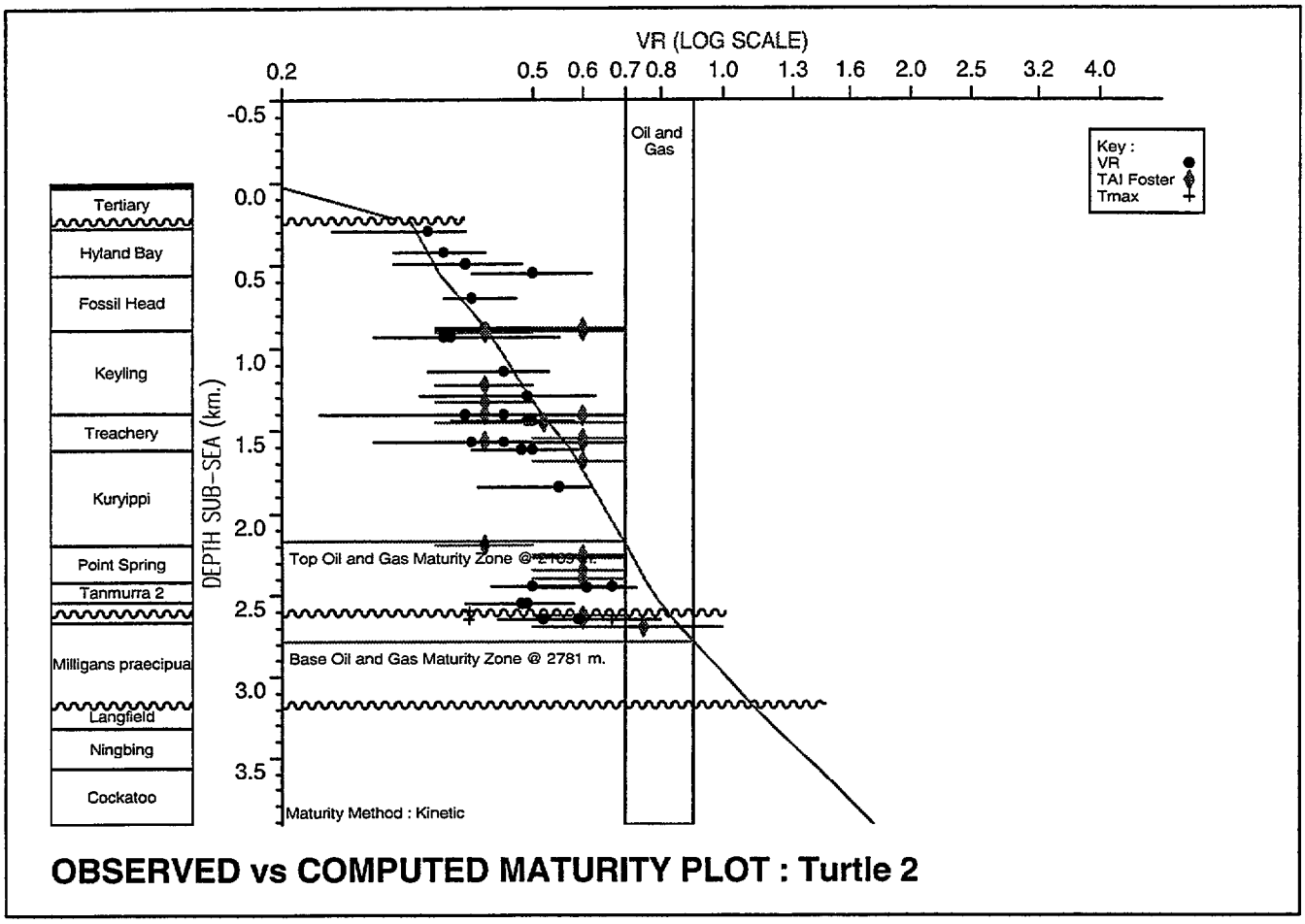

OBSERVED vs COMPUTED MATURITY PLOT : Turtle 2

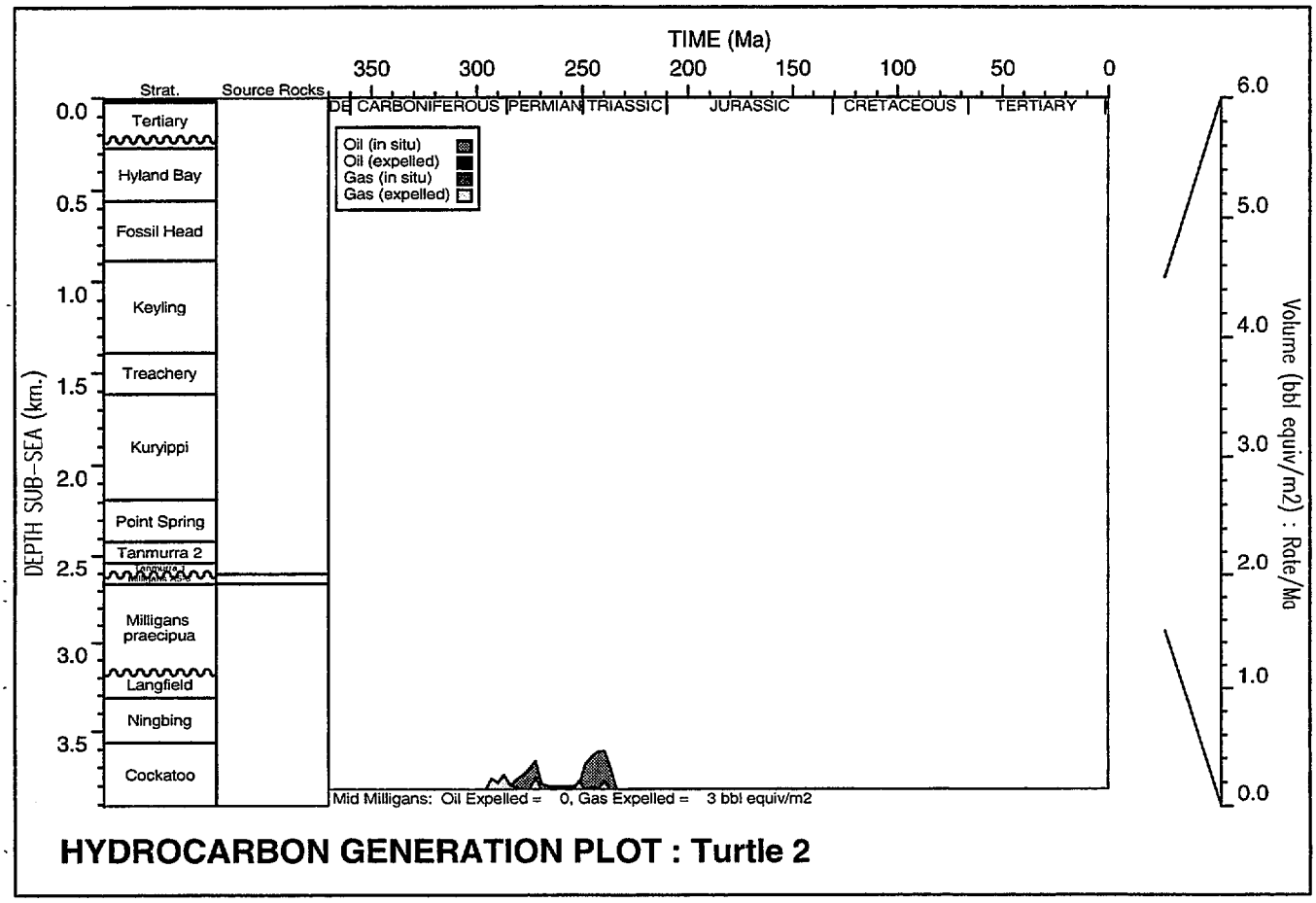

HYDROCARBON GENERATION PLOT : Turtle 2

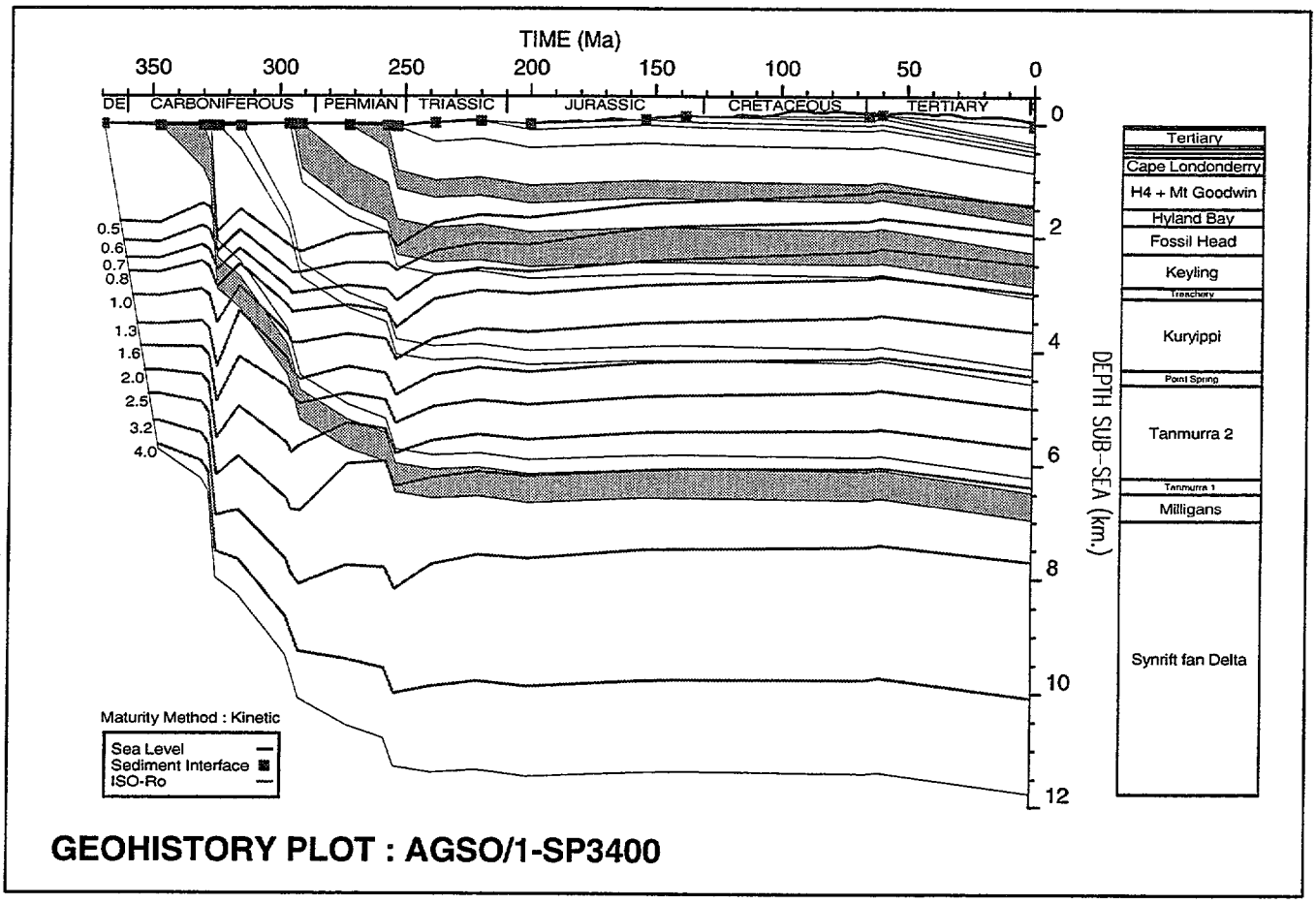

GEOHISTORY PLOT : AGSO/1-SP3400

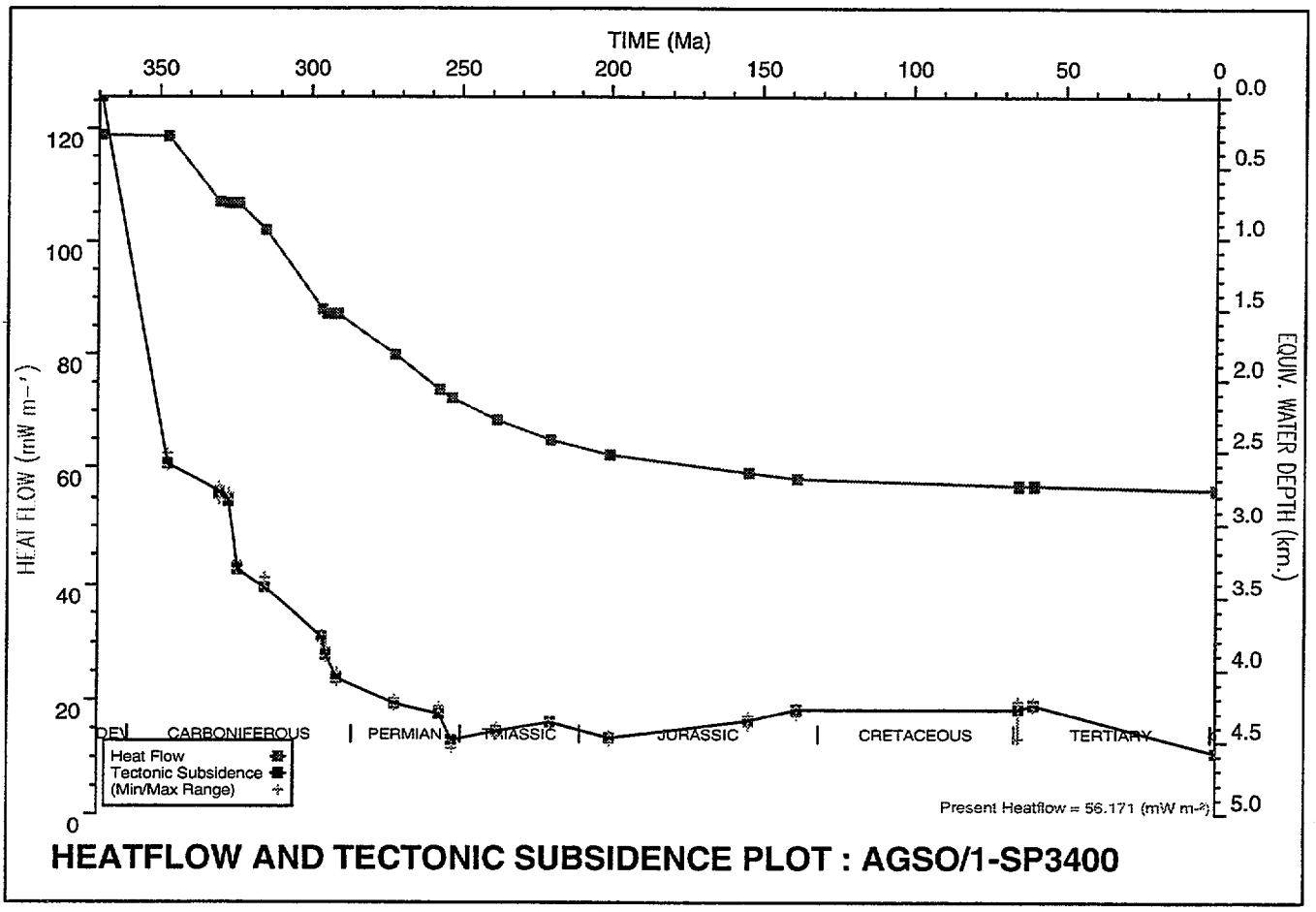

HEATFLOW AND TECTONIC SUBSIDENCE PLOT : AGSO/1-SP3400

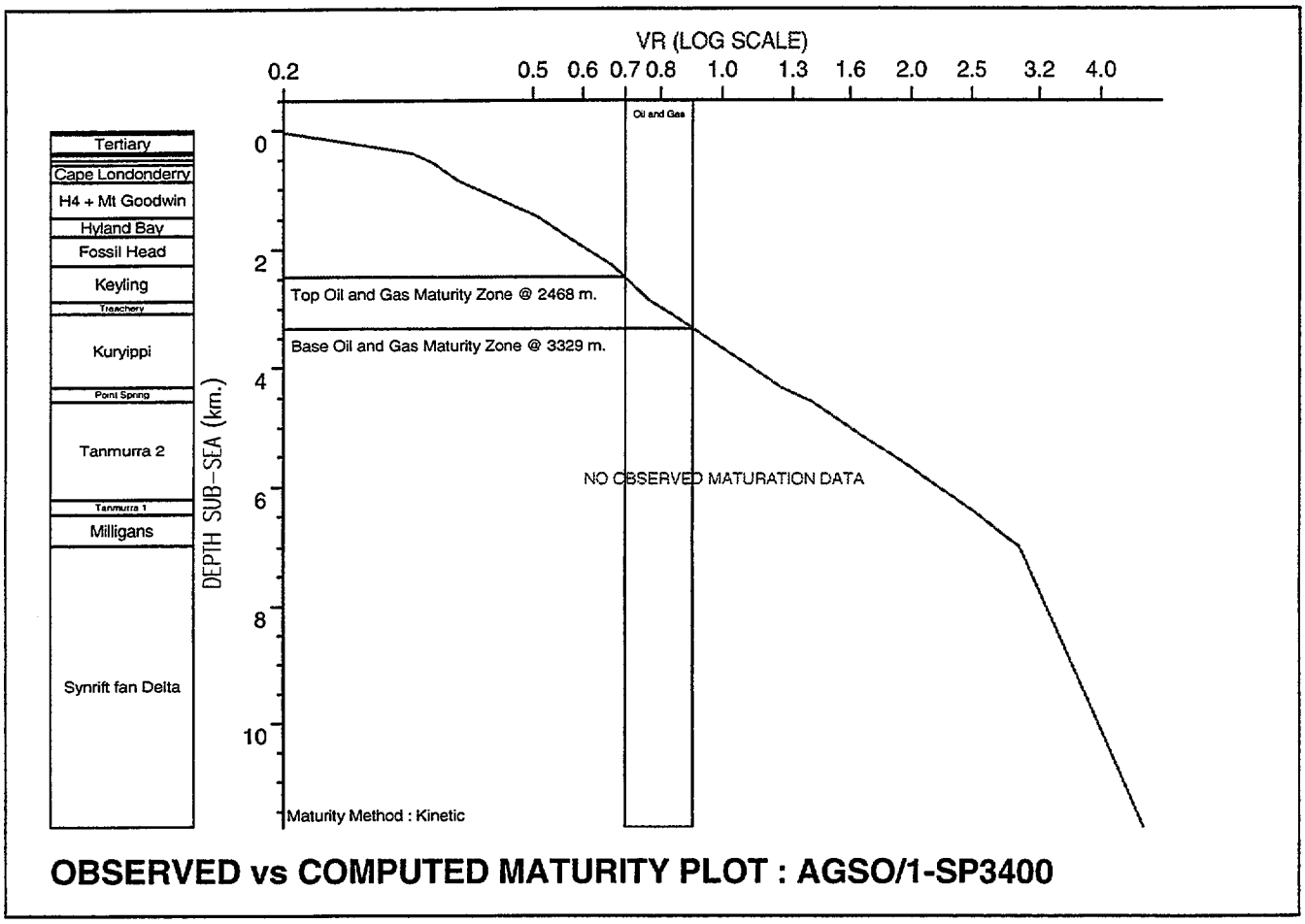

OBSERVED vs COMPUTED MATURITY PLOT : AGSO/1-SP3400

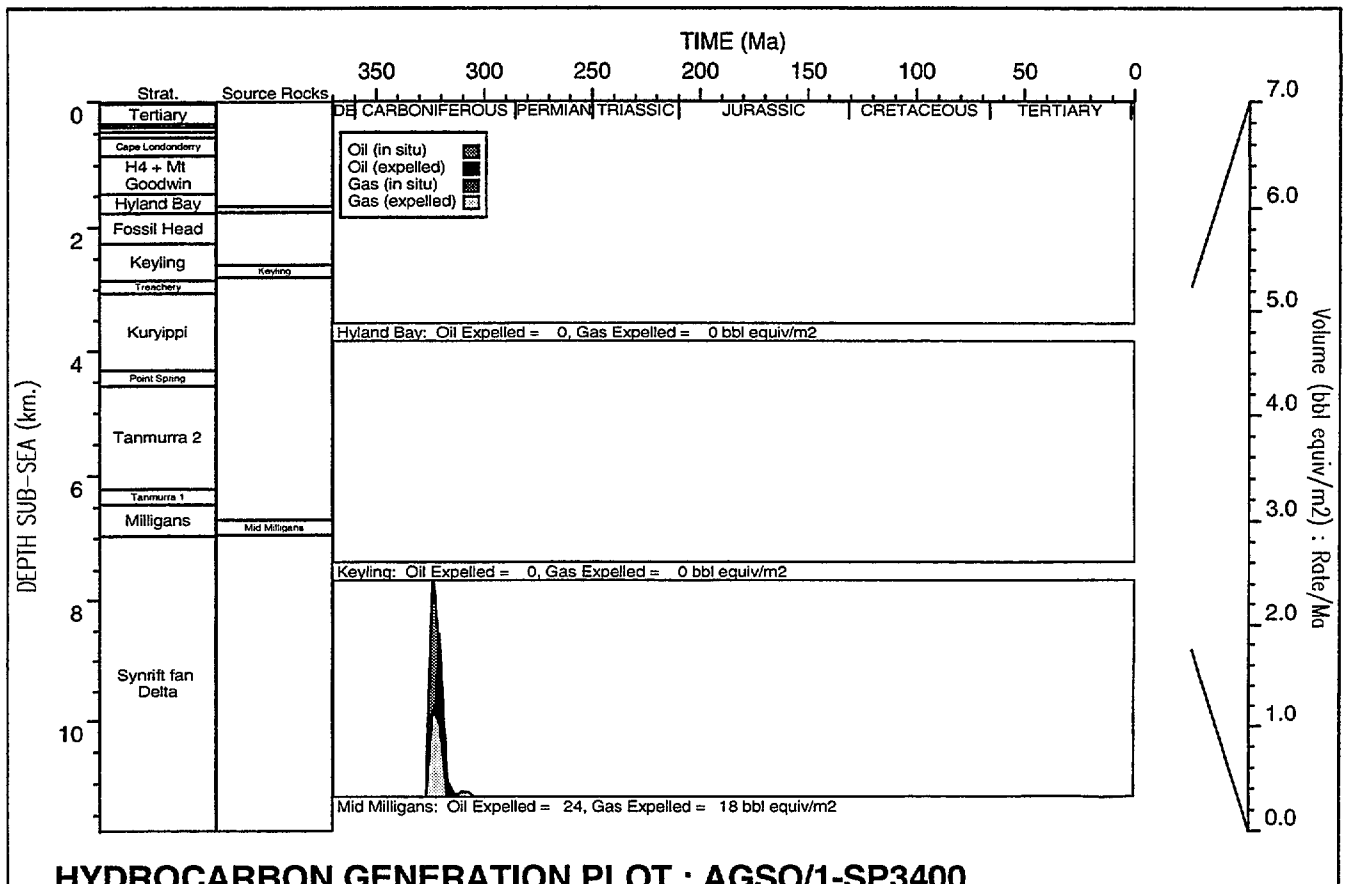

HYDROCARBON GENERATION PLOT : AGSO/1-SP3400

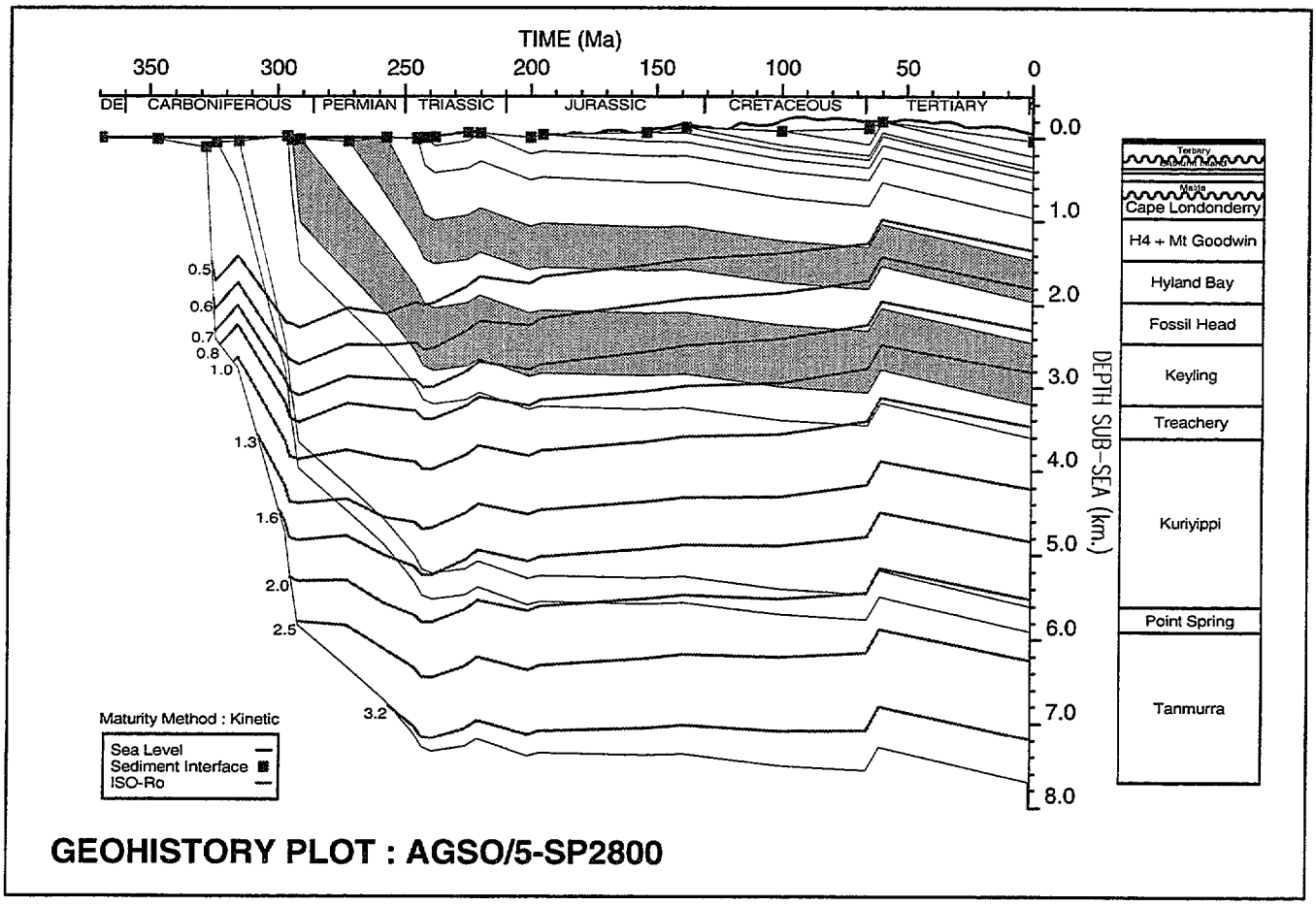

GEOHISTORY PLOT : AGSO/5-SP2800

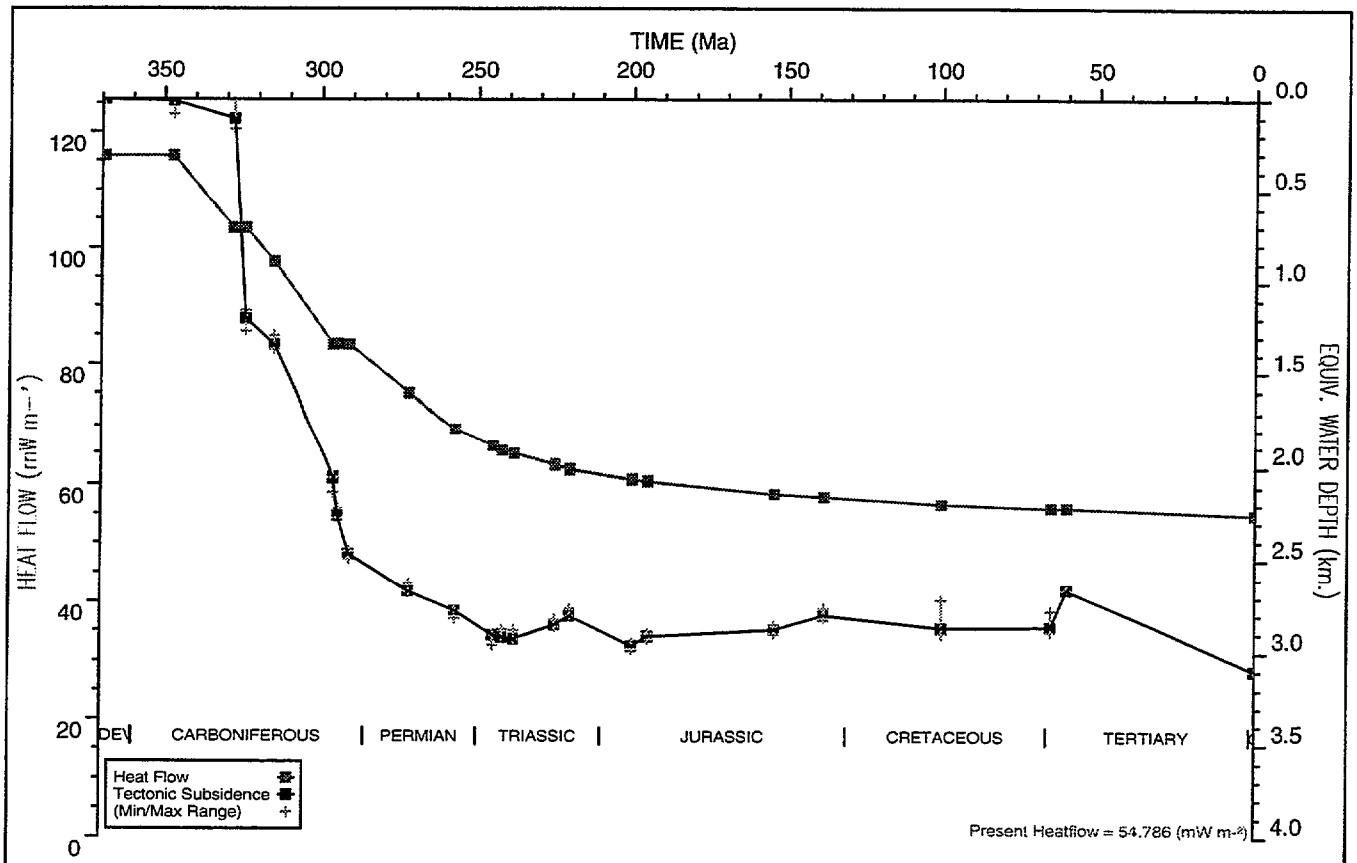

HEATFLOW AND TECTONIC SUBSIDENCE PLOT : AGSO/5-SP2800

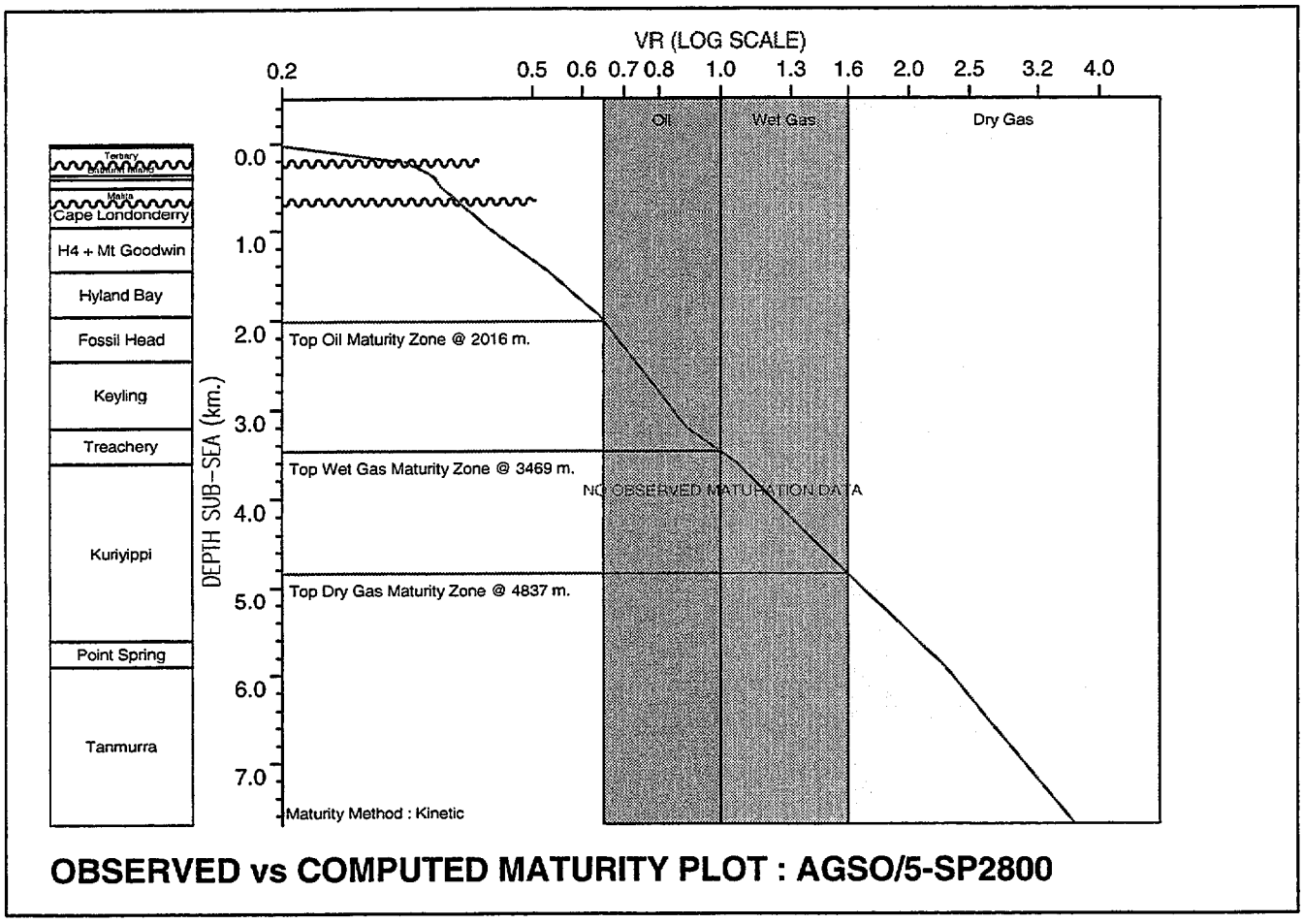

OBSERVED vs COMPUTED MATURITY PLOT : AGSO/5-SP2800

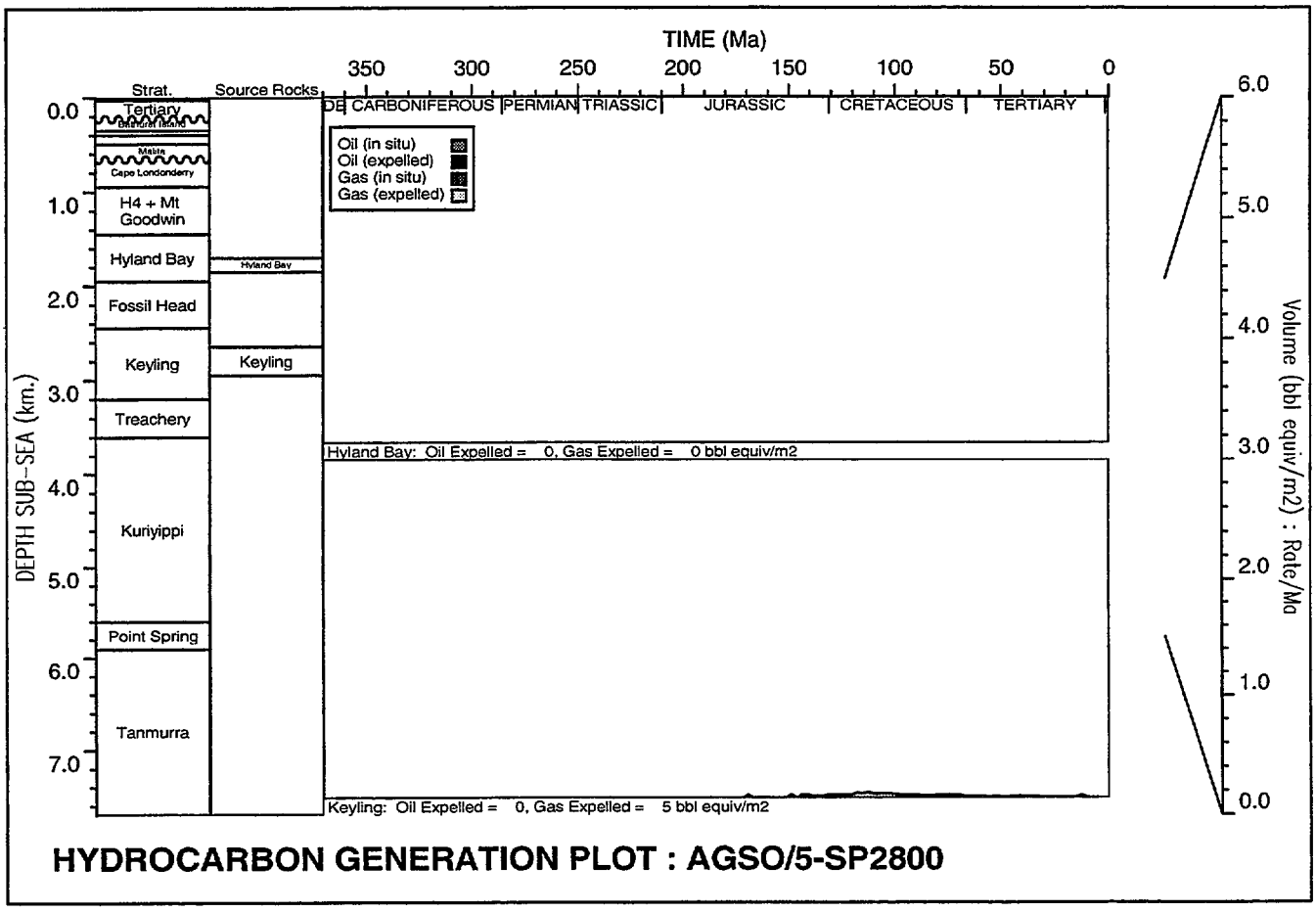

HYDROCARBON GENERATION PLOT : AGSO/5-SP2800

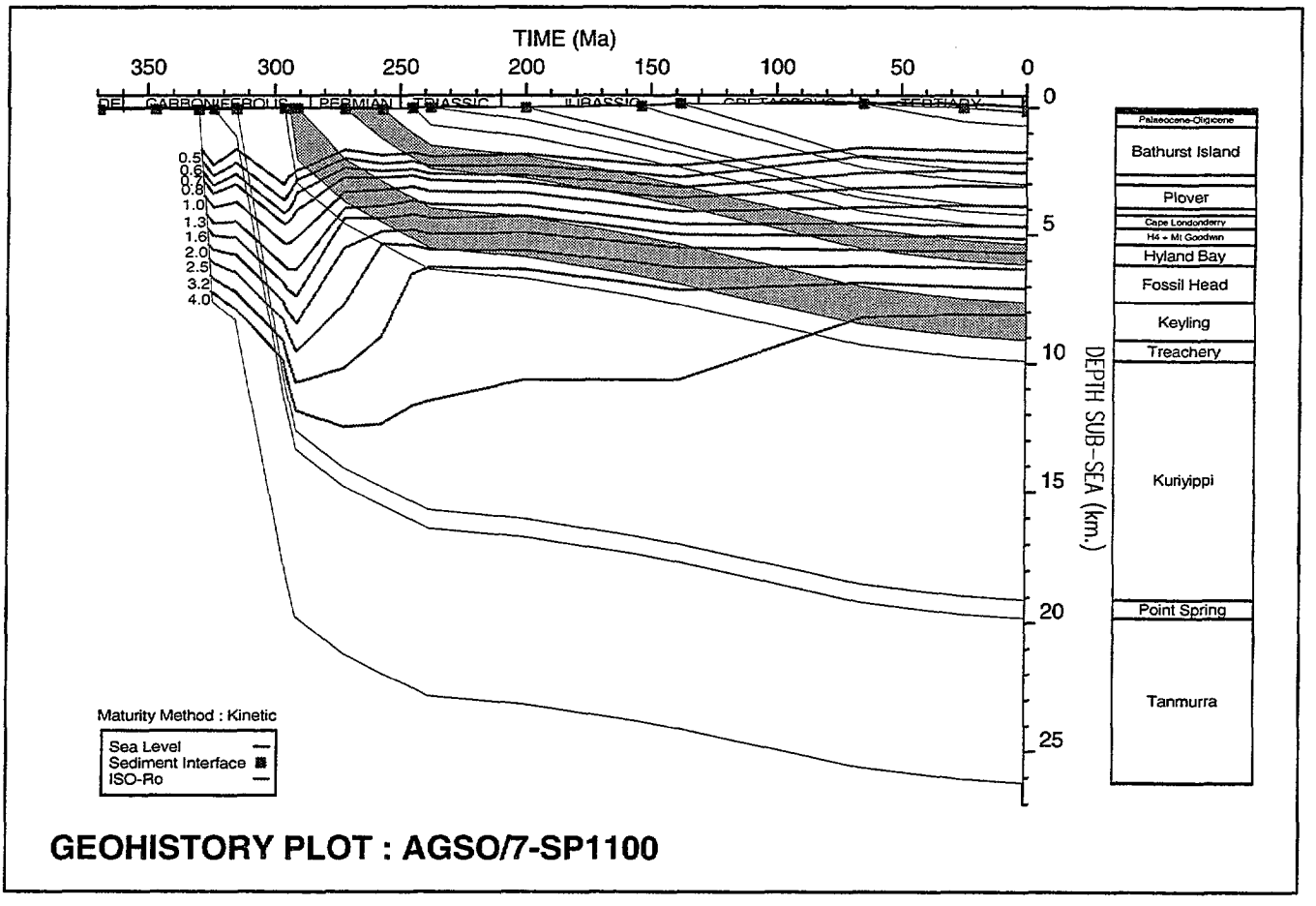

GEOHISTORY PLOT : AGSO/7-SP1100

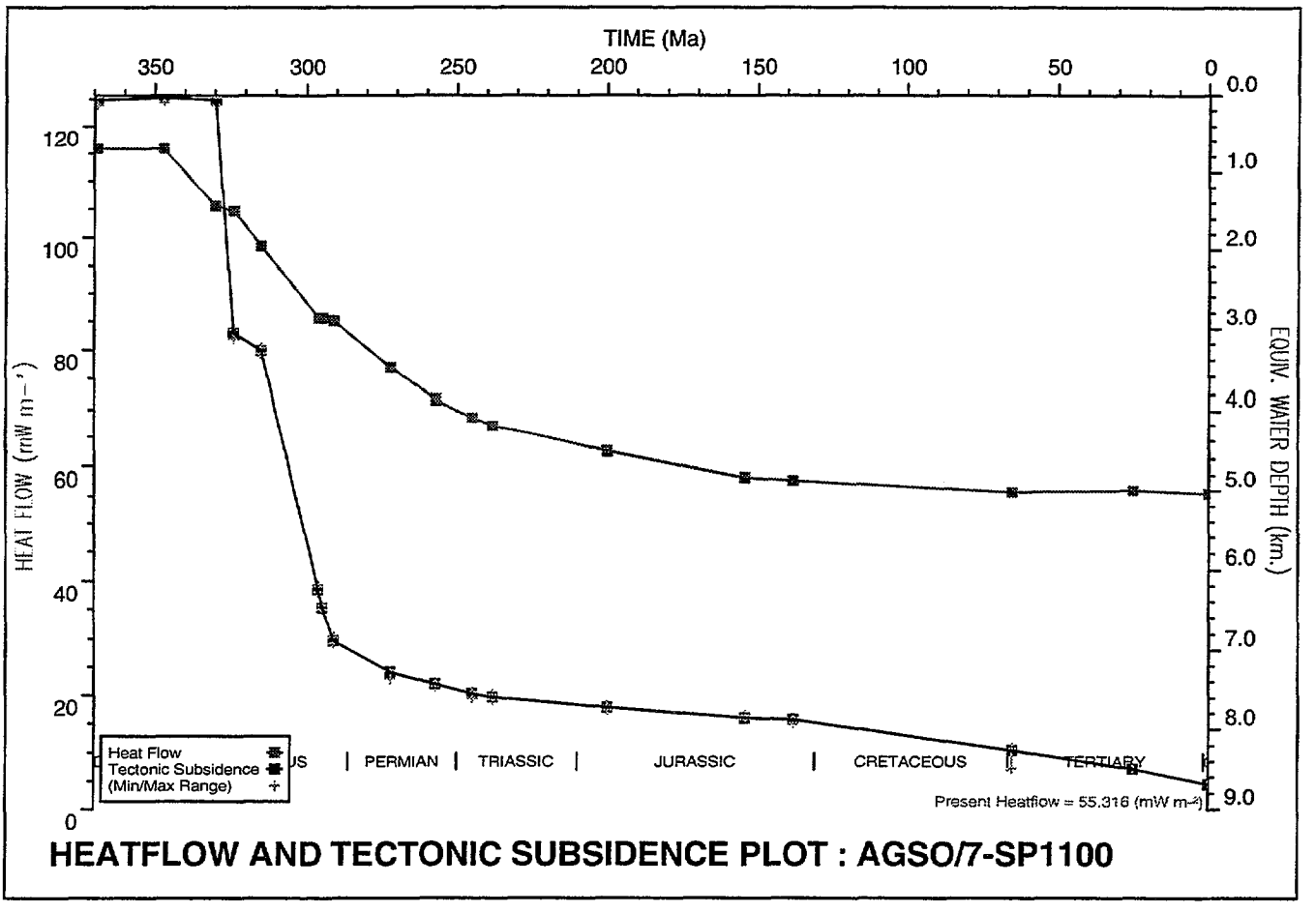

HEATFLOW AND TECTONIC SUBSIDENCE PLOT : AGSO/7-SP1100

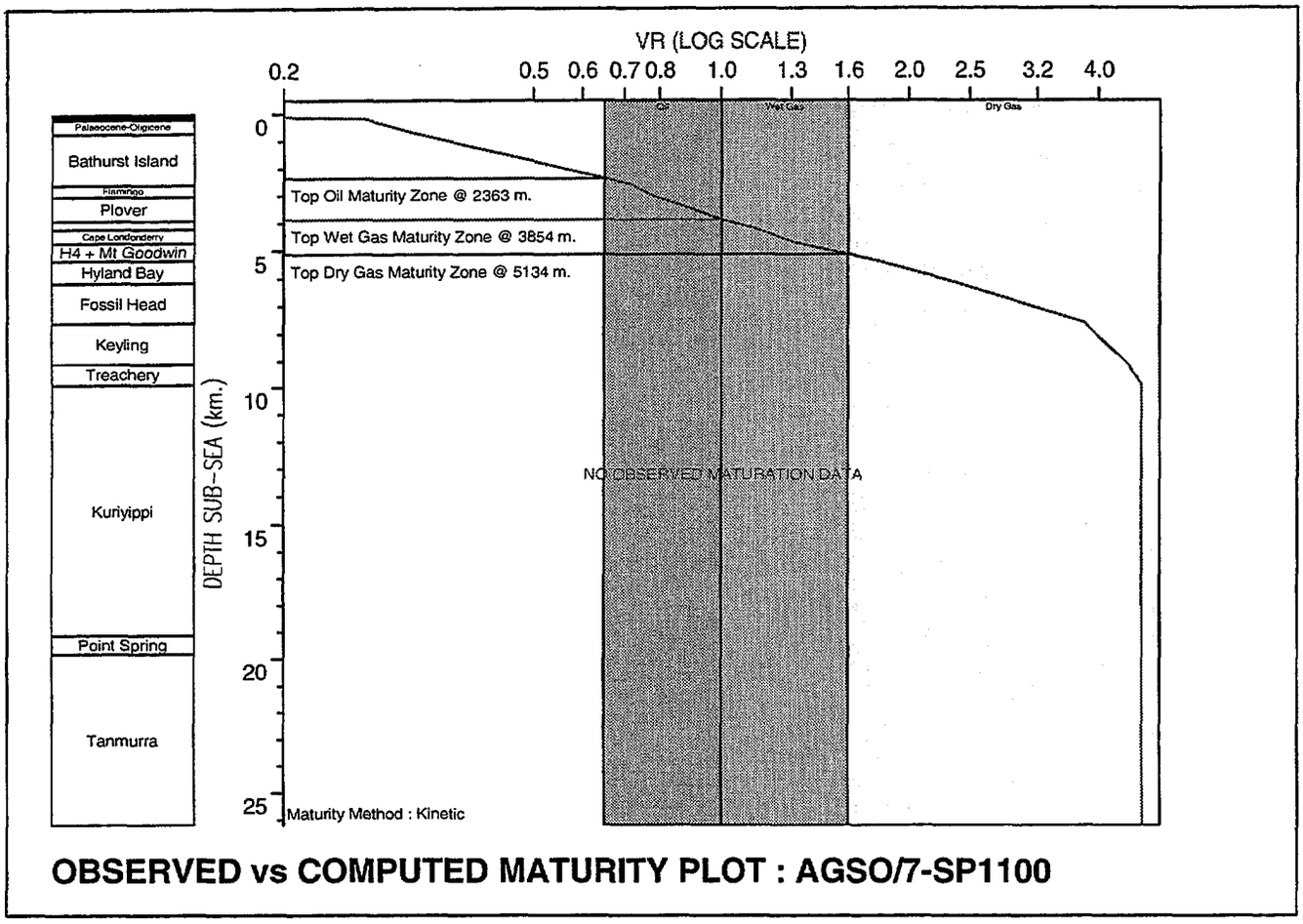

OBSERVED vs COMPUTED MATURITY PLOT : AGSO/7-SP1100

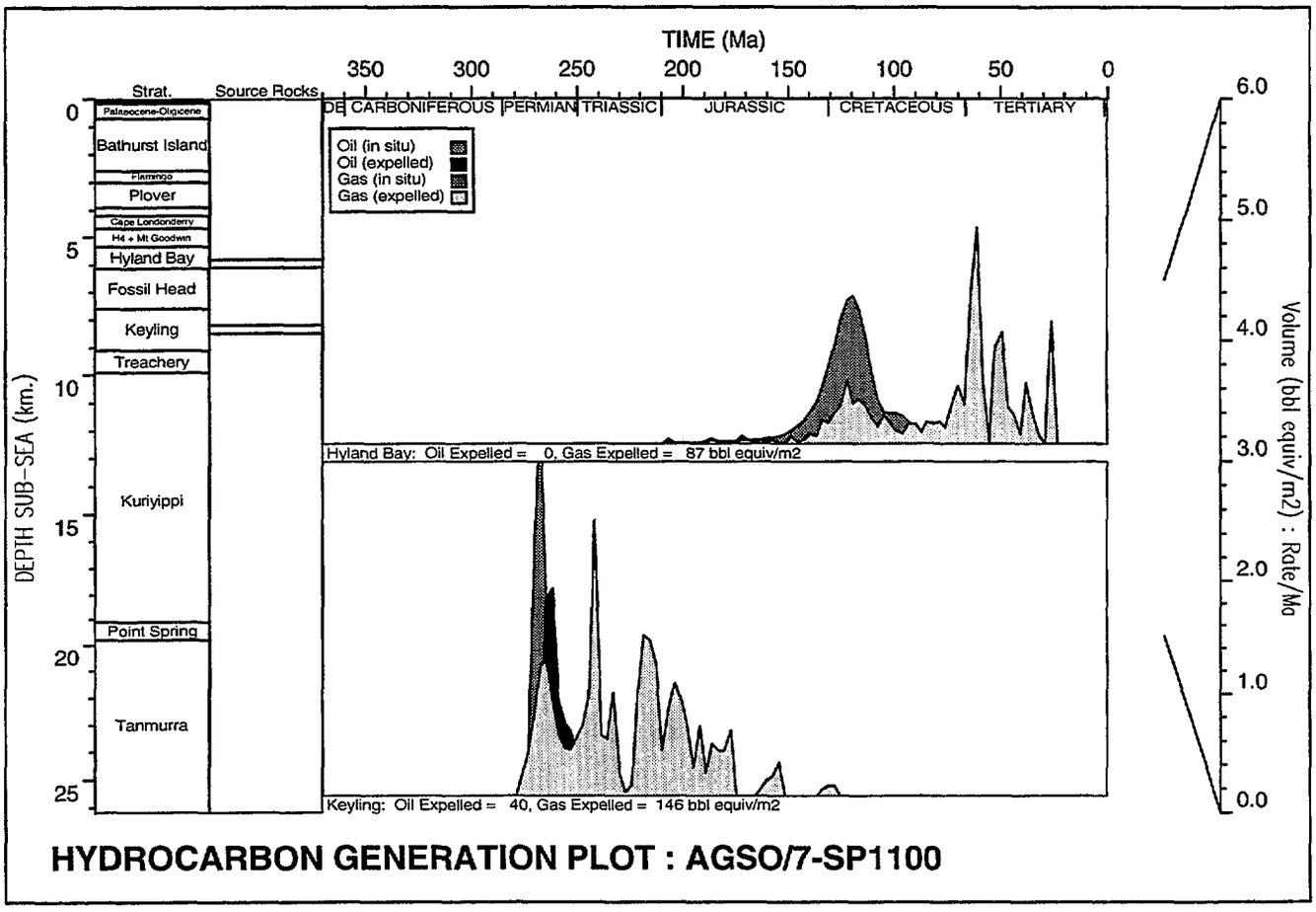

HYDROCARBON GENERATION PLOT : AGSO/7-SP1100

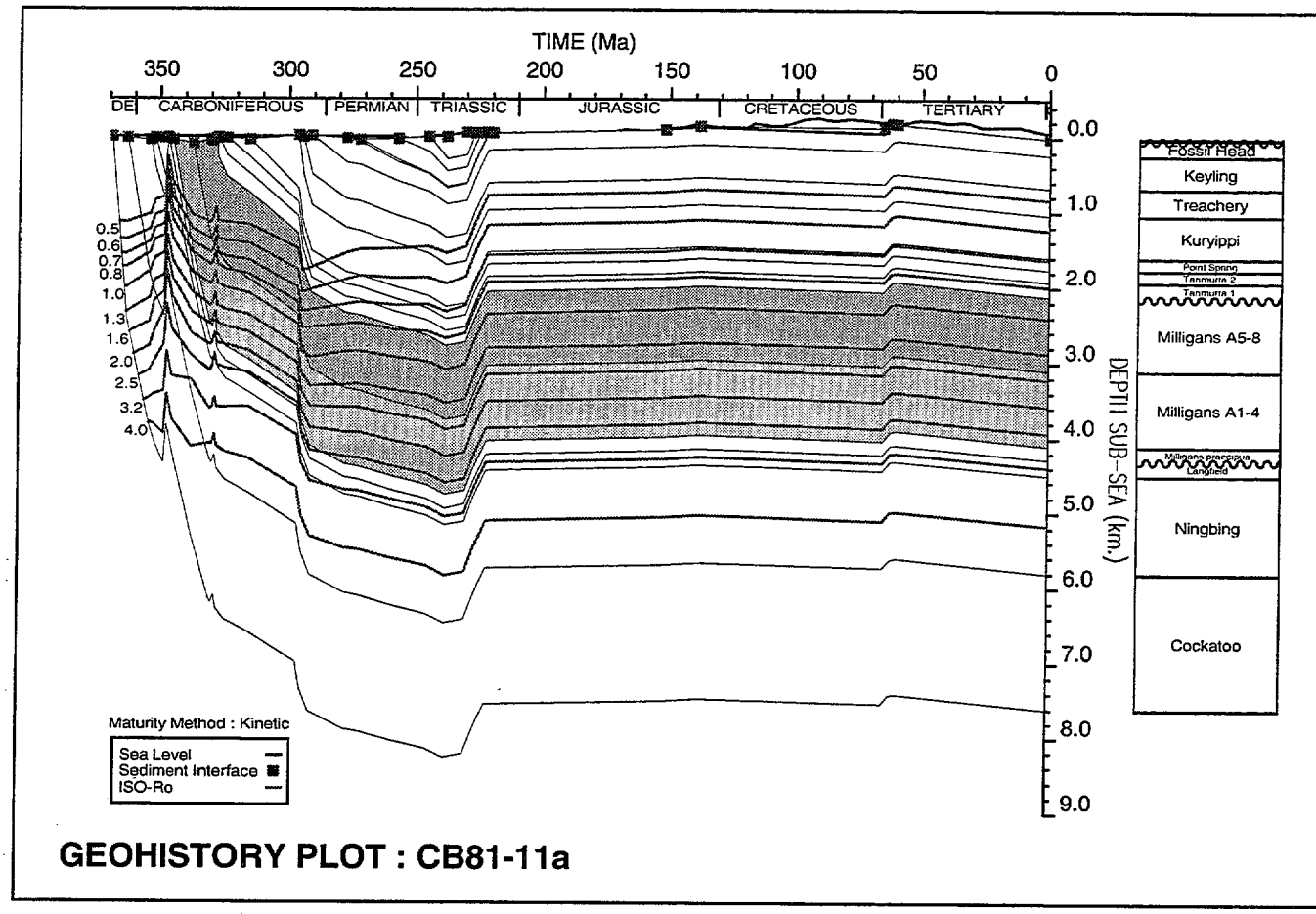

GEOHISTORY PLOT : CB81-11a

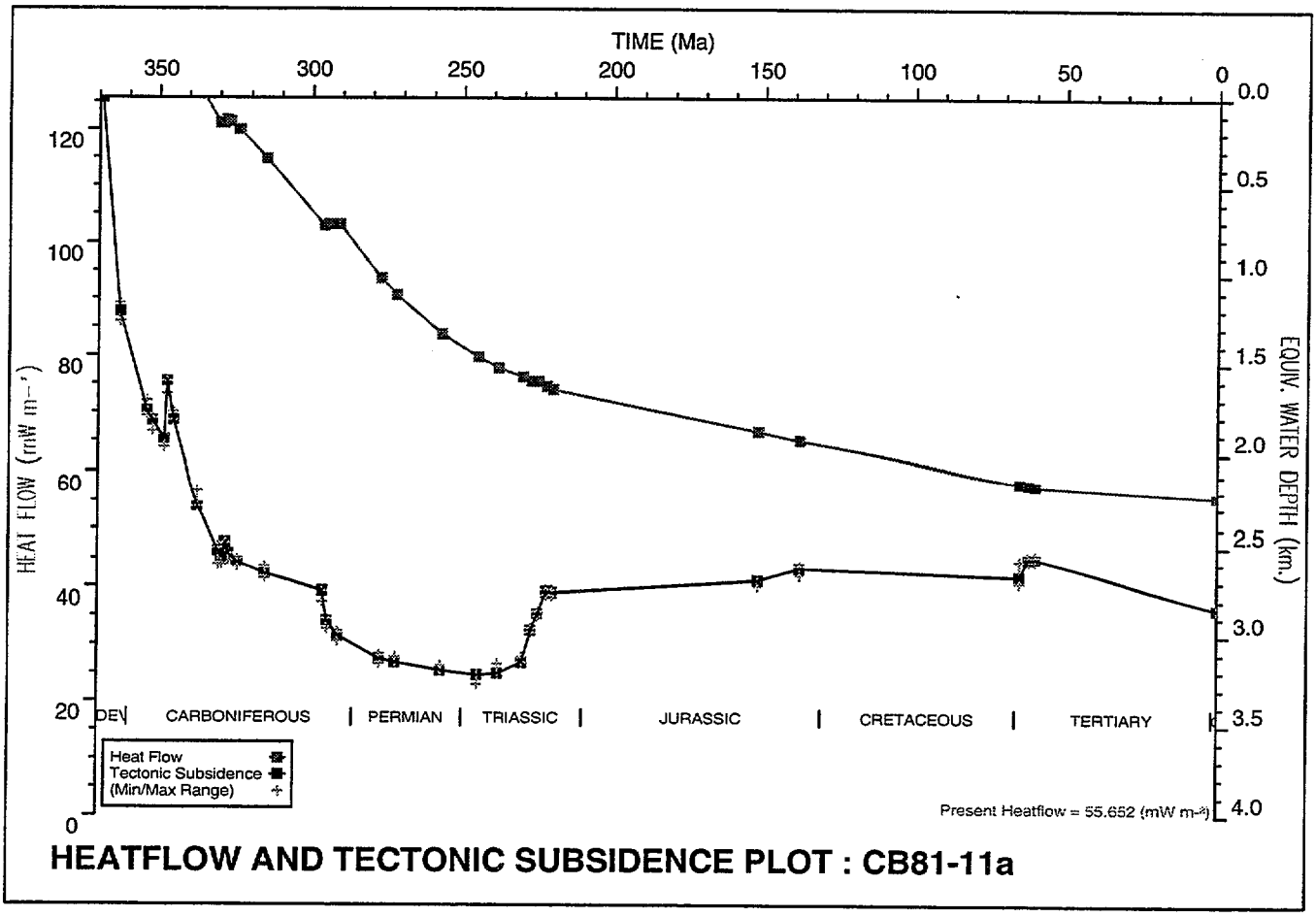

HEATFLOW AND TECTONIC SUBSIDENCE PLOT : CB81-11a

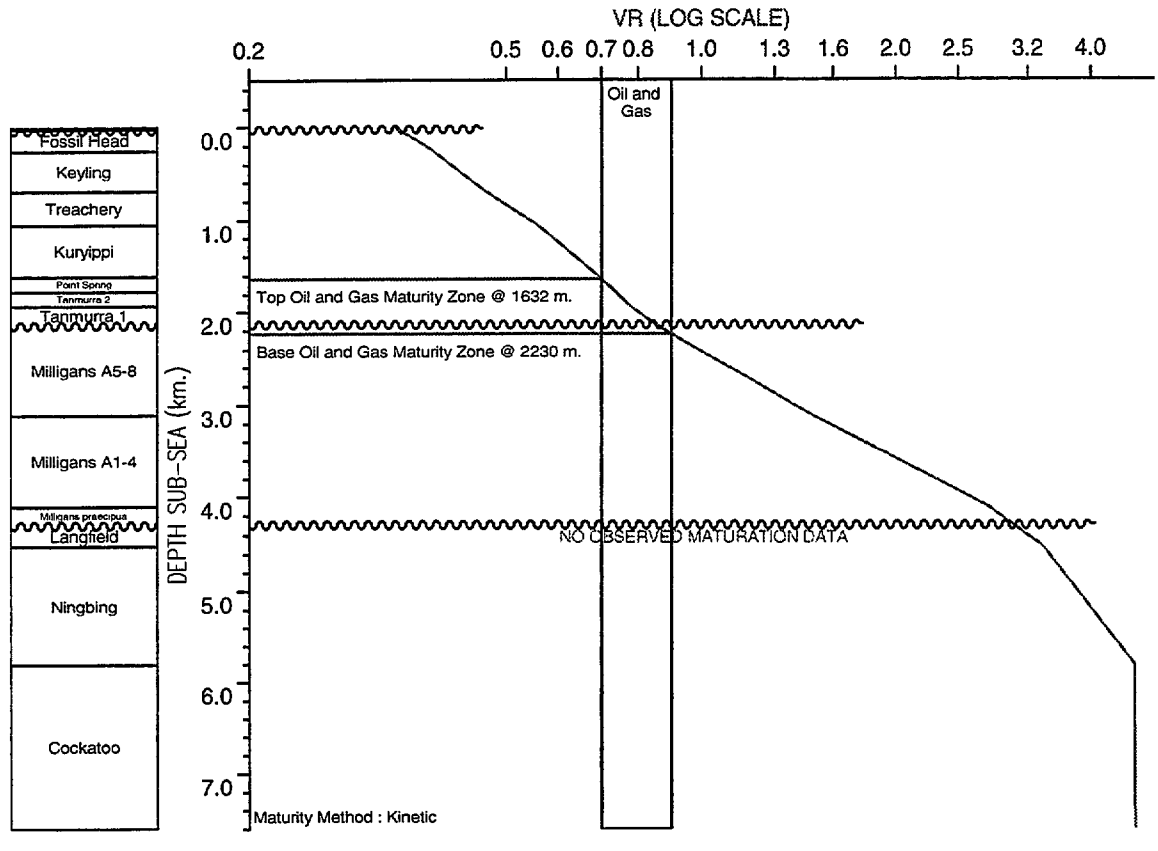

OBSERVED vs COMPUTED MATURITY PLOT : CB81-11a

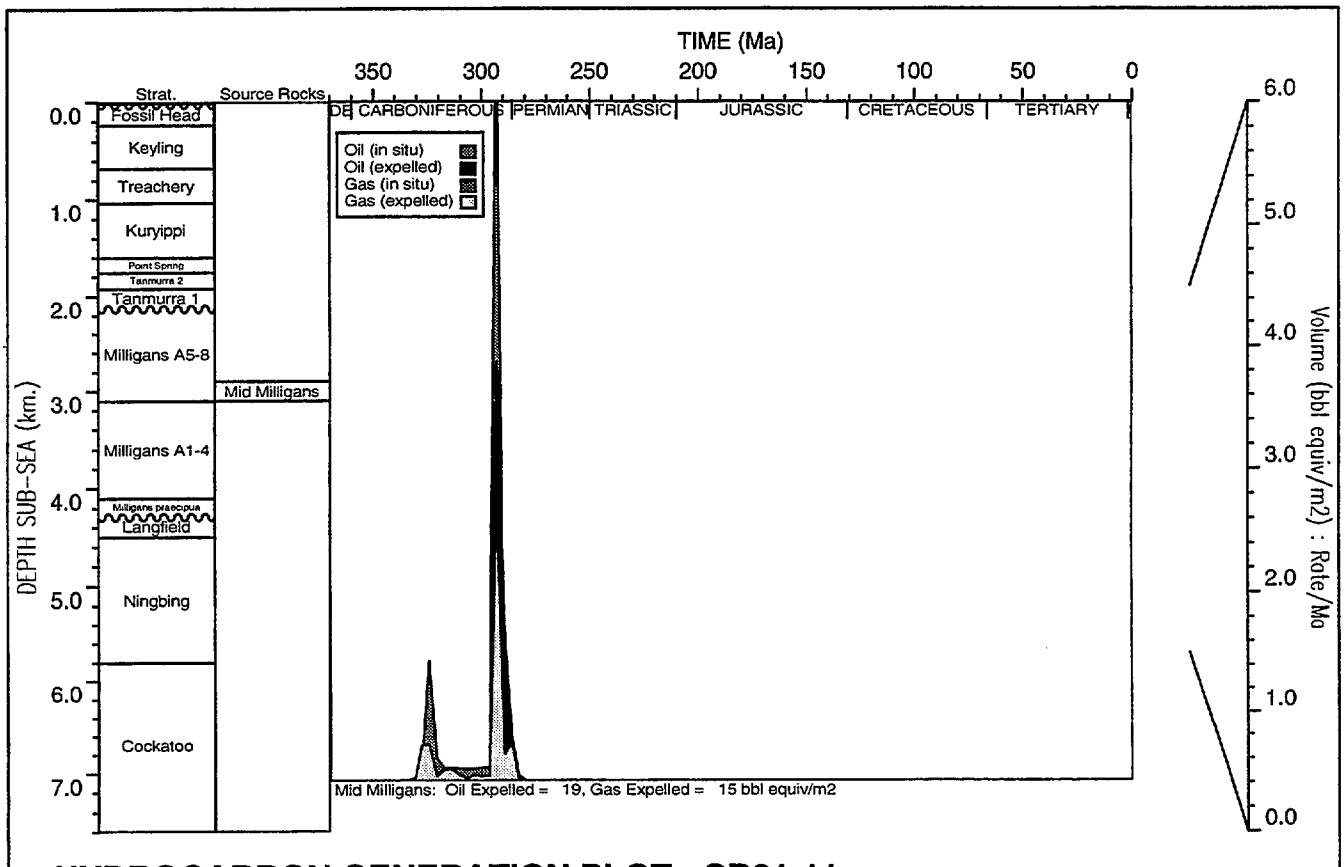

HYDROCARBON GENERATION PLOT : CB81-11a

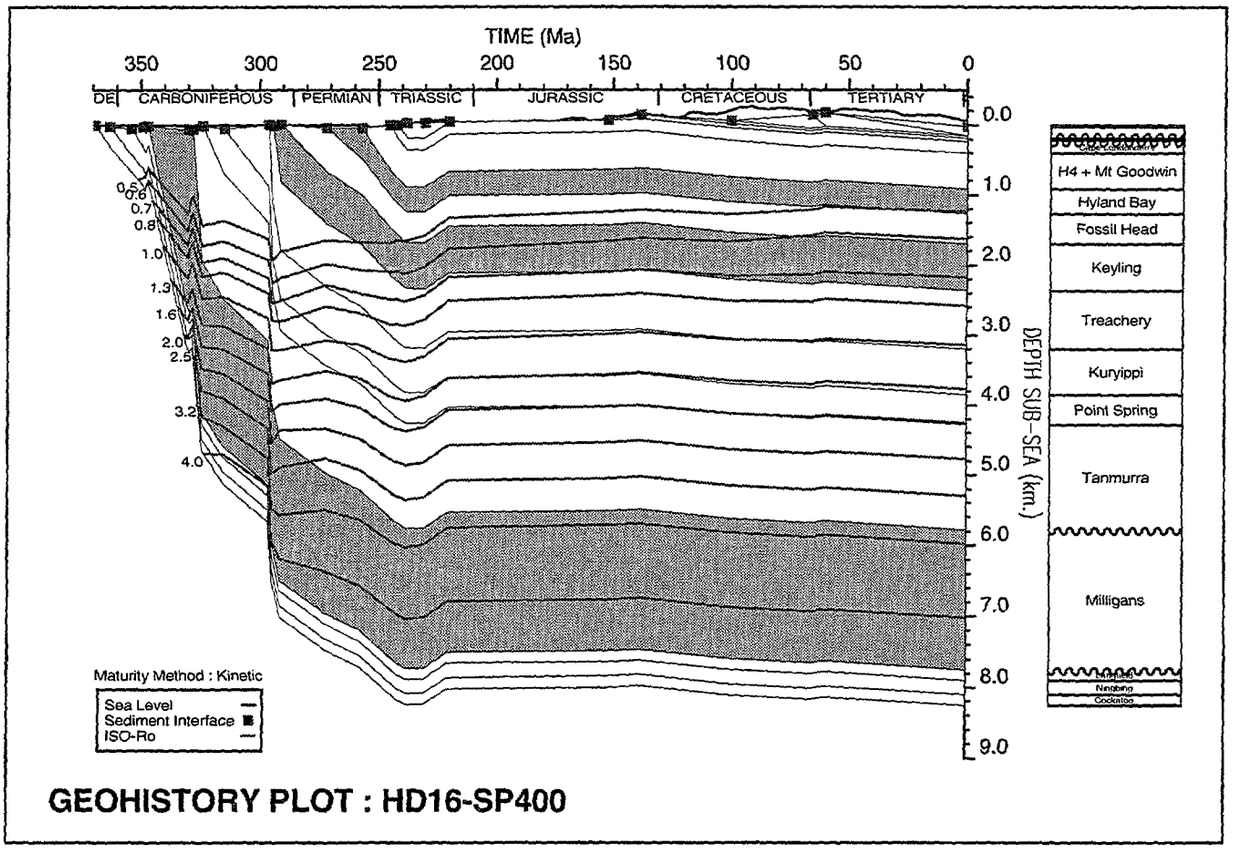

GEOHISTORY PLOT : HD16-SP400

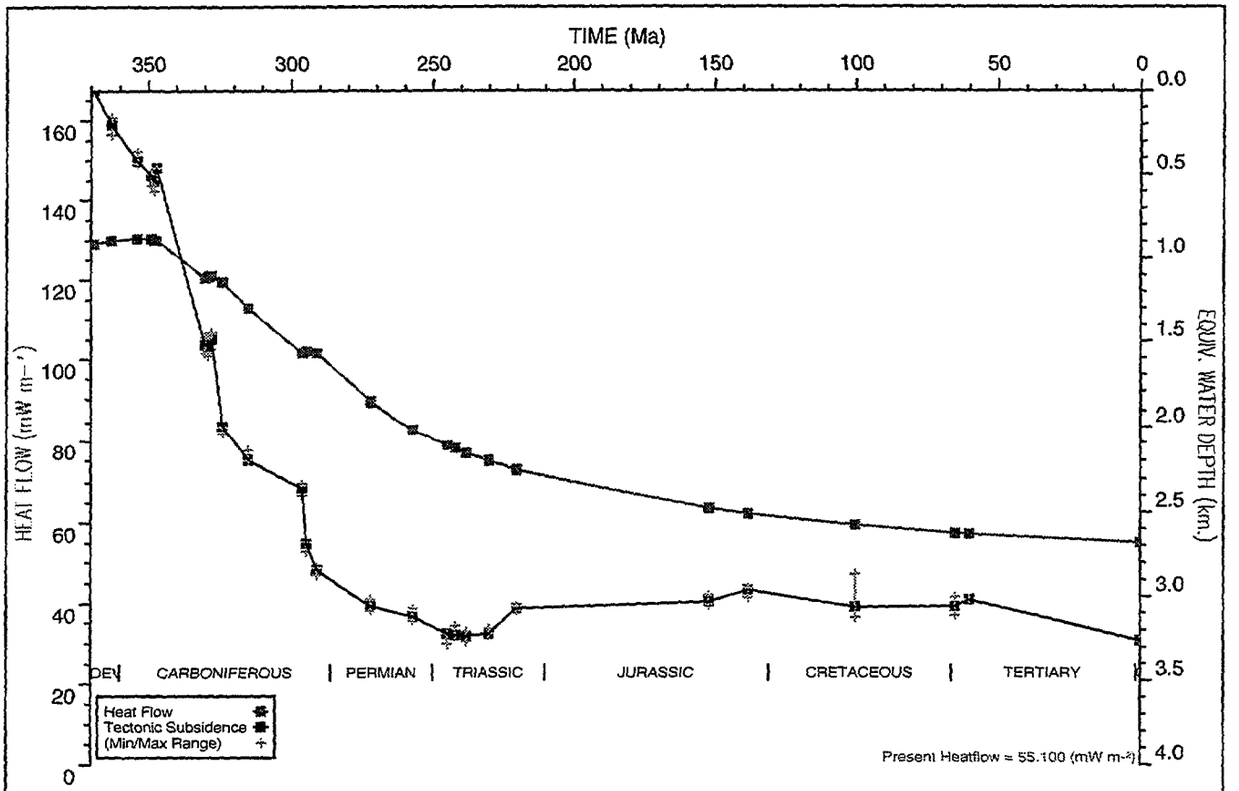

HEATFLOW AND TECTONIC SUBSIDENCE PLOT : HD16-SP400

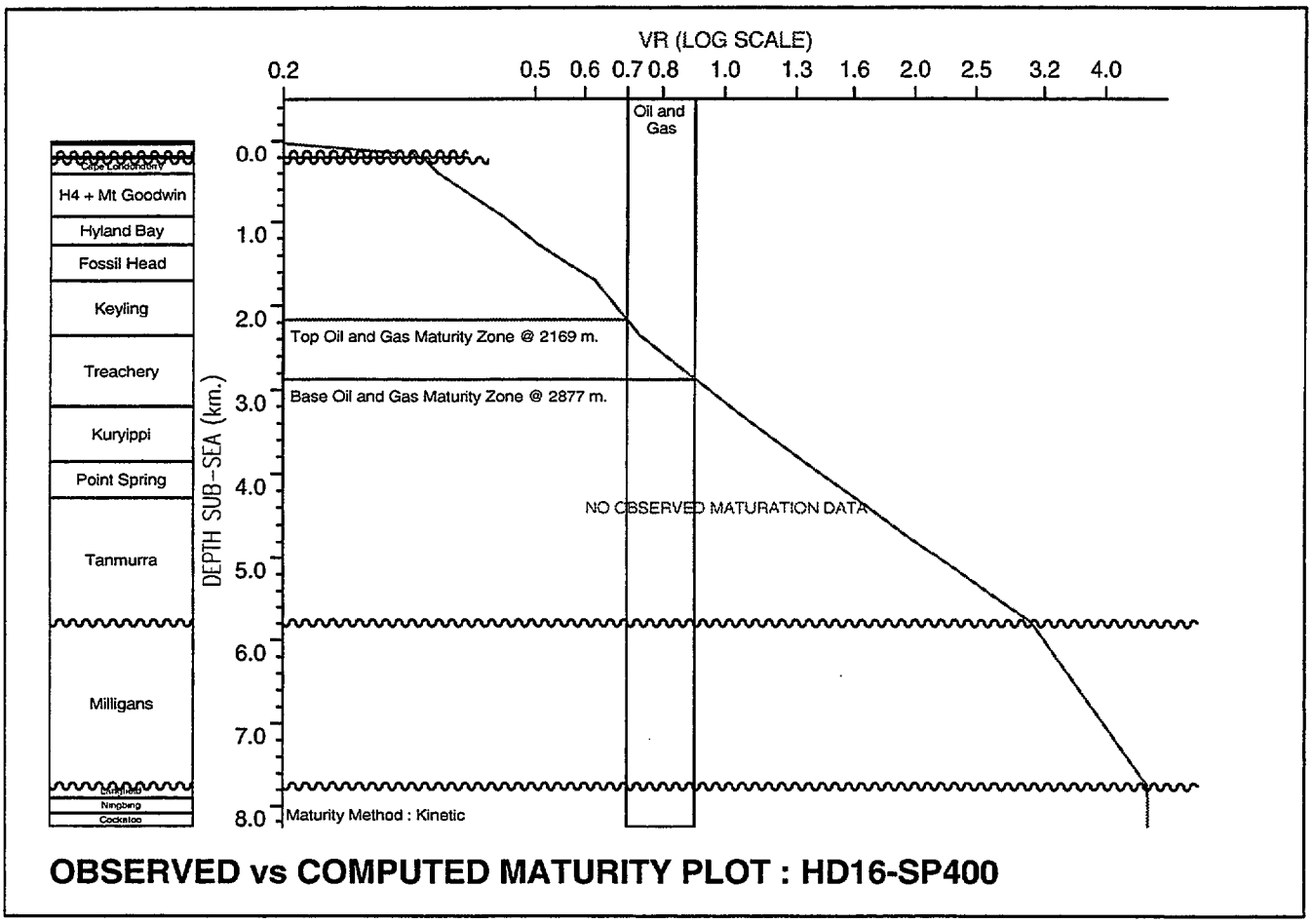

OBSERVED vs COMPUTED MATURITY PLOT : HD16-SP400

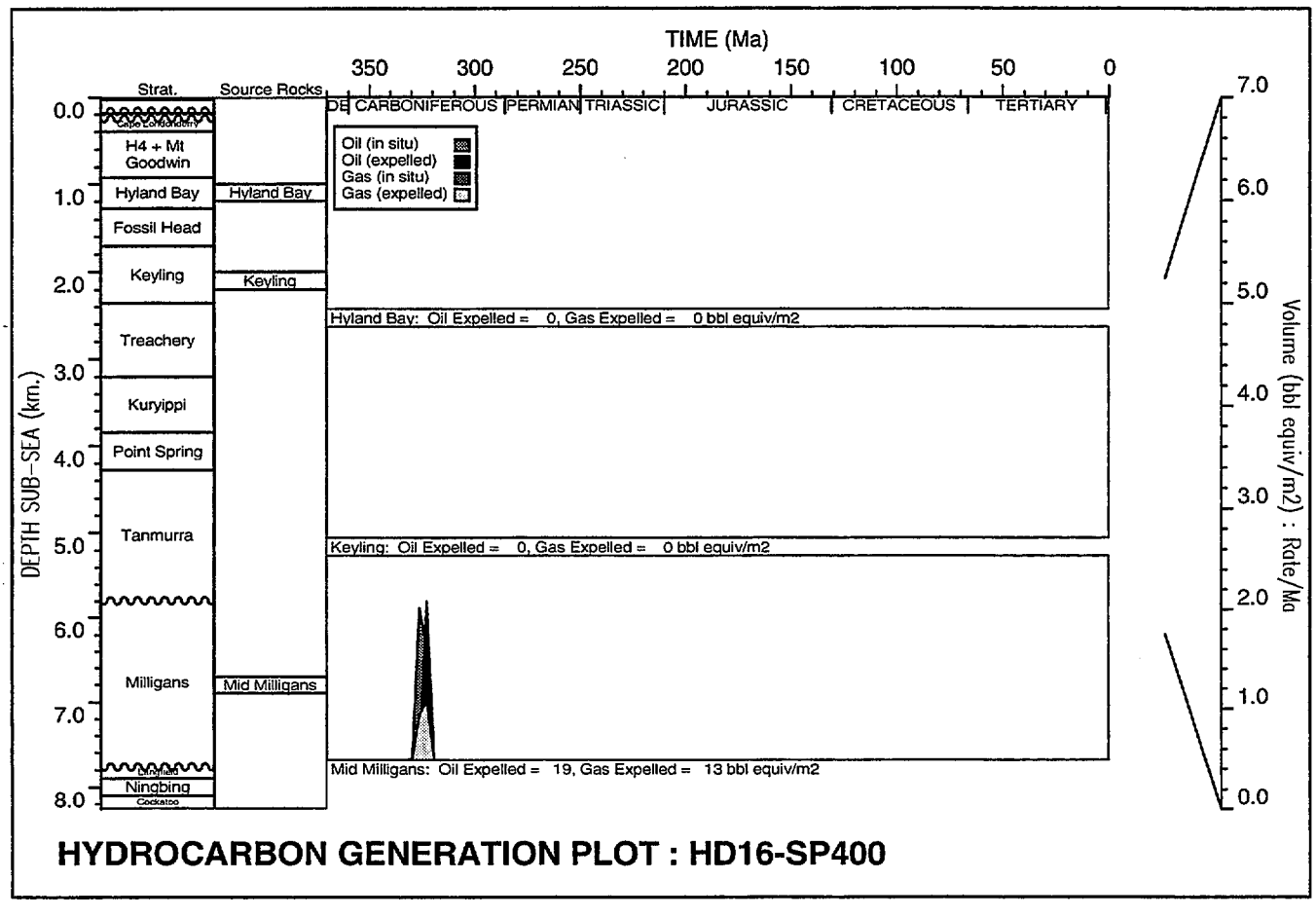

HYDROCARBON GENERATION PLOT : HD16-SP400

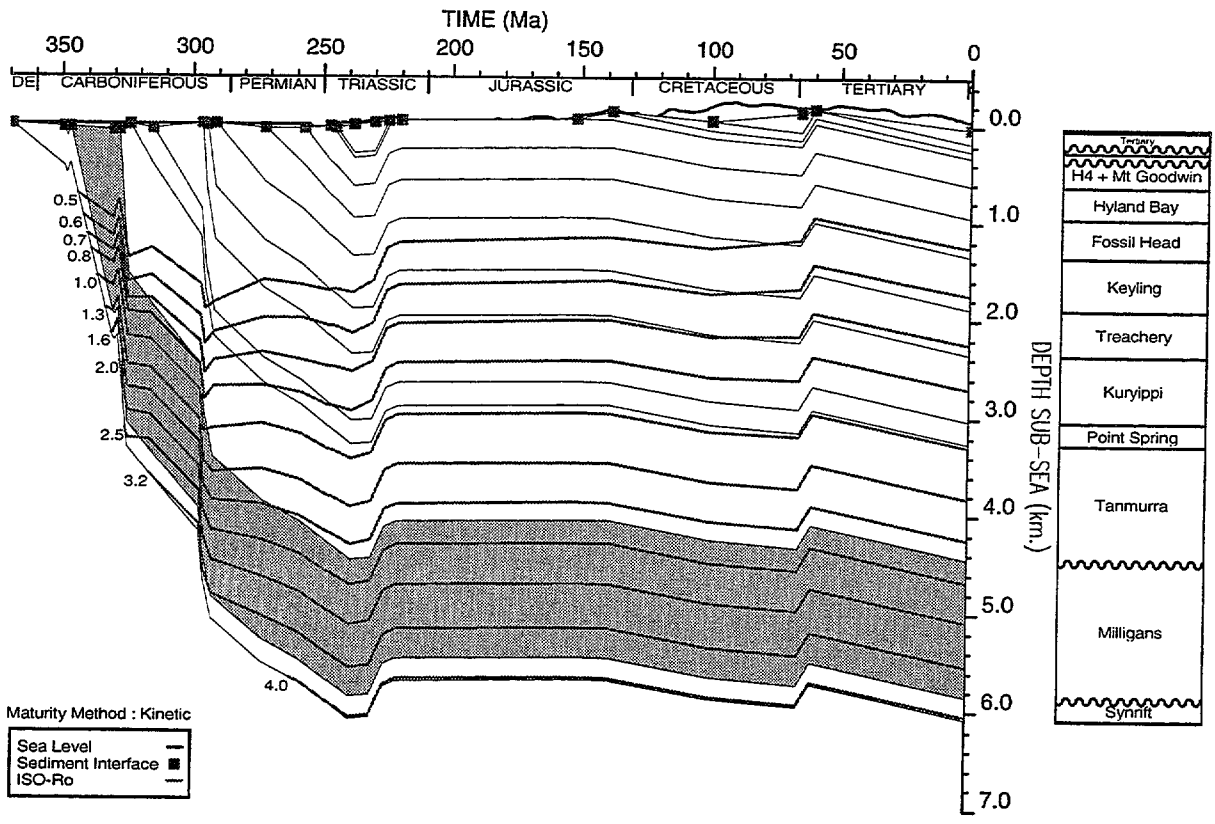

GEOHISTORY PLOT : HD16-SP1050

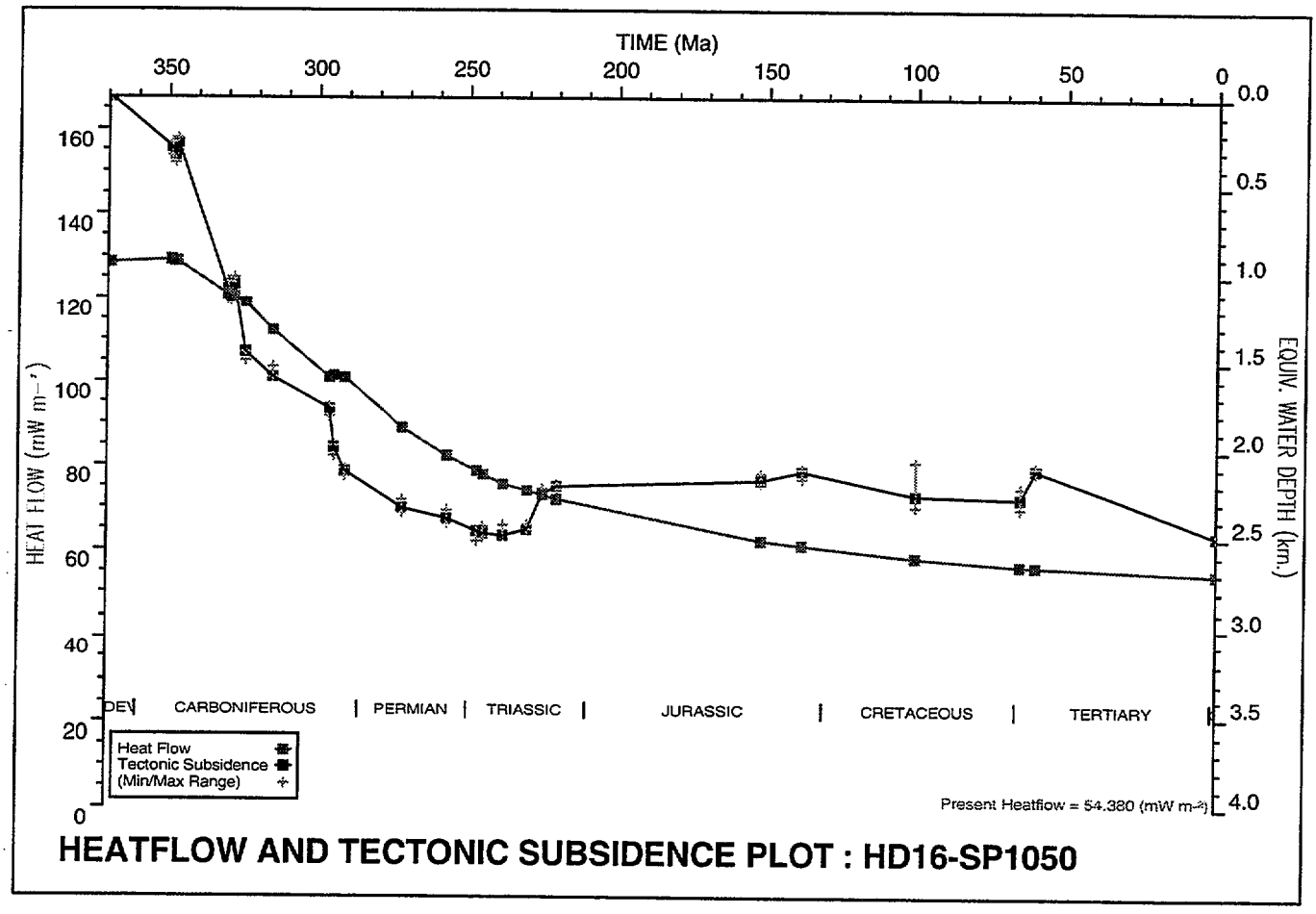

HEATFLOW AND TECTONIC SUBSIDENCE PLOT : HD16-SP1050

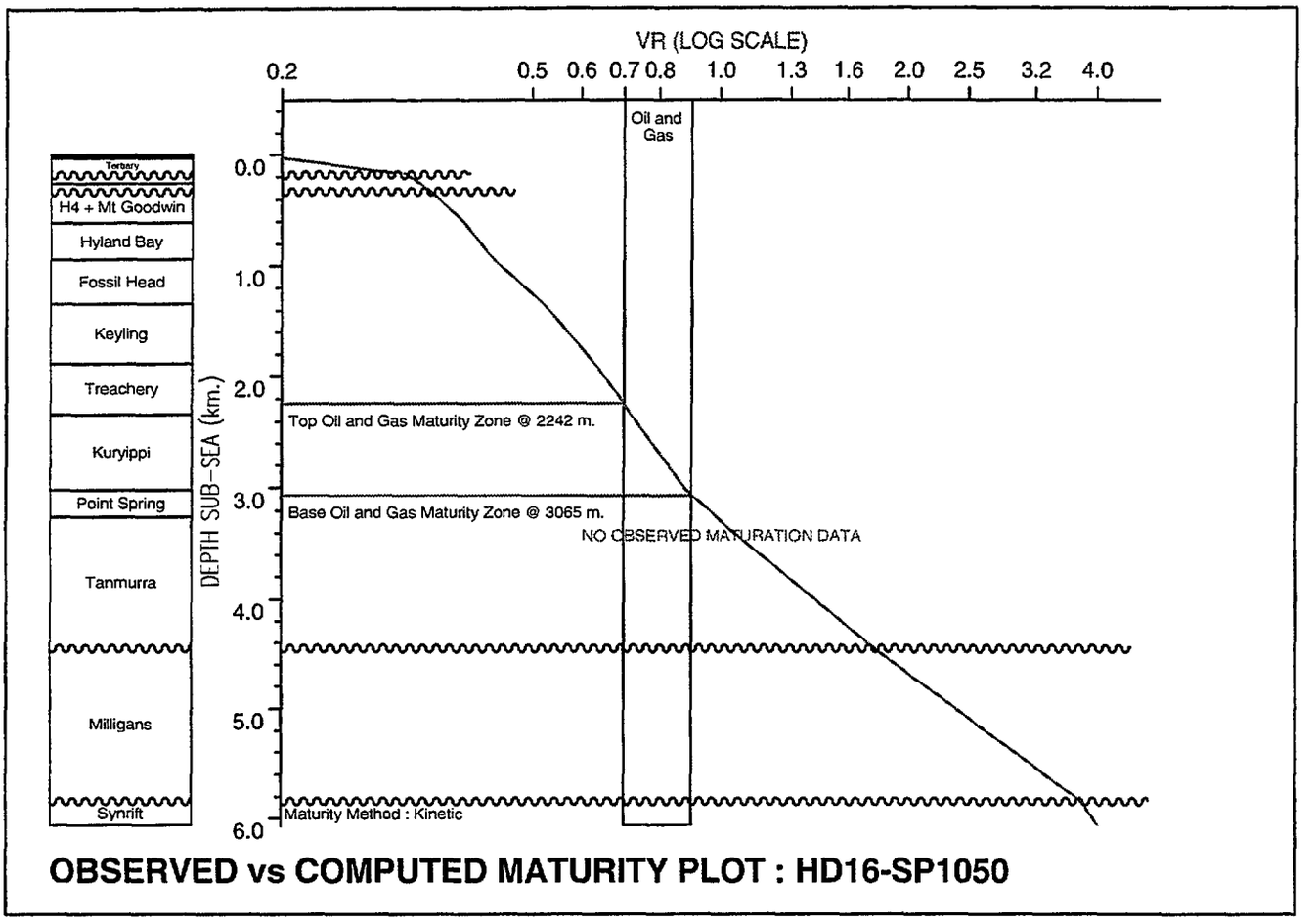

OBSERVED vs COMPUTED MATURITY PLOT : HD16-SP1050

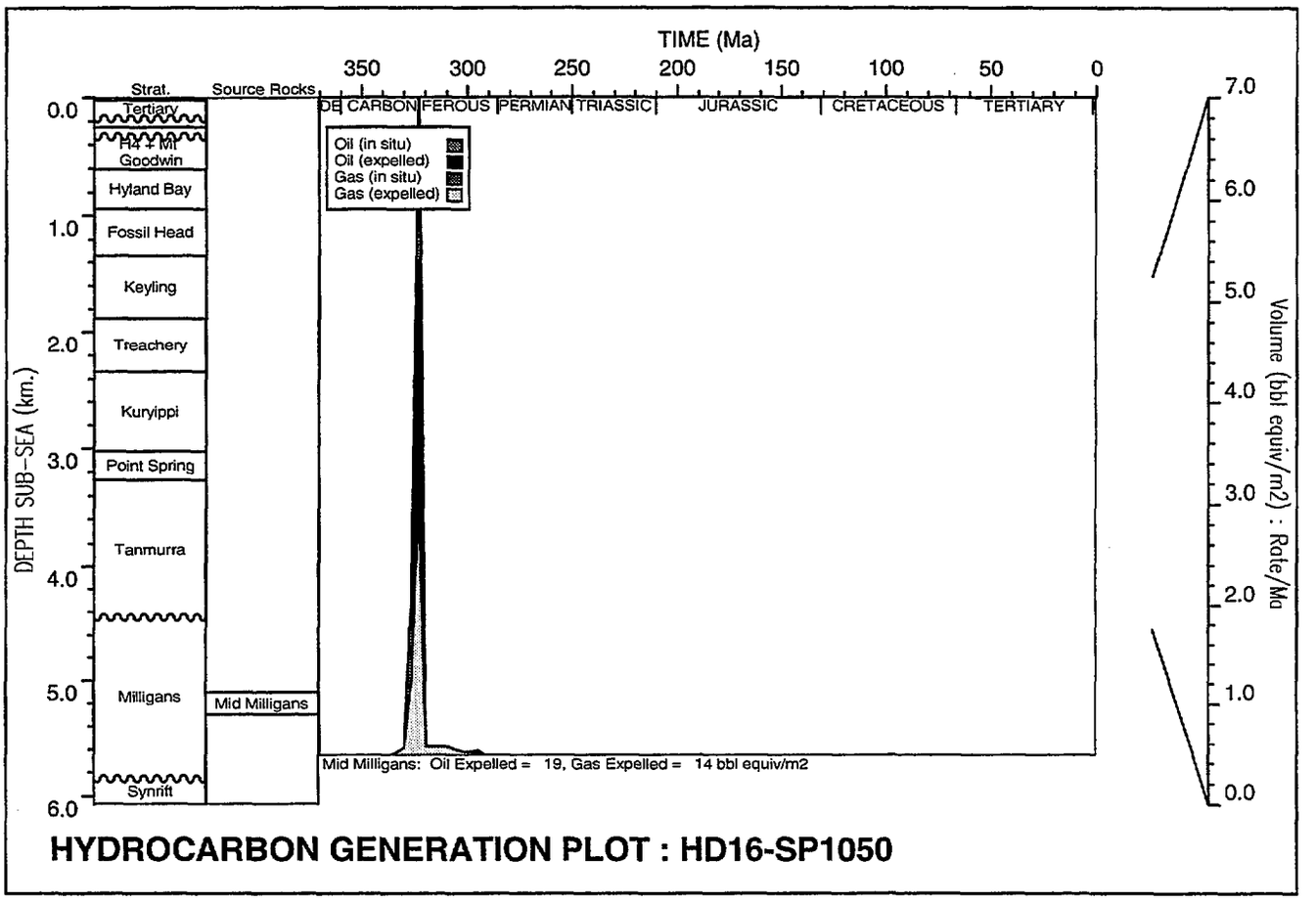

HYDROCARBON GENERATION PLOT : HD16-SP1050

Appendix C: Kerogen Kinetic Data

The following kerogen kinetic analyses were undertaken by AGSO's Isotope and Organic Geochemistry Laboratories (see Edwards & Summons, 1996, appendix A).

Modelled kerogen for Milligans source unit based on sample #7925
Modelled kerogen for Keyling and Hyland Bay source units based on sample #8484

Sample #8539:

Extracted Rock, Spirit Hill-1, 199 m, Milligans Supersequence, Shale
TOC = 1.71 % , HI = 60

Frequency factor = 5.8204E +12 s^{-1}

Percent	Activation energy (cal/mol)
0.00	42000.
0.46	43000.
0.82	44000.
1.50	45000.
0.00	46000.
0.00	47000.
0.00	48000.
0.00	49000.
42.75	50000.
17.78	51000.
9.06	52000.
0.00	53000.
2.94	54000.
6.31	55000.
0.00	56000.
0.00	57000.
8.38	58000.

Sample #8539:

Carboniferous Kerogen, Spirit Hill-1, 199 m, Milligans Supersequence.

Frequency factor = 3.3389E +13 s^{-1}

Percent	Activation energy (cal/mol)
0.00	44000.
0.00	45000.
0.84	46000.
0.93	47000.
1.81	48000.
0.89	49000.
0.00	50000.
0.00	51000.
43.83	52000.
15.45	53000.
30.04	54000.
0.00	55000.
0.47	56000.
2.00	57000.
0.00	58000.
2.16	59000.
0.00	60000.
1.58	61000.

Sample #8544:

Extracted Rock, Spirit Hill-1, 670-671m, Ningbing Supersequence, Shale
TOC = 0.73 %, HI = 123

Frequency factor = 2.8568E +13 s^{-1}

Percent	Activation energy (cal/mol)
0.00	43000.
0.05	44000.
0.00	45000.
0.20	46000.
1.76	47000.
0.00	48000.
0.00	49000.
0.00	50000.
0.00	51000.
0.00	52000.
55.61	53000.
18.53	54000.
8.80	55000.
0.00	56000.
7.41	57000.
0.00	58000.
0.00	59000.
0.00	60000.
7.65	61000.

Sample #8544:

Devonian Kerogen, Spirit Hill-1, 670-671 m, Ningbing Supersequence

Frequency factor = 1.2036E +14 s^{-1}

Percent	Activation energy (cal/mol)
0.00	45000.
0.92	46000.
0.00	47000.
0.20	48000.
2.92	49000.
0.00	50000.
3.85	51000.
0.00	52000.
0.05	53000.
29.97	54000.
21.25	55000.
35.62	56000.
0.00	57000.
0.31	58000.
0.62	59000.
0.00	60000.
0.00	61000.
4.30	62000.

Sample #8484:

Permian Extracted Rock, Flat Top-1, 1661-1664 m, Keyling Supersequence, Coal
TOC = 31%, HI = 295

Frequency factor = 1.1663E +14 s^{-1}

Percent	Activation energy (cal/mol)
0.00	46000.
0.00	47000.
0.00	48000.
0.00	49000.
0.00	50000.
0.00	51000.
0.00	52000.
0.00	53000.
66.84	54000.
0.00	55000.
15.56	56000.
3.68	57000.
5.34	58000.
3.52	59000.
0.00	60000.
2.85	61000.
0.00	62000.
2.21	63000.

Sample #8989:

Permian Extracted Rock, Kinmore-1, 1470-1473 m, Keyling Supersequence, Shale
TOC = 6.65 %, HI = 283

Frequency factor = 2.7237E +14 s^{-1}

Percent	Activation energy (cal/mol)
0.00	46000.
0.00	47000.
0.00	48000.
0.00	49000.
0.00	50000.
0.00	51000.
0.00	52000.
0.00	53000.
0.00	54000.
63.99	55000.
0.00	56000.
15.62	57000.
7.34	58000.
5.55	59000.
0.00	60000.
1.81	61000.
0.00	62000.
0.00	63000.
5.69	64000.

Sample #7925:

Extracted Rock, NBF1002, 208 m, Milligans Supersequence, Shale
TOC = 3.67 %, HI = 292

Frequency factor = 2.1920E +13 s^{-1}

Percent	Activation energy (cal/mol)
0.00	43000.
0.00	44000.
0.00	45000.
0.00	46000.
0.00	47000.
0.00	48000.
0.00	49000.
0.00	50000.
90.68	51000.
0.27	52000.
9.05	53000.
0.00	54000.
0.00	55000.
0.00	56000.
0.00	57000.
0.00	58000.

Oil versus Gas Bond Frequencies

Since the bulk chemical kinetics for the Milligans Bed kerogen (# 7925) is dominated by a single activation energy at 51 kcal/mole with a bond frequency of 300 mg HC/gTOC (equal to Rock Eval HI), the proportion of the bond frequencies that is gas (C_1-C_5 hydrocarbons) and oil (C_{6+} hydrocarbons) was determined by pyrolysis - gas chromatography - mass spectrometry (py-gc-ms), as plotted below. Using external gas standards for quantitation, the amounts of gas and oil were calculated to give a gas-to-oil ratio (GOR) of 0.5. Using this GOR value, bond frequencies of 100 and 200 mg HC/gTOC were applied to the kerogen-to-gas and kerogen-to-oil WinBury kinetics.

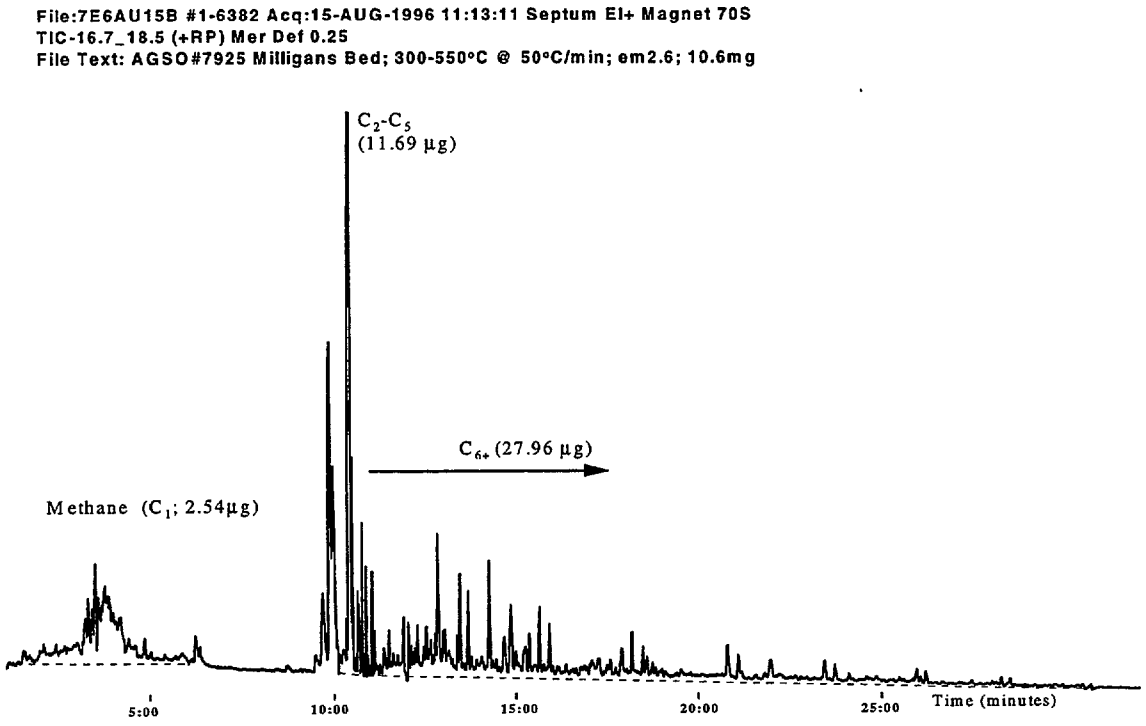

Pyrolysis - gas chromatography - mass spectrometry trace of kerogen concentrate # 7925.

In the case of the modelled Keyling and Hyland Bay kerogens, the proportion of the bond frequencies that is gas (C1-C5 hydrocarbons) and oil (C6+ hydrocarbons) was determined by analogy to similar Gondwanan source rocks in the East Australian Basins (C.J. Boreham, AGSO, July 1996).

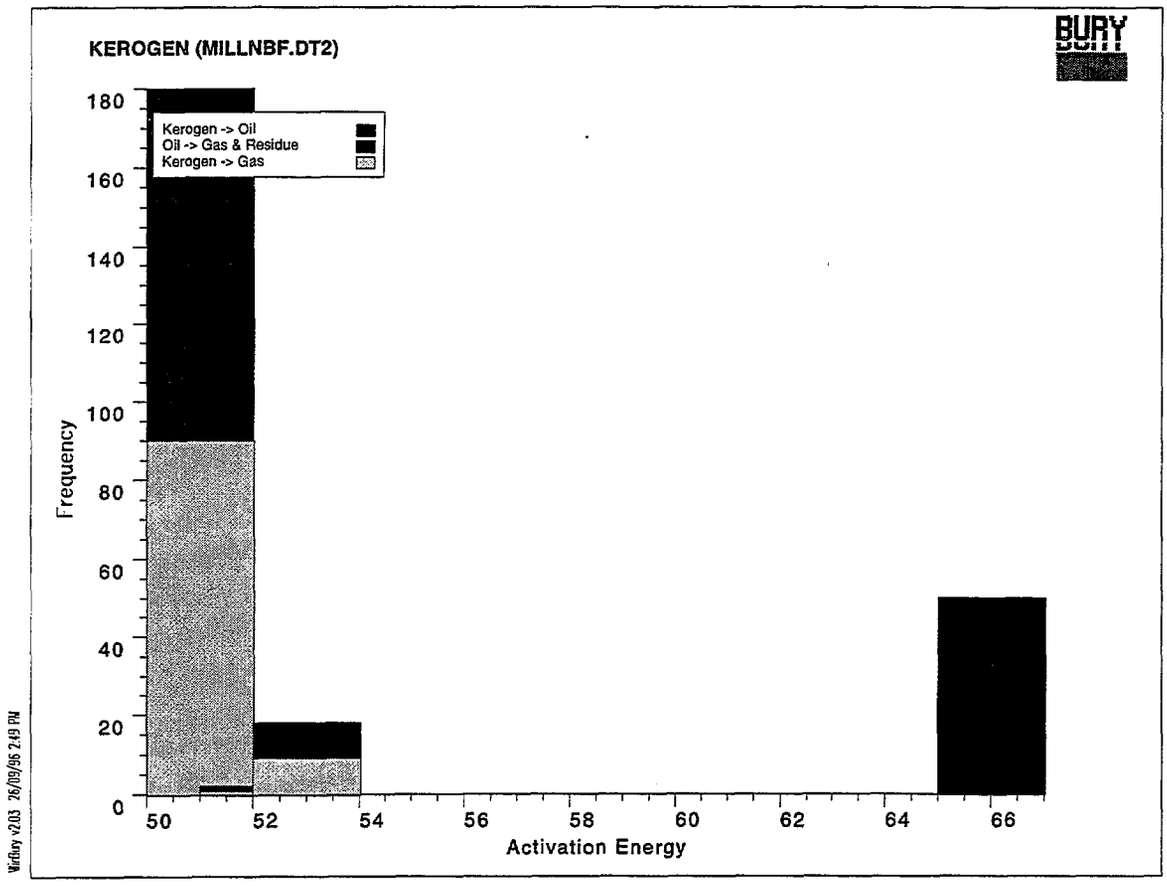

	NO	Activation Energy	Rate Constant	Bond Frequency	Reactant Code	Product Code
1	1	51	6.7E+0026	180.00	1	2
2	2	51	6.7E+0026	90.00	1	5
3	3	52	6.7E+0026	2.00	1	2
4	4	52	6.7E+0026	1.00	1	5
5	5	53	6.7E+0026	18.00	1	2
6	5	53	6.7E+0026	9.00	1	5
7	5	66	3.5E+0029	50.00	2	5

KINETICS : MILLNBF.DT2

Kerogen kinetic data modelled for the mid-Milligans source unit.

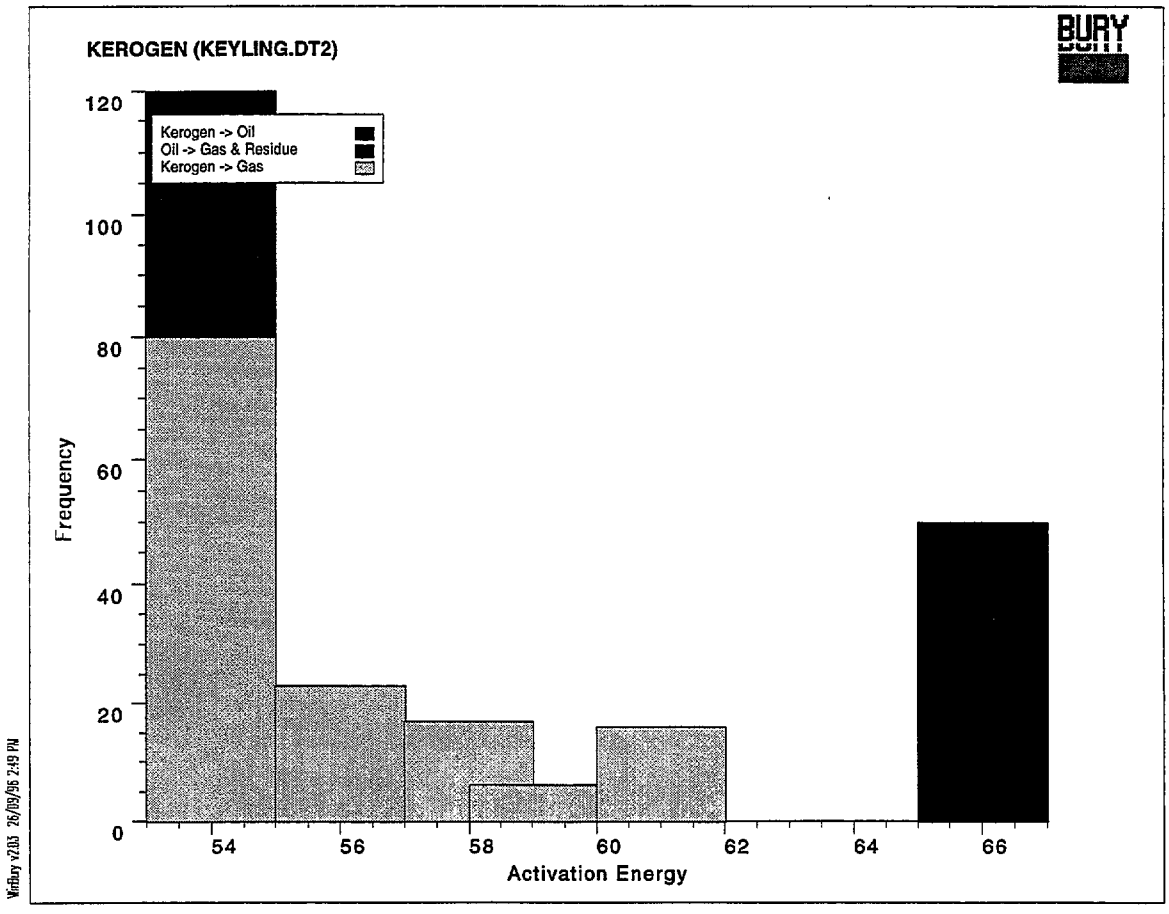

	NO	Activation Energy	Rate Constant	Bond Frequency	Reactant Code	Product Code
1	1	54	3.6E+0027	120.00	1	2
2	2	54	3.6E+0027	80.00	1	5
3	3	56	3.6E+0027	23.00	1	2
4	4	56	3.6E+0027	23.00	1	5
5	5	58	3.6E+0027	11.00	1	2
6	6	58	3.6E+0027	17.00	1	5
7	7	59	3.6E+0027	4.00	1	2
8	8	59	3.6E+0027	6.00	1	5
9	9	61	3.6E+0027	16.00	1	5
10	10	66	3.5E+0029	50.00	2	5

KINETICS : KEYLING.DT2

Kerogen kinetic data modelled for the Keyling source unit.

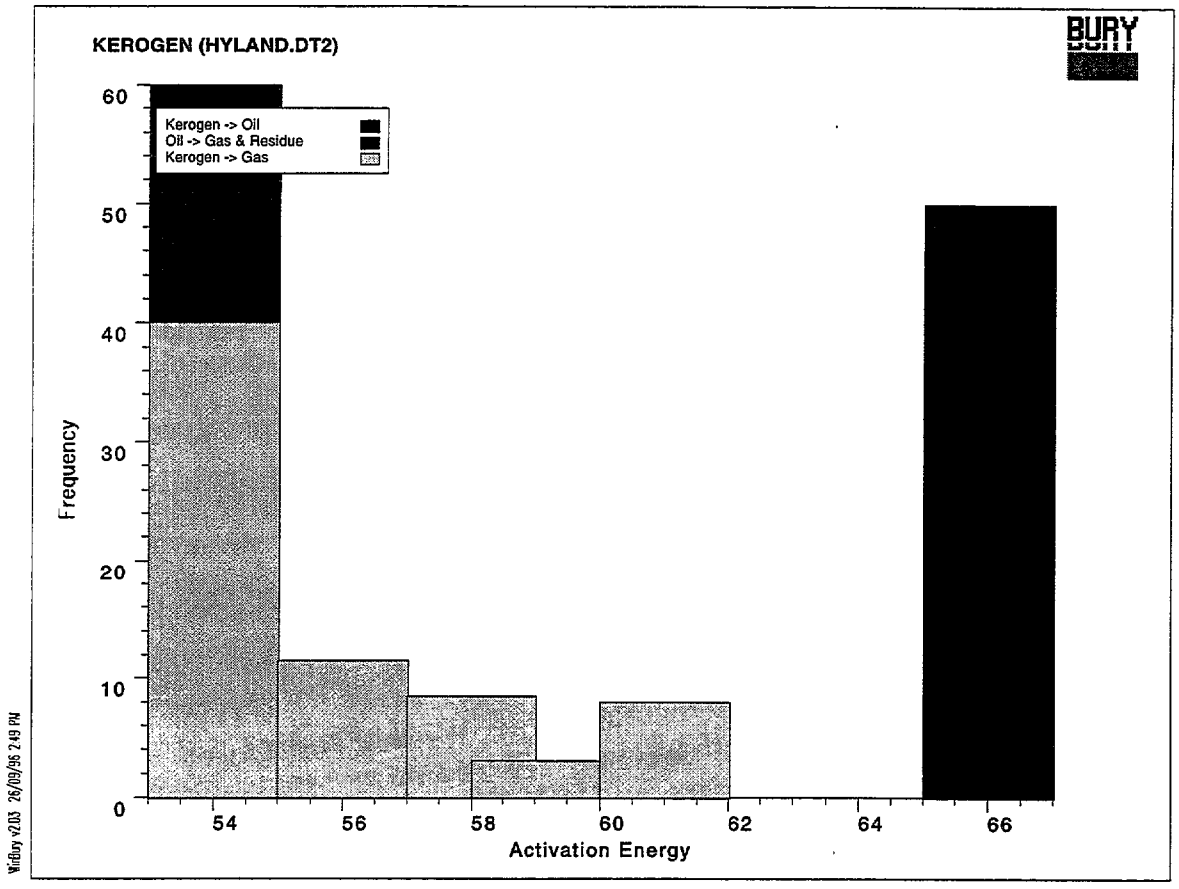

	NO	Activation Energy	Rate Constant	Bond Frequency	Reactant Code	Product Code
1	1	54	3.6E+0027	60.00	1	2
2	2	54	3.6E+0027	40.00	1	5
3	3	56	3.6E+0027	11.50	1	2
4	4	56	3.6E+0027	11.50	1	5
5	5	58	3.6E+0027	5.50	1	2
6	6	58	3.6E+0027	8.50	1	5
7	7	59	3.6E+0027	2.00	1	2
8	8	59	3.6E+0027	3.00	1	5
9	9	61	3.6E+0027	8.00	1	5
10	10	66	3.5E+0029	50.00	2	5

KINETICS : HYLAND.DT2

Kerogen kinetic data modelled for the Hyland Bay source unit